

# **Stereoselective synthesis of vicinal diols with enzymatic cascade reactions**

Inaugural-Dissertation

zur Erlangung des Doktorgrades  
der Mathematisch-Naturwissenschaftlichen Fakultät  
der Heinrich-Heine-Universität Düsseldorf

vorgelegt von

**Justyna Katarzyna Kulig**  
aus Oppeln

Jülich, September 2013

aus dem Institut für Bio- und Geowissenschaften 1: Biotechnologie  
des Forschungszentrum Jülich GmbH  
der Heinrich-Heine Universität Düsseldorf

Gedruckt mit der Genehmigung der  
Mathematisch-Naturwissenschaftlichen Fakultät der  
Heinrich-Heine-Universität Düsseldorf

Referent: Prof. Dr. Martina Pohl  
Korreferent: Prof. Dr. Vlada Urlacher

Tag der mündlichen Prüfung: 19.07.2013

## Selbstständigkeitserklärung

Hiermit versichere ich an Eides Statt, dass die vorgelegte Dissertation von mir selbständig und ohne unzuverlässige fremde Hilfe unter Beachtung der “Grundsätze zur Sicherung guter wissenschaftlicher Praxis an der Heinrich-Heine-Universität” erstellt worden ist.

Bisher habe ich keine erfolglosen Promotionsversuche unternommen.

---

Ort, Datum

---

Justyna Kulig

“One never notices what has been done, one can only  
see what remains to be done”

Maria Skłodowska-Curie (1867-1934)



# Abstract

---

Alcohol dehydrogenases are of high interest for the stereoselective synthesis of building blocks with multi-chiral centres. They are implemented for single enzymatic reduction or oxidation steps or be part of synthetic enzymatic multi-step cascades for the production of industrially relevant chiral synthons.

Although biotransformations with alcohol dehydrogenases are widespread, enzymes, which accept sterically demanding substrates, especially  $\alpha$ -hydroxy ketones, are not common in nature. Therefore chemical methods for the synthesis of chiral 1,2-diols are still first choice.

As a drawback, alcohol dehydrogenases require expensive nicotinamide cofactors such as NAD(H) or NADP(H) for their activity. Prices of these cofactors prevent their application in stoichiometric amounts and therefore regeneration of nicotinamide cofactors is an essential issue for biotechnological purposes. Therefore a co-substrate is required that is transformed to the respective co-product in equimolar amounts relative to the product. This co-product has to be separated from the product or must be removed *in situ*, which decreases atom- and process economy.

In this work the carboligation of two inexpensive aldehydes catalysed by ThDP-dependent enzymes is combined with a subsequent reduction of the intermediately formed  $\alpha$ -hydroxy ketone by alcohol dehydrogenases. Therefore, a suitable cofactor regeneration system with smart *in situ* co-product removal had to be developed in order to gain high eco-efficiency of the synthetic enzyme cascade. To achieve the aim, the following work packages were addressed:

1. Investigation of the substrate range of eight available alcohol dehydrogenases with focus on reduction of bulky-bulky  $\alpha$ -hydroxy ketones;
2. Determination of the stereoselectivity of the first and the second step of the synthetic cascade;
3. Selection of the most promising enzyme(s) for the reduction of  $\alpha$ -hydroxy ketones (which turned out to be the alcohol dehydrogenase from *Ralstonia* sp.) and its detailed biochemical characterisation with focus on the reduction of  $\alpha$ -hydroxy ketones;
4. Evaluation of a suitable cofactor regeneration system (substrate-coupled and enzyme-coupled approach) for the enzymatic 2-step synthesis, where smart

implementation of co-substrates (benzyl alcohol or ethanol) allows *in situ* removal of the co-product (benzaldehyde or acetaldehyde) from the second cascade step by reusing it in the first catalytic step (carboligation) of the cascade;

5. Reaction engineering of the synthetic multi-enzymatic cascade with assistance of mathematical modelling, to optimise the overall yield of the synthetic cascade.

During this work two synthetic recycling cascade reactions using a substrate-coupled and an enzyme-coupled approach for cofactor regeneration were developed. For the substrate-coupled approach benzyl alcohol was used as co-substrate, and the co-product benzaldehyde was reused as a substrate in the carboligation step. For the enzyme-coupled approach ethanol was chosen as a co-substrate and the resulting acetaldehyde was also reused as substrate for the C–C bond formation.

Whereas good conversions (> 70%), but moderate stereoselectivities (dr *syn/anti* 9:1) were obtained for the production of (1*R*,2*R*)-1-phenylpropane-1,2-diol in cascade reactions using the substrate-coupled approach, the enzyme-coupled approach yielded excellent conversions (> 95%) and diastereoselectivities (*de* > 99%).

Furthermore, during this thesis the most promising alcohol dehydrogenase from *Ralstonia* sp. for the reduction of  $\alpha$ -hydroxy ketones was subject of crystallisation studies for X-ray structural investigations in order to explain its high potential for conversion of especially bulky substrates.

# Kurzfassung

Alkoholdehydrogenasen sind für die stereoselektive Synthese von Molekülen mit mehreren chiralen Zentren von großer Bedeutung. Sie können entweder für einzelne enzymatische Reduktions- bzw. Oxidationsschritte oder als Teil von synthetischen enzymatischen mehrstufigen Kaskaden für die Produktion von industriell relevanten chiralen Synthesebausteinen verwendet werden.

Obwohl Biotransformationen mit Alkoholdehydrogenasen weit verbreitet sind, sind Enzyme, die sterisch anspruchsvolle Substrate, insbesondere  $\alpha$ -Hydroxyketone, akzeptieren, in der Natur selten. Daher sind chemische Verfahren für die Synthese von chiralen 1,2-Diolen bisher die erste Wahl.

Ein Nachteil der Verwendung von Alkoholdehydrogenasen sind teure Nicotinamidcofaktoren wie NAD(H) oder NADP(H), die für die Katalyse benötigt werden. Die hohen Preise dieser Cofaktoren verhindern ihren Einsatz in stöchiometrischen Mengen. Aus diesem Grund ist die Regeneration von Nicotinamidcofaktoren ein wichtiges Thema für biotechnologische Anwendungen. Dazu wird ein Cosubstrat verwendet, das während der enzymatischen Cofaktorregenerierung in äquimolaren Mengen, relativ zum Produkt; zum entsprechenden Coprodukt umgesetzt wird. Dieses Coprodukt muss vom Produkt abgetrennt oder *in situ* entfernt werden. Dies verringert sowohl die Atomökonomie als auch die Wirtschaftlichkeit des Prozesses.

In dieser Arbeit wird die Carboligation von zwei kostengünstigen Aldehyden durch Thiamindiphosphat-abhängige Enzyme katalysiert und mit einer anschließenden Reduktion des intermediär gebildeten  $\alpha$ -Hydroxyketons zum 1,2-Diol durch Alkoholdehydrogenasen kombiniert. Dafür musste eine geeignete Cofaktorregenerierung mit *in situ* Coproduktentfernung entwickelt werden, um eine hohe Ökoeffizienz der synthetischen Enzymkaskade sicherzustellen. Um dieses Ziel zu erreichen, wurden folgende Arbeitspakete behandelt:

1. Untersuchung des Substratspektrums von acht verfügbaren Alkoholdehydrogenasen mit Fokus auf die Reduzierung sterisch anspruchsvoller  $\alpha$ -Hydroxyketone;
2. Bestimmung der Stereoselektivität der ersten und der zweiten Stufe der synthetischen Kaskade;

3. Auswahl des vielversprechendsten Enzyms für die Reduktion von  $\alpha$ -Hydroxyketonen (hier die Alkoholdehydrogenase aus *Ralstonia* sp.) und seine detaillierte biochemische Charakterisierung mit Fokus auf die Reduktion von  $\alpha$ -Hydroxyketonen;
4. Evaluierung eines geeigneten Cofaktorregenerationssystems (Substrat-gekoppelter und Enzym-gekoppelter Ansatz) zur enzymatischen 2-Schritt-Synthese, wobei die intelligente Wahl der Cosubstrate (Benzylalkohol bzw. Ethanol) eine *in situ*-Entfernung der gebildeten Coprodukte (Benzaldehyd bzw. Ethanol) des zweiten Kaskadenschritts durch dessen Wiederverwendung in der ersten katalytischen Stufe der Kaskade (Carboligation) ermöglicht;
5. Reaktionstechnische Optimierung der synthetischen multi-enzymatischen Kaskade mit Hilfe mathematischer Modellierung zur Optimierung der Ausbeute der gesamten Kaskade.

Während dieser Arbeit wurden zwei synthetische Recycling-Kaskadenreaktionen mit einem Substrat-gekoppelten und einem Enzym-gekoppelten Ansatz für die Cofaktorregenerierung entwickelt. Für den Substrat-gekoppelten Ansatz wurde Benzylalkohol als Cosubstrat verwendet und das entstehende Nebenprodukt Benzaldehyd als Substrat in dem Carboligationsschritt wiederverwendet. Bei dem Enzym-gekoppelten Ansatz mit Ethanol als Cosubstrat wurde das resultierende Acetaldehyd ebenfalls als Substrat für die C-C-Verknüpfung wiederverwendet.

Während gute Umsätze (> 70%), jedoch begleitet von mäßiger Stereoselektivität (dr *syn/anti* 9:1), für die Herstellung des (1*R*,2*R*)-1-Phenylpropan-1,2-diols in der Kaskadenreaktionen unter Verwendung der Substrat-gekoppelten Ansatzes erzielt wurden, ergab der Enzym-gekoppelte Ansatz ausgezeichnete Umsätze (> 95%) und Diastereoselektivität (*de* > 99%).

Des Weiteren wurden während dieser Arbeit für die, bezüglich der Reduktion von  $\alpha$ -Hydroxyketonen, vielversprechendste Alkoholdehydrogenase aus *Ralstonia* sp. Kristallisationsstudien für die Röntgenstrukturanalyse durchgeführt, um das hohe Potenzial zur Umwandlung von insbesondere sterisch anspruchsvollen Substraten zu erklären

## List of publications

---

1. “*Stereoselective synthesis of bulky 1,2-diols with alcohol dehydrogenases*”  
Justyna Kulig, Robert C. Simon, Christopher A. Rose, Syed M. Husain, Matthias Häckh, Steffen Lüdeke, Kirsten Zeitler, Wolfgang Kroutil, Martina Pohl and Dörte Rother  
Catalysis Science & Technology, **2012**, 2(8), 1580-1589 (*selected as Hot Article*)
2. “*Biochemical characterization of an alcohol dehydrogenase from Ralstonia sp.*”  
Justyna Kulig, Amina Frese, Wolfgang Kroutil, Martina Pohl and Dörte Rother  
Biotechnology & Bioengineering, **2013**, 110(7), 1838-1848
3. “*Stereoselective synthesis of 1,2-diols with synthetic enzyme cascades including smart in situ cofactor regeneration and co-product recycling*”  
Justyna Kulig, Wolfgang Wiechert, Martina Pohl and Dörte Rother  
ChemCatChem, **2013**, *submitted*
4. “*Structures of alcohol dehydrogenases from Ralstonia and Sphingobium spp. reveal the molecular basis for their recognition of ‘bulky-bulky’ ketones*”  
Henry Man, Kinga Kedziora, Justyna Kulig, Annika Frank, Ivan Lavandera-Garcia, Vincente Gotor-Fernandez, Dörte Rother, Sam Hart, Johan P. Turkenburg and Gideon Grogan  
Topics in Catalysis, **2013**, *accepted*

## List of oral presentations

1. *“Modular synthetic enzyme cascades for the production of valuable chiral precursors”*  
Justyna Kulig, Torsten Sehl, Wolfgang Kroutil, John M. Ward, Helen C. Hailes, Wolfgang Wiechert, Martina Pohl and Dörte Rother (*presenting author*)  
MECP2012: Multistep Enzyme-Catalyzed Processes 2012, April 10-13, **2012**, Graz, Austria
2. *“Modular synthetic enzyme cascades for the production of valuable chiral precursors”*  
Justyna Kulig, Torsten Sehl, Wolfgang Kroutil, John M. Ward, Helen C. Hailes, Wolfgang Wiechert, Martina Pohl and Dörte Rother (*presenting author*)  
VU Amsterdam, June **2012**, Amsterdam, The Netherlands (*invited presentation*)
3. *“Novel double recycling cascade reactions with the potent Ca-stabilized alcohol dehydrogenase from Ralstonia sp.”*  
Justyna Kulig (*presenting author*), Amina Frese, Robert C. Simon, Wolfgang Kroutil, Martina Pohl and Dörte Rother  
ZING Conference on Biocatalysis, December 4-7, **2012**, Xcaret, Mexico
4. *“Modular synthetic enzyme cascades for the production of chiral diols and amino alcohols”*  
Torsten Sehl, Justyna Kulig, Robert Westphal, Alvaro Baraibar, Andre Jakoblinnert, Jochen Wachtmeister, Martina Pohl and Dörte Rother (*presenting author*)  
ECCE<sub>9</sub> & ECAB<sub>2</sub>: 9th European Congress of Chemical Engineering and 2nd European Congress of Applied Biotechnology, April 21-25, **2013**, The Hague, The Netherlands

## List of poster presentations

---

1. *"Identification and characterisation of enzymes for the synthesis of chiral diols"*  
Justyna Kulig (presenting author), Wolfgang Wiechert, Martina Pohl and Dörte Gocke  
Biocat 2010, August 29 – September 2, **2010**, Hamburg, Germany
2. *"Stereoselective 2-step synthesis of chiral 1,2-diols"*  
Justyna Kulig (presenting author), Wolfgang Kroutil, Frank Hollmann, Wolfgang Wiechert, Martina Pohl and Dörte Gocke  
BIOTRAINS meeting, December 2-4, **2010**, Basel, Switzerland
3. *"Enzymatic 2-step synthesis: From aldehydes to chiral vicinal diols"*  
Justyna Kulig (presenting author), Robert C. Simon, Wolfgang Kroutil, Frank Hollmann, Wolfgang Wiechert, Martina Pohl and Dörte Rother  
Frontiers in White Biotechnology, June 21-22, **2011**, Delft, The Netherlands
4. *"Enzymatic 2-step synthesis: From aldehydes to chiral vicinal diols"*  
Justyna Kulig (presenting author), Robert C. Simon, Wolfgang Kroutil, Frank Hollmann, Wolfgang Wiechert, Martina Pohl and Dörte Rother  
"Biotransformations 2011" DECHEMA Summer School, August 22-25, **2011**, Bad Herrenalb, Germany
5. *"Enzymatic toolboxes for the synthesis of chiral diols"*  
Justyna Kulig (presenting author), Robert C. Simon, Wolfgang Kroutil, Frank Hollmann, Wolfgang Wiechert, Martina Pohl and Dörte Rother  
Marie Curie Researchers Symposium "SCIENCE – Passion, Mission, Responsibilities", September 25-27, **2011**, Warsaw, Poland
6. *"Via enzyme toolboxes to chiral diols"*  
Justyna Kulig (presenting author), Robert C. Simon, Wolfgang Kroutil, Frank Hollmann, Wolfgang Wiechert, Martina Pohl and Dörte Rother  
BIOTRANS 2011: Conference of industrial process, research and development, October 2-6, **2011**, Giardini Naxos, Italy

7. *“2-step enzymatic synthesis of bulky 1,2-diols”*  
Justyna Kulig (*presenting author*), Robert C. Simon, Wolfgang Kroutil, Martina Pohl and Dörte Rother  
MECP2012: Multistep Enzyme-Catalyzed Processes 2012, April 10-13, **2012**, Graz, Austria
8. *“Synthetic enzyme cascades for the production of valuable chiral diols and amino alcohols”*  
Justyna Kulig, Torsten Sehl, Wolfgang Kroutil, John M. Ward, Helen C. Hailes, Wolfgang Wiechert, Martina Pohl, Dörte Rother (*presenting author*)  
Gordon Conference on Biocatalysis, Jun **2012**, Smithfield, Rhode Island, USA
9. *“Modular synthetic enzyme cascades for the stereoselective production of chiral diols and amino alcohols with whole cells”*  
Jochen Wachtmeister (*presenting author*), Andre Jakoblinnert, Justyna Kulig, Torsten Sehl, Martina Pohl and Dörte Rother  
ZING Conference on Biocatalysis, December 4-7, **2012**, Xcaret, Mexico
10. *“Modular synthetic enzyme cascades for the stereoselective production of chiral diols from cheap aldehydes with whole cells”*  
Jochen Wachtmeister (*presenting author*), Andre Jakoblinnert, Justyna Kulig and Dörte Rother  
ECCE<sub>9</sub> & ECAB<sub>2</sub>: 9th European Congress of Chemical Engineering and 2nd European Congress of Applied Biotechnology, April 21-25, **2013**, The Hague, The Netherlands



# Acknowledgements

---

I would like to express my gratitude to all the people who became a part of my PhD project. Especially, I would like to thank:

Apl. Prof. Dr. Martina Pohl for the great opportunity to work on the project under excellent working conditions at the institute as well as for her outstanding supervision, patience and motivation during the course of this thesis.

Dr. Dörte Rother for her extraordinary commitment to the project, the excellent supervision as an executive supervisor, for many valuable hints and her inspiring motivation.

Prof. Dr. Vlada Urlacher for her kind effort to evaluate this work as a co-referee.

Prof. Dr. Wolfgang Wiechert for the continuous interest in my PhD project, his helpful suggestions, many fruitful discussions and his valuable input to the project.

Dr. Gideon Grogan and his team from York Structure Biology Laboratory at University of York (United Kingdom), for a very fruitful cooperation in frame of this project. Especially, I would like to express my gratitude, for the opportunity to learn some of the secrets of protein crystallisation during my research stay in York.

During the time at Forschungszentrum Jülich GmbH many people of the Biocatalysis and Biosensor group supported my work. I would like to thank all of them, especially:

Amina Frese for her high motivation and her commitment in her bachelor project;

Doris Hahn for never giving up cloning despite all obstacles;

Dr. Daniel Minör for his assistance in whole cell catalysis experiments, for sharing his knowledge about cofactor regeneration systems;

Dr. Robert C. Simon for priceless assistance and many discussions about chemical syntheses.

Furthermore, I would like to thank Lilia Arnold, Ilona Frindi-Wosch, Heike Offermann, and Ursula Mackfeld for their very valuable advice and help in laboratory.

Additionally, I would like to thank my former and present colleagues of the Biocatalysis and Biosensors group: Alvaro Baraibar, Aischarya Brahma, Tina Gerhards, Andre Jakoblinert, Daniel Jussen, Roland Moussa, Daniel Okrob, Carlo Schmitz, Victoria Steffen, Jochen Wachtmeister, Robert Westphal, and Kerstin Würges for the hilarious working atmosphere, their priceless support in laboratory, fruitful discussions as well as for their valuable help by teaching and improvement of my German language.

At this point I would like to express my sincere gratitude to Torsten Sehl for interesting and fruitful nightlong discussions about biochemistry, enzymology and cascade reactions as well as his guidance through the German grammar rules.

I am very thankful Marianne Hess and Maria Lauer for their big help in every-day situations.

In addition, I would like to express my acknowledgement to Dr. Kirsten Zeitler, Prof. Dr. Marion Ansorge-Schumacher, Prof. Dr. Andreas Schmid, and Prof. Dr. Michael Müller for a pleasant cooperation in frame of this project.

This work would not have been possible without the financial support of Marie Curie Initial Training Network (BIOTRAINS, grant agreement: 258331) for which I am very grateful. Here I also would like to thank all BIOTRAINS members, but especially Prof. Dr. Wolfgang Kroutil, Dr. Ivan Lavandera, and Dr. Frank Hollmann for pleasant cooperations and fruitful discussions during the meetings all over Europe.

Last, but not least, I would like to thank my family and my long-standing friends Anna Kucia and Paweł Markowicz for their constant support and encouragement.

# Table of content

<b>1. INTRODUCTION</b>	<b>1</b>
1.1. Concept of Green Chemistry	2
1.2. Industrial biotechnology	3
1.3. Enzymes in biocatalysis	5
1.4. Classification of enzymes	7
1.5. Oxidoreductases classification	8
1.6. Alcohol dehydrogenases/Ketoreductases	9
1.7. Cofactor regeneration	10
1.7.1. Substrate-coupled approach	11
1.7.2. Enzyme-coupled approach	11
1.8. Mechanism of alcohol dehydrogenases	12
1.9. Chiral pharmaceuticals	15
1.10. Chiral 1,2-diols as building blocks	17
1.11. Production of 1,2-diols	19
1.11.1. Chemical methods	19
1.11.2. Enzymatic methods	22
1.11.2.1. First step: carbonylation by ThDP-dependent enzymes	24
1.11.2.1.1. Benzaldehyde lyase	26
1.11.2.1.2. Benzoylformate decarboxylase	26
1.11.2.1.3. Acetohydroxyacid synthase	26
1.11.2.1.4. Pyruvate decarboxylase	27
1.11.2.2. Second step: oxidoreduction by alcohol dehydrogenases	27
1.11.2.2.1. Carbonyl reductase from <i>Candida parapsilosis</i>	27
1.11.2.2.2. ADH from <i>Flavobacterium frigidimaris</i>	28
1.11.2.2.3. ADH from horse liver	28
1.11.2.2.4. ADH from <i>Lactobacillus brevis</i>	29
1.11.2.2.5. ADH from <i>Ralstonia</i> sp.	29
1.11.2.2.6. ADH from <i>Sphingobium yanoikuyae</i>	29
1.11.2.2.7. ADH from <i>Thermoanaerobacter brockii</i>	30
1.11.2.2.8. ADH from <i>Thermoanaerobacter</i> sp.	30
1.11.2.2.9. ADH from <i>Thermus</i> sp.	31
1.12. Synthetic cascade reactions	31
1.13. Reaction/Process engineering	33

<b>2. PUBLICATIONS</b>	<b>36</b>
<b>Publication I</b>	<b>37</b>
Stereoselective synthesis of bulky 1,2-diols with alcohol dehydrogenases	
<b>Publication II</b>	<b>55</b>
Biochemical characterization of an alcohol dehydrogenase from <i>Ralstonia</i> sp.	
<b>Publication III</b>	<b>79</b>
Stereoselective synthesis of 1,2-diols with synthetic enzyme cascades including <i>in situ</i> cofactor regeneration and co-product recycling	
<b>Publication IV</b>	<b>101</b>
Structures of alcohol dehydrogenases from <i>Ralstonia</i> and <i>Sphingobium</i> spp. reveal the molecular basis for their recognition of 'bulky-bulky' ketones	
 <b>3. DISCUSSION</b>	 <b>119</b>
3.1. Overview of publications	119
3.2. Alcohol dehydrogenases as versatile catalysts	121
3.3. Stereoselectivity of ADHs	125
3.4. Biochemical characterisation of ADH from <i>Ralstonia</i> sp.	128
3.4.1. Purification and storage stability	128
3.4.2. Effect of salts	129
3.4.3. Determination of the native molecular weight of RADH	130
3.4.4. pH- and temperature optima	130
3.4.5. Substrate range for oxidation and reduction	131
3.4.6. Steady-state kinetic parameters	131
3.4.7. Activity in organic solvents	133
3.5. Preparations to crystallise RADH	134
3.5.1. Cloning RADH into a vector with cleavable tag	134
3.5.2. Expression and purification of His-RADH	134
3.5.3. Crystallisation and structure analysis of RADH	136
3.6. Reaction engineering	139
3.6.1. Optimisation of the cofactor regeneration system	139
3.6.1.1. Substrate-coupled approach	140
3.6.1.2. Enzyme-coupled approach	140
3.6.2. Synthetic cascade reaction	141
3.6.2.1. Cascade reaction using substrate-coupled cofactor regeneration	141
3.6.2.2. Cascade reaction using enzyme-coupled cofactor regeneration	145

3.6.2.3. Comparison of cascade reactions using the substrate- and enzyme coupled approach	146
3.6.2.4. Further cascade reactions	146
<b>4. CONCLUSIONS AND FUTURE PERSPECTIVES</b>	<b>147</b>
<b>5. APPENDIX</b>	<b>149</b>
5.1. DNA sequence of RADH (without His-tag)	150
5.2. Protein sequence of RADH (without His-tag)	150
5.3. Primers for RADH subcloning	151
5.4. DNA sequence of His-RADH	151
5.5. Protein sequence of His-RADH	151
5.6. Protein sequence of His-RADH: after His-tag cleavage	152
5.7. General procedure for subcloning	152
5.8. Thermocycler program for LIC-cloning	153
5.9. Protocol for His-RADH purification using IMAC	153
5.10. DNA sequence of strep-SADH	154
5.11. Protein sequence of strep-SADH	155
<b>6. REFERENCES</b>	<b>156</b>

# List of abbreviations

(1 <i>R</i> ,2 <i>R</i> )-diol	(1 <i>R</i> ,2 <i>R</i> )-1-phenylpropane-1,2-diol
(1 <i>R</i> ,2 <i>S</i> )-diol	(1 <i>R</i> ,2 <i>S</i> )-1-phenylpropane-1,2-diol
(1 <i>S</i> ,2 <i>R</i> )-diol	(1 <i>S</i> ,2 <i>R</i> )-1-phenylpropane-1,2-diol
(1 <i>S</i> ,2 <i>S</i> )-diol	(1 <i>S</i> ,2 <i>S</i> )-1-phenylpropane-1,2-diol
2-HPP	2-hydroxypropiophenone, 2-hydroxy-1-phenylpropan-1-one
ADH	alcohol dehydrogenase
ADHT	alcohol dehydrogenase from <i>Thermoanaerobacter</i> sp.
AHAS-I	isoenzyme I of acetohydroxyacid synthase from <i>Escherichia coli</i>
Arg	arginine
Asn	asparagine
Asp	aspartic acid
ATP	adenosine triphosphate
BAL	benzaldehyde lyase from <i>Pseudomonas fluorescens</i>
BFD	benzoylformate decarboxylase from <i>Pseudomonas putida</i>
CPCR	carbonyl reductase from <i>Candida parapsilosis</i>
Cys	cysteine
<i>de</i>	diastereomeric excess
dNTP	deoxynucleoside triphosphate
DMF	<i>N,N</i> -dimethylformamide
DMSO	dimethyl sulfoxide
<i>dr</i>	diastereomeric ratio
<i>ee</i>	enantiomeric excess
EA	ethyl acetate
EC	Enzyme Commission
EMA	European Medicines Agency
EPA	United States Environmental Protection Agency
ExPASy	Expert Protein Analysis System (Bioinformatics resource portal)
FAD	flavin adenine dinucleotide
FADH	alcohol dehydrogenase from <i>Flavobacterium frigidimaris</i>
FDA	United States Food and Drugs Administration
FOR	forward primer
Glu	glutamic acid
His	histidine
His-RADH	His-tagged alcohol dehydrogenase from <i>Ralstonia</i> sp. (fusion protein)
HLADH	Horse liver alcohol dehydrogenase

HRV 3C	3C protease from human rhinovirus type 14
IMAC	immobilised metal ion affinity chromatography
IPTG	isopropyl- $\beta$ -D-1-thiogalactopyranoside
KdcA	$\alpha$ -keto acid decarboxylase from <i>Lactococcus lactis</i>
LBADH	alcohol dehydrogenase from <i>Lactobacillus brevis</i>
LIC	ligation independent cloning
MeCN	acetonitrile
MenD	2-succinyl-5-enolpyruvyl-6-hydroxy-3-cyclohexadiene-1-carboxylate synthase from <i>Escherichia coli</i>
MCS	multiple cloning site
MDR	medium-chain dehydrogenase/reductase
MTBE	methyl <i>tert</i> -butyl ether
MTHF	2-methyltetrahydrofuran
n.a.	not available
NAD <sup>+</sup>	oxidised form of nicotinamide adenine dinucleotide
NADP <sup>+</sup>	oxidised form of nicotinamide adenine dinucleotide phosphate
NADH	reduced form of nicotinamide adenine dinucleotide
NADPH	reduced form of nicotinamide adenine dinucleotide phosphate
n.d.	not determined
Ni-NTA	nitrilotriacetic acid chelated with Ni <sup>2+</sup> ions
PAC	phenylacetylcarbinol, 1-hydroxy-1-phenylpropan-1-one
PCR	polymerase chain reaction
PEG	polyethylene glycol
PDC	pyruvate decarboxylase
PQQ	pyrroloquinoline quinone
<i>rac</i>	racemic
RADH	alcohol dehydrogenase from <i>Ralstonia</i> sp.
REV	reverse primer
SADH	alcohol dehydrogenase from <i>Sphingobium yanoikuyae</i>
SDR	short-chain dehydrogenase/reductase
SEC	size exclusion chromatography
strep-	streptavidin tag
TADH	alcohol dehydrogenase from <i>Thermus</i> sp. ATN1
TBADH	alcohol dehydrogenase from <i>Thermoanaerobacter brockii</i>
TEA	triethanolamine, tris-(2-hydroxyethyl)amine
ThDP	thiamine diphosphate
THF	tetrahydrofuran
TR1	transition state 1
TR2	transition state 2
TRIS	2-amino-2-hydroxymethylpropane-1,3-diol
UV	ultraviolet

# I Introduction

---



## 1.1 Concept of Green Chemistry

In order to maintain wealth, health and social justice alternative ways for the production of goods and energy supply need to be established to replace fossil fuel based feed stocks. Industrial (white) biotechnology is a key element and cutting-edge technology for the vision of a bio-based economy. Strongly connected to the policy of bio-based economy is the concept of *Green Chemistry*, which is defined as “design of chemical products and processes to reduce or eliminate the use and generation of hazardous substances” (Anastas and Warner 1998; Anastas and Williamson 1996; Horvath and Anastas 2007).

The concept of *Green Chemistry* consists of 12 principles, which were originally published in 1998 by Paul Anastas and John Warner, agents of the United States Environmental Protection Agency (EPA). These rules give a kind of roadmap for chemists how to implement green chemistry in chemical processes (Anastas and Warner 1998; Anastas and Williamson 1996; Horvath and Anastas 2007). They include:

- **PREVENTION** – prevention of waste production instead of remediation;
- **HIGH ATOM ECONOMY** – design of synthetic methods to maximise incorporation of all used materials in the overall process;
- **LESS HAZARDOUS CHEMICAL SYNTHESSES** – design of synthetic methods to minimise toxicity to human health and the environment;
- **SAFER CHEMICALS** – design of chemical products to affect their desired function and simultaneously minimise their toxicity;
- **SAFER SOLVENTS AND AUXILIARIES** – if possible, minimisation of the use of auxiliaries substances; if impossible – auxiliaries should be made benign;
- **HIGH ENERGY EFFICIENCY** – reduction of energy requirements of the overall process; if possible, mild conditions (ambient temperature and pressure) should be used;
- **RENEWABLE FEEDSTOCKS** – renewable raw materials or feedstock should be applied whenever it is practicable;
- **REDUCED DERIVATISATION** – reduction of unnecessary derivatisation steps, which can produce additional waste;
- **CATALYSIS** – catalytic amounts are favoured over stoichiometric reagents;
- **DEGRADABLE COMPOUNDS** – design of chemical products that break down into innocuous products and do not persist in the environment;

- **REAL-TIME ANALYSIS FOR POLLUTION PREVENTION** – development of analytical methodologies for real-time, in-process monitoring and control prior to formation of hazardous substances;
- **INHERENTLY SAFER CHEMISTRY FOR ACCIDENT PREVENTION** – selection of substances and their formulation used in a chemical process in order to minimise the potential for chemical accidents, including releases, explosions and fires.

Recently, a modified generalisation of the 12 rules of *Green Chemistry* was summarised in one word, the acronym *PRODUCTIVELY* (Tang et al. 2005) (see below).

<b>P</b>	– prevent waste
<b>R</b>	– renewable materials
<b>O</b>	– omit derivatisation steps
<b>D</b>	– degradable chemical products
<b>U</b>	– use of safe synthetic methods
<b>C</b>	– catalytic reagents
<b>T</b>	– temperature, pressure ambient
<b>I</b>	– in-process monitoring
<b>V</b>	– very few auxiliary substrates
<b>E</b>	– E-factor, maximise feed in product
<b>L</b>	– low toxicity of chemical products
<b>Y</b>	– yes, it is safe

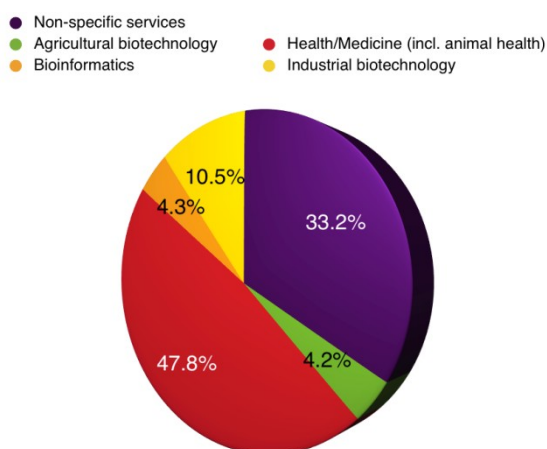
In the new *PRODUCTIVELY* concept the order of some rules was changed and some of the principles were combined in one point. The simplified approach allows rapid understanding of the idea of *Green Chemistry*.

## 1.2 Industrial biotechnology

All known biotechnological processes depend on enzymes – either in resting or living whole-cell systems or isolated biocatalysts (Höfer et al. 2009). These biological systems are implemented in the industrial biotechnology (also known in Europe as white biotechnology) for the manufacture of valuable products, improvement of industrial chemical processes, production of alternative energy (or “bioenergy”) and biomaterials. Furthermore, biotechnological processes are commonly used for the production of enzymes for textile, cosmetics, pharmaceuticals and for food-, pulp- and paper industry (Kirk et al. 2002; Kjellin and Johansson 2010; Sabale and Rane 2012; Torres et al. 2012; Vellard 2003). In 2012 in Germany 10.5% of all biotechnological companies were classified with focus on industrial (white) biotechnology (Figure 1) (Ding et al. 2012).

Biocatalysis, in which natural/biological catalysts are employed for the synthesis of organic compounds, is a key technology according to the *Green Chemistry* principles (see paragraph 1.1). Biocatalysis opens access to sustainable processes *via*

production of highly valuable products (e.g. chemicals, materials and fuels) from renewable resources by simultaneous reduction of energy consumption and waste production.



**Figure 1.** Main activities of German biotechnology companies (only one classification per company) (Ding et al. 2012).

Impressively, with biocatalysis almost every kind of chemical reaction seems to be accessible (Faber 2011). As mentioned above biocatalytical reactions can be conducted by isolated enzymes or with whole-cells. Both approaches have their advantages and disadvantages (Table 1). The major advantage of isolated cells is a lack of side reactions, which frequently occurs in whole-cell catalysis. On the other side, whole-cell biocatalysis does not require additional cofactor regeneration systems that have to be developed for every single reaction catalysed with isolated enzymes. Depending on the requirements of the final product, isolated enzymes as well as whole-cells find broad industrial applications, but (partially) purified enzymes are predominantly implemented. Processes with isolated enzymes are established for food and textiles processing, and they are also used as supplements for the production of feed and detergents, whereas whole cell systems are generally employed in the field of special chemicals providing a broad range of methods and processes (Bommarius and Riebel 2004; Höfer et al. 2009).

In spite of the broad possibilities of enzyme-catalysed processes, biocatalysis and biotransformations are still often only the second choice in fine chemical industry (Meyer et al. 2013). This is caused by various factors; among them are e.g. substrate load limitations (e.g. poor substrate solubilities in aqueous systems) and sometimes low conversions (Table 2). Only if the requirements mentioned in Table 2 are fulfilled or no alternative chemical processes are available, biocatalysis is implemented nowadays. But the number of processes is continuously increasing (Meyer et al. 2013).

**Table 1.** Advantages and disadvantages of isolated enzymes and whole cells as biocatalysts (Faber 2011).

Biocatalyst	Form	Advantages	Disadvantages
Isolated enzymes	Any	Simple apparatus, simple workup, better productivity due to a higher concentration tolerance	Cofactor recycling necessary, limited enzyme stabilities
	Dissolved in water	High enzyme activities	Side reaction possible, low solubility of hydrophobic compounds, workup requires extraction
	Suspended in organic solvents	Easy to perform, easy workup, hydrophobic compounds are soluble, easy enzyme recovery	Reduced activities and stabilities
	Immobilised	Easy enzyme recovery	Loss of activity during immobilisation
Whole cells	Any	No additional cofactor recycling system necessary, no enzyme purification required	Expensive equipment, tedious workup due to large volumes, low productivity due to lower concentration tolerance, side reactions likely due to uncontrolled metabolism
	Growing culture	Higher activities	Large biomass, enhanced metabolism, more by-products, process control difficult
	Resting cells	Workup easier, reduced metabolism, fewer by-products	Lower activities
	Immobilised cells	Cell reuse possible	Lower activities

**Table 2.** Requirements for biotransformations in large scale (Hollmann et al. 2011; Huisman et al. 2010).

Parameter	Value
Substrate concentration	> 100 g L <sup>-1</sup>
Conversion	> 95% in 24 h
Stereoselectivity	> 99.5% <i>ee</i>
Substrate-to-enzyme ratio	> 50 (kg kg <sup>-1</sup> )
Cofactor concentration	< 0.5 g L <sup>-1</sup> (< 0.5 mM)

### 1.3 Enzymes in biocatalysis

The application of biocatalysts can have many advantages, where homogeneous and heterogeneous catalysis in organic chemistry fails. Among them are the following features:

- **ENZYMES ARE OFTEN VERY EFFICIENT AND RAPID.** Enzymes catalyse reactions up to 10<sup>8</sup>-10<sup>10</sup>-fold faster in comparison to non-catalysed reactions (Menger 1993; Wolfenden 2011; Wolfenden and Snider 2001; Zechel and Withers 2000). As an outcome, chemical reactions require 0.5-1 mol% of catalysts, whereas most of enzymatic reactions are conducted with 10<sup>-3</sup>-10<sup>-4</sup> mol% (500-10 000-fold less) (Faber 2011).

- **ENZYMES ARE ENVIRONMENTALLY FRIENDLY.** In contrast to chemical catalysts (e.g. heavy metals or hazardous and toxic catalysts), enzymes are eco-friendly, since they are biodegradable.
- **ENZYMES WORK UNDER MILD CONDITIONS.** The largest number of enzymes works under mild conditions regarding pH-value (between pH 5-8) and temperature (20-40 °C). There are some exceptions, where enzymes are working under unconventional conditions (extremely high/low temperatures and pHs), which are typical for enzymes isolated from extremophile microorganisms. For instance, for an alcohol dehydrogenase from *Flavobacterium frigidimaris* the temperature optimum was determined to be 70 °C, moreover the enzyme is stable at high temperatures (half-life: 50 minutes, 60°C) (Kazuoka et al. 2007). Other examples are glucoamylases isolated from *Picrophilus oshimae*, *Picrophilus torridus* and *Thermoplasma acidophilum*. These enzymes are able to catalyse reactions under harsh conditions like a pH-optimum of 2 and a temperature optimum of 90 °C (half-life: 20 hours, 90 °C for *Picrophilus oshimae* and 24 hours, 90 °C for *Picrophilus torridus* and *Thermoplasma acidophilum*) (Serour and Antranikian 2002). Enzymatic reactions under mild conditions minimise difficulties with isomerisation, epimerisation, racemisation, rearrangement, decomposition, protection/deprotection steps and other unwanted side reactions which are very common in chemical reactions (Lin et al. 2011).
- **ENZYMES CAN BE COMBINED, E.G. IN CASCADES.** Since most of enzymes are capable to catalyse reactions under mild conditions, which for a number of enzymes are similar, there is a possibility of combining several catalytic steps in one reaction vessel yielding valuable product. In addition, enzymes have been successfully combined with chemical reactions for the production of important chiral synthons (Borchert et al. 2012; Gauchot et al. 2010, Husain et al. 2011).
- **ENZYMES ARE NOT LIMITED TO THEIR NATURAL REACTION.** A number of enzymes are known to accept a broad substrate range, which is not limited only to its known natural set of substrates. Further, some enzymes catalyse more than one type of reaction. These combined features are defined as enzyme promiscuity. Enzyme promiscuity can be classified into:
  - **CONDITION PROMISCUITY** – where the enzyme is able to catalyse reactions under various conditions which are different from natural conditions, e.g. anhydrous media, higher temperatures or pHs;
  - **SUBSTRATE PROMISCUITY** – where enzymes show a broader substrate range compared to the physiologically predominantly converted substrate in the natural organisms;

- **CATALYTIC PROMISCUITY** – where enzymes clearly show different transition states during the reaction cycle. Here two different catalytic promiscuities can be distinguished:
  - **ACCIDENTAL** – where a side reaction is catalysed by the wild-enzyme;
  - **INDUCED** – a new reaction is established by one or several mutations rerouting the reaction catalysed of the wild-enzyme (Hult and Berglund 2007).

Aforementioned advantages of enzymes are very important, but one of the most crucial features of enzymes is that they catalyse chemical reactions highly stereoselectively. Three types of selectivity can be distinguished:

- **CHEMOSELECTIVITY** – defined as “**which** functional group will react”. In detail: a reaction is performed by acting specifically on only one functional group in the presence of others. In chemistry usual functional groups that should not be transformed, have to be protected;
- **REGIOSELECTIVITY** – defined as “**where** functional group will react”. Enzymes are able to distinguish differences between functional groups, which are identical but located in various positions;
- **STERESELECTIVITY** – means “which stereoisomer reacts or from which site a prochiral compound is attacked”. In detail: a reaction is catalysed stereoselectively, when one stereoisomer is preferentially formed.

#### 1.4 Classification of enzymes

Enzymes are classified by the *Enzyme Commission* that categorised all enzymes into six main groups depending on the reaction they catalyse (Table 3).

Each enzyme in the classification has its own number, represented as follows:

#### **EC A.B.C.D.**

where:

A – class of enzyme (one of the six enzyme classes of Table 3)

B – enzyme subclass (e.g. for oxidoreductases, it displays the type of electron donors which are oxidised)

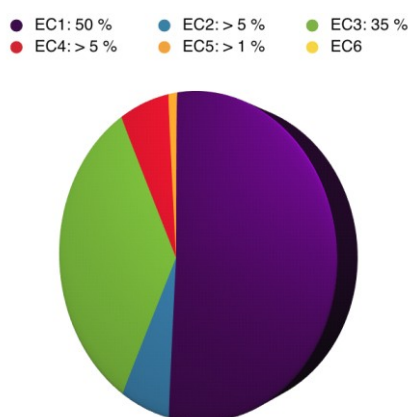
C – enzyme sub-subclass (e.g. for oxidoreductases, it displays for each type of electron donor the type of electron acceptor involved)

D – enzyme sub-sub-subclass (running number, which is sometimes required to characterise new subdivisions in a sub-subclass).

**Table 3.** Enzyme classification according to the *Enzyme Commission* (EC).

EC number	Enzyme class	Catalysed reaction
1	Oxidoreductases	Oxidation/reduction reactions, e.g. oxidoreductases
2	Transferases	Transfer of functional group from one molecule to another, e.g. transaminases
3	Hydrolases	Hydrolysis of various bonds, e.g. lipases
4	Lyases	Synthesis or cleavage of covalent bonds (without ATP consumption), e.g. decarboxylases
5	Isomerases	Isomerisation within a single molecule, e.g. isomerases
6	Ligases	Connection of two molecules by consumption of ATP, e.g. synthetases

Currently, all enzyme classes, despite the ligases, are industrially applied in the pharma-, food industry-, agrochemicals-, cosmetics- and polymer- sector and others. According to their application enzymes distribute as follows (Meyer et al. 2013) (Figure 1):



**Figure 2.** Distribution of enzyme classes in industrial applications for the production of blockbusters (small molecule pharmaceuticals) (Meyer et al. 2013).

According to the Figure 1 oxidoreductases (EC 1, 50%) and hydrolases (EC 3, 35%) are the most frequently used enzyme classes for the production of fine chemicals (Meyer et al. 2013).

### 1.5 Oxidoreductases classification

Oxidoreductases can be divided in 23 subgroups depending on the catalysed reaction (Boyce and Tipton 2005) (Table 4).

Of highest interest in applied biocatalysis are oxidoreductases from the subgroups of dehydrogenases (EC 1.1) and oxygenases (EC 1.13 and EC 1.14).

**Table 4.** Classification of oxidoreductases according to their catalysed reaction (Boyce and Tipton 2005).

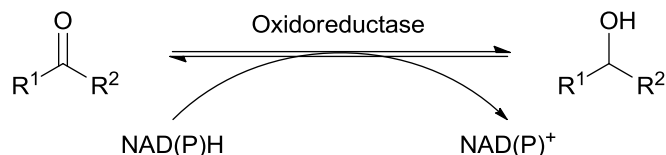
No.	Enzyme subclass	Catalysed reaction
1	EC 1.1	Acting on the CH–OH group of donors
2	EC 1.2	Acting on the aldehyde or oxo group of donors
3	EC 1.3	Acting on the CH–CH group of donors
4	EC 1.4	Acting on the CH–NH <sub>2</sub> group of donors
5	EC 1.5	Acting on the CH–NH group of donors
6	EC 1.6	Acting on NADH or NADPH
7	EC 1.7	Acting on other nitrogenous compounds as donors
8	EC 1.8	Acting on sulfur group of donors
9	EC 1.9	Acting on a heme group of donors
10	EC 1.10	Acting on diphenols and related compounds as donors
11	EC 1.11	Acting on peroxide as acceptor
12	EC 1.12	Acting on hydrogen as donor
13	EC 1.13	Acting on single donors with O <sub>2</sub> as oxidant and incorporation of paired oxygen into the substrate (oxygenases). The oxygen incorporated needs not to be derived from O <sub>2</sub> .
14	EC 1.14	Acting on paired oxygen donors with O <sub>2</sub> as oxidant and incorporation or reduction of oxygen. The oxygen incorporated needs not to be derived from O <sub>2</sub> .
15	EC 1.15	Acting on superoxide as acceptor
16	EC 1.16	Oxidising metal ions
17	EC 1.17	Acting on CH or CH <sub>2</sub> groups
18	EC 1.18	Acting on iron-sulfur proteins as donor
19	EC 1.19	Acting on reduced flavodoxin as donor
20	EC 1.20	Acting on phosphorus or arsenic as donors
21	EC 1.21	Acting on X–H and Y–H to form an X–Y bond
22	EC 1.22	Acting on halogens in donors
23	EC 1.97	Other oxidoreductases

Dehydrogenases (e.g. alcohol dehydrogenases, EC 1.1.1.1) are implemented for asymmetric reduction of ketones, aldehydes and other derivatives with carbonyl groups and for oxidation of alcohols to the corresponding aldehydes or ketones. Oxygenases (e.g. Baeyer-Villiger monooxygenases) are frequently used for monooxygenations, transformations of ribonucleotides, stereospecific epoxidations, and oxidation of esters and lactones (Meyer et al. 2013).

## 1.6 Alcohol dehydrogenases/Ketoreductases

Alcohol dehydrogenases (ADHs) belong to the oxidoreductases class (Table 3). They catalyse reversible oxidoreduction reactions (Figure 2). The reaction is catalysed by the transfer of reducing equivalents between donor and acceptor molecules. The reducing equivalents are defined electrons (e.g. produced by artificial electron transferring agents or electrodes) or hydride ions (de Torres et al. 2012; Kim and Yoo 2009).



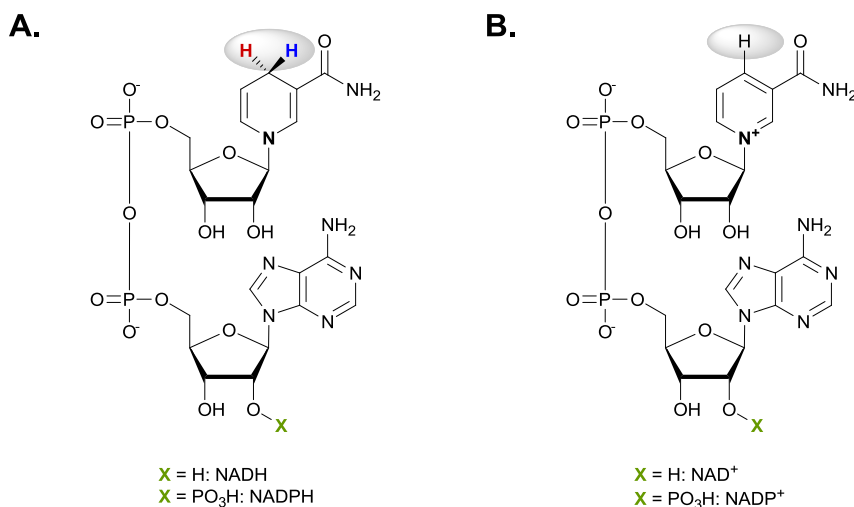


**Figure 3.** General reaction scheme of oxidoreductases.

For instance, reduction of the prochiral keto group (acceptor) occurs by the transfer of hydride ion from the reduced cofactor (donor) to the carbonyl group yielding an alcohol (Figure 3). The reaction in general is highly stereospecific (Patel 2000). Depending on the reaction conditions (pH-value) reduction or oxidation is favoured yielding alcohols or ketones, respectively.

### 1.7 Cofactor regeneration

ADHs require nicotinamide adenine dinucleotide (phosphate) cofactors (NAD(H) or (NADP(H))) for their activity (Figure 4). Since these cofactors are expensive (see Table 5), it is uneconomic to apply them in equimolar concentration. To overcome cost limitations in large-scale applications cofactor regeneration is essential.



**Figure 4.** Nicotinamide adenine dinucleotide (phosphate) cofactor. **A.** Reduced form, **B.** Oxidised form.

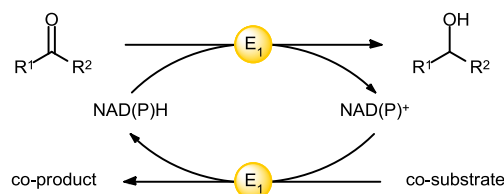
**Table 5.** Cost of nicotinamide adenine dinucleotide cofactors (Biomol GmbH, Hamburg, Germany; state: May 2013).

Cofactor	Price EUR/mol
NAD <sup>+</sup>	13 260
NADH	45 780
NADP <sup>+</sup>	97 588
NADPH	414 001

According to the classification of Chenault and Whitesides (Chenault and Whitesides 1987) there are five general methods for cofactor regeneration: biological, chemical, electrochemical, photochemical and enzymatic cofactor regenerations. The latter is the currently preferred one in industrial applications (Chenault and Whitesides 1987; Liu and Wang 2007; Wichmann and Vasic-Racki 2005) and can be further classified into substrate-coupled and enzyme-coupled approaches.

### 1.7.1 Substrate-coupled approach

In the substrate-coupled approach only one enzyme for the main reaction and the regeneration reaction (Figure 5) is required. Often ethanol or 2-propanol are used as co-substrates for the regeneration reaction. During the recycling reaction acetaldehyde or acetone, respectively, are formed.



**Figure 5.** Substrate-coupled cofactor regeneration.

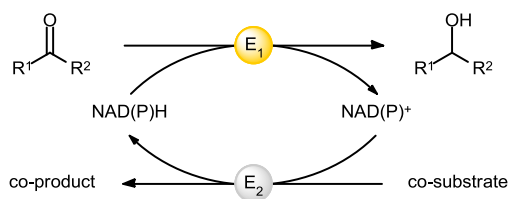
Some biocatalytical processes employing substrate-coupled cofactor regeneration require removal of the co-product formed, since it may affect the activity and stability of the enzyme when present in high concentrations (Goldberg et al. 2007). The reversibility of the reduction reaction should be also considered. This reversibility can occur when pH optima for the reduction and oxidation reaction are close to each other or even overlap. Then overall conversion depends on the equilibrium constant. High conversions can be achieved by a combination of high co-substrate concentrations and smart co-product removal (Stillger et al. 2002).

There are a number of lab-scale and industrial-scale applications for the substrate-coupled regeneration approach using alcohol dehydrogenases from *Thermoanaerobacter Brockii* (TBADH) (Bastos et al. 1999; Bastos et al. 2002), *Candida parapsilosis* (Stillger et al. 2002), horse liver (Virto et al. 1995), and *Lactobacillus brevis* (Daußmann et al. 2006a; Daußmann et al. 2006b).

### 1.7.2 Enzyme-coupled approach

For the enzyme-coupled approach the main reaction is catalysed by one enzyme and the regeneration reaction is catalysed by another enzyme (Figure 6). Currently various dehydrogenases are commonly applied. Among them are: glucose

dehydrogenase from *Bacillus cereus* (Wong and Drueckhammer 1985; Wong et al. 1985) and *Bacillus subtilis* (Hilt et al. 1991). During this reaction glucose (co-substrate) is oxidised to gluconic acid (co-product), which makes pH control necessary. Other well established regeneration enzymes are formate dehydrogenases from *Candida boidinii* (Peters et al. 1993b; Zelinski et al. 1999) and *Pseudomonas* sp. (Karzanov et al. 1989; Müller et al. 1978; Tishkov et al. 1993). Here formate is oxidised to carbon dioxide as a co-product, which can be easily removed from the reaction vessel by evaporation.



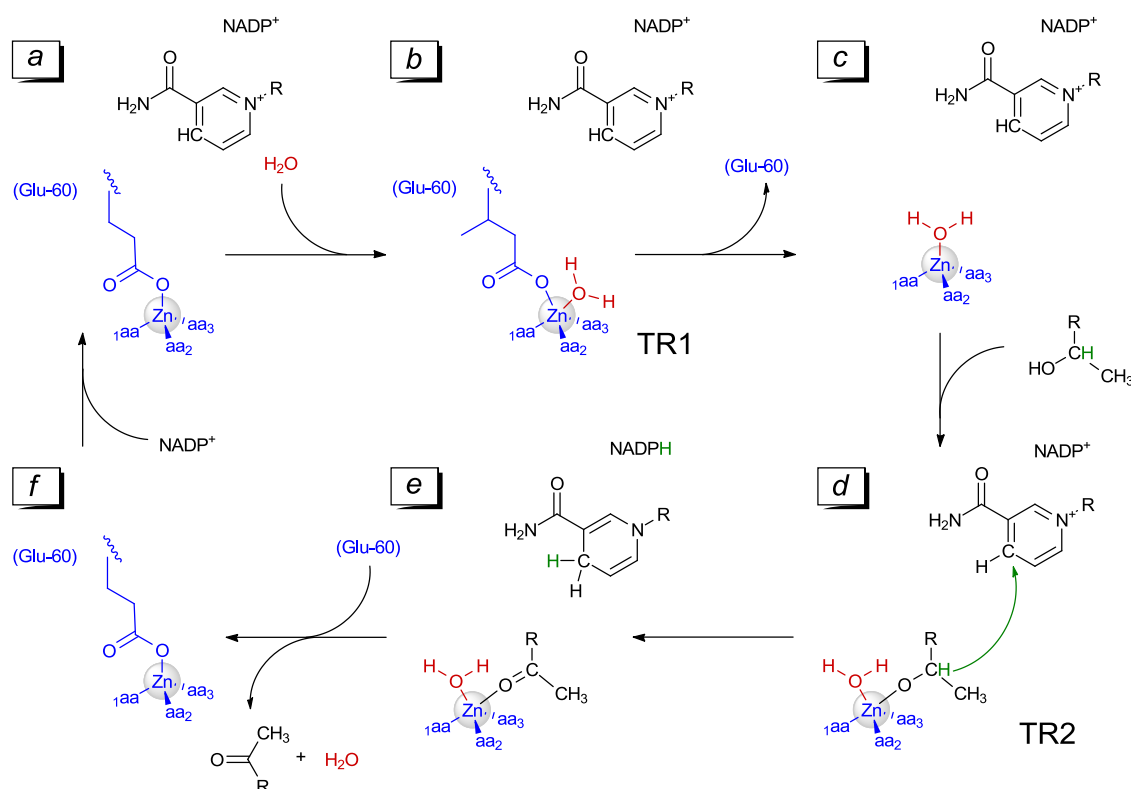
**Figure 6.** Enzyme-coupled cofactor regeneration.

### 1.8 Mechanism of alcohol dehydrogenases

For Zn-dependent alcohol dehydrogenases several catalytic mechanisms based on the mechanism of horse liver alcohol dehydrogenase (HLADH) are proposed (Auld 2001; Dunn et al. 1986). Differences in the suggested mechanism are a consequence of missing time-resolved structural information about intermediate states during catalysis. In addition, the zinc ion is silent in several spectroscopic techniques and therefore knowledge about intermediate states is limited (Kleifeld et al. 2003a).

The mechanism of Zn-dependent alcohol dehydrogenases was solved on the example of oxidation catalysed by the enzyme isolated from *Thermoanaerobacter brockii* (TBADH) (Kleifeld et al. 2003a).

Alcohol dehydrogenase from *Thermoanaerobacter brockii* (TBADH) is a bacterial enzyme that oxidises primary and secondary alcohols to the respective aldehydes and ketones in the presence of  $\text{NADP}^+$ , with primary alcohols being less preferred (Lamed and Zeikus 1981). The tetrameric enzyme with a molecular weight of 37 652 Da per subunit consist of 352 amino acids (Peretz and Burstein 1989). Only one single zinc ion per subunit was discovered, which has a catalytic function (Bogin et al. 1997).



**Figure 7.** Proposed mechanism of the Zn-dependent alcohol dehydrogenase from *Thermoanaerobacter brockii* (TBADH) on the example of the oxidation of secondary alcohols, where aa<sub>1</sub>: Cys-37, aa<sub>2</sub>: His-59, aa<sub>3</sub>: Asp-150. **a**: holoenzyme; the zinc ion remains tetrahedrally coordinated when bound to NADP<sup>+</sup>; **b**: the first transient complex (TR1) represents the coordination of a water molecule before the exchange of Glu-60 residue; **c**: dissociation of the Glu-60 residue results in a tetrahedral zinc ion with a bound water molecule; **d**: binding of the substrate (here alcohol); by formation of alcoholate *via* a hydride transfer the TR2 intermediate is produced; **e**: product formation; **f**: dissociation of product, cofactor and a water molecule and subsequent binding of the Glu-60 residue yield into the initial conformation (according to (Kleinfeld et al. 2003a)).

The tetrahedral coordination sphere of the catalytic zinc ion that directly takes part in the reaction mechanism, is coordinated by Asp-150, His-59, Cys-37, and Glu-60 (Kleinfeld et al. 2003b; Korkhin et al. 1998) (Figure 7A). Glu-60 is strictly conserved in all members of this ADH-family but has no essential influence on TBADH activity, which was confirmed by site-directed mutagenesis studies on this amino acid (Kleinfeld et al. 2003b).

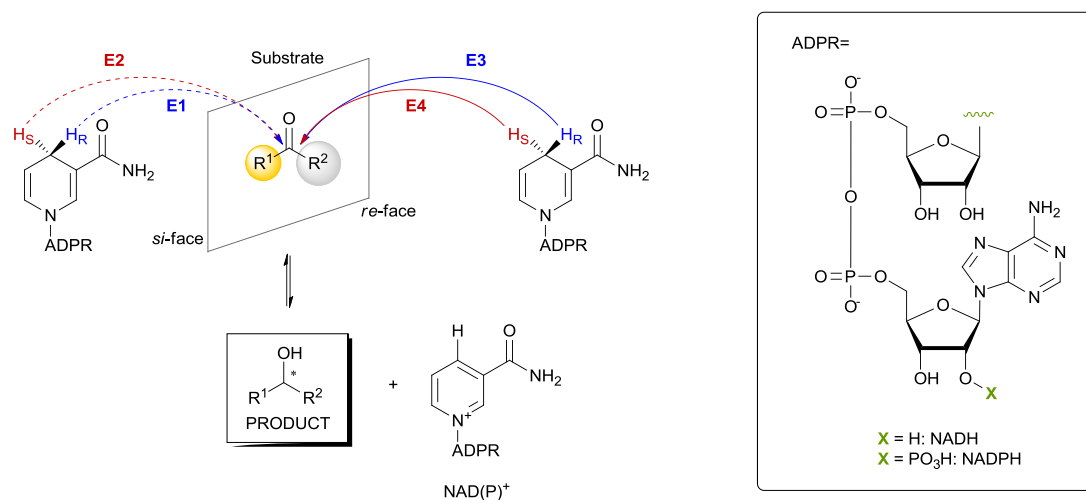
The reaction cycle starts with binding of one water molecule to the zinc ion, forming a pentacoordinated zinc ion (first pentacoordinated intermediate state, transition state TR1) (Figure 7B). Subsequently, the coordinative binding of Glu-60 is released and the tetrahedral coordination state is restored (Figure 7C). It was found that the transition state TR1 has a short life-time, which suggests its role as an intermediate for the state TR2. In the next step the substrate (here: alcohol) is bound to the zinc ion resulting in the formation of the second pentacoordinated transition state of zinc (TR2). Here the reaction between the oxidised cofactor and TR2 occurs by transfer of a hydride ion of the substrate molecule to the cofactor

(Figure 7D), resulting in the formation of the reduced cofactor and the product (here: aldehyde or ketone) that is released (Figure 7E). Finally, the original state is restored by replacing the water molecule in the tetrahedral coordination sphere through Glu-60 (Figure 7F) (Kleifeld et al. 2003a).

Conclusively the oxidation of an alcohol involves a net removal of two hydrogen atoms from the substrate (Figure 7C), first a proton abstraction and second a hydride ion transfer from the substrate to the cofactor.

The reverse reaction, the ADH-catalysed reduction of prochiral aldehydes or ketones, proceeds in four stereochemical patterns (E1-E4) (Figure 8) depending on:

- nucleophilic attack of a hydride ion on the  $sp^2$ -hybridised carbonyl C-atom from the *re*- (E1, E2) or *si*-face (E3, E4). *Re*-face is defined with the carbonyl group oriented upwards, the small substituent ( $R_1$ ) on the left site and large on the right site ( $R_2$ ) (Figure 8);
- the reduced nicotinamide cofactor contains two diastereotropic hydrogens ( $H_S$ , pro-*S* and  $H_R$ , pro-*R*). Consequently, pro-*R* (E1, E3) or pro-*S* (E2, E4) hydride attack of the prochiral substrate may result in products with different stereoselectivity (Figure 8).



**Figure 8.** Hydride transfer from cofactor (NAD(P)H) to carbonyl group. ADPR: adenosine diphosphate ribose; E1-E4: different kinds of enzymes, where E1 and E3 – pro-*R* configuration, E2 and E4 – pro-*S* configuration;  $R^1$ - $R^2$ : substituents, where  $R^1 < R^2$ .

Some known alcohol dehydrogenases can be assigned to one of the four general patterns of determine stereoselectivity (E1-E4). For instance:

- **E1** (pro-*R*/*si*-face): alcohol dehydrogenases from *Pseudomonas* sp. (Bradshaw et al. 1992a) and *Lactobacillus kefir* (Bradshaw et al. 1992b);
- **E2** (pro-*S*/*si*-face): glycerol dehydrogenase from *Geotrichum candidum* (Nakamura et al. 1990; Nakamura et al. 1992; Nakamura et al. 1988),

dihydroxyacetone reductase *Mucor javanicus* (Dutler et al. 1977; Hochuli et al. 1977);

- **E3** (pro-*R*/*re*-face): alcohol dehydrogenases from yeast (Prelog 1964), horse liver (Davies and Jones 1979; Jones 1986; Jones et al. 1976; Lam et al. 1988), *Thermoanaerobacter brockii* (Drueckhammer et al. 1988; Drueckhammer et al. 1987; Keinan et al. 1986a; Keinan et al. 1986b), and *Moraxella* sp. (Velonia et al. 1999);
- **E4** (pro-*S*/*re*-face): is not common among the ADH enzyme family (de Wildeman et al. 2007; Fang et al. 1995).

Most ADHs transfer hydrogen in pro-*R* conformation to the *re*-face (E3 pathway) of the carbonyl group, defined as the Prelog-rule. By contrast, only few ADHs were found that follow the anti-Prelog rule, where the nucleophilic attack occurs from the *si*-face of the carbonyl group (E1 pathway) (Bradshaw et al. 1992a) (Bradshaw et al. 1992b).

## 1.9 Chiral pharmaceuticals

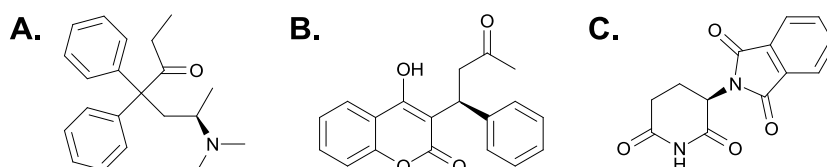
Chirality and stereochemistry are not new concepts in chemistry, although before 1992 there was not large interest in stereoselective syntheses. In 1992 FDA (US Food and Drugs Administration) and EMA (European Medicines Agency) introduced requirements for drug producers to investigate and characterise each enantiomer as well as the racemic mixture of all racemic drugs entering the market (Richards and McCague 1997). FDA and EMA also recommended the redevelopment of registered racemates as single stereoisomers (chiral switch).

Chirality of drugs is of high importance in terms of possible toxic effects. There are several examples, where just one enantiomer is the biologically active one or exhibits the desired effect and the other enantiomer is inactive or causes dangerous side effects or even where interconversion of one enantiomer into the other one occurs. Three examples are: (I) methadone, (II) warfarin and (III) thalidomide.

- **METHADONE** – is a synthetic opioid used for treatment of opioid dependency. The racemic mixture of the drug has some side effects such as risk of cardiac adverse events and sudden death (Krantz et al. 2009a; Krantz et al. 2009b). Opioid activity is found in (*R*)-methadone (therapeutic effects, Figure 9A), whereas (*S*)-methadone exhibits the mentioned lethal effects (Eap et al. 2007). Metabolism of each enantiomer of *rac*-methadone proceeds similar, where the mutual competitive inhibition occurs.
- **WARFARIN** – is a drug available in a racemic mixture, where (*S*)-warfarin has a significantly higher therapeutic potential (Scott 1993). It is an anti-

coagulant agent used for the treatment of thrombosis and thromboembolism. Patients treated with warfarin indicate a wide dosing range in order to place the narrow therapeutic window between overcoagulation and undercoagulation (Scott 1993). (*R*)-warfarin (Figure 9B) is strongly interfering the treatment since it inhibits the metabolism of (*S*)-warfarin.

- **THALIDOMIDE** – was introduced as a racemic mixture in the late 1950s as a nauseant and sedative drug. Later, it was reported that the (*R*)-enantiomer (Figure 9C) is responsible for sedative affects (Eriksson et al. 2000; Hoglund et al. 1998), whereas (*S*)-enantiomer was found to be teratogenic (Blaschke et al. 1979; Heger et al. 1994). Further publications reported that the chiral centre in thalidomide is unstable (Reist et al. 1998) resulting in fast interconversion of (*S*)- and (*R*)-enantiomers in humans (Eriksson et al. 2001). Therefore a treatment with only the (*R*)-enantiomer is still of risk and should be evaluated carefully. Nowadays the drug is still used for treatment of multiple myeloma (Kropff et al. 2012; Palumbo 2010; Wang et al. 2012; Yakoub-Agha et al. 2012), erythema nodosum leprosum (Chen et al. 2010; Joglekar and Levin 2004; Villahermosa et al. 2005) and alleviating symptoms of HIV (Haslett et al. 1999). Additionally, research is ongoing concerning application of thalidomide for the treatment of various kind of cancer (Efsthathiou and Logothetis 2009; Fanelli et al. 2003; Hashimoto et al. 2004; Nguyen et al. 1997; Reck and Gatzemeier 2010; Singhal and Mehta 2001; Zeldis 2005; Zhou et al. 2002).

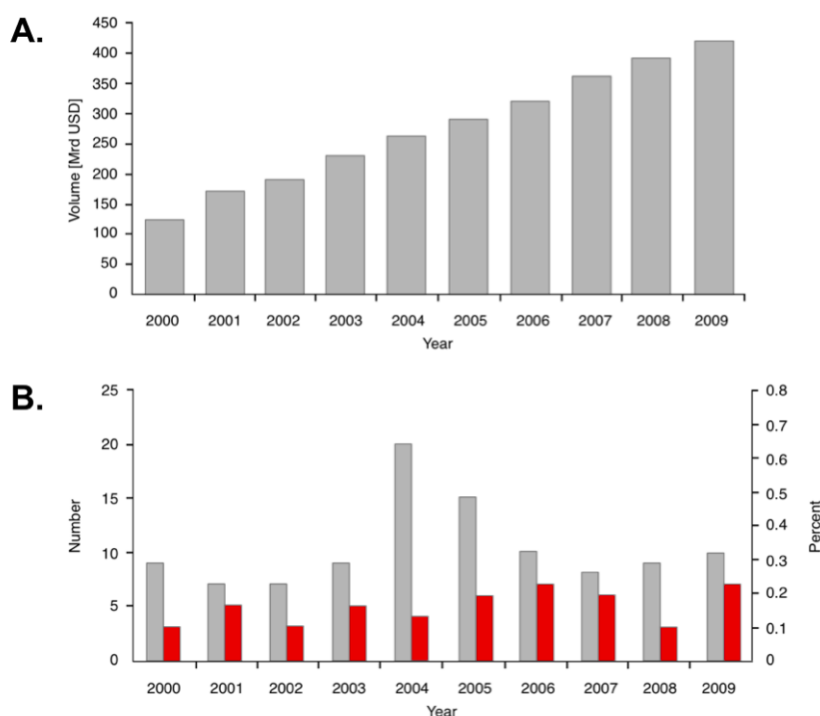


**Figure 9.** (*R*)-enantiomers of chiral pharmaceuticals. A. (*R*)-methadone, B. (*R*)-warfarin, C. (*R*)-thalidomide.

Besides, there are many more similar examples that demonstrate the dangerous effects for health and therewith the importance for stereoselective syntheses. As a consequence of the costly and time consuming test procedure most companies decided to implement new chiral products in optically pure form (Faber and Patel 2000; Margolin 1993), which resulted in an increase of newly developed single-enantiomeric drugs significantly (Figure 10) (Agranat et al. 2002; Chir TU-Berlin 2011).

There are three possible pathways to gain single stereoisomer of desired compounds (Faber 2001; Gadler et al. 2006; Richards and McCague 1997; Turner 2010) (Faber 2011):

- **THE CHIRALITY POOL** – where the desired chiral centre is provided (e.g. isolated from natural sources) and conserved during further catalytic steps;
- **RESOLUTION METHODS** – where racemates are separated into single stereoisomers;
- **ASYMMETRIC SYNTHESIS** – where a single stereoisomer is produced by the introduction of an asymmetry centre into a prochiral (non-chiral) molecule.



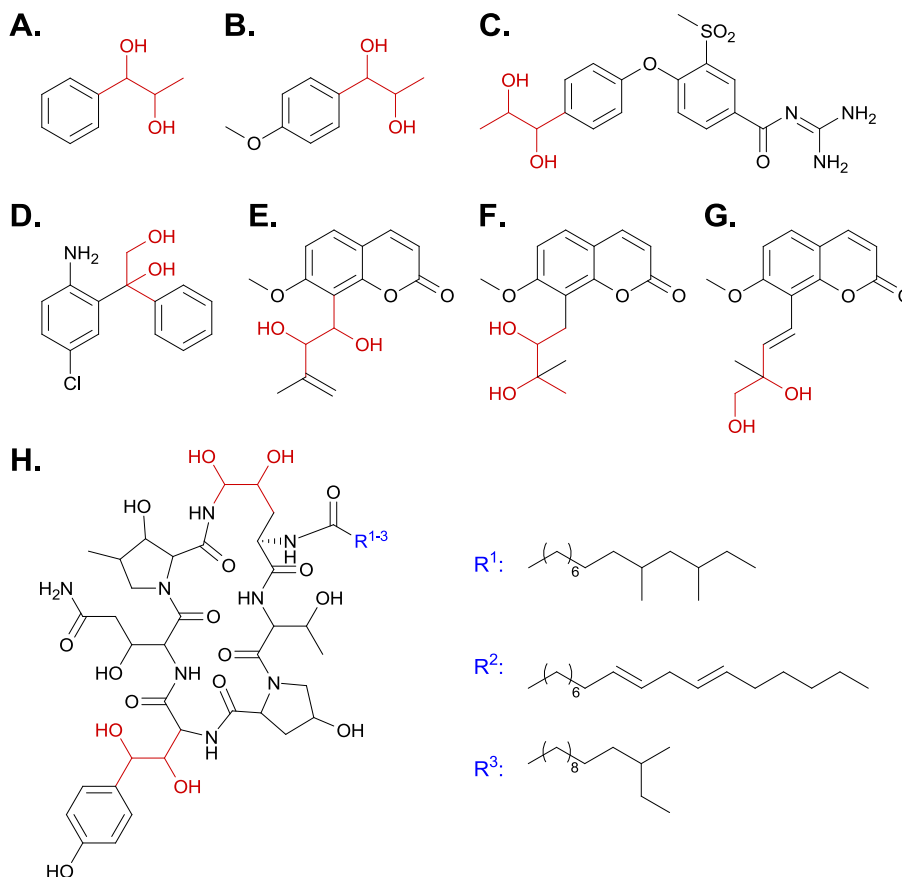
**Figure 10.** **A.** Worldwide sales of chiral pharmaceuticals (2000-2009). **B.** Number of approved drugs with priority status of the top 20 US American pharmaceutical companies (based on their sales, red columns). The efficiency of research of small pharmaceutical companies (based on their research output) of key medicines is much higher than the top 20 (grey columns) (Chir TU-Berlin 2011).

### 1.10 Chiral 1,2-diols as building blocks

Chiral 1,2-diols find broad application as drugs as well as synthons for pharmaceuticals (Figure 11), agrochemicals and chiral catalysts. Currently, chiral 1,2-diols are successfully implemented as medicines for the treatment of neurodegenerative diseases (Figure 11A) (Brown et al. 1998; Brown et al. 2001; Brown and Ren 2002) or show anti-inflammatory, gastroprotectory and anti-sepsis activity (Figure 11B) (Freire et al. 2005; Lee et al. 2003; Song and Son 2003). Further, a wide utilisation of 1,2-diols as building blocks is reported for syntheses of e.g. cardiovascular agents (Figure 11C) (Lang et al. 1994), (*S*)-etifoxine (an



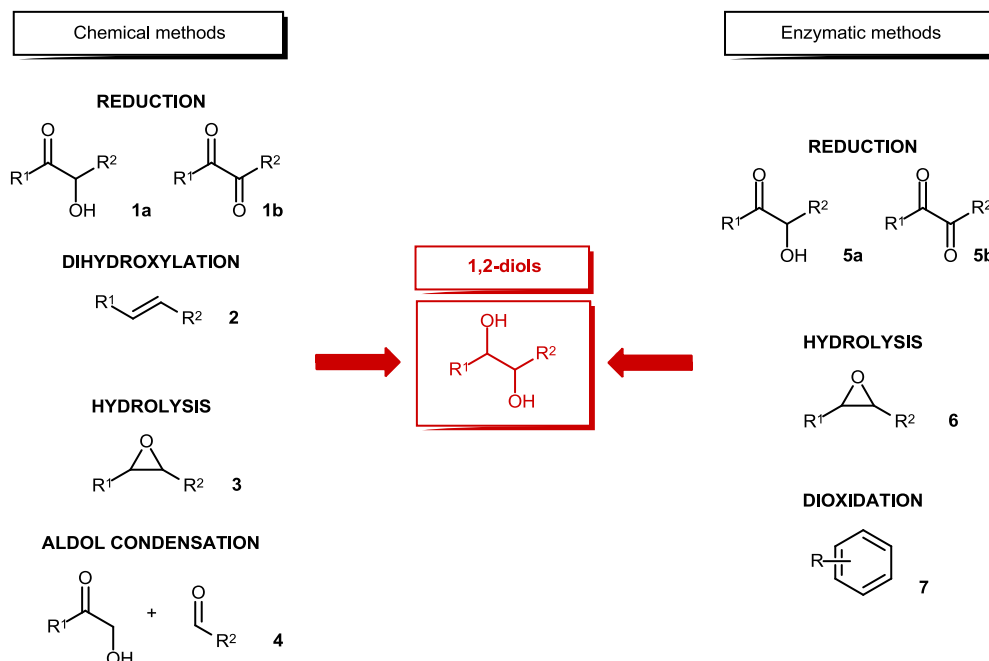
anxiolytic and anti-convulsant drug, Figure 10D) (Putman et al. 2007) and anti-tumor agents (Figure 11E-G) (Ito et al. 1999). The 1,2-diol moiety is also found in some anti-fungal antibiotics from the pneumocandin family, for instance: pneumocandin A<sub>0</sub> (Figure 11H, R<sup>1</sup>), echinocandin B (Figure 10H, R<sup>2</sup>) and mulundocandin (Figure 11H, R<sup>3</sup>).



**Figure 11.** 1,2-Dihydroxy functions are widely spread among pharmaceuticals and in drug synthons. **A.** drug for treatment of neurodegenerative diseases (Brown et al. 1998; Brown et al. 2001; Brown and Ren 2002), **B.** anti-inflammantory, gastroprotector drug with additional anti-septic activity (Freire et al. 2005; Lee et al. 2003; Song and Son 2003), **C.** cardiovascular agents (Lang et al. 1994), **D.** building block for the synthesis of (*S*)-etifoxine (Putman et al. 2007), **E-G.** anti-tumor agent on Epstein-Barr virus (Ito et al. 1999), **H:** anti-fungal drugs of the pneumocandin type: R<sup>1</sup>: pneumocandin A<sub>0</sub>, R<sup>2</sup>: echinocandin B, R<sup>3</sup>: mulundocandin.

## 1.11 Production of 1,2-diols

Production of 1,2-diols can be conducted using chemical or enzymatic methods (Figure 12).



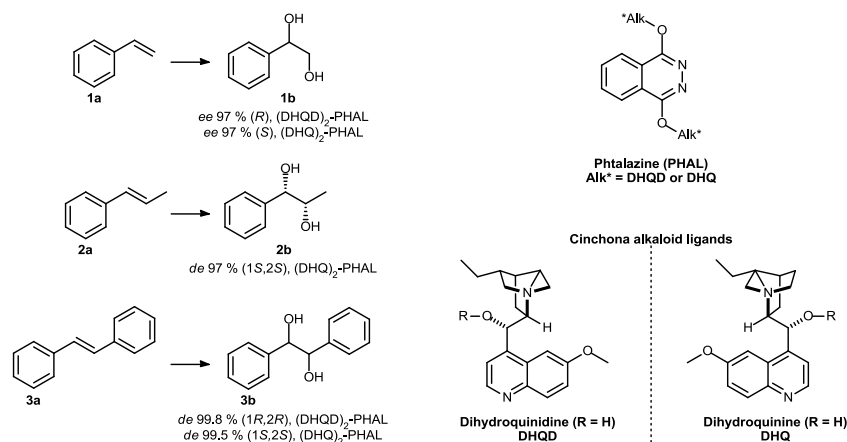
**Figure 12.** Production of 1,2-diols by chemical and enzymatic methods.

## 1.11.1 Chemical methods

There are various chemical methods for the production of 1,2-diols. Among them are: reduction of  $\alpha$ -hydroxy ketones or  $\alpha$ -diketones (Figure 12, **1a,b**) using hydride transfer agents such as  $\text{NaBH}_4$ ,  $\text{LiAlH}_4$  or  $\text{Zn}(\text{BH}_4)_2$  (Johnson and Klein 1979; McMahon et al. 1981; Noyori et al. 1979; Yamada and Koga 1970), Sharpless dihydroxylation of alkenes (Figure 12, **2**) (Sharpless et al. 1992), hydrolysis of epoxides (Figure 12, **3**) (Tokunaga et al. 1997; Wang et al. 2008) or asymmetric aldol condensation (Figure 12, **4**) (Guillena et al. 2006; Notz and List 2000).

The chemical reduction of aliphatic  $\alpha$ -hydroxy ketones (Figure 12, **1a**) to the respective 1,2-diols catalysed by aluminium hydride reagents (such as  $\text{LiAlH}_4$ ,  $\text{AlH}_3$ ,  $[\text{LiAl}(\text{OMe})_3\text{H}]$  and  $[\text{LiAl}(\text{O}-t\text{-Bu})_3\text{H}]$ ) showed only low stereoselectivities (Katzenellenbogen and Bowlus 1973; Bowlus and Katzenellenbogen 1974). Better results were achieved by chelation-controlled reduction with  $\text{Zn}(\text{BH}_4)_2$  resulting mainly in the formation of *anti*-1,2-diols with higher stereoselectivity compared to  $\text{LiAlH}_4$ -catalysed reactions (Nakata et al. 1983). The reactions were shown mainly for the reduction of aliphatic  $\alpha$ -hydroxy ketones and only few examples of araliphatic  $\alpha$ -hydroxy ketones were shown with good yields and moderate

stereoselectivities (Bowlus and Katzenellenbogen 1974; Katzenellenbogen and Bowlus 1973; Nakata et al. 1983).



**Figure 13.** Examples of Sharpless dihydroxylation of olefins with excellent stereoselectivities. Alk\* = Cinchona alkaloid ligands (DHQD or DHQ), PHAL = phtalazine, DHQD = dihydroquinidine, DHQ = dihydroquinine (Kolb et al. 1994)

Most recently a comprehensive investigation of borohydride-catalysed reductions of araliphatic  $\alpha$ -hydroxy ketones was reported by Husain et al. (Husain et al., 2011). They reduced aromatic  $\alpha$ -hydroxy ketones with very good conversion but with moderate stereoselectivity. Whereas excellent diastereoselectivities (formation of *anti*-1,2-diol, *de* > 99%) were obtained in several cases using Zn(BH<sub>4</sub>)<sub>2</sub> (Husain et al. 2011).

An alternative route is the reduction of  $\alpha$ -diketones (Figure 12, **1b**) to the respective 1,2-diols, which was also reported for the production of sterically demanding 1,2-diols (e.g. benzils). Therefore various chiral ruthenium complexes or organocatalyst were employed. Unfortunately, the products could be obtained only as mixtures of *syn*- and *anti*-diastereoisomers (Ikariya and Blacker 2007; Murata et al. 1999).

Another method especially for the production of 1,2-diols, is the Sharpless dihydroxylation of alkenes (Figure 12, **2**). Here application of another dangerous catalyst, namely OsO<sub>4</sub>, is required, which is a very expensive, toxic and reactive catalyst. Reactions can be successfully applied for the hydroxylation of *E*-alkenes gaining *syn*-1,2-diols with good stereoselectivities (up to 99% depending on the substrate) using chiral ligands (Figure 13) (Kolb et al. 1994). For instance, dihydroxylation of styrene (**1a**) yields the respective 1,2-diol (**1b**) with high stereoselectivity of 97% for both, (*R*)- and (*S*)-enantiomers. Similar result were obtained with *trans*-1-phenyl-1-propene (**2a**) yielding the (1*S*,2*S*)-1-phenylpropane-1,2-diol (**2b**). Excellent stereoselectivities of > 99% were achieved for the dihydroxylation of (*E*)-1,2-diphenylethene (**3a**) to (1*R*,2*R*)- and (1*S*,2*S*)-1,2-diphenylethane-1,2-diol (**3b**), respectively (Kolb et al. 1994). In contrast, syntheses of *anti*-1,2-diols are limited by the availability of *Z*-alkenes, which are hardly accessible since respective synthetic methods are less established than for *E*-alkenes.

Moreover, the thermodynamic control favours the lower-in-energy *E*-alkenes (Kolb et al. 1994; Siau et al. 2012). Further, for the synthesis of *anti*-1,2-diols applying Sharpless dihydroxylation, stereoselectivities are generally only moderate (below 90%) (Kolb et al. 1994).

Hydrolysis of epoxides (Figure 12, 3) is another method which also often requires hazardous and toxic catalysts. The reaction proceeds very often under acidic conditions in order to gain vicinal diols. For instance, kinetic resolution of racemic epoxides using water and chiral cobalt-based salen complexes gave high yields and high enantioselectivities (*ee* up to 98%) for the resulting 1,2-diols (Tokunaga et al. 1997). Recently, a modified method of epoxides hydrolysis was reported (Wang et al. 2008), where epoxide ring-opening was catalysed by hot water (60-100 °C) without any addition of catalysts. Furthermore, Wang et al. showed that addition of other nucleophiles such as azides and thiophenol could also effectively open epoxide rings in hot water. Although hot water-promoted hydrolysis of epoxides gives very high yields (up to 99%), only moderate diastereoselectivities were achieved (Wang et al. 2008).

Further, 1,2-diols can be obtained by aldol condensation (Figure 12, 4). A key challenge of the reaction is the simultaneous control of regio-, diastereo- and enantioselectivity when asymmetric ketones are applied. The L-proline-catalysed aldol condensation gives good conversions (up to 95%) and moderate stereoselectivities (*dr* 20:1) (Notz and List 2000). Guillena et al. presented a modified aldol condensation of aldehydes and  $\alpha$ -alkoxyacetone. For the reaction a combination of L-proline with BINAM-prolinamides were used yielding the *anti*-1,2-diol with moderate enantioselectivity (*ee* up to 85%). Highest regio- and diastereoselectivities (*ee* up to 98%) for the *anti*-1,2-stereoisomer were gained when  $\alpha$ -methoxyacetone as a substrate (in DMF at 0 °C) was used (Guillena et al. 2006). Finally, a novel synthetic strategy toward the asymmetric synthesis of vicinal diols bearing a tertiary centre was developed. The novel method involves (I) the dinuclear Mg-catalysed asymmetric addition of ethyl diazoacetate to aldehydes, (II) oxidation of the diazo functionality and (III) diastereoselective alkyl transfer of various organometallics into chiral  $\beta$ -hydroxy- $\alpha$ -ketoesters in order to gain a versatile range of 1,2-diols with high yields (up to 99% depending on the substrate), high diastereoselectivities (*dr* up to > 20:1) and chirality transfer (up to > 99%). Chirality transfer is defined as ratio of the enantioselectivity of the product to the enantioselectivity of the substrate (Trost et al. 2012).

Since chemical syntheses of vicinal diols often are conducted with low stereoselectivities, there is a necessity to separate all stereoisomers, which is not an easy task. The successful separation of racemic 1,2-diols was described for the 1,2-diphenylethanediol as an example, where several additional chemical steps (e.g. synthesis of borate complexes, addition of chiral amino acid derivatives and (*S*)-

proline in benzene, treatment with hydrochloric acid) were required in order to gain highly stereoselective (1*R*,2*R*)-product (*de* 99%) (Periasamy 1996).

To conclude: the chemical methods described above have some main drawbacks besides the use of hazardous chemicals: often low stereoselectivity and no access to all stereoisomers of the compound of interest.

#### 1.11.2 Enzymatic methods

Enzymatic methods are a good alternative for the stereoselective synthesis of 1,2-diols avoiding the use of hazardous chemicals and harsh reaction conditions (Sheldon 2008). Three main routes to 1,2-diols are described: (I) reduction of  $\alpha$ -diketones by alcohol dehydrogenases (Figure 12, **5b**), (II) reduction of  $\alpha$ -hydroxy ketones (Figure 12, **5a**), and (III) hydrolysis of epoxides by epoxide hydrolases (Figure 12, **6**) are available.

Reduction of  $\alpha$ -diketones (Figure 12, **5b**) by alcohol dehydrogenases is one of the common enzymatic methods for the production of vicinal diols. Therefore the NADH-dependent diacetyl reductase from *Bacillus stearothermophilus* was applied. The enzyme accepts a large diversity of side chains of various size (mainly aliphatic side chains including cyclic compounds) yielding (1*S*,2*S*)-diols with high enantiomeric excess (*ee* up to > 98%) (Bortolini et al. 1997). A similar substrate spectrum (aliphatic  $\alpha$ -diketones) was found for reductions using whole cells of Baker's yeast, *Aspergillus niger*, *Geotrichum candidum*, and *Rodhotrula rubla* (Besse et al. 1993; Boutoute et al. 1998). However, these reactions were catalysed with only moderate regioselectivities (high formation of  $\alpha$ -hydroxy ketones as a side product) and enantioselectivities (Boutoute et al. 1998). Furthermore, reduction of diacetyl using cells from *Pichia farinose* IAM 4682 yielded the 1,2-diol with low stereoselectivities (Ideka et al. 1996).

Suitable enzymes for the reduction of  $\alpha$ -diketones (such as diacetyl or *n*-heptane-2,3-dione) are an alcohol dehydrogenase from *Rhodococcus ruber* DSM44541 (isolated yield up to 93% and *de* up to > 99%) (Edegger et al. 2006) and the alcohol dehydrogenases from *Lactobacillus brevis*, *Thermoanaerobacter* sp. and *Rhodococcus ruber* (Kurina-Sanz et al. 2009). The latter catalysing the reduction of long-chain aliphatic  $\alpha$ -diketones with excellent conversions (up to > 99%) and stereoselectivities (*ee* > 99%). Whereas, short-chain aliphatic  $\alpha$ -diketones were reduced with lower conversions (higher formation of  $\alpha$ -hydroxy ketones as side products) and stereoselectivities (Kurina-Sanz et al. 2009).

Another method for the synthesis of vicinal diols is the hydrolysis of epoxides (Figure 12, **6**) catalysed by epoxide hydrolases. These enzymes have been found in plants (Blée and Schuber 1995), insects (Linderman et al. 1995), bacteria (Mischitz

et al. 1995a), filamentous fungi (Morisseau et al. 1997) and mammals (Mueller et al. 1995; Oesch 1972; Pace-Asciak and Lee 1989; Watabe et al. 1981; Zeldin et al. 1995). The ring opening leads to the formation of the corresponding *anti*-configured 1,2-diol (Orru et al. 1999). Satisfactory sources from bacteria, such as *Rhodococcus* and *Nocardia* spp. (Kroutil et al. 1997; Mischitz et al. 1995b; Osprian et al. 1997) or fungi as for example *Aspergillus* and *Beauveria* spp. (Chen et al. 1993; Pedragosa et al. 1996) have been identified. Bacterium *Nocardia* EH1 showed almost complete enantioselectivity for kinetic resolution of 2-methyl-1,2-epoxyheptane, yielding enantiopure (*R*)-diol and (*S*)-epoxide (Osprian et al. 1997).

Also the resolution of racemic monosubstituted, 2,2- or 2,3-disubstituted oxiranes was studied, where diverse fungi and bacteria were applied for biotransformations displaying high enantioselectivities (Bala and Chimni 2010; Orru et al. 1999).

Furthermore, Bellucci and coworkers reported highly stereoselective biotransformations of racemic epoxides such as ( $\pm$ )-3,4-epoxytetrahydropyran to a single diol enantiomer (Bellucci et al. 1989; Hodgson et al. 1996). Most recently, a hydrolysis of cyclopentane- and cyclohexane oxides and *N*-benzyloxycarbonyl-3,4-epoxypyrrolidine using an epoxide hydrolase from *Sphingomonas* sp. HXN-200 afforded the corresponding (*R,R*)-vicinal diols with high enantioselectivity (*ee* 86-93%) and high yields (90-99%) (Wu et al. 2013). Improvement of stereoselectivity of the epoxide hydrolase-catalysed reactions to the respective 1,2-diols was recently reported by the addition of ionic liquids (Chiappe et al. 2007).

Stereoselective synthesis of vicinal diols can be also feasible with dioxygenases (Figure 12, 7). Oxidation of mono- and poly-cyclic aromatic ring systems (toluene-derivatives) was reported yielding *syn*-diols. Diversely mono-substituted benzenes were oxidised to the respective *syn*-2,3-diols with high enantioselectivities (*ee* 98%). The same tendency was observed for the oxidations of di- and poly-diversely substituted benzenes, where *syn*-diols with high enantioselectivities (*ee* up to 98%) were gained (Boyd and Sheldrake 1998).

Most recently, an enzymatic reduction of diversely substituted  $\alpha$ -hydroxy ketones (Figure 12, 5a) to the respective 1,2-diols was described using whole cells of *Pichia glucozyma*. Thereby 1,2-diols with high conversions (up to > 80%) and diastereoselectivities (*syn:anti* > 98:2) were obtained. Unfortunately, the respective enzyme(s) responsible for these reactions is/are not known yet (Husain et al. 2011). Also good conversions (up to 90%) and excellent stereoselectivities (*ee* up to > 99%) were obtained for the reductions of araliphatic diversely substituted  $\alpha$ -hydroxy ketones to the respective diols using an enzyme system from carrot (*Daucus carota*) (Liu et al. 2012).

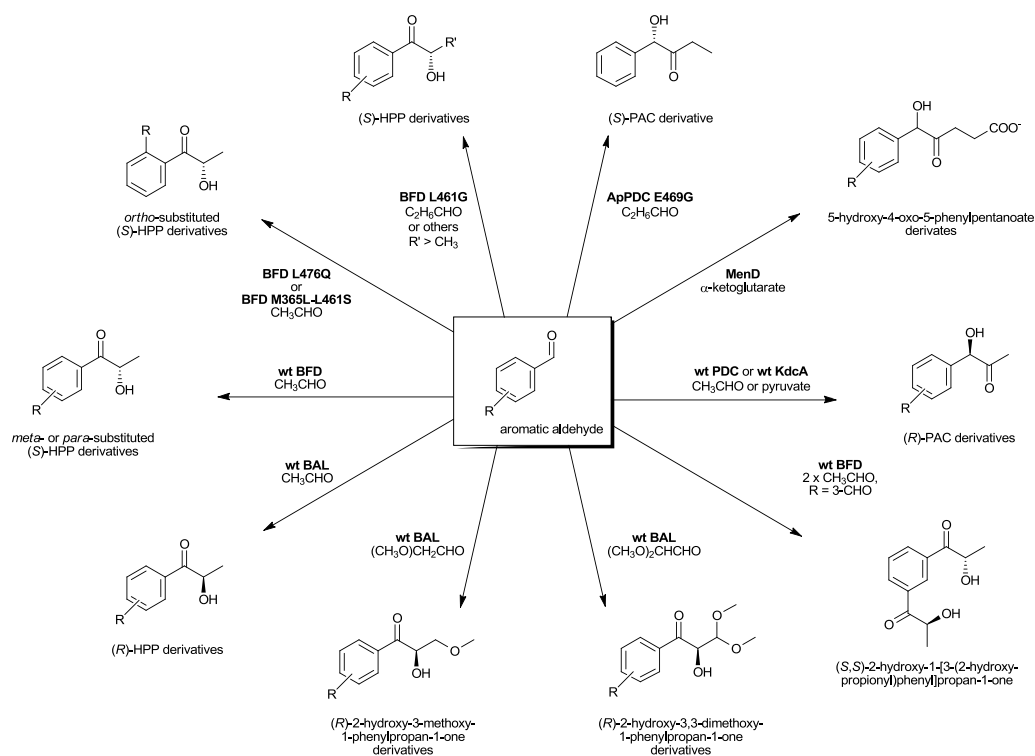
A novel and valuable method is a 2-step enzymatic synthesis of 1,2-diols. The first step is the carboligation of two inexpensive aldehydes catalysed by thiamine diphosphate (ThDP)-dependent lyase yielding  $\alpha$ -hydroxy ketones, which are

subsequently reduced in the second step by NAD(P)H-dependent alcohol dehydrogenases. This method was first described by Kihumbu in 2002 for the production of all four stereoisomers of 1-phenylpropane-1,2-diol (Kihumbu et al. 2002). Very high enantiomeric and diastereomeric excesses of 98-99% could be reached. However, this work was limited to the reduction of (*R*)- and (*S*)-2-hydroxy-1-phenylpropan-1-one (2-HPP) to the all possible stereoisomers of the 1,2-diol ((1*R*,2*R*)-, (1*R*,2*S*)-, (1*S*,2*R*)- and (1*S*,2*R*)-1-phenylpropane-1,2-diol) and it was not further assigned to other substrates.

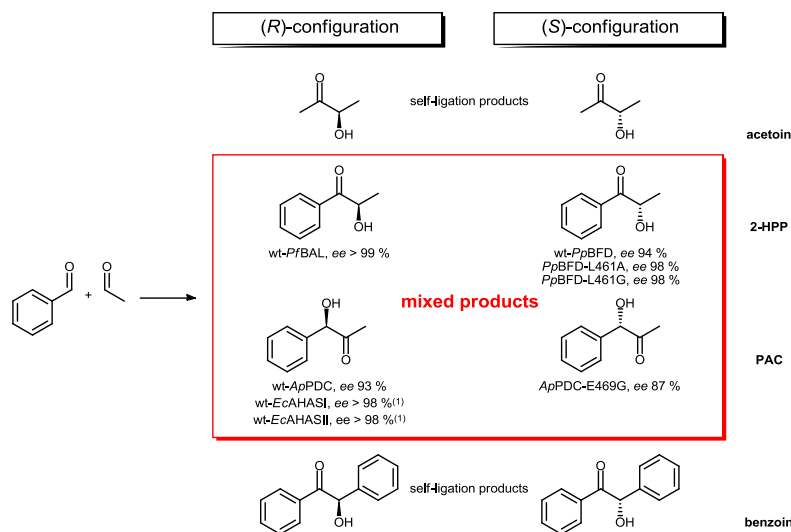
#### 1.11.2.1 First step: carboligation by ThDP-dependent enzymes

The first step is the carboligation of two inexpensive aldehydes catalysed by a thiamine diphosphate (ThDP)-dependent lyase yielding  $\alpha$ -hydroxy ketones with high regio-, chemo- and enantioselectivity (Figure 14) (Müller et al. 2009; Müller et al.; Hailes et al. 2013).

Within the group of Pohl/Rother at the IGB-1 at Forschungszentrum Jülich GmbH a toolbox of ThDP-dependent enzymes was created giving access to a broad platform of diversely substituted  $\alpha$ -hydroxy ketones with high stereoselectivity (Figure 14). The toolbox encompass 23 wild type enzymes (e.g. benzaldehyde lyase (BAL), benzoylformate decarboxylase (BFD), acetohydroxyacid synthase (AHAS), pyruvate decarboxylase (PDC), etc.) and > 100 variants of them. By smart combination of substrates and ThDP-dependent enzyme a desired  $\alpha$ -hydroxy ketones can be synthesised with excellent regio-, chemo- and enantioselectivity (Müller et al. 2009; Müller et al. 2013).



**Figure 14.** Platform of diversely substituted  $\alpha$ -hydroxy ketones (adapted and modified from (Müller et al. 2009))



**Figure 15.** Carboligation of benzaldehyde and acetaldehyde using defined ThDP-dependent enzymes yielding mixed  $\alpha$ -hydroxy ketone with high enantioselectivity ( $ee > 99\%$ ). 2-HPP = 2-hydroxy-1-phenylpropan-1-one; PAC = 1-hydroxy-1-phenylpropan-2-one, phenylacetylcarbinol; *PfBAL* = benzaldehyde lyase from *Pseudomonas fluorescens* (Janzen et al. 2006); *PpBFD* = benzoylformate decarboxylase from *Pseudomonas putida* and its variants (Gocke et al. 2008; Iding et al. 2000); *ApPDC* = pyruvate decarboxylase from *Acetobacter pasteurianus* (Rother et al. 2011) and its variant (Gerhards et al. 2012); *EcAHASI*, *EcAHASII* – acetohydroxyacid synthase isoenzyme I and II, respectively from *Escherichia coli* (Engel et al. 2003); <sup>(1)</sup> – pyruvate as a donor instead of acetaldehyde.

For instance, the combination of acetaldehyde and benzaldehyde can yield four enantiomeric products, but the main interest in this work is on all four enantiomers of the two mixed products (Figure 15).



#### 1.11.2.1.1 Benzaldehyde lyase

Benzaldehyde lyase (BAL) is an enzyme isolated from *Pseudomonas fluorescens* Biovar I. The natural role of the enzyme is catabolic cleavage of aromatic acylloins to respective aldehydes, which are next catabolised in  $\beta$ -ketoadipate pathway (Janzen et al. 2006). The enzyme requires for its activity two cofactors, thiamin diphosphate (0.1 mM) and divalent  $Mg^{2+}$  (2.5 mM) cations (Fraga and Hinrichsen 1994; Hinrichsen et al. 1994; Janzen et al. 2006).

BAL is an extremely useful enzyme for biotransformations, since it is able to catalyse lyase and ligase reactions (cleavage and formation of benzoin, respectively). Detailed biochemical characterisation of the enzyme revealed that the enzyme is stable between pH 6 to 8, which is the pH-optimum for the lyase and ligase activity. Furthermore, BAL shows extremely high initial rate activities, a broad substrate scope and excellent stereoselectivities ( $ee > 99\%$  depending on substrates) (Janzen et al. 2006).

#### 1.11.2.1.2 Benzoylformate decarboxylase

Benzoylformate decarboxylase (BFD) was found in the mandelate catabolism of bacteria such as *Pseudomonas putida*, *Acinetobacter calcoaceticus* and *Pseudomonas aeruginosa* (Barrowman and Fewson 1985; Barrowman et al. 1986; Hegeman 1970). The enzyme is responsible for the non-oxidative decarboxylation of benzoylformate to benzaldehyde. Besides BFD catalyses also the carboligation of benzaldehyde (upon decarboxylation of benzoylformate) and acetaldehyde (Iding et al. 2000; Wilcocks et al. 1992). BFD shows similar pH-optima to BAL: for the carboligation starting from benzoylformate and acetaldehyde a pH-optimum between 6.0 and 8.5 was found, whereas for the pH-optimum is shifted to 7.5-8.5, if benzaldehyde and acetaldehyde are used as substrates (Iding et al. 2000). The carboligation of two molecules yields valuable  $\alpha$ -hydroxy ketones with high stereoselectivity (up to  $ee > 99\%$ ) (Iding et al. 2000). The carboligation of benzaldehyde and acetaldehyde gives (*S*)-2-HPP with high enantioselectivity ( $ee$  92-94%) (Iding et al. 2000; Wilcocks et al. 1992). Meanwhile several variants of BFD with improved stereoselectivity for the production of (*S*)-2-HPP ( $ee$  98%) were prepared, namely BFD-L461A and BFD-L461G (Demir et al. 2001; Gocke et al. 2008; Iding et al. 2000; Lingen et al. 2003).

#### 1.11.2.1.3 Acetohydroxyacid synthase

Acetohydroxyacid synthases are key enzymes in plants, fungi and bacteria, which catalyse *de novo* synthesis of the branched-chain amino acids (Bar-Ilan et al. 2001; Chipman et al. 1998; Chipman et al. 2005; McCourt and Duggleby 2005).

Isoenzyme I of acetohydroxyacid synthase (AHAS-I) isolated from *Escherichia coli* is a ThDP-dependent enzyme, which requires besides ThDP,  $Mg^{2+}$  ions and FAD for its activity. The enzyme catalyses the carboligation of an  $\alpha$ -keto acid (acceptor, here: pyruvate) and aldehyde (donor, here: benzaldehyde) yielding an (*R*)- $\alpha$ -hydroxy ketone (here: PAC) with very high enantioselectivity (*ee* > 98%) (Engel et al. 2003; Engel et al. 2004a; Engel et al. 2004b; Engel et al. 2005; Vinogradov et al. 2005; Vinogradov et al. 2006). The pH-optimum for carboligation of pyruvate and benzaldehyde was found at pH 6.5-8.0 (Chien et al. 2010). Besides, carboligation starting from two aldehydes such as acetaldehyde and benzaldehyde is catalysed with significantly lower activity (Schmitz 2012).

#### 1.11.2.1.4 Pyruvate decarboxylase

Pyruvate decarboxylase from *Acetobacter pasteurianus* (ApPDC) is an enzyme responsible for the oxidative metabolism of lactic acid to acetaldehyde and carbon dioxide. Acetaldehyde is subsequently oxidised to its final product, acetic acid (Rother et al. 2011). Recently it was found that the (*R*)-selective enzyme is capable to catalyse the synthesis of (*R*)- $\alpha$ -hydroxy ketones. Genetic modification of the wild enzyme yielded the variant ApPDC E469G that gave access to (*S*)- $\alpha$ -hydroxy ketones using aliphatic donor aldehydes and benzaldehyde as the acceptor. Best results were obtained with propanal as the donor (*ee* 89%) under the conditions tested (Rother et al. 2011).

#### 1.11.2.2 Second step: oxidoreduction by alcohol dehydrogenases

The proof-of-principle of combination of ThDP-dependent enzymes with ADHs was already shown by Kihumbu for the production of four stereoisomers of 1-phenylpropane-1,2-diol in 2-step 2-pot synthesis through reduction of the intermediate, 2-HPP (Kihumbu et al. 2002).

An extended investigation of the substrate scope of available oxidoreductases with a focus on the reduction of diversely substituted  $\alpha$ -hydroxy ketones was first conducted in this thesis.

##### 1.11.2.2.1 Carbonyl reductase from *Candida parapsilosis*

Carbonyl reductase from *Candida parapsilosis* (CPCR) was first isolated from the strain DSM 70125 and biochemically characterised by Peters et al. (Peters et al. 1993a). The same enzyme was later isolated by Yamamoto et al. from a related strain IFO 0369 and expressed in *E. coli* (Yamamoto et al. 1999). CPCR consists of

336 amino acids per subunit (Yamamoto et al. 1999) and forms a dimer. The carbonyl reductase is an NADH- and  $\text{Zn}^{2+}$ -dependent enzyme, which belongs to the medium-chain dehydrogenase family (Jakoblinnert et al. 2012). The (*S*)-selective enzyme displays a broad substrate range and therefore is employed for a number of various processes such as production of valuable alcohols (Matsuyama et al. 2011), hydroxy esters (Peters et al. 1993c) and propargylic alcohols (Schubert et al. 2001). Furthermore, the enzyme was successfully employed for biotransformations in an enzyme membrane reactor (Laue et al. 2001), an enzyme emulsion reactor (Liese et al. 1998) and a biphasic reactor (van den Wittenboer et al. 2009). Most recently, the enzyme overexpressed in *E. coli* was implemented as a whole cell biocatalyst for biotransformation in neat organic substrates with excellent conversions yielding up to  $500 \text{ g L}^{-1}$  of enantiopure alcohol (Jakoblinnert et al. 2011).

#### 1.11.2.2.2 ADH from *Flavobacterium frigidimaris*

The NAD(H)-dependent medium-chain dehydrogenase (MDR) was isolated from the psychrotolerant *Flavobacterium frigidimaris* (FADH). The enzyme consists of 344 amino acids per subunit and forms a tetramer. Furthermore, the enzyme contains two  $\text{Zn}^{2+}$ -ions per subunit (see chapter 1.8). FADH shows a broad temperature range for activity between  $0^\circ\text{C}$  and  $85^\circ\text{C}$  with an activity maximum at  $70^\circ\text{C}$ . The (*S*)-selective enzyme displays a broad substrate range for the reduction of aliphatic aldehydes and ketones (Kazuoka et al. 2007).

#### 1.11.2.2.3 ADH from horse liver

Commercially available HLADH is a NAD(H)-dependent medium-chain dehydrogenase. The enzyme consists of 374 amino acids per subunit (Jörnvall 1970) and forms a dimer (Ramaswamy et al. 1994). HLADH contains two  $\text{Zn}^{2+}$ -ions per subunit (one structural and one catalytical) (see chapter 1.8) (Bränden et al. 1973; Eklund et al. 1976). The (*S*)-selective enzyme is frequently used e.g. for reductions of aldehydes (Bowen et al. 1986; Bradshaw et al. 1992c; Giacomini et al. 2007), ketones (Jones and Schwartz 1981; Jones and Takemura 1982; Krawczyk and Jones 1989; Lam et al. 1988; Shigematsu et al. 1995; Willaert et al. 1988), oxidation of alcohols (Adolph et al. 1991; Dalziel and Dickinso 1966; Jones and Lok 1979; Lemiere et al. 1988; Merritt and Tomkins 1959) and esterase reaction (Tsai 1982). HLADH was successfully implemented for numbers of cofactor regeneration processes (Itozawa and Kise 1993; Itozawa and Kise 1995; Virto et al. 1995). Furthermore, the enzyme in immobilised form was successfully used for biocatalysis (Itozawa and Kise 1995; Sotolongo et al. 1999).

#### 1.11.2.2.4 ADH from *Lactobacillus brevis*

The NADP(H)-dependent short-chain dehydrogenase (SDR) isolated from *Lactobacillus brevis* (LBADH) consists of 241 amino acids per subunit and forms a tetramer (Riebel 1996). LBADH requires for its activity  $Mg^{2+}$ -ions (Niefind et al. 2003; Niefind et al. 2000; Schlieben et al. 2005). The enzyme shows pH-optimum for reduction at pH 6.5-8.5, whereas optimum for oxidation is between pH 7-10 (Kulishova 2010). The (*R*)-selective enzyme (Niefind et al. 2003; Niefind et al. 2000; Schlieben et al. 2005) has a broad substrate scope including linear and branched aliphatic as well as aromatic aldehydes and ketones, propargylic and allylic ketones, diketones, ketoesters and acetophenone and its derivatives (Leuchs and Greiner 2011). LBADH is also active towards  $\alpha$ -hydroxy ketones (Kihumbu et al. 2002). Further, the enzyme is used in industrial processes, e.g. for the production of ethyl-(3*R*)-hydroxybutanoate (Daußmann et al. 2006b; Liese 2006).

#### 1.11.2.2.5 ADH from *Ralstonia* sp.

Alcohol dehydrogenase from *Ralstonia* sp. (RADH) consists of 249 amino acids per subunit and belongs to a short-chain dehydrogenases family (Lavandera et al. 2008a). The enzyme was found to be specifically useful for reductions of bulky-bulky ketones containing two sterically demanding substituents (Lavandera et al. 2008a). The reductions employing the recombinant enzyme from *E. coli* were catalysed with activities up to  $17.4 \mu\text{mol h}^{-1} \text{g}^{-1}$  and moderate stereoselectivities (*ee* 40-95%), depending on the substrate and the implemented cofactor regeneration system (Lavandera et al. 2008c). Substrate-coupled cofactor regeneration was optimised using ethanol (10 vol%) and 2-propanol (5 vol%) at pH 7.5 and pH 7.0, respectively (Lavandera et al. 2008c). Better activities up to  $32.4 \mu\text{mol h}^{-1} \text{g}^{-1}$  (*ee* > 99%) were obtained with bulky-bulky ketones and glucose dehydrogenase (GDH) for cofactor regeneration (Lavandera et al. 2008a).

In purified form the enzyme with streptavidine tag (strep-RADH) was only implemented for the reduction of aldoxime to the respective alcohol proving first chemo-promiscuous activity of RADH (Ferreira-Silva et al. 2010).

Biochemical characterisation of isolated RADH was first performed in frame of this thesis.

#### 1.11.2.2.6 ADH from *Sphingobium yanoikuyae*

A further well suited enzyme for the reduction of bulky-bulky ketones is alcohol dehydrogenase from *Sphingobium yanoikuyae* (SADH) (Lavandera et al. 2008b; Lavandera et al. 2008c). As RADH, the enzyme belongs to the short-chain

dehydrogenases superfamily and consists of 262 amino acids per subunit (Lavandera et al. 2008b).

The recombinant enzyme overexpressed in *E. coli* catalyses the reduction of sterically hindered ketones with higher activities (up to  $18.6 \mu\text{mol h}^{-1} \text{g}^{-1}$ ) than RADH and moderate stereoselectivities (*ee* 59-97%), depending on the reduced substrate and implemented cofactor regeneration system (Lavandera et al. 2008c). It was found that for SADH-catalysed reactions suitable co-substrates for cofactor regeneration are 2-propanol (5 vol%) and ethanol (5 vol%) with pH-optima of 7.0 and 8.0, respectively (Lavandera et al. 2008c).

Lyophilised *E. coli* cells containing overexpressed SADH were implemented successfully for dynamic kinetic resolution of *rac*-methylcarbinols, e.g. hexanophenone with good to very good enantiomeric excesses (*ee* 89% (*S*) and *ee* 97% (*S*) using ethanol and 2-propanol for cofactor regeneration, respectively) (Lavandera et al. 2008b). As with RADH detailed biochemical characterisation of the purified enzyme is still missing.

#### 1.11.2.2.7 ADH from *Thermoanaerobacter brockii*

The alcohol dehydrogenase isolated from *Thermoanaerobacter brockii* (TBADH) consists of 352 amino acids per subunit and is a medium chain,  $\text{Zn}^{2+}$ - and NADP(H)-dependent enzyme (see chapter 1.8) which forms a tetramer (Peretz and Burstein 1989; Peretz et al. 1997). The enzyme is applied for biotransformations of chloro-substituted aliphatic ketones (Keinan et al. 1986a; Keinan et al. 1986b) and furanyl ketones (Drueckhammer et al. 1988). TBADH is used for industrial applications mainly for cofactor regeneration (enzyme-coupled approach) (Bastos et al. 1999; Bastos et al. 2002; Keinan et al. 1986b; Korkhin et al. 1998; Röthig et al. 1990), since it displays high activity towards aliphatic primary and secondary alcohols (Lamed and Zeikus 1981). Therefore TBADH was also tested for cofactor regeneration in the present thesis.

#### 1.11.2.2.8 ADH from *Thermoanaerobacter* sp.

The (*S*)-selective alcohol dehydrogenase isolated from *Thermoanaerobacter* sp. (ADHT) is another  $\text{Zn}^{2+}$ - and NADP(H)-dependent medium-chain dehydrogenase, which consists of 352 amino acids per subunit (Daußmann and Hennemann 2009). The enzyme displays broad substrate scope toward aldehydes and ketones (Daußmann and Hennemann 2009) and it was employed for biotransformations in isolated and immobilised form (Trivedi et al. 2005; Trivedi et al. 2006) for the stereoselective production of (*R*)- and (*S*)-allylic alcohols (chemoenzymatic method)

(Sgalla et al. 2007), 1,2-diols (Kihumbu et al. 2002) and (*S*)-1-phenylethanol, respectively (Trivedi et al. 2005; Trivedi et al. 2006).

#### 1.11.2.2.9 ADH from *Thermus* sp.

The (*S*)-selective alcohol dehydrogenase from *Thermus* sp. (TADH) consists of 347 amino acids per subunit, which classifies the enzyme as an MDR (medium-chain dehydrogenases/reductases) protein superfamily (Jörnvall et al. 2010). In the sequence of TADH a typical zinc-binding motif was found. Furthermore, the enzyme is strongly inhibited by addition of EDTA indicating metal-dependency. The crystal structure of TADH is still missing and therefore the metal-dependency still could not be confirmed. TADH is an NAD(H)-dependent enzyme with broad substrate range including aliphatic and aromatic aldehydes, aliphatic and cyclic ketones. By contrast, aromatic ketones are reduced with significantly lower velocities. These reactions result in formation of (*S*)-alcohols with high stereoselectivity (*ee* > 99%) (Höllrigl et al. 2008).

### 1.12 Synthetic cascade reactions

Cascade reactions are common in nature. In metabolic pathways of living cells, a synchronised regulation of a number of enzymatic reactions without isolation of intermediates occurs.

According to Ricca *et al.* (Ricca et al. 2011) a synthetic biocatalytic cascade reaction is a reaction system, where two or more reactions are carried out concurrently in the same reaction vessel using at least one biocatalyst. This encompasses multi-enzymatic, chemo-enzymatic, and enzyme-initiated spontaneous sequences (Ricca et al. 2011). Modular cascade processes have many advantages, but also some drawbacks, which are summarised in Table 6.

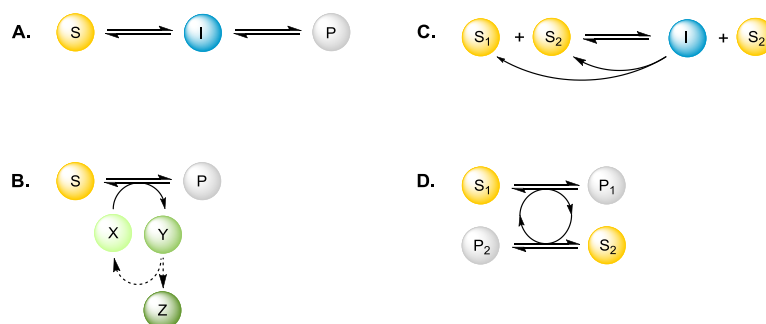
Most importantly, with synthetic cascade reactions in one pot economic and environmental benefits, such as reduction of intermediate steps or waste production, can be gained. Besides, cascade reactions give the opportunity to shift reaction equilibria to the direction of the desired product. Therewith higher space-time yields (Junceda 2008) can be reached, which is not possible in time separated multi-step processes. Apart from these significant advantages, the main drawbacks of multi-step modular cascade reactions are highly varying reaction rates of different biocatalysts in one pot. Therefore reaction engineering is often a crucial step in order to achieve reasonable conversions for each step of the cascade.

**Table 6.** Advantages and disadvantages of modular cascade reactions conducted concurrently in one pot (Junceda 2008).

Advantages	Disadvantages
<ul style="list-style-type: none"> <li>– Less intermediate steps</li> <li>– Less solvent and reaction volume</li> <li>– Shorter cycle times</li> <li>– Higher space-time yields</li> <li>– Less waste (atom economy)</li> </ul>	<ul style="list-style-type: none"> <li>– Catalysts are often incompatible with each other</li> <li>– Reaction rates may be very different</li> <li>– Difficulties of finding optimum conditions (pH, temperature, solvent, etc.)</li> </ul>

Depending on the process used, four cascade “designs” can be distinguished (Figure 16):

- A. **LINEAR CASCADE** – is a classical approach of the cascade reaction, where a single substrate is transformed *via* one or more intermediate steps to a single product (Figure 16A). This kind of domino reaction helps to reduce waste and save time required for purification of intermediates (Ricca et al. 2011). Linear cascade can proceed in:
- **SEQUENTIAL MODE** – where addition of catalysts to the reaction vessel proceeds subsequently;
  - **SIMULTANEOUS MODE** – where catalysts are added to the reaction vessel at the same time;
- B. **ORTHOGONAL CASCADE** – the substrate conversion to the desired product is coupled with additional reactions in order to recycle cofactors or cosubstrates, or to remove by-products (Figure 16B) (Ricca et al. 2011).
- C. **CYCLIC CASCADE** – one out of a mixture of substrates (e.g. racemate) is selectively transformed to an (prochiral) intermediate, which is subsequently converted back to the starting material (one of enantiomer) (Figure 16C). By repeated reactions one enantiomer is accumulated, while the other one is subsequently reverted into the starting substrates (Ricca et al. 2011).



**Figure 16.** Cascade reactions can be classified by four different designs. **A.** Linear cascade; **B.** Orthogonal cascade, **C.** Cyclic cascade, **D.** Parallel cascade, (Ricca et al. 2011); Abbreviations: S = substrate, I = intermediate, P = product, X = co-substrate, Y = co-product or by-product, Z = another product.

- D. **PARALLEL CASCADE** – two different substrates are simultaneously converted to two valuable products of interest (Figure 16D). These reactions are very often catalysed in the presence of co-substrates or cofactors (Ricca et al. 2011).

### 1.13 Reaction/Process engineering

Enzyme reaction engineering allows identification of optimal reaction parameters for the multi-enzymatic cascades. Since cascade reactions combine various enzymes with different features, it is necessary to find optimal conditions for these enzymes (e.g. pH, temperature, enzyme-, substrate-, cofactor concentrations) in order to gain highest possible productivity.

Enzyme-catalysed biotransformations have to be well planned. Some requirements have to be considered, such as:

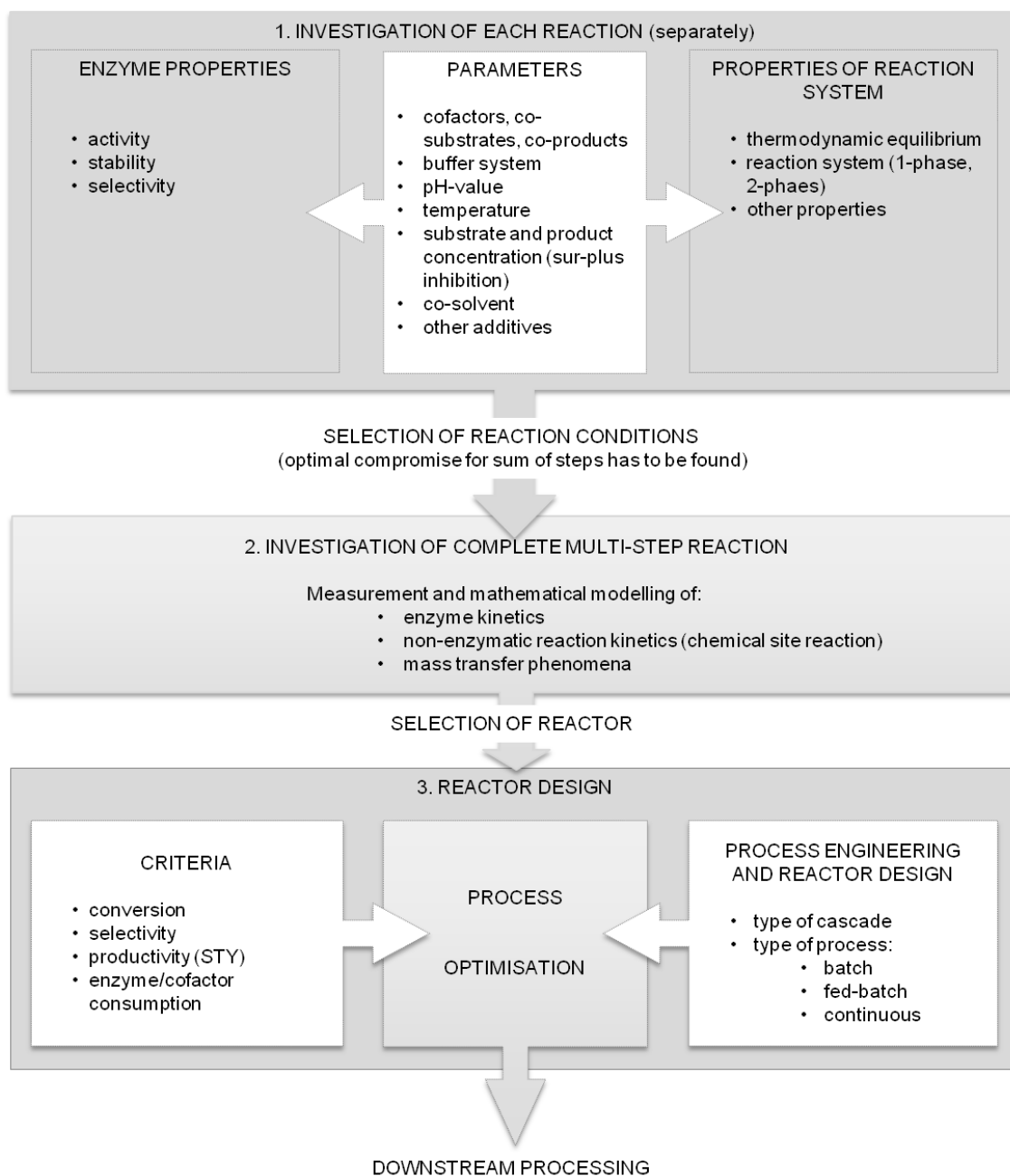
- **PRODUCT** – which should be obtained in high optical purity and (optimally) without by-product formation;
- **ENZYME** – its applicability for the cascade has to be confirmed in advance. It does not only need to accept the substrate of interest, but further has to be as active, stable and selective as possible. These data have to be available in advance to select an appropriate biocatalyst;
- **SUBSTRATES** – substrate selection strongly depends on its availability and price (Drauz and Waldmann 2002). Further, a smart selection may result in the development of desired cascade types, e.g. recycling cascades with *in situ* co-product removal, what was conducted in frame of this thesis.

The goal of the reaction engineering is to find conditions where following requirements are at least partially fulfilled:

- high reaction selectivity
- high optical purity of the product
- high space time yield/conversions (productivity) of the optimised reaction
- low enzyme and cofactor use per mass unit of product (Drauz and Waldmann 2002) (Table 2).

Generally, process development consists of three steps, including investigation of the (I) reaction system, (II) reaction kinetics, and (III) optimal process engineering and reactor design (Figure 17).





**Figure 17.** Steps of process optimisation in enzyme reaction engineering (Drauz and Waldmann 2002, modified).

**I. INVESTIGATION OF THE REACTION SYSTEM** can be subdivided into two parts:

a. *Enzyme properties* have to be tested regarding:

- Activity, selectivity and stability, concerning pH, temperature, suitable buffer, and additives (e.g. metal-ions as stabilisation agents);
- Optimal substrate, product, co-substrate (e.g. for cofactor regeneration) concentrations. Here, additionally the enzyme activity and possible sur-plus inhibition should be investigated;

- b. *Other features* of the reaction system (e.g. equilibrium constant of reversible reactions, pH- and temperature-effects on substrate and products solubility, etc.).

**II. INVESTIGATION OF REACTION KINETICS.** Here a detailed analysis of kinetic parameters should be performed under optimised reaction conditions described in point I. Once all required kinetic data are available, mathematical reaction modelling should be applied in order to calculate theoretical conversions of investigated process. Mathematical reaction modelling can be a helpful tool to detect bottlenecks during process optimisation.

**III. INVESTIGATION OF OPTIMAL PROCESS ENGINEERING AND REACTOR DESIGN** is the reactor design and evaluation of the optimal process mode (e.g. type of cascade).

## II Publications

---

## Publication I

---

### “Stereoselective synthesis of bulky 1,2-diols with alcohol dehydrogenases”

Justyna Kulig, Robert C. Simon, Christopher A. Rose, Syed M. Husain, Matthias Häckh, Steffen Lüdeke, Kirsten Zeitler, Wolfgang Kroutil, Martina Pohl and Dörte Rother

Catalysis Science and Technology, 2012

Vol. 2(8), 1580-1589

DOI: 10.1039/C2CY20120H

Reproduced by permission of The Royal Society of Chemistry  
(<http://pubs.rsc.org/en/Content/ArticleLanding/2012/CY/c2cy20120h>)

# Catalysis Science & Technology

View Online / Journal Homepage  
Dynamic Article Links 

Cite this: DOI: 10.1039/c2cy20120h

www.rsc.org/catalysis

PAPER

## Stereoselective synthesis of bulky 1,2-diols with alcohol dehydrogenases†

Justyna Kulig,<sup>a</sup> Robert C. Simon,<sup>†ab</sup> Christopher A. Rose,<sup>c</sup> Syed Masood Husain,<sup>d</sup> Matthias Häckh,<sup>d</sup> Steffen Lüdeke,<sup>d</sup> Kirsten Zeitler,<sup>c</sup> Wolfgang Kroutil,<sup>b</sup> Martina Pohl<sup>a</sup> and Dörte Rother<sup>\*a</sup>

Received 28th February 2012, Accepted 26th March 2012

DOI: 10.1039/c2cy20120h

Although biotransformations implementing alcohol dehydrogenases (ADHs) are widespread, enzymes which catalyse the reduction and oxidation of sterically demanding substrates, especially 2-hydroxy ketones, are still rare. To fill this gap eight ADHs were investigated concerning their potential to reduce bulky 2-hydroxy ketones. All of these enzymes showed good activities along with excellent enantio- (ee > 99%) and diastereoselectivities (de > 99%). Due to their differences in substrate preferences and stereoselectivity a broad range of diastereomerically pure 1,2-diols is now accessible via biotransformation. Best results were obtained using the alcohol dehydrogenase from *Ralstonia* sp. (*Cupriavidus* sp.) (RADH), which showed a broad substrate range, especially for sterically demanding compounds. Aromatic 2-hydroxy ketones, like (*R*)-2-hydroxy-1-phenylpropan-1-one ((*R*)-2-HPP), were reduced much faster than aliphatic or aromatic aldehydes (e.g. benzaldehyde) under the applied conditions. Additionally (*R*)- as well as (*S*)-2-hydroxy ketones were converted with high diastereoselectivities (de > 99%). RADH, which was up to now only studied as a whole cell biocatalyst overexpressed in *E. coli*, was purified and thoroughly characterised concerning its catalytic properties.

### 1. Introduction

A key interest in organic chemistry is the synthesis of chiral building blocks.<sup>1</sup> Among these, sterically demanding chiral 1,2-diols with two chiral centres are of high interest since they find versatile application as synthons for chemical catalysts, agrochemicals and pharmaceuticals.<sup>2–4</sup> However, the development of methods covering the synthesis of all forms of the stereoisomers is still challenging. The production of enantiomerically pure 1,2-diols has been described using chemical and enzymatic methods. Since four stereoisomers can occur, the chemical synthesis of chiral 1,2-diols is not a trivial task. An approved method is the synthesis of *syn*-1,2-diols applying Sharpless dihydroxylation of (*E*)-olefins. It results in high

stereoselectivities, while the synthesis of *anti*-1,2-diols is limited by the availability of (*Z*)-olefins.<sup>5</sup> Moreover, the Sharpless asymmetric dihydroxylation requires the application of potassium osmate(VI) dihydrate (K<sub>2</sub>OsO<sub>4</sub>·2H<sub>2</sub>O), which is a dangerous and toxic catalyst. Therefore, the enzymatic approach is an attractive alternative. Here the synthesis takes place under mild conditions yielding chiral diols with high chemo-, regio- and stereoselectivity. Different biocatalytic routes to chiral alcohols have been described using oxidoreductases, hydrolases and lyases, either with isolated enzymes or whole cells.<sup>6</sup>

One powerful approach toward chiral 1,2-diols is the reduction of the prochiral keto group of 2-hydroxy ketones via NAD(P)H-dependent oxidoreductases. The reduction of small and small-bulky 2-hydroxy ketones, such as (*R*)- and (*S*)-2-hydroxy-1-phenylpropan-1-one (2-HPP, **9**), using alcohol dehydrogenases from *Lactobacillus brevis* (LBADH) and *Thermoanaerobacter* sp. (ADHT) has already been described earlier.<sup>7,8</sup> However, there is still a gap of enzymes accepting bulky-bulky substrates which has to be filled. Bulky-bulky<sup>3</sup> 2-hydroxy ketones are defined as 2-hydroxy ketones possessing two substituents which are larger than ethyl, azido-, cyano-, or halomethyl groups. Recently, the biocatalytic reduction of bulky-bulky 2-hydroxy ketones such as methoxy-substituted (*R*)-2-HPP and benzoin derivatives was described using whole cells of *Pichia glucozyma*.<sup>9</sup> Unfortunately, the respective enzyme(s) responsible for this reaction is/are not yet known.

An alcohol dehydrogenase identified from *Ralstonia* sp. DSM 6428 (also known as *Cupriavidus* sp. DSM 6428) has earlier been described by Kroutil's group as a suitable enzyme for the reduction

<sup>a</sup> Institute of Bio- and Geosciences, IBG-1: Biotechnology, Forschungszentrum Jülich GmbH, 52425 Jülich, Germany. E-mail: do.rother@fz-juelich.de; Fax: +49 2461-613870; Tel: +49 2461-616772

<sup>b</sup> Institute of Chemistry, Organic and Bioorganic Chemistry, University of Graz, Heinrichstrasse 28, 8010 Graz, Austria

<sup>c</sup> Institute of Organic Chemistry, University of Regensburg, Universitätsstrasse 31, 93053 Regensburg, Germany

<sup>d</sup> Institute of Pharmaceutical Sciences, University of Freiburg, Albertstrasse 25, 79104 Freiburg, Germany

† Electronic supplementary information (ESI) available: The vector maps of RADH and SADH, cloning, expression and purification procedures of recombinant ADHs, tables with all crude extract data as well as infrared and vibrational circular dichroism spectra are presented. See DOI: 10.1039/c2cy20120h

\* Present address: Institute of Chemistry, Organic and Bioorganic Chemistry, University of Graz, Heinrichstrasse 28, 8010 Graz, Austria



of bulky-bulky ketones by whole cell biotransformations.<sup>3</sup> Motivated by these results, we started a broader screening of available ADHs concerning their activity towards various 2-hydroxy ketones, which was initially performed using crude extracts of recombinant *E. coli* cells overexpressing the respective enzymes: alcohol dehydrogenases from *Thermoanaerobacter* sp. (ADHT), *Flavobacterium frigidimarum* (FADH), horse liver (HLADH), *Lactobacillus brevis* (LBADH), *Ralstonia* sp. (RADH), *Sphingobium yanoikuyae* (SADH), *Thermus* sp. (TADH), and carbonyl reductase from *Candida parapsilosis* (CPCR). Among these ADHT, LBADH and RADH showed promising activity towards 2-hydroxy ketones, with RADH being most active towards bulky-bulky 2-hydroxy ketones. Therefore its high potential for the synthesis of chiral diols was studied in more detail.

## 2. Material and methods

### 2.1. Origin of chemicals

All chemicals for chemical syntheses were of high analytical grade and purchased from Sigma (Steinheim, Germany), Aldrich (Steinheim, Germany), Fluka (Steinheim, Germany), Merck (Darmstadt, Germany) and Roth (Karlsruhe, Germany). NADPH and NADH were purchased from Biomol (Hamburg, Germany).

### 2.2. Chemical and biochemical synthesis of 2-hydroxy ketones

The 2-hydroxy ketones **5–8**, **10–11** and **13–14** were bought from one of the above-mentioned companies. Phenylacetylcarbinol, PAC ((*R*)-**12**), was received from BASF AG and purified as described below. The 2-hydroxy ketones **18–27** and **32–34** were obtained *via* carbene-catalysed regioselective chemical syntheses as recently described.<sup>10,11</sup> 2-Hydroxy ketones *rac*-**9**, (*R*)-**9**, (*S*)-**9**, (*R*)-**28** and (*S*)-**28** were chemically or biotransformations as described in the following.

***rac*-2-Hydroxy-1-phenylpropan-1-one (*rac*-**9**).** The synthesis was carried out according to the literature.<sup>12</sup> Our spectroscopic data are in full agreement with those previously published.<sup>13,14</sup>  $R_f$  (PE/EtOAc 90/10) = 0.27.  $^1\text{H-NMR}$  (600 MHz,  $\text{CDCl}_3$ ): 1.46 (d,  $^3J_{3,2}$  = 7.1 Hz, 3 H, 3-H), 3.80 (brs, 1 H, OH), 5.17 (q,  $^3J_{2,3}$  = 7.1 Hz, 1 H, 2-H), 7.51 ( $m_c$ , 2 H, arom.-H), 7.62 ( $m_c$ , 1 H, arom.-H), 7.93 ( $m_c$ , 2 H, arom.-H) ppm.  $^{13}\text{C-NMR}$  (151 MHz,  $\text{CDCl}_3$ ): 22.3 (C-3), 69.3 (C-2), 128.7 (arom.-CH), 128.9 (arom.-CH), 134.0 (arom.-C<sub>ipso</sub>), 202.4 (C-1) ppm. GC-MS (EI, 70 eV):  $m/z$  (%) = 150 [ $\text{M}^+$ ] (15), 105 [ $\text{C}_7\text{H}_5\text{O}^+$ ] (100), 77 [ $\text{C}_6\text{H}_5^+$ ] (37).

**(*R*)-2-Hydroxy-1-phenylpropan-1-one ((*R*)-**9**).** The synthesis was carried out as described elsewhere.<sup>7,15</sup> Spectroscopic data are in full agreement with those previously published.

**(*S*)-2-Hydroxy-1-phenylpropan-1-one ((*S*)-**9**).** The substrate was synthesised as previously described.<sup>16,17</sup> Spectroscopic data are again in full agreement with the literature.

**(*R*)-1-Hydroxy-1-phenylpropan-2-one ((*R*)-**12**).** The crude product was provided by BASF as mentioned above and purified by common methods. The resulting yellow oil has a purity of >96% (GC and NMR) and an ee of 84% ((*R*)-**12**).  $^1\text{H-NMR}$  (600 MHz,  $\text{CDCl}_3$ ): 2.08 (s, 3 H,  $\text{CH}_3$ ), 4.30 (brs, 1 H, OH), 5.09

(brs, 1 H, 1-H), 7.31–7.40 (m, 5 H, arom.-H) ppm.  $^{13}\text{C-NMR}$  (151 MHz,  $\text{CDCl}_3$ ): 25.3 ( $\text{CH}_3$ ), 80.2 (C-2), 127.4 (arom.-CH), 128.8 (arom.-CH), 129.1 (arom.-CH), 138.1 (arom.-C<sub>ipso</sub>), 207.2 (C-1) ppm. GC-MS (70 eV):  $m/z$  (%) = 150 [ $\text{M}^+$ ] (55), 107 [ $\text{C}_7\text{H}_7\text{O}^+$ ] (75), [ $\text{C}_2\text{H}_3\text{O}^+$ ] (33).

**(*R*)-2-Hydroxy-1-(4-methoxyphenyl)propan-1-one ((*R*)-**28**).** The synthesis was performed as described in ref. 18. Spectroscopic data fully agreed with those previously published.

**(*S*)-2-Hydroxy-1-(4-methoxyphenyl)propan-1-one ((*S*)-**28**).** The synthesis was carried out according to the literature.<sup>16,17</sup> Spectroscopic data are in full agreement with those previously published.

The biocatalytic syntheses of 2-hydroxy ketones **15–17**, **29–30** and **31** were conducted as previously described.<sup>19–22</sup>

### 2.3. Cloning, expression and purification of recombinant ADHs

Cloning, expression and purification procedures of recombinant ADHs can be found in the ESI.†

### 2.4. Enzyme activity assays

Activity measurements of ADHs were performed spectrophotometrically at 340 nm by determining the consumption of NAD(P)H at 30 °C in a half-micro cuvette (total volume: 1 mL) for 60 seconds. One unit (U) of activity is defined as the amount of enzyme which catalyses the consumption of 1  $\mu\text{mol}$  of NAD(P)H per minute in an appropriate buffer system (see Table 2) at 30 °C. The standard activity tests were conducted using benzaldehyde (10 mM) (ADHT and RADH) or acetophenone (10 mM) (LBADH) as substrate. All activity measurements were performed in triplicate.

**Investigation of the substrate ranges with crude cell extracts.** The reaction mixture for screening the activities of the crude cell extracts contained 10 mM of each substrate and 0.2 mM NAD(P)H in 50 mM TEA-HCl buffer, pH 7.0, if not otherwise stated (Table 2 and Table S2, ESI†). Background activity was determined with crude cell extracts prepared from an empty vector control of the respective recombinant strains which was subtracted from activities of crude cell extracts containing the respective ADHs.

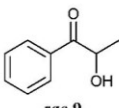
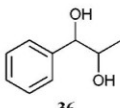
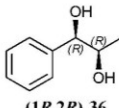
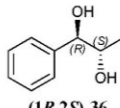
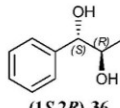
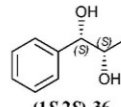
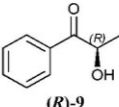
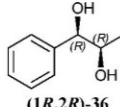
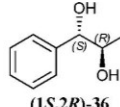
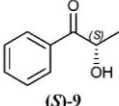
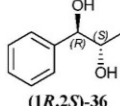
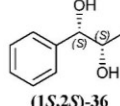
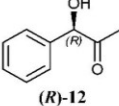
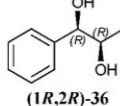
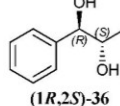
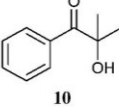
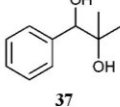
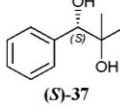
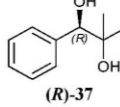
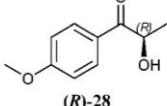
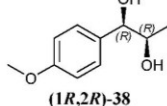
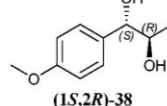
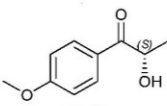
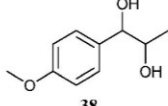
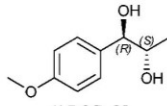
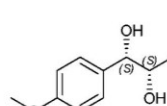
**Investigation of the substrate specificity for RADH.** The activity assay was conducted under optimised conditions for the reduction reaction. The assay mixture contained 10 mM of each substrate, if not otherwise stated (Table 4) and 0.2 mM of NADPH in 50 mM TEA-HCl buffer with 0.8 mM  $\text{CaCl}_2$ , pH 7.5. For the activity assay 6.5  $\mu\text{g mL}^{-1}$  of isolated RADH was applied.

**Determination of the protein concentration.** For determination of the protein concentration, the method of Bradford<sup>23</sup> using bovine serum albumin as a standard (Fermentas) was applied.

### 2.5. Chemical syntheses of reference compounds

In Table 1 all possible products of the enzymatic reduction of *rac*-**9**, (*R*)-**9**, (*S*)-**9**, **10**, (*R*)-**12**, (*R*)-**28** and (*S*)-**28** are summarised. Reduction of the prochiral carbonyl group of **10** can only yield the (*R*)- or (*S*)-diol **37** (Table 1). The reduction of *rac*-**9**, (*R*)-**9**, (*S*)-**9** and (*R*)-**12** may yield four stereoisomers of 1-phenylpropane-1,2-diol (**36**), whereas the reduction of (*R*)-**28** and (*S*)-**28** can theoretically give up to four

**Table 1** Synthesised stereoisomers of different 1,2-diols as reference compounds

Substrate		Products			
					
					
					
					
					
					
					

stereoisomers of the 1-(4-methoxyphenyl)-propane-1,2-diol (**38**) depending on the employed enzyme. As will be seen in the discussion, neither a racemisation nor a tautomerisation occurs under the applied conditions for the enzymatic reductions.

In order to assign the absolute configuration of the enzymatically obtained 1,2-diols, compounds **36–38** were chemically synthesised as described below.

$^1\text{H}$ -NMR and  $^{13}\text{C}$ -NMR spectra were recorded on a Bruker Advance-DRX 600 spectrometer in  $\text{CDCl}_3$  with TMS ( $\text{Me}_4\text{Si}$ ) as the internal standard. Chemical shifts are given in ppm relative to the  $\text{Me}_4\text{Si}$  ( $^1\text{H}$ ,  $\text{Me}_4\text{Si}$  = 0 ppm) or relative to the resonance of the solvent ( $^{13}\text{C}$ ,  $\text{CDCl}_3$  = 77.2 ppm). GC-MS analysis was performed on a Varian CP-3800/Saturn 2000 instrument equipped with HP-5 column (30 m  $\times$  0.32 mm  $\times$  0.25  $\mu\text{m}$ ). The sample analysis (1  $\mu\text{L}$ ) was carried out in following program:

injection temperature: 60  $^\circ\text{C}$  and kept constant for 3 min, then in a slope 20.0  $^\circ\text{C min}^{-1}$  temperature was increased to 180  $^\circ\text{C}$  and subsequently kept constant for 5 min. Optical rotation was measured at 20  $^\circ\text{C}$  on a Jasco P-2000 polarimeter using the sodium D-line.

**(2R,3R)-2-Methyl-3-phenyloxirane (35).** The substrate for further synthesis of **36** was synthesised according to a modified procedure of Klawonn *et al.*<sup>24</sup> Briefly, to a stirred solution of *meta*-chloroperoxybenzoic acid (*m*-CPBA, 1.60 g, 10.5 mmol) in 10 mL of dry diethyl ether, *trans*- $\beta$ -methylstyrene (1.18 g, 10.0 mmol) at 0  $^\circ\text{C}$  was added dropwise. The reaction was continued for further 12 h until no *trans*- $\beta$ -methylstyrene could be detected anymore by thin layer chromatography (TLC). The reaction was stopped by addition of saturated



NaHCO<sub>3</sub> (50 mL) and then extracted four times with ethyl acetate (EtOAc, 4 × 20 mL). The combined organic layers were dried over MgSO<sub>4</sub>, filtrated and concentrated under reduced pressure. Subsequent filter flash chromatography on silica (eluent: PE/EtOAc 96/4) yielded the epoxide in 92% yield (1.23 g, 9.2 mmol) as a colourless oil. Spectroscopic data are in full agreement with those previously published.<sup>24</sup> *R*<sub>f</sub> [(PE/EtOAc 96/4) = 0.52]. <sup>1</sup>H-NMR (600 MHz, CDCl<sub>3</sub>): 1.45 (d, <sup>3</sup>J<sub>Me,2</sub> = 5.2 Hz, 3 H, Me), 3.03 (dq, <sup>3</sup>J<sub>2,1</sub> = 2.1 Hz, <sup>3</sup>J<sub>2,Me</sub> = 5.2 Hz, 1 H, 2-H), 3.57 (d, <sup>3</sup>J<sub>1,2</sub> = 2.2 Hz, 1 H, 1-H), 7.24–7.35 (m, 5 H, arom.-H) ppm. <sup>13</sup>C-NMR (151 MHz, CDCl<sub>3</sub>): 17.9 (C-3), 59.0 (C-2), 59.5 (C-2), 125.6 (arom.-CH), 128.0 (arom.-CH), 128.4 (arom.-CH), 137.8 (arom.-C<sub>ipso</sub>) ppm. GC-MS (70 eV): *m/z* (%) = 135 [(M – H)<sup>+</sup>] (100), 118 [C<sub>8</sub>H<sub>6</sub>O<sup>+</sup>] (33), 105 [C<sub>8</sub>H<sub>9</sub><sup>+</sup>] (23), 91 [C<sub>7</sub>H<sub>7</sub><sup>+</sup>] (20).

***syn/anti*-1-Phenylpropane-1,2-diol (36).** According to a known literature procedure,<sup>25</sup> the epoxide (35) (1.10 g, 8.20 mmol) was suspended in 18 mL millipore water. The reaction was run for 24 h at 60 °C and monitored by TLC. After complete consumption of the starting material, the reaction mixture was extracted four times with EtOAc (4 × 20 mL) and the combined organic layers were dried over Na<sub>2</sub>SO<sub>4</sub>. The organic phase was filtrated and concentrated under reduced pressure. Subsequent filter flash chromatography on silica gel (eluent: PE/EtOAc 70/30) yielded 85.5% of the diol 36 (1.07 g, 7.02 mmol) as a colourless oil in a diastereomeric mixture (dr [*syn/anti*] = 60/40). The oil slowly crystallised upon resting *syn*-diol.<sup>7</sup> *R*<sub>f</sub> [(PE/EtOAc 70/30) = 0.17]. <sup>1</sup>H-NMR (600 MHz, CDCl<sub>3</sub>): 1.04 (d, <sup>3</sup>J<sub>1,2</sub> = 6.3 Hz, 3 H, CH<sub>3</sub>), 2.69 (brs, 1 H, OH), 2.90 (brs, 1 H, OH), 3.84 (dq, <sup>3</sup>J<sub>2,3</sub> = 6.7 Hz, <sup>3</sup>J<sub>2,1</sub> = 6.3 Hz, 1 H, 2-H), 4.34 (brd, <sup>3</sup>J<sub>3,2</sub> = 7.3 Hz, 1 H, 3-H), 7.28–7.35 (m, 5 H, arom.-H) ppm. <sup>13</sup>C-NMR (151 MHz, CDCl<sub>3</sub>): 18.8 (C-3), 72.2 (C-2), 79.5 (C-1), 126.9 (arom.-CH), 128.2 (arom.-CH), 128.5 (arom.-CH), 141.1 (arom.-C<sub>ipso</sub>) ppm. GC-MS (70 eV): *m/z* (%) = 135 [(M – OH)<sup>+</sup>] (15), 108 [C<sub>7</sub>H<sub>7</sub>O<sup>+</sup>] (95), 45 [C<sub>2</sub>H<sub>5</sub>O<sup>+</sup>] (20).

***syn*-1-Phenylpropane-1,2-diol ((1*R*,2*R*)-36 and (1*S*,2*S*)-36).** According to the literature,<sup>26</sup> *N*-methylmorpholine-*N*-oxide (NMO, 1.54 g, 13.2 mmol) and potassium osmate K<sub>2</sub>OsO<sub>4</sub>·2H<sub>2</sub>O (14.1 mg, 42.4 μmol) were suspended in 10 mL of a 60/40 acetone/water mixture. To this solution *trans*-β-methylstyrene (500 mg, 4.23 mmol, dissolved in 10 mL of a 60/40 acetone/water solution) was added dropwise over a time period of 20 minutes. The mixture was stirred until no more starting material could be detected (TLC control; ~2 hours) and the reaction was then stopped by the addition of Na<sub>2</sub>SO<sub>3</sub> (1.25 g, 9.94 mmol). The reaction mixture was poured into 50 mL millipore water and was extracted four times with dichloromethane (4 × 15 mL). The combined organic layers were dried over MgSO<sub>4</sub>, filtrated and concentrated under reduced pressure. Subsequent filter flash chromatography on silica (eluent: PE/EtOAc 70/30) gained the diastereomerically pure product [dr (*syn/anti*) > 99/1] in 99% yield (640 mg, 4.20 mmol) as a colourless powder.

**(1*S*,2*S*)-1-Phenylpropane-1,2-diol ((1*S*,2*S*)-36) and (1*R*,2*R*)-1-phenylpropane-1,2-diol ((1*R*,2*R*)-36).** According to the literature,<sup>27</sup> the alpha or beta reagent for Sharpless asymmetric dihydroxylation (AD-mix, 1.4 g) for the synthesis of (1*S*,2*S*)-36 or (1*R*,2*R*)-36,

respectively, was dissolved in 5 mL *tert*-butyl alcohol (*t*-BuOH) and 5 mL millipore water. The solution was cooled to 0 °C and treated with methanesulfonamide, CH<sub>3</sub>SO<sub>2</sub>NH<sub>2</sub> (81 mg, 852 μmol for (1*S*,2*S*)-36 and 95 mg, 1.0 mmol for (1*R*,2*R*)-36). After the addition of *trans*-β-methylstyrene, the reaction mixture was stirred for 12 hours in the case of (1*S*,2*S*)-36 and for 15 hours in the case of (1*R*,2*R*)-36, respectively, and then the reaction was stopped by the addition of Na<sub>2</sub>SO<sub>3</sub> (1.5 g, 11.9 mmol). The solution was poured into 30 mL millipore water and extracted four times with dichloromethane (4 × 15 mL). The combined organic layers were dried over Na<sub>2</sub>SO<sub>4</sub>, filtrated and concentrated under reduced pressure. Subsequent filter flash chromatography (eluent: PE/EtOAc 70/30) yielded 96% (124 mg, 0.81 mmol) of the diastereomerically pure enantiomer of the diol (1*S*,2*S*)-36 (dr [*syn/anti*] > 99/1; ee > 96%) as a colourless solid. Spectroscopic data are in full agreement with those previously published. [*α*]<sub>D</sub><sup>20</sup> = +53.8 (c 0.42, CHCl<sub>3</sub>, dr [*syn/anti*] > 99/1; ee > 96%). Literature data:<sup>7</sup> [*α*]<sub>D</sub><sup>20</sup> = +54.3 (c 1.9, CHCl<sub>3</sub>, de 98%). Diol (1*R*,2*R*)-36 was gained (dr [*syn/anti*] > 99/1; ee > 96%) with 85% yield (130 mg, 0.85 mmol) as a colourless solid. Spectroscopic data are in full agreement with those previously published. [*α*]<sub>D</sub><sup>20</sup> = –51.3 (c 0.46, CHCl<sub>3</sub>, dr [*syn/anti*] > 99/1; ee > 97%). Literature value for the opposite enantiomer:<sup>7</sup> [*α*]<sub>D</sub><sup>20</sup> = +54.3 (c 1.9, CHCl<sub>3</sub>, de 98%).

**2-Methyl-1-phenylpropane-1,2-diol (37).** According to the literature,<sup>26</sup> *N*-methylmorpholine-*N*-oxide (NMO, 1.10 g, 9.38 mmol) and the potassium osmate K<sub>2</sub>OsO<sub>4</sub>·2H<sub>2</sub>O (11.2 mg, 30.3 μmol) were suspended in 10 mL of a 60/40 acetone/water mixture. To this solution 2-methyl-1-phenyl-1-propene (400 mg, 3.03 mmol) was added dropwise (dissolved in 10 mL of a 60/40 acetone/water solution) within 20 minutes. The mixture was stirred until no more starting material could be detected (TLC control; ~3 hours) and then the reaction was stopped by the addition of Na<sub>2</sub>SO<sub>3</sub> (1.20 g, 9.38 mmol). The reaction mixture was poured into 50 mL millipore water and was extracted four times with dichloromethane (4 × 15 mL). The combined organic layers were dried over MgSO<sub>4</sub>, filtrated and concentrated under reduced pressure. Subsequent filter flash chromatography on silica (eluent: PE/EtOAc 70/30) yielded the diastereomerically pure [dr (*syn/anti*) > 99/1] product in 97% yield (489 mg, 2.95 mmol) as a colourless powder. Spectroscopic data are in full agreement with those previously published.<sup>28</sup> *R*<sub>f</sub> [(PE/EtOAc 80/20) = 0.11]. <sup>1</sup>H-NMR (600 MHz, CDCl<sub>3</sub>): 1.10 (s, 3 H, Me at C-2), 1.24 (s, 3 H, Me at C-2), 2.05 (brs, 1 H, OH at C-2), 2.55 (brd, <sup>3</sup>J<sub>OH,1</sub> = 2.5 Hz, 1 H, OH at C-1), 4.53 (brs, 1 H, 1-H), 7.25–7.39 (m, 5 H, arom.-CH) ppm. <sup>13</sup>C-NMR (151 MHz, CDCl<sub>3</sub>): 23.9 (Me at C-2), 26.6 (Me at C-2), 73.4 (C-2), 80.9 (C-1), 127.4 (arom.-CH), 127.9 (arom.-CH), 128.0 (arom.-CH), 140.6 (arom.-C<sub>ipso</sub>) ppm. GC-MS (70 eV): *m/z* (%) = 165 [(M – H)<sup>+</sup>] (1), 149 [C<sub>10</sub>H<sub>19</sub>O<sub>3</sub><sup>+</sup>] (90), 108 [C<sub>7</sub>H<sub>7</sub>O<sup>+</sup>] (100), 59 [C<sub>3</sub>H<sub>7</sub>O<sup>+</sup>] (60).

**(*S*)-2-Methyl-1-phenylpropane-1,2-diol ((*S*)-37) and (*R*)-2-methyl-1-phenylpropane-1,2-diol ((*R*)-37).** According to the literature,<sup>27</sup> the alpha or beta reagent for Sharpless asymmetric dihydroxylation (AD-mix, 0.7 g) for the synthesis of (*S*)-37 or (*R*)-37, respectively, was dissolved in 5 mL *t*-BuOH and 5 mL millipore water.



The solution was cooled to 0 °C and treated with methanesulfonamide, CH<sub>3</sub>SO<sub>2</sub>NH<sub>2</sub> (48 mg, 0.5 mmol). After the addition of 2-methyl-1-phenyl-1-propene (66.1 mg, 0.5 mmol), the reaction mixture was stirred at the same temperature for two days and then the reaction was stopped by the addition of Na<sub>2</sub>SO<sub>3</sub> (0.75 g, 5.95 mmol). The solution was poured into 30 mL millipore water and extracted four times with dichloromethane (4 × 15 mL). The combined organic layers were dried over Na<sub>2</sub>SO<sub>4</sub>, filtrated and concentrated under reduced pressure. Subsequent filter flash chromatography (eluent: PE/EtOAc 70/30) yielded the diastereomerically pure enantiomer of the diol ((*S*)-**37**) (dr [*syn/anti*] > 99/1; ee > 92%) in 94% yield (78.4 mg, 0.47 mmol) as a colourless solid. Spectroscopic data are in full agreement with those previously published. [ $\alpha$ ]<sub>D</sub><sup>20</sup> = +17.6 (c 0.56, EtOH, dr [*syn/anti*] > 99/1; ee > 92%). Literature value for the opposite enantiomer:<sup>28</sup> [ $\alpha$ ]<sub>D</sub><sup>20</sup> = -17.1 (c 1.0, EtOH, ee 91%). The diol ((*R*)-**37**) was obtained (dr [*syn/anti*] > 99/1; ee > 96%) in 97% yield (80.4 mg, 0.48 mmol) as a colourless solid. Spectroscopic data are in full agreement with those previously published. [ $\alpha$ ]<sub>D</sub><sup>20</sup> = -18.1 (c 0.54, EtOH, dr [*syn/anti*] > 99/1; ee > 96%). Literature value:<sup>28</sup> [ $\alpha$ ]<sub>D</sub><sup>20</sup> = -17.1 (c 1.0, EtOH, ee 91%).

**1-(4-Methoxyphenyl)propane-1,2-diol (**38**)**. To a stirred solution of *meta*-chloroperoxybenzoic acid (*m*-CPBA, 1.24 g, 8.11 mmol) in 10 mL dry diethyl ether was added *trans*-anethole (741 mg, 5.0 mmol) at 0 °C. The reaction mixture was stirred until no starting material could be detected (TLC control, ~12 hours). The reaction was stopped by the addition of saturated NaHCO<sub>3</sub> (50 mL) and then extracted four times with small portions of EtOAc (4 × 20 mL). Combined organic layers were dried over MgSO<sub>4</sub>, filtrated and concentrated under reduced pressure. The remaining liquid was diluted with 16 mL millipore water and heated to 60 °C for 24 hours. After cooling to room temperature, the solution was poured into saturated NaHCO<sub>3</sub> solution (50 mL) and extracted four times with small portions of EtOAc (4 × 20 mL). Combined organic layers were dried over MgSO<sub>4</sub>, filtrated and concentrated under reduced pressure. Subsequent filter flash chromatography on silica (eluent: PE/EtOAc 70/30) afforded a significant amount of the starting material and a diastereomeric mixture (dr [*syn/anti*] = 50/50) of the diol (**38**) in 23% yield (208 mg, 1.14 mmol). Spectroscopic data are in full agreement with those previously published. *R*<sub>f</sub> [(PE/EtOAc 70/30) = 0.14]. GC-MS (70 eV) = 181 [(M-H)<sup>+</sup>] (5), 137 [C<sub>8</sub>H<sub>9</sub>O<sub>2</sub><sup>+</sup>] (100), 77 (C<sub>6</sub>H<sub>5</sub><sup>+</sup>) (19). Melting point: 95 °C; literature value: 98 °C.

*syn*:<sup>29,30</sup> <sup>1</sup>H NMR (600 MHz, CDCl<sub>3</sub>): 1.03 (d, <sup>3</sup>*J*<sub>Me,2</sub> = 6.3 Hz, 3 H, CH<sub>3</sub>), 2.57 (brd, <sup>3</sup>*J*<sub>OH,2</sub> = 3.1 Hz, 1 H, OH), 2.63 (brd, <sup>3</sup>*J*<sub>OH,1</sub> = 3.1 Hz, 1 H, OH), 3.80 (s, 3 H, OMe), 3.82 (ddq, <sup>3</sup>*J*<sub>2,1</sub> = 7.2 Hz, <sup>3</sup>*J*<sub>2,Me</sub> = 6.2 Hz, <sup>3</sup>*J*<sub>2,OH</sub> = 3.0 Hz, 1H, 2-H), 4.31 (d, <sup>3</sup>*J*<sub>1,2</sub> = 7.6 Hz, 1H, 1-H), 6.88 (d, <sup>3</sup>*J*<sub>1',2'</sub> = 8.7 Hz, 2H, arom.-H), 7.25 (d, <sup>3</sup>*J*<sub>2',1'</sub> = 8.7 Hz, 2 H, arom.-H) ppm. <sup>13</sup>C-NMR (151 MHz, CDCl<sub>3</sub>): 18.8 (C-3), 55.3 (OMe), 72.3 (C-2), 79.2 (C-1), 113.9 (arom.-CH), 128.0 (arom.-CH), 133.2 (arom.-C<sub>ipso</sub>), 159.5 (arom.-C<sub>ipso</sub>) ppm.

*anti*:<sup>31</sup> <sup>1</sup>H NMR (600 MHz, CDCl<sub>3</sub>): 1.09 (d, <sup>3</sup>*J*<sub>Me,2</sub> = 6.4 Hz, 3 H, CH<sub>3</sub>), 2.50 (brs, 1 H, OH), 2.77 (brs, 1 H, OH), 3.80 (s, 3 H, OMe), 3.97 (ddq, <sup>3</sup>*J*<sub>2,1</sub> = 4.4 Hz, <sup>3</sup>*J*<sub>2,Me</sub> = 6.4 Hz, <sup>3</sup>*J*<sub>2,OH</sub> = 10.8 Hz, 1 H, 2-H), 4.59 (d, <sup>3</sup>*J*<sub>1,2</sub> = 4.5 Hz, 1 H, 1-H), 6.89 (d, <sup>3</sup>*J*<sub>1',2'</sub> = 8.7 Hz, 1 H, arom.-H), 7.28 (d, <sup>3</sup>*J*<sub>2',1'</sub> = 8.7 Hz,

1 H, arom.-H) ppm. <sup>13</sup>C-NMR (151 MHz, CDCl<sub>3</sub>): 17.5 (C-3), 55.3 (OMe), 71.3 (C-2), 77.3 (C-1), 113.8 (arom.-CH), 127.9 (arom.-CH), 132.5 (arom.-C<sub>ipso</sub>), 159.3 (arom.-C<sub>ipso</sub>) ppm.

***syn*-1-(4-Methoxyphenyl)propane-1,2-diol ((1*R*,2*R*)-**38** and (1*S*,2*S*)-**38**)**. To a stirred solution<sup>26</sup> of *N*-methylmorpholine-*N*-oxide (NMO, 1.23 g, 10.46 mmol) and potassium osmate K<sub>2</sub>OsO<sub>4</sub>·2H<sub>2</sub>O (12.4 mg, 33.7 μmol) in 10 mL a mixture of the *trans*-anethole (500 mg, 3.37 mmol) was added dropwise (dissolved in 10 mL of a 60/40 acetone/water solution). The mixture was stirred until no more starting material could be detected (TLC control; 2 hours) and the reaction was then stopped by the addition of Na<sub>2</sub>SO<sub>3</sub> (978 mg, 7.76 mmol). The reaction mixture was poured into 50 mL millipore water and was extracted four times with small portions of dichloromethane (4 × 15 mL). Combined organic layers were dried over MgSO<sub>4</sub>, filtrated and concentrated under reduced pressure. Subsequent filter flash chromatography on silica (eluent: PE/EtOAc 70/30) afforded the product with >86% yield (530 mg, 2.91 mmol) as a colourless powder. Spectroscopic data are in agreement with those previously published.<sup>29,30</sup>

**(1*S*,2*S*)-1-(4-Methoxyphenyl)propane-1,2-diol ((1*S*,2*S*)-**38** and (1*R*,2*R*)-1-(4-methoxyphenyl)propane-1,2-diol ((1*R*,2*R*)-**38**)**. The syntheses were conducted by employing the same procedure as described above for (1*R*,2*R*)-**36** and (1*S*,2*S*)-**36**. As substrate the *trans*-anethole (148 mg, 1.0 mmol) was added and the reactants were stirred for 48 hours. The reaction was stopped by the addition of Na<sub>2</sub>SO<sub>3</sub> (1.5 g, 11.90 mmol), and the mixture was poured into 30 mL millipore water and extracted four times with small portions of dichloromethane (4 × 15 mL). Combined organic layers were dried over Na<sub>2</sub>SO<sub>4</sub>, filtrated and concentrated under reduced pressure. Subsequent filter flash chromatography (eluent: PE/EtOAc 70/30) afforded the diastereomerically pure enantiomer of (1*S*,2*S*)-**38** (dr [*syn/anti*] > 99/1; ee > 96%) in 89% yield (162 mg, 0.89 mmol) as a colourless solid. Spectroscopic data are in full agreement with those previously published, [ $\alpha$ ]<sub>D</sub><sup>20</sup> = +51.9 (c 0.50, CHCl<sub>3</sub>, dr [*syn/anti*] > 99/1; ee > 96%). Diol (1*R*,2*R*)-**38** was gained (dr [*syn/anti*] > 99/1; ee > 96%) with 89% yield (162 mg, 0.89 mmol) as a colourless solid. Spectroscopic data: [ $\alpha$ ]<sub>D</sub><sup>20</sup> = -51.2 (c 0.50, CHCl<sub>3</sub>, dr [*syn/anti*] > 99/1; ee > 96%). The absolute configuration was confirmed by vibrational circular dichroism (VCD) analysis of the corresponding acetone derivatives **39** (see ESI† for details and experimental and calculated VCD-spectra).

## 2.6. Set-up of biotransformations

The stereoselectivity of all different ADH-catalysed reductions was determined using racemic or enantiomerically pure 2-hydroxy ketones (Table 3). Asymmetric biotransformations were conducted in 1.5 mL Eppendorf vials at 20 °C under constant shaking (500 rpm) for 24 hours in a total volume of 1 mL. The following conditions were used: TEA-HCl buffer (50 mM), pH 7.0, if not otherwise stated (Table S2, ESI†), 2-hydroxy ketone (10 mM), NADPH (1 mM), crude cell extracts containing overexpressed ADHs (2 mg mL<sup>-1</sup>) or isolated RADH (0.2 mg mL<sup>-1</sup>), respectively.

### 2.7. Chiral analysis of biotransformation products

Samples (1  $\mu$ L) were analysed by gas chromatography on a chiral CP-chirasil-DEX CB column (25 m  $\times$  0.25 mm  $\times$  0.25  $\mu$ m, Varian, Germany) with a flame ionisation detector (FID) and hydrogen as the carrier gas. Separation and determination of the enantiomeric excess of the non-derivatised stereoisomers of 1-phenylpropane-1,2-diol (**36**) was carried out using the following program: injection temperature: 140  $^{\circ}$ C, isotherm run for 30 min. The retention times of the stereoisomers (**36**) were as follows:  $R_{t(1S,2S)-36}$  = 24.1 min,  $R_{t(1R,2R)-36}$  = 25.8 min,  $R_{t(1S,2R)-36}$  = 27.4 min,  $R_{t(1R,2S)-37}$  = 28.5 min. The retention times of *anti*-diols (**36**) were assigned according to the literature.<sup>7</sup> For separation and determination of the enantiomeric excess of 2-methyl-1-phenylpropane-1,2-diol (**37**) the following program was applied: injection temperature: 110  $^{\circ}$ C, then in a linear gradient of 2.5  $^{\circ}$ C min<sup>-1</sup> the temperature was increased to 160  $^{\circ}$ C. The retention times of the enantiomers of 2-methyl-1-phenylpropane-1,2-diol (**37**) were:  $R_{t(S)-37}$  = 21.9 min,  $R_{t(R)-37}$  = 22.5 min. The determination of the diastereomeric excess of the stereoisomers of 1-(4-methoxyphenyl)propane-1,2-diol (**38**) was conducted by nuclear magnetic resonance (<sup>1</sup>H NMR).

## 3. Results and discussion

### 3.1. Activity-screening of ADHs

To study the potential of the eight well established oxidoreductases for the reduction of different 2-hydroxy ketones to 1,2-diols, initial tests were conducted with crude cell extracts of the recombinant strains. Additionally, some aldehydes and ketones were tested to complete the substrate range for small compounds. Among the eight enzymes only ADHT, LBADH and RADH showed significant activity towards the tested 2-hydroxy ketones under the applied conditions (Table S2 and Table S3, ESI<sup>†</sup>).

The first tests using crude cell extracts demonstrated the high potential of the three selected enzymes for the reduction of a broad range of 2-hydroxy ketones.

Almost every substrate could be reduced by at least one of the enzymes. ADHT and LBADH showed higher activities towards aliphatic substrates, whereas RADH clearly preferred sterically demanding mixed aromatic-aliphatic 2-hydroxy ketones. Also the sterically hindered substrate **10** was reduced by RADH effectively. Since the kinetic parameters for the reduction of the 2-hydroxy ketones are not yet known, the activities cannot be compared in terms of maximal velocities; they could be significantly higher at different substrate concentrations.

Conclusively, these initial results suggested that a broad range of chiral 1,2-diols was accessible by these three enzymes. In the following their stereoselectivity was studied for selected reactions.

### 3.2. Stereoselectivity studies

The three selected enzymes were investigated towards their stereoselectivity for the reduction reaction of seven different 2-hydroxy ketones (Table 3). The stereochemistry of the reduction products was determined by referring to the absolute configuration of the respective *syn*-diols (1*R*,2*R*)-**36**, (1*S*,2*S*)-**36**, (1*R*,2*R*)-**38**, and (1*S*,2*S*)-**38** from asymmetric Sharpless synthesis (Table 1). This allowed for assignment of retention times from chiral solid phase gas chromatography to a particular

**Table 2** Substrate specificity of crude cell extracts containing over-expressed alcohol dehydrogenases. The activity towards aldehydes, ketones and 2-hydroxy ketones was measured in triplicate following the consumption of NADPH (0.2 mM) at 340 nm at 30  $^{\circ}$ C. *c*—concentration; n.a.—activity not detectable; n.d.—activity not determined; 2-HPP—2-hydroxy propiophenone = 2-hydroxy-1-phenylpropan-1-one (**9**); (*R*)-PAC—phenylacetylcarbinol = 1-hydroxy-1-phenylpropan-2-one (**12**); Benzooin—2-hydroxy-1,2-diphenylethanone (**13**);  $\alpha$ -pyridoin—2-hydroxy-1,2-di(pyridine-2-yl)ethanone (**14**)

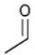
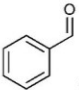
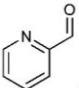
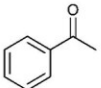
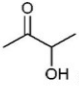
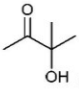
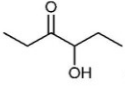
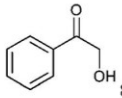
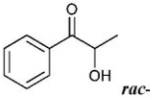
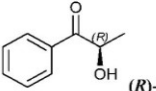
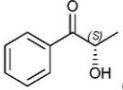
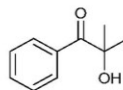
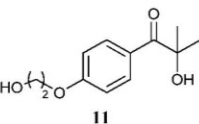
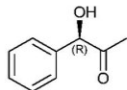
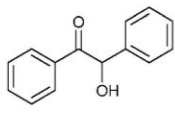
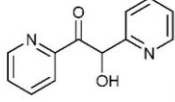
Substrate	c/mM	Specific activity/U mg <sup>-1</sup>		
		ADHT	LBADH	RADH
Aldehydes				
	10	6.0 ± 0.3	109.8 ± 3.1	n.a.
	10	5.9 ± 0.2	8.0 ± 0.1	3.0 ± 0.1
	10	7.7 ± 0.2	4.2 ± 0.0	4.1 ± 0.0
Ketones				
	10	7.7 ± 0.2	89.6 ± 1.0	2.4 ± 0.0
2-Hydroxy ketones: aliphatic				
	10	18.1 ± 0.1	127.8 ± 3.7	0.5 ± 0.0
	10	13.3 ± 0.3	36.7 ± 0.4	6.6 ± 0.1
	10	6.4 ± 0.3	66.1 ± 0.9	4.8 ± 0.1
2-Hydroxy ketones: 2-HPP and derivatives thereof				
	10	4.2 ± 0.1	28.7 ± 0.2	5.6 ± 0.1
	10	0.8 ± 0.0	3.5 ± 0.0	112.2 ± 7.2
	10	2.2 ± 0.2	3.0 ± 0.0	239.9 ± 7.6



Table 2 (continued)

Substrate	c/mM	Specific activity/U mg <sup>-1</sup>		
		ADHT	LBADH	RADH
 ( <i>S</i> )-9	10	2.9 ± 0.0	3.2 ± 0.1	10.0 ± 0.1
 10	10	4.4 ± 0.5	0.3 ± 0.0	21.5 ± 0.4
 11	5	0.7 ± 0.2	0.0 ± 0.0	4.1 ± 0.1
2-Hydroxy ketones: PAC				
 ( <i>R</i> )-12	10	3.5 ± 0.0	20.4 ± 0.2	36.3 ± 1.8
2-Hydroxy ketones: benzoin and α-pyridoin				
 13	10	0.1 ± 0.0	n.d.	n.a.
 14	10	0.5 ± 0.0	0.1 ± 0.0	0.6 ± 0.0

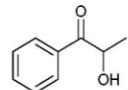
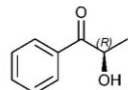
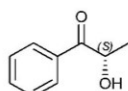
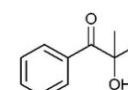
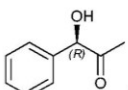
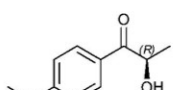
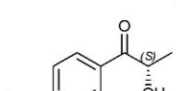
configuration of both *syn*-diols and the corresponding *anti*-diols. The chiroptical data for *syn*-36, (*R*)-37 and (*S*)-37 were in agreement with the literature values for the expected configurations.<sup>7,28</sup> Absolute configuration of the *syn*-38 enantiomers was confirmed by vibrational circular dichroism (VCD) analysis (see ESI† for spectra and details).

The only achiral substrate **10** was reduced by all three oxidoreductases with high stereoselectivity. Thereby LBADH yielded the (*S*)-enantiomer, while the other two gave the (*R*)-enantiomer with an ee of >99%.

The other tested substrates in Table 3 already contain one chiral centre ((*R*)-9, (*S*)-9, (*R*)-12, (*R*)-28 and (*S*)-28). This chiral centre is maintained during biotransformation in all cases and has no visible chiral induction on the formation of the second chiral centre, except substrate (*S*)-28, in which the diastereomeric excess drops to 87%. Under the applied reaction conditions we could not observe any racemisation or tautomerisation of the 2-hydroxy ketones. This is a clear advantage of the enzymatic approach. Almost all of the tested substrates were reduced with very high stereoselectivity (ee and de > 99%).

Conclusively, *syn*- and *anti*-1,2-diols with high diastereoselectivity were obtained by the appropriate choice of the biocatalyst.

Table 3 Stereoselectivity of selected biotransformations using crude cell extracts containing overexpressed alcohol dehydrogenases and purified RADH, respectively. ee and de were determined by chiral GC or <sup>1</sup>H NMR analyses. Reaction conditions: TEA-HCl (50 mM, pH 7.0), 30 °C, NADPH (1 mM), *rac*-9, (*R*)-9, (*S*)-9, **10**, (*R*)-12, (*R*)-28 and (*S*)-28 (10 mM, respectively), ADHs crude cell extract (2 mg mL<sup>-1</sup>) or purified RADH (0.2 mg mL<sup>-1</sup>), reaction time 24 h

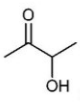
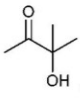
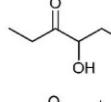
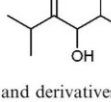
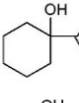
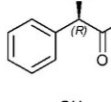
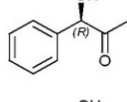
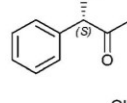
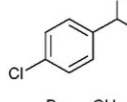
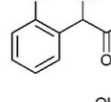
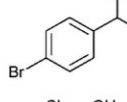
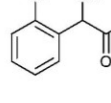
Substrate	Oxidoreductase		
	ADHT	LBADH	RADH
 <i>rac</i> -9	<i>dr</i> ( <i>syn/anti</i> ) 23.6:1 <sup>a</sup>	<i>dr</i> ( <i>syn/anti</i> ) 1:1 <sup>a</sup>	<i>dr</i> ( <i>syn/anti</i> ) 2:1 <sup>a</sup> 4:1 <sup>b</sup>
 ( <i>R</i> )-9	<i>de</i> > 99% ( <i>syn</i> ) <sup>a</sup>	<i>de</i> > 99% ( <i>anti</i> ) <sup>a</sup>	<i>de</i> > 99% ( <i>syn</i> ) <sup>a,b</sup>
 ( <i>S</i> )-9	<i>de</i> > 99% ( <i>anti</i> ) <sup>a</sup>	<i>de</i> > 99% ( <i>syn</i> ) <sup>a</sup>	<i>de</i> > 99% ( <i>anti</i> ) <sup>a,b</sup>
 10	<i>ee</i> > 99% <sup>a</sup>	<i>ee</i> > 99% <sup>a</sup>	<i>ee</i> > 99% <sup>a,b</sup>
 ( <i>R</i> )-12	<i>de</i> > 99% ( <i>anti</i> ) <sup>a</sup>	<i>de</i> 89% ( <i>syn</i> ) <sup>a</sup>	<i>de</i> > 99% ( <i>anti</i> ) <sup>a,b</sup>
 ( <i>R</i> )-28	n.d.	n.d.	<i>de</i> > 99% ( <i>syn</i> ) <sup>b,c,d</sup>
 ( <i>S</i> )-28	n.d.	n.d.	<i>de</i> 87% ( <i>anti</i> ) <sup>b,c</sup>

ee—enantiomeric excess, de—diastereomeric excess, dr—diastereomeric ratio, n.d.—not determined.<sup>a</sup> Employing crude cell extracts with overexpressed ADHs. <sup>b</sup> Employing purified RADH. <sup>c</sup> de determined by <sup>1</sup>H NMR measurement. <sup>d</sup> Absolute configuration confirmed by VCD studies.

The diastereomeric ratio of the *syn/anti*-diols provided information about the enzyme's selectivity towards the two respective enantiomers of the substrate. This was specifically tested with both enantiomers of 2-HPP (**9**), which were accepted by all tested enzymes and reduced selectively. Whereas LBADH reduced both enantiomers with the same velocity under the applied conditions, RADH and ADHT preferred the (*R*)-enantiomer of **9** yielding diastereomeric ratios (*syn/anti*) of 2:1 (RADH) and 23.6:1 (ADHT), respectively.

LBADH showed inverse stereoselectivity compared to the other tested oxidoreductases. Interestingly for all of these enzymes, the location of the already existing chiral centre in

**Table 4** Initial rate activities of RADH towards the reduction of different 2-hydroxy ketones. Measurements were performed spectrophotometrically in 50 mM TEA buffer, 0.8 mM calcium chloride, pH 7.5 at 30 °C by following the decrease of NADPH (0.2 mM) at 340 nm for 60 s. Each reaction contained 6.5  $\mu\text{g mL}^{-1}$  RADH

Substrate	<i>c</i> /mM	Specific activity/U $\text{mg}^{-1}$
<b>Acyloins</b>		
	10	$1.1 \pm 0.0$
	10	$9.8 \pm 0.0$
	10	$5.1 \pm 0.1$
	10	$0.8 \pm 0.1$
<b>PAC and derivatives thereof</b>		
	10	$49.3 \pm 1.1$
	10	$61.9 \pm 1.9$
	10	$19.0 \pm 0.5$
	10	$60.0 \pm 2.4$
	Saturated	$0.7 \pm 0.1$
	Saturated	$0.9 \pm 0.0$
	Saturated	$0.1 \pm 0.1$
	1	$0.2 \pm 0.0$

**Table 4 (continued)**

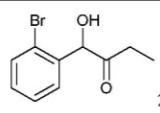
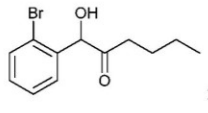
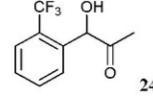
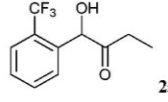
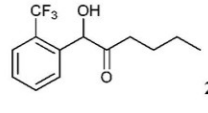
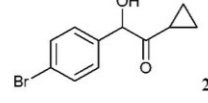
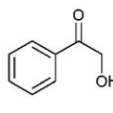
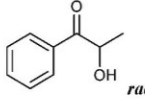
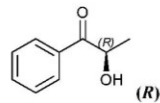
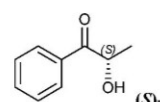
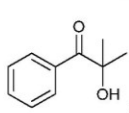
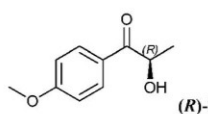
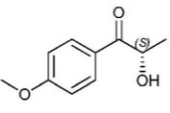
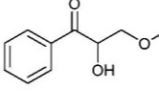
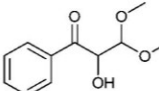
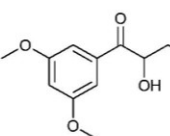
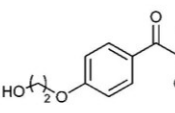
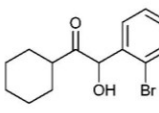
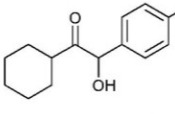
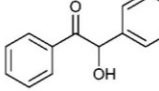
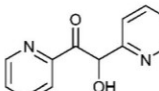
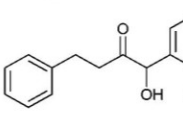
Substrate	<i>c</i> /mM	Specific activity/U $\text{mg}^{-1}$
	5	$0.2 \pm 0.0$
	1	$0.2 \pm 0.1$
	5	$0.5 \pm 0.0$
	5	$1.1 \pm 0.1$
	1	$0.3 \pm 0.0$
	Saturated	$0.6 \pm 0.2$
<b>2-HPP and derivatives thereof</b>		
	10	$4.3 \pm 0.1$
	10	$259.2 \pm 3.5$
	10	$362.6 \pm 1.9$
	10	$17.1 \pm 0.3$
	10	$44.4 \pm 0.5$
	10	$138.7 \pm 1.8$

Table 4 (continued)

Substrate	c/mM	Specific activity/U mg <sup>-1</sup>
 (S)-28	10	17.4 ± 0.2
 29	10	0.6 ± 0.0
 30	10	0.2 ± 0.1
 31	10 <sup>a</sup>	Absorption limitation
 11	5	6.2 ± 0.3
Other substrates		
 32	Saturated	0.1 ± 0.0
 33	Saturated	0.00
 13	Saturated	0.00
 14	Saturated <sup>b</sup>	0.4 ± 0.0
 34	Saturated	0.3 ± 0.0

<sup>a</sup> Absorption limitations occurred already at 1 mM of substrate concentration. <sup>b</sup> Saturated substrate solution, diluted two-fold because of absorption limitations.

two similar 2-hydroxy ketones resulted in the formation of inverse product stereoselectivities, e.g. (R)-PAC ((R)-12) and (R)-HPP ((R)-9) were reduced to the respective *anti*- and *syn*-diols. With ADHT and RADH (R)-2-HPP ((R)-9) was

reduced (R)-selectively to the *syn*-product (1R,2R)-36, while (R)-PAC ((R)-12) was reduced (S)-selectively yielding the *anti*-product (1R,2S)-36. Besides, LBADH catalysed also the formation of the *syn*-diol (1R,2R)-36 by (R)-selective reduction of (R)-PAC ((R)-12) (Table 3). This was caused by the orientation of the substrate in the enzymes' active sites, where the cofactor's hydride ion attack could occur either from the *si*-face of the reduced molecule or from the *re*-face, depending on the enzyme.<sup>32,33</sup>

These data demonstrate that at least all four different stereoisomers of the methyl-phenylpropanediols are now accessible with the three tested ADHs, depending on the chirality of the starting compound and the stereoselectivity of the enzyme.

### 3.3. Detailed characterisation of RADH's substrate range

The high potential of RADH to reduce bulky-bulky 2-hydroxy ketones (Table 2) motivated us to characterise the catalytic potential of this enzyme in more detail. Therefore, a purification procedure was established to get access to the pure biocatalyst by avoiding potential side effects of the crude cell extract, and to allow quantitative measurements. Detailed characterisation of the enzyme, which will be published elsewhere (manuscript in preparation) revealed the addition of CaCl<sub>2</sub> as essential to maintain the stability of the purified enzyme. To analyse the substrate range of RADH in more detail, its initial rate activities towards the reduction of 34 different 2-hydroxy ketones were analysed.

A screening of 2-hydroxy ketones with isolated RADH confirmed the trend already observed with crude cell extracts, demonstrating that this enzyme was extremely active towards the reduction of bulky-bulky compounds. The highest activity among the tested substrates was found with (R)-2-HPP ((R)-9), which was reduced to the respective vicinal 1,2-diol with about 360 U mg<sup>-1</sup>, followed by racemic 2-HPP (*rac*-9), with a specific activity of 260 U mg<sup>-1</sup>, and (R)-*p*-methoxy-2-HPP ((R)-28) with about 140 U mg<sup>-1</sup>. However, these activities could not be compared in absolute numbers as they do not necessarily represent the maximal velocity.

Regarding two very similar molecules such as (R)-2-HPP ((R)-9) and (R)-PAC ((R)-12), the relative position of the hydroxyl- and the keto group has significant impact on RADH's activity, since (R)-2-HPP ((R)-9) is about 6-fold faster converted to the respective 1,2-diol than (R)-PAC ((R)-12). This goes along with data obtained with the crude cell extract where a similar difference (6.5-fold) was observed (Table 2).

Our results demonstrate that RADH prefers 2-HPP-derivatives as excellent substrates for reductions. Although PAC and its derivatives are reduced with good activities as well, the reduction of the keto function next to the aromatic ring seems to be preferred over the reduction of the keto group next to the aliphatic side chain. Additionally, although the activity towards the sterically extremely demanding bulky-bulky substrates 14 and 34 is rather low, it is worth pointing out that they are converted at all.

As already visible with the crude cell extract, the chiral centre of chiral substrates has a strong influence on the specific activity of the RADH. For example (S)-*p*-methoxy-2-HPP ((S)-28) is reduced with a specific activity of 17 U mg<sup>-1</sup> while the (R)-enantiomer ((R)-28) is reduced 8-fold faster (139 U mg<sup>-1</sup>). The same holds for (R)-2-HPP ((R)-9) and (S)-2-HPP ((S)-9),



supporting the results obtained with crude cell extracts (Table 2). An inverse situation was observed in the case of 1-hydroxy-1-phenylbutan-2-one ((*R*)-**17**, (*S*)-**17**), where the (*S*)-enantiomer ((*S*)-**17**) is reduced 3-fold faster than the (*R*)-enantiomer ((*R*)-**17**).

The enzyme exhibits severe activity differences towards substrates not only with respect to the position of the carbonyl group but also regarding the configuration of the adjacent asymmetric chiral carbon atom.

Conclusively not only the position of the hydroxyl group to be reduced has a strong influence on the enzyme's activity but also the configuration of the asymmetric carbon atom is decisive.

Therewith the results obtained with the purified enzyme confirm the data obtained with crude cell extracts (Table 3). The only difference was a shift of the ratio of *syn* and *anti* diol formation from racemic 2-HPP from 2:1 (crude cell extract) to 4:1 (purified RADH).

#### 4. Conclusions and outlook

We demonstrated the high potential of biocatalysis for the stereoselective synthesis of a broad range of 1,2-diols starting from chiral 2-hydroxy ketones. Among the enzymes tested, ADHT, LBADH and especially RADH showed high catalytic activities and stereoselectivities and enable the excess to all stereoisomers of a respective 1,2-diol, particularly to *anti*-diols.

RADH was isolated for the first time and a protocol to keep the enzyme stable in buffer was established. The reduction activity of the isolated enzyme was studied with 34 different 2-hydroxy ketones (Table 4), where only two (benzoin **13** and 2-(4-bromophenyl)-1-cyclohexyl-2-hydroxyethanone **33**) did not show any activity at all, which might be due to the low solubility of these compounds. Highest activities were observed with (*R*)-2-HPP ((*R*)-**9**) and its 4-methoxy derivative ((*R*)-**28**) with a methyl group next to the prochiral carbonyl group.

In our ongoing studies RADH is evaluated in biotransformations in order to elucidate the stability of the enzyme in a purified form and to identify optimal reaction parameters.

#### Acknowledgements

This work was financed by the Marie Curie Initial Training Network "BIOTRAINS—a European biotechnology training network for the support of chemical manufacturing", grant agreement no. 238531, and partially financed by the DFG (German Research Foundation) in frame of the Research Group FOR 1296.

#### Notes and references

- 1 M. Hall and A. S. Bommaris, *Chem. Rev.*, 2011, **111**, 4088–4110.
- 2 T. Daußmann, H. G. Hennemann, T. C. Rosen and P. Dünkemann, *Chem. Eng. Technol.*, 2006, **78**, 249–255.
- 3 I. Lavandera, A. Kern, B. Ferreira-Silva, A. Glieder, S. de Wildeman and W. Kroutil, *J. Org. Chem.*, 2008, **73**, 6003–6005.
- 4 R. N. Patel, *Coord. Chem. Rev.*, 2008, **252**, 659–701.
- 5 H. C. Kolb, M. S. VanNieuwenhze and K. B. Sharpless, *Chem. Rev.*, 1994, **94**, 2483–2547.
- 6 K. Goldberg, K. Schroer, S. Lütz and A. Liese, *Appl. Microbiol. Biotechnol.*, 2007, **76**, 237–248.
- 7 D. Kihumbu, T. Stillger, W. Hummel and A. Liese, *Tetrahedron: Asymmetry*, 2002, **13**, 1069–1072.
- 8 S. Shanmuganathan, D. Natalia, L. Greiner and P. Dominguez de Maria, *Green Chem.*, 2012, **14**, 94–97.
- 9 S. M. Husain, T. Stillger, P. Dünkemann, M. Lodige, L. Walter, E. Breitling, M. Pohl, M. Burchner, I. Krossing, M. Müller, D. Romano and F. Molinari, *Adv. Synth. Catal.*, 2011, **353**, 2359–2362.
- 10 S. E. O'Toole, C. A. Rose, S. Gundala, K. Zeitler and S. J. Connon, *J. Org. Chem.*, 2011, **76**, 347–357.
- 11 C. A. Rose, S. Gundala, S. J. Connon and K. Zeitler, *Synthesis*, 2011, 190–198.
- 12 C. Q. Chen, X. H. Feng, G. Z. Zhang, Q. Zhao and G. S. Huang, *Synthesis*, 2008, 3205–3208.
- 13 S. B. Sopaci, I. Simsek, B. Tural, M. Volkan and A. S. Demir, *Org. Biomol. Chem.*, 2009, **7**, 1658–1664.
- 14 P. Dominguez de Maria, T. Stillger, M. Pohl, S. Wallert, K. Drauz, H. Gröger, H. Trauthwein and A. Liese, *J. Mol. Catal. B: Enzym.*, 2006, **38**, 43–47.
- 15 A. S. Demir, M. Pohl, E. Janzen and M. Müller, *J. Chem. Soc., Perkin Trans. 1*, 2001, 633–635.
- 16 T. Dünwald, A. S. Demir, P. Siegert, M. Pohl and M. Müller, *Eur. J. Org. Chem.*, 2000, 2161–2170.
- 17 N. Kurlmann, M. Lara, M. Pohl, W. Kroutil and A. Liese, *J. Mol. Catal. B: Enzym.*, 2009, **61**, 111–116.
- 18 A. S. Demir, O. Sesenoglu, E. Eren, B. Hosrik, M. Pohl, E. Janzen, D. Kolter, R. Feldmann, P. Dünkemann and M. Müller, *Adv. Synth. Catal.*, 2002, **344**, 96–103.
- 19 D. Rother, G. Kolter, T. Gerhards, C. L. Berthold, E. Gauchenova, M. Knoll, J. Pleiss, M. Müller, G. Schneider and M. Pohl, *ChemCatChem*, 2011, **3**, 1587–1596.
- 20 P. Dominguez de Maria, M. Pohl, D. Gocke, H. Gröger, H. Trauthwein, T. Stillger, L. Walter and M. Müller, *Eur. J. Org. Chem.*, 2007, 2940–2944.
- 21 P. Lehwald, M. Richter, C. Rohr, H. W. Liu and M. Müller, *Angew. Chem., Int. Ed.*, 2010, **49**, 2389–2392.
- 22 A. S. Demir, O. Sesenoglu, P. Dünkemann and M. Müller, *Org. Lett.*, 2003, **5**, 2047–2050.
- 23 M. M. Bradford, *Anal. Biochem.*, 1976, **72**, 248–254.
- 24 M. Klawonn, M. K. Tse, S. Bhor, C. Dobler and M. Beller, *J. Mol. Catal. A: Chem.*, 2004, **218**, 13–19.
- 25 Z. Wang, Y. T. Cui, Z. B. Xu and J. Qu, *J. Org. Chem.*, 2008, **73**, 2270–2274.
- 26 N. Schöne, *Doctoral thesis*, Universität Stuttgart, 2007.
- 27 K. B. Sharpless, W. Amberg, Y. L. Bennani, G. A. Crispino, J. Hartung, K. S. Jeong, H. L. Kwong, K. Morikawa, Z. M. Wang, D. Q. Xu and X. L. Zhang, *J. Org. Chem.*, 1992, **57**, 2768–2771.
- 28 S. Negishi, H. Ishibashi and J. Matsuo, *Org. Lett.*, 2010, **12**, 4984–4987.
- 29 S. Trudeau, J. B. Morgan, M. Shrestha and J. P. Morken, *J. Org. Chem.*, 2005, **70**, 9538–9544.
- 30 J. B. Morgan, S. P. Miller and J. P. Morken, *J. Am. Chem. Soc.*, 2003, **125**, 8702–8703.
- 31 D. Acetti, E. Brenna and C. Fuganti, *Tetrahedron: Asymmetry*, 2007, **18**, 488–492.
- 32 T. Matsuda, R. Yamanaka and K. Nakamura, *Tetrahedron: Asymmetry*, 2009, **20**, 513–557.
- 33 K. Nakamura, R. Yamanaka, T. Matsuda and T. Harada, *Tetrahedron: Asymmetry*, 2003, **14**, 2659–2681.

### Stereoselective synthesis of bulky 1,2-diols with alcohol dehydrogenases

Justyna Kulig<sup>a</sup>, Robert Simon<sup>a,b</sup>, Christopher A. Rose<sup>c</sup>, Kerstin Zeitler<sup>c</sup>, Wolfgang Kroutil,  
Martina Pohl<sup>a</sup> and Dörte Rother<sup>a</sup>

<sup>a</sup>Institute of Bio- and Geosciences, IBG-1: Biotechnology, Forschungszentrum Jülich GmbH, 52425 Jülich,  
Germany

<sup>b</sup>Institute of Chemistry, Organic and Bioorganic Chemistry, University of Graz, Heinrichstrasse 28, 8010 Graz,  
Austria

<sup>c</sup>Institute of Organic Chemistry, University of Regensburg, Universitätsstrasse 31, 93053 Regensburg, Germany

### Supplementary Information

Table of contents:

1. Cloning, expression and purification of recombinant ADHs
2. Activity-screening of ADHs
3. Determination of absolute configuration of (1*R*,2*R*)-**38** and (1*S*,2*S*)-**38**
4. References

## 1. Cloning, expression and purification of recombinant ADHs

### 1.1. Strains and plasmids

*Escherichia coli* strains BL21(DE3) and DH5 $\alpha$ , as well as the pET-22b(+) vector were purchased from Novagen (Madison, USA). The strain DH5 $\alpha$  was used as a host organism for cloning, whereas BL21(DE3) was implemented for expression.

The cloning vectors p\_RADH and p\_SADH containing sequence optimised *radh* and *sadh* genes<sup>1, 2</sup> were subcloned as described below. The corresponding genes were synthesised by GeneArt. The *adh*t gene was synthesised by Sloning BioTechnology GmbH, Germany. The HLADH was purchased from Evocatol (Düsseldorf, Germany). The CPCR-clone was obtained from the research group of M. Ansorge-Schumacher (Berlin, Germany). The LBADH-clone was obtained from W. Hummel (Jülich, Germany). The FADH-clone was kindly provided by T. Oikawa (Kansai University, Japan) and the clone with TADH was from A. Schmid (Dortmund, Germany). References concerning the cloning strategies of these respective genes can be found in the literature mentioned in Table 1.

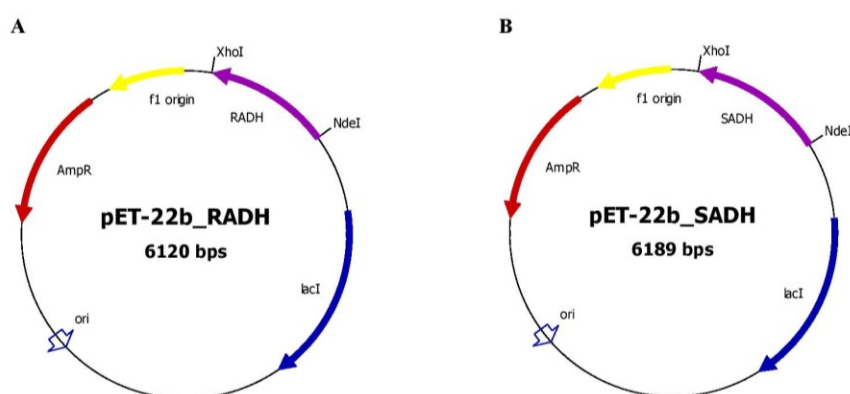
**Table 1.** Details concerning vector harbouring the genes for the studied oxidoreductases and conditions of cell cultivation.

	ADHT	CPCR	FADH	Oxidoreductase		RADH	SADH	TADH
	pET-22b(+)	pET-26b(+)	pET-3b	HLADH	LBADH	pET-22b(+)	pET-22b(+)	pET-11b
Antibiotic	Amp	Kan	Amp	–	Amp	Amp	Amp	Amp
Antibiotic concentration [ $\mu\text{g mL}^{-1}$ ]	100	50	100	–	100	100	100	100
Additive	ZnCl <sub>2</sub> , 1 mM	–	–	–	–	–	–	–
Reference	this work	<sup>3</sup>	<sup>4</sup>	synthetic gene	<sup>5</sup>	this work	this work	<sup>6</sup>

Amp – ampicillin, Kan – kanamycin

### 1.2. Subcloning of *radh* and *sadh*

The *radh* and *sadh* genes were subcloned into the expression vectors pET-22b(+) by digestion with the restriction enzymes *Nde*I and *Xho*I (Figure 1). To obtain sufficient plasmid for sequencing and further studies, *E. coli* DH5 $\alpha$  was transformed with the plasmids pET-22b(+)\_RADH and pET-22b(+)\_SADH, respectively.<sup>7</sup> Positive clones were selected on lysogeny broth (LB) agar plates using ampicillin sodium salt ( $100 \mu\text{g mL}^{-1}$ ) for selection. Gene sequences were confirmed by sequencing. For enzyme production, the genes were overexpressed in *E. coli* BL21(DE3).



**Figure 1.** Vector maps of RADH (A) and SADH (B) cloned into the high-copy plasmid pET-22b(+).



### 1.3. Expression and purification of recombinant ADHs

#### 1.3.1. Expression

Cultivation of *E. coli* cells carrying the respective *adh* genes were grown in shaking flasks (150 rpm) at 37 °C in 1 L of LB medium<sup>8</sup> supplemented with appropriate amounts of antibiotics (100 µg mL<sup>-1</sup> of ampicillin or 50 µg mL<sup>-1</sup> of kanamycin depending on the vector) and further required additives (Tab. 1). Protein expression was initiated by the addition of isopropyl-β-D-1-thiogalactopyranoside (IPTG, 1 mM final concentration), when the optical density at 600 nm reached 0.7. The bacterial cultures were incubated for further 5 hours at 30 °C (in case of RADH and SADH at 20 °C). The cells were harvest by centrifugation (15,900 × g, 40 min, 4 °C, centrifuge Beckmann AV-J20XP) and stored at -20 °C until further use.

Cells containing the RADH plasmid were grown in a 9 L bioreactor (Infors, Switzerland) in LB medium supplemented with glucose (15 g L<sup>-1</sup>) and ampicillin sodium salt (100 µg mL<sup>-1</sup>) for selective growth. Cultivation was carried out without further optimisation. Growth was followed by measurements of the optical density at 600 nm. IPTG was added (0.7 mM, final concentration) when the optical density reached 0.8. Further growth was followed at 22 °C for 20 hours during the production phase. The cells were harvested by centrifugation (15,900 × g, 40 min, 4 °C), and stored at -20 °C. From a 9 L culture approximately 180 g wet weight cells were obtained.

#### 1.3.2. Cell disruption

*E. coli* BL21(DE3) cells containing the respective ADH, were resuspended in TEA-HCl or Tris-HCl buffer (50 mM, pH 7.0) supplemented with magnesium and calcium chloride, if necessary (Tab. 2) and lysozyme (1 mg mL<sup>-1</sup>). Cell disintegration was performed by ultrasonification (Hielscher, sonotrode S1, cycle 0.5, amplitude 40, about 1 mL of cell suspension, 20 % w v<sup>-1</sup>) on ice in 20 seconds intervals for a total time of 3 minutes. Cell debris was removed by centrifugation (20,800 × g, 40 min, 4 °C). These crude cell extracts were used for the initial screening towards the reduction of various 2-hydroxy ketones.

To obtain larger quantities of RADH for enzyme purification, cells of *E. coli* BL21(DE3)-RADH were resuspended (about 50 mL of cell suspension, 20 % w v<sup>-1</sup>) as described above but at pH 7.5 and disrupted with the sonotrode S3 for 3 minutes at 3 minutes interval for a total of 15 minutes. Cell debris was removed by centrifugation (48,250 × g, 40 min, 4 °C).

**Table 2.** Buffer systems for cell disruption and activity assays for the different oxidoreductases.

	Oxidoreductase							
	ADHT	CPCR	FADH	HLADH	LBADH	RADH	SADH	TADH
Buffer	Tris-HCl	TEA-HCl	Tris-HCl	TEA-HCl	TEA-HCl	TEA-HCl	TEA-HCl	Tris-HCl
Concentration [mM]	50	50	50	50	50	50	50	50
pH	7.0	7.0	7.0	7.0	7.0	7.0	7.0	7.0
Additive	–	–	–	–	MgCl <sub>2</sub>	CaCl <sub>2</sub>	–	–
Additive concentration [mM]	–	–	–	–	1.0	0.8	–	–

#### 1.3.3. Purification of RADH

##### *Gel filtration*

The crude cell extract of RADH was first desalted using a Sephadex G-25 column (880 mL) (GE Healthcare, Sweden), which was previously equilibrated with TEA-HCl, 10 mM, pH 7.5. The desalting procedure was performed with a flow rate of 10 mL min<sup>-1</sup> and the eluate was collected in 10

mL fractions. Protein-containing fractions were determined at 280 nm, pooled and applied to anion-exchange chromatography for further purification.

#### Anion-exchange chromatography

The desalted crude cell extract (130 mL) was loaded onto a Q-Sepharose Fast Flow column (diameter: 1.6 cm, gel bed volume: 28 mL) (GE Healthcare, Sweden), which was equilibrated with at least three column volumes of equilibration buffer (TEA-HCl, 50 mM, pH 7.5) prior to use. After removal of unbound proteins by washing with equilibration buffer, elution was started with a linear NaCl-gradient (0-200 mM) within 150 minutes. The flow rate was set to 1 mL min<sup>-1</sup> and the eluate was collected in 10 mL fractions. RADH-containing fractions eluted with 150 mM NaCl. The collected fractions were subjected to an activity assay and SDS-PAGE electrophoresis. Fractions containing active RADH were pooled and again desalted using the Sephadex G-25 column with the same procedure as described above. Freeze-dried RADH was stored at -20 °C.

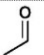
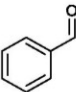
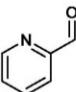
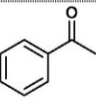
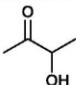
### 1.4. SDS electrophoresis

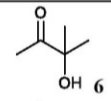
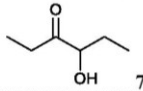
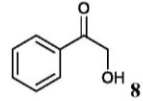
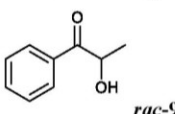
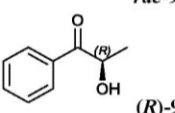
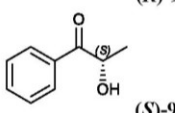
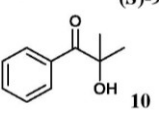
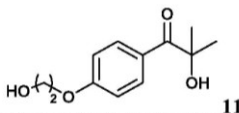
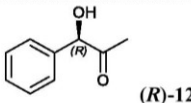
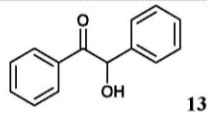
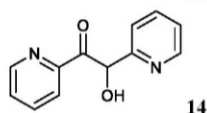
SDS-PAGE<sup>9</sup> was carried out on 4-12% NuPAGE<sup>®</sup> Novex Bis-Tris gels (Invitrogen). For the estimation of the molecular weight of proteins the PageRuler<sup>™</sup> Plus Prestained Protein Ladder (10-250 kDa, Fermentas) was used. The gel was stained in SimplyBlue<sup>™</sup> SafeStain (Invitrogen) or with the SilverXpress<sup>®</sup> Silver Staining Kit (Invitrogen).

## 2. Activity-screening of ADHs

**Table 3.** Substrate specificity of crude cell extracts containing overexpressed alcohol dehydrogenases. The reduction activity towards aldehydes, ketones and 2-hydroxy ketones is measured in triplicate by consumption of NADPH (0.2 mM) at wavelengths of 340 nm at 30°C.

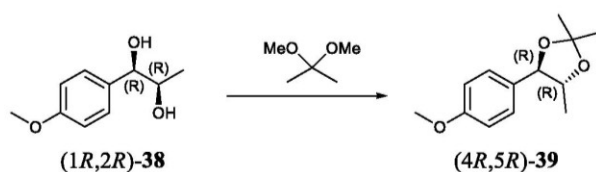
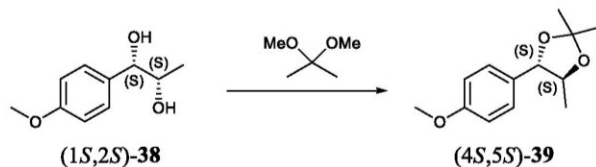
n.a. – activity not detectable; n.d. – activity not determined; CPCR – *Candida parapsilosis* carbonyl reductase, FADH – *Flavobacterium frigidimaris* alcohol dehydrogenase, HLADH – Horse liver alcohol dehydrogenase, SADH – *Sphingobium yanoikuyae* alcohol dehydrogenase, TADH – *Thermus* sp. alcohol dehydrogenase. HPP – 2-hydroxy propiophenone = 2-hydroxy-1-phenylpropan-1-one (9); PAC – phenylacetylcarbinol = 1-hydroxy-1-phenylpropan-2-one (12, here only (*R*)-enantiomer); Benzoin – 2-hydroxy-1,2-diphenylethanone (13);  $\alpha$ -pyridoin – 2-hydroxy-1,2-di(pyridine-2-yl)ethanone (14).

Substrate	Concentration [mM]	Specific activity [U mg <sup>-1</sup> ]				
		CPCR	FADH	HLADH	SADH	TADH
Aldehydes						
 1	10	0.26±0.00	1.41±0.00	0.96±0.01	n.a.	0.68±0.00
 2	10	0.12±0.00	4.12±0.03	0.54±0.02	0.03±0.00	0.40±0.00
 3	10	n.a.	1.47±0.02	0.12±0.01	n.a.	0.01±0.00
Ketones						
 4	10	n.a.	n.a.	n.a.	n.a.	0.54±0.00
2-Hydroxy ketones: aliphatic						
 5	10	n.a.	n.a.	n.a.	n.a.	n.a.

Substrate	Concentration [mM]	CPCR	Specific activity [U mg <sup>-1</sup> ]			
			FADH	HLADH	SADH	TADH
 6	10	n.a.	n.a.	n.a.	n.a.	n.a.
 7	10	n.a.	n.a.	n.a.	n.a.	n.a.
<b>2-Hydroxy ketones: 2-HPP and derivatives</b>						
 8	10	n.a.	n.a.	n.a.	n.a.	n.a.
 <i>rac</i> -9	10	n.d.	n.d.	n.d.	n.d.	n.d.
 ( <i>R</i> )-9	10	n.d.	n.d.	n.d.	n.d.	n.d.
 ( <i>S</i> )-9	10	n.d.	n.d.	n.d.	n.d.	n.d.
 10	10	n.a.	n.a.	n.a.	n.a.	n.a.
 11	5	n.a.	n.a.	n.a.	n.a.	n.a.
<b>2-Hydroxy ketones: PAC</b>						
 ( <i>R</i> )-12	10	n.d.	n.d.	n.d.	n.d.	n.d.
<b>2-Hydroxy ketones: Benzoin and α-pyridoin</b>						
 13	saturated	n.d.	n.d.	n.d.	n.d.	n.d.
 14	saturated	n.a.	n.a.	n.a.	n.a.	n.a.

### 3. Determination of absolute configuration of (1*R*,2*R*)-**38** and (1*S*,2*S*)-**38**

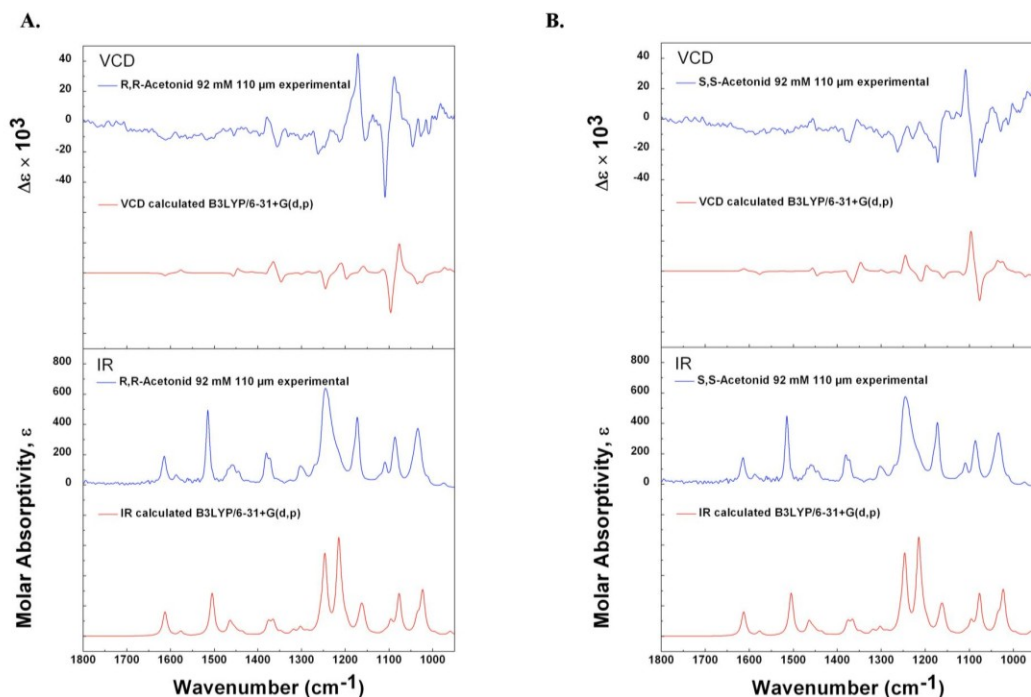
The diols (1*R*,2*R*)-**38** and (1*S*,2*S*)-**38** (10 mg, 0.05 mmol) were dissolved in dry dichloromethane (700 µL) and 2,2-dimethoxypropane (34 µL, 0.27 mmol, 5 eq.) before catalytic amounts of *p*-toluenesulfonic acid (2 mg) were added at 0°C. The reaction mixtures were stirred at room temperature for 30 min, subsequently quenched with saturated aqueous NaHCO<sub>3</sub>, and extracted with dichloromethane. Combined organic layers were washed with brine, dried over MgSO<sub>4</sub> and concentrated under reduced pressure. Subsequent filter flash chromatography (EtOAc/cyclohexane 30/70) yielded (4*R*,5*R*)-**39** (9.9 mg, 81 %) and (4*S*,5*S*)-**39** (8.5 mg, 85 %). (4*R*,5*R*)-**39**: [α]<sub>D</sub><sup>20</sup> = −0.13 (c 0.5, CH<sub>3</sub>CN); (4*S*,5*S*)-**39**: [α]<sub>D</sub><sup>20</sup> = +0.15 (c 0.5, CH<sub>3</sub>CN).

Scheme 1. Preparation of (4*R*,5*R*)-**39**Scheme 2. Preparation of (4*S*,5*S*)-**39**

$^1\text{H}$  NMR ( $\text{CDCl}_3$ ):  $\delta$  (ppm) = 1.26 (d,  $J$  = 6.0 Hz, 3H,  $\text{CHCH}_3$ ), 1.50, 1.55 (s, 6H,  $\text{CH}_3$ ), 3.81 (s, 3H,  $\text{OCH}_3$ ), 3.81-3.88 (m, 1H,  $\text{CHCH}_3$ ), 4.42 (d,  $J$  = 8.6 Hz, 1H,  $\text{CHCHCH}_3$ ), 6.88-6.92 (m, 2H,  $\text{CH}_{\text{arom}}$ ), 7.28-7.32 (m, 2H,  $\text{CH}_{\text{arom}}$ ).

$^{13}\text{C}$  NMR ( $\text{CDCl}_3$ ):  $\delta$  (ppm) = 16.1 ( $\text{CHCH}_3$ ), 27.1, 27.4 ( $\text{CH}_3$ ), 55.3 ( $\text{OCH}_3$ ), 79.1, 84.6 ( $\text{CH-O}$ ), 108.2, 129.5 ( $\text{C}_{\text{arom}}$ ), 113.9, 127.9 ( $\text{CH}_{\text{arom}}$ ), 159.6 ( $\text{C-OCH}_3$ ).

The absolute configurations of (4*R*,5*R*)-**39** and (4*S*,5*S*)-**39** were determined by vibrational circular dichroism (VCD) and quantum chemical calculations (GAUSSIAN 09). FT-VCD and FT-IR spectra were recorded on a Bruker Tensor 27 FTIR spectrometer equipped with a Bruker PMA 50 VCD side-bench module with a resolution of  $4\text{ cm}^{-1}$  in a  $100\text{ }\mu\text{m}$  BaF<sub>2</sub> cell.



**Figure 2.** The experimental (blue) and the calculated (red) spectra, for the acetonides (4*R*,5*R*)-**39** (A) and (4*S*,5*S*)-**39** (B). Experimental IR and VCD spectra of (4*R*,5*R*)-**39** and (4*S*,5*S*)-**39** (92 mM in  $\text{CDCl}_3$ ) and the Boltzmann-weighted average of theoretical IR and VCD spectra ( $\text{B}_3\text{LYP}/6\text{-}31\text{G}^*$ ) were calculated for four conformers of (4*R*,5*R*)-**39** and (4*S*,5*S*)-**39**.

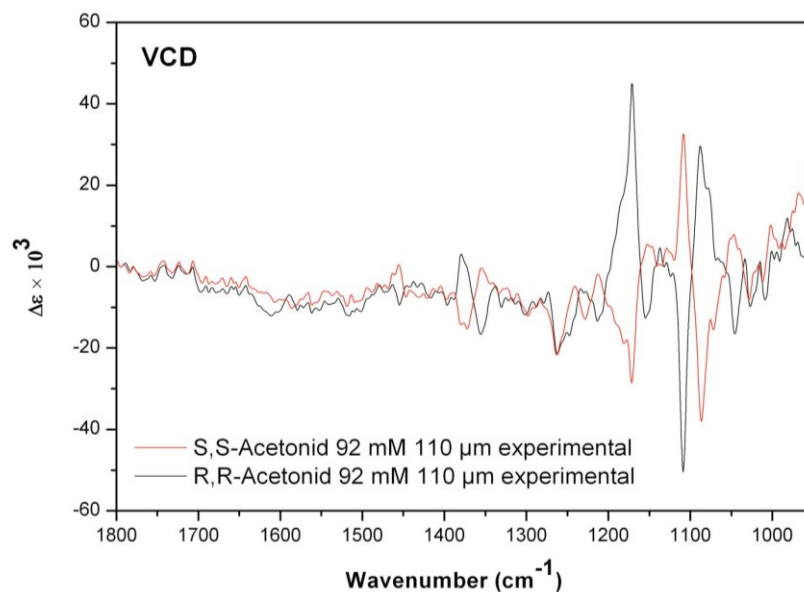


Figure 3. Superposed VCD-spectra of (4*R*,5*R*)-**39** and (4*S*,5*S*)-**39**.

#### 4. References

1. I. Lavandera, A. Kern, B. Ferreira-Silva, A. Glieder, S. de Wildeman and W. Kroutil, *J. Org. Chem.*, 2008, **73**, 6003-6005.
2. I. Lavandera, A. Kern, V. Resch, B. Ferreira-Silva, A. Glieder, W. M. F. Fabian, S. de Wildeman and W. Kroutil, *Org. Lett.*, 2008, **10**, 2155-2158.
3. M. Bhattacharjee, Doctoral thesis, RWTH Aachen University, 2006.
4. D. A. Ullisch, Diploma thesis, RWTH Aachen University, 2007.
5. B. Riebel, PhD Doctoral thesis, Heinrich-Heine-Universität Düsseldorf, 1996.
6. F. Hollmann, A. Kleeb, K. Otto and A. Schmid, *Tetrahedron: Asymmetry*, 2006, **17**, 867-868.
7. D. Hanahan, *J. Mol. Biol.*, 1983, **166**, 557-580.
8. J. Sambrook, Russel, Dawid W., *Molecular cloning: a laboratory manual.*, Cold Spring Harbor, New York, 2001.
9. U. K. Laemmli, *Nature*, 1970, **227**, 680-685.

## Publication II

---

“Biochemical characterization of an alcohol dehydrogenase from *Ralstonia* sp.”

Justyna Kulig, Amina Frese, Wolfgang Kroutil, Martina Pohl  
and Dörte Rother

Biotechnology and Bioengineering, 2013

Vol. 110(7), 1838-1848

DOI: 10.1002/BIT.24857



## ARTICLE

BIOTECHNOLOGY  
and  
BIOENGINEERINGBiochemical Characterization of an Alcohol Dehydrogenase From *Ralstonia* sp.Justyna Kulig,<sup>1</sup> Amina Frese,<sup>1</sup> Wolfgang Kroutil,<sup>2</sup> Martina Pohl,<sup>1</sup> Dörte Rother<sup>1</sup><sup>1</sup>Institute of Bio- and Geosciences, IBC-1: Biotechnology, Forschungszentrum Jülich GmbH, 52425 Jülich, Germany; telephone: +49-2461-616772; fax: +49-2461-613870; e-mail: do.rother@fz-juelich.de<sup>2</sup>Department of Chemistry, Organic and Bioorganic Chemistry, University of Graz, Graz, Austria

**ABSTRACT:** Stereoselective reduction towards pharmaceutically potent products with multi-chiral centers is an ongoing hot topic, but up to now catalysts for reductions of bulky aromatic substrates are rare. The NADPH-dependent alcohol dehydrogenase from *Ralstonia* sp. (RADH) is an exception as it prefers sterically demanding substrates. Recent studies with this enzyme indicated outstanding potential for the reduction of various  $\alpha$ -hydroxy ketones, but were performed with crude cell extract, which hampered its detailed characterization. We have established a procedure for the purification and storage of RADH and found a significantly stabilizing effect by addition of  $\text{CaCl}_2$ . Detailed analysis of the pH-dependent activity and stability yielded a broad pH-optimum (pH 6–9.5) for the reduction reaction and a sharp optimum of pH 10–11.5 for the oxidation reaction. The enzyme exhibits highest stability at pH 5.5–8 and 8–15°C; nevertheless, biotransformations can also be carried out at 25°C (half-life 80 h). Under optimized reaction parameters a thorough study of the substrate range of RADH including the reduction of different aldehydes and ketones and the oxidation of a broad range of alcohols was conducted. In contrast to most other known alcohol dehydrogenases, RADH clearly prefers aromatic and cyclic aliphatic compounds, which makes this enzyme unique for conversion of space demanding substrates. Further, reductions are catalyzed with extremely high stereoselectivity (>99% enantio- and diastereomeric excess). In order to identify appropriate substrate and cofactor concentrations

for biotransformations, kinetic parameters were determined for NADP(H) and selected substrates. Among these, we studied the reduction of both enantiomers of 2-hydroxypropionophenone in more detail.

Biotechnol. Bioeng. 2013;110: 1838–1848.

© 2013 Wiley Periodicals, Inc.

**KEYWORDS:** alcohol dehydrogenase; *Ralstonia* sp.; *Cupriavidus* sp.; calcium dependency; bulky substrates

## Introduction

Until now only a few alcohol dehydrogenases (ADHs) and carbonyl reductases were found as promising enzymes for a broad scope of biotransformations of sterically demanding compounds. For instance the alcohol dehydrogenase from *Lactobacillus brevis* was successfully employed as a robust biocatalyst for stereoselective reduction of prochiral ketones (Leuchs and Greiner, 2011). Further leading examples are the ADHs isolated from *Thermoanaerobacter brockii* (Röthig et al., 1990), *Candida boidinii* (Bommarius et al., 1995), *Rhodococcus erythropolis* (Gröger et al., 2004) and *Saccharomyces cerevisiae* (Katz et al., 2003) and the carbonyl reductase from *Candida parapsilosis* (Stillger et al., 2002), which are currently implemented in stereoselective biotransformations at lab- as well as industrial-scale (de Wildeman and Sereinig, 2011; Faber et al., 2010).

All mentioned ADHs and carbonyl reductase are metal-ion dependent enzymes, where the metal-ion can have a catalytic and/or a structure stabilizing effect on the enzyme. Examples are the  $\text{Zn}^{2+}$ -dependent ADHs from *T. brockii* (Bogin et al., 1997) and horse liver (Maret et al., 1979), where zinc ions have structural and catalytic functions. The alcohol dehydrogenase from *L. brevis* is stabilized by  $\text{Mg}^{2+}$ -ions (Niefind et al., 2003).

Alcohol dehydrogenase from *Ralstonia* sp. DSM 6428 (also known as *Cupriavidus* sp.) was found to be suitable for

Abbreviations: 2-HPP, 2-hydroxy-1-phenylpropan-1-one, 2-hydroxypropionophenone; ADH, alcohol dehydrogenase; ADHT, *Thermoanaerobacter* sp. alcohol dehydrogenase; LBADH, *Lactobacillus brevis* alcohol dehydrogenase; RADH, *Ralstonia* sp. (*Cupriavidus* sp.) alcohol dehydrogenase; SEC, size exclusion chromatography; TEA, tris-(2-hydroxyethyl)amine; TRIS, 2-amino-2-hydroxymethylpropane-1,3-diol.

Correspondence to: D. Rother

Contract grant sponsor: Marie Curie Initial Training Network in frame of project "BIOTRAINS—a European biotechnology training network for the support of chemical manufacturing"

Contract grant number: 238531

Additional supporting information can be found in the online version of this article.

Received 4 September 2012; Revision received 21 December 2012;

Accepted 22 January 2013

Accepted manuscript online 4 February 2013;

Article first published online 22 February 2013 in Wiley Online Library

(http://onlinelibrary.wiley.com/doi/10.1002/bit.24857/abstract)

DOI 10.1002/bit.24857

the reduction of sterically hindered ketones in whole cell biotransformations (Lavandera et al., 2008a). Recently, we applied the purified enzyme for bioreductions of a broad range of alpha-hydroxy ketones, where the enzyme shows outstanding activities.

Comparison of RADH to well-known ADHs from *L. brevis* (LBADH) and *Thermoanaerobacter* sp. (ADHT) showed significantly higher specific activities. ADHT and LBADH towards aliphatic alpha-hydroxy ketones, whereas RADH demonstrated a clear preference for the reduction of araliphatic alpha-hydroxy ketones. Moreover, bulky substrates were reduced with high enantio- and diastereoselectivities (Kulig et al., 2012). In previous studies it became obvious that the isolated RADH, although very active, is not stable under the applied reaction conditions (half-life ~6 h). Therefore, a detailed biochemical characterization was conducted in order to improve the applicability of the high potential of the enzyme for the transformation of sterically demanding substrates. Here we describe an easy procedure to stabilize the enzyme and investigated appropriate reaction parameters for the reduction of carbonyl compounds and the oxidation of alcohols.

## Materials and Methods

### Chemicals

All chemicals were of analytical grade. Alcohols (1–12), aldehydes (13, 15–30), and ketones (31–40, 42–44) were purchased from Sigma–Aldrich (Steinheim, Germany). Acetaldehyde (14) and acetophenone (41) were commercially available from Fluka (Steinheim, Germany) and Merck (Darmstadt, Germany), respectively. NADP(H) was purchased from Biomol (Hamburg, Germany).

### Expression of Recombinant RADH

RADH cloned into the vector pET-22b(+) was expressed in *E. coli* BL21(DE3) from Novagen (Madison, WI) as described previously (Kulig et al., 2012). Cultivation and cell disruption procedures were described elsewhere as well (Kulig et al., 2012).

### Purification

Here three purification protocols of RADH were applied depending on the purpose of the biochemical study. The first was conducted without  $\text{Ca}^{2+}$  ions, while for the second and third protocol 0.2 and 0.8  $\text{mmol L}^{-1}$   $\text{CaCl}_2$ , respectively, were added to all buffers. All purification steps were performed in TEA–HCl buffer, 50  $\text{mmol L}^{-1}$ , pH 7.5 supplemented with defined concentrations of  $\text{CaCl}_2$ , if needed. All purification steps were carried out at room temperature (20–25°C). The three-step purification protocol employed a size

exclusion chromatography (SEC) for initial desalting of the crude cell extracts, which was necessary to allow proper binding of the enzyme to the anion exchanger. After anion exchange chromatography a second SEC was used in order to remove the sodium chloride and to adjust a proper concentration of calcium ions for enzyme storage (Kulig et al., 2012).

### Storage Stability

In order to find suitable storage conditions for RADH, the purified and desalted enzyme was stored in four different ways: (I) in desalting buffer (TEA–HCl, 10  $\text{mmol L}^{-1}$ , pH 7.5) at 8°C, (II) same as (I) but stored at –20°C, (III) in a mixture of 50% (v/v) glycerol and desalting buffer (stored at –20°C) and (IV) freeze-dried and stored at –20°C. For comparison, residual activity was followed over time using the standard reduction assay.

### SDS Electrophoresis

SDS–PAGE (Laemmli, 1970) was carried out on a 4–12% NuPAGE<sup>®</sup> Novex Bis–Tris gels (Invitrogen, Carlsbad, CA). For protein molecular weight estimations prestained protein ladder PageRuler<sup>™</sup> Plus (10–250 kDa, Fermentas, Rockford, IL) was applied. The gel was stained in SimplyBlue<sup>™</sup> SafeStain (Invitrogen) or by applying SilverXpress<sup>®</sup> Silver Staining Kit (Invitrogen; Supplementary Information, Fig. S4A).

### Determination of the Protein Concentration

For determination of protein concentrations the Bradford method (Bradford, 1976) was applied using bovine serum albumin (Fermentas) as a standard, whereby the Bradford solution was prepared by ourselves.

### Determination of the Native Molecular Weight

The native molecular weight of RADH was determined by SEC using a Superdex<sup>™</sup> 200 column (diameter: 26 mm, length: 63 cm, gel bed volume: 334 mL, RADH loaded: 1.7 mL, RADH concentration: 3  $\text{mg mL}^{-1}$ ; GE Healthcare, Uppsala, Sweden). The column was equilibrated with 50  $\text{mmol L}^{-1}$  TEA–HCl buffer, pH 7.5 containing 150  $\text{mmol L}^{-1}$  NaCl. The native molecular weight of RADH was calculated according to a calibration curve obtained with different standard proteins (for details see Supplementary Information, Fig. S4B).

### Oxidation Assay

Initial rate activities were measured spectrophotometrically at 340 nm by following the formation (reduction) of



NADPH at 30°C in semi-micro cuvettes (total volume 1 mL) for 1 min. One unit (U) of enzyme is defined as the amount of enzyme that catalyzes the production of 1  $\mu\text{mol}$  NADPH per min at 30°C for the respective substrate. The standard oxidation reaction contained 100  $\text{mmol L}^{-1}$  cyclohexanol and 0.5  $\text{mmol L}^{-1}$  NADP<sup>+</sup> in 50  $\text{mmol L}^{-1}$  glycine-NaOH buffer pH 10.5 including 0.8  $\text{mmol L}^{-1}$  CaCl<sub>2</sub>. Due to high activity of cyclohexanol, even small changes in optima and stability due to changes of reaction conditions could be detected sensitively. All activity measurements were performed in triplicate.

### Reduction Assay

Initial rate activities for reductions were measured spectrophotometrically at 340 nm by following the consumption (oxidation) of NADPH at 30°C in semi-micro cuvettes (total volume 1 mL) for 1 min. One unit (U) of enzyme is defined as the amount of enzyme that catalyzes the consumption of 1  $\mu\text{mol}$  of NADPH per min at 30°C for the respective substrate. The standard reduction assay contained 10  $\text{mmol L}^{-1}$  benzaldehyde and 0.2  $\text{mmol L}^{-1}$  NADPH in 50  $\text{mmol L}^{-1}$  TEA-HCl buffer pH 7.5 including 0.8  $\text{mmol L}^{-1}$  CaCl<sub>2</sub>.

### Effect of Salts

The effect of different metal chlorides on the initial rate activity of RADH was studied using the standard reduction assay containing 1  $\text{mmol L}^{-1}$  of the respective chloride. Relative activities were calculated based on the initial activity determined for RADH without salts. Salts which did not reduce the initial rate activity (NaCl, KCl, CaCl<sub>2</sub>, MgCl<sub>2</sub>) were further tested concerning their effect on the enzyme stability at 0°C. Therefore, the decrease of activity was followed using the standard reduction assay containing 1  $\text{mmol L}^{-1}$  of the respective salt until a significant drop of activity (of about 20%) was observed.

### Effect of pH

For estimation of the pH optima of the oxidation and reduction reaction initial rate activities were measured using different buffers for the reduction and oxidation assay (citrate-phosphate, 50  $\text{mmol L}^{-1}$ , pH 4.0–7.0; TEA-HCl, 50  $\text{mmol L}^{-1}$ , pH 7.0–8.0; TRIS-HCl, 50  $\text{mmol L}^{-1}$ , pH 7.0–8.5; glycine-NaOH, 50  $\text{mmol L}^{-1}$ , pH 8.5–12.0, all supplemented with CaCl<sub>2</sub>, 0.8  $\text{mmol L}^{-1}$ ). To study the pH-dependent stability, the enzyme was incubated in the different buffers at different pH-values at 25°C and residual activity was followed using the reduction assay until complete deactivation was observed.

### Effect of Temperature

For determination of the temperature optimum initial, rate activities were determined with the reduction assay between 15 and 60°C. The substrate solution was preheated in the temperature-controlled slide of the spectrophotometer (Shimadzu UV-1601) until the desired temperature was reached. The temperature was additionally controlled with an external thermocoupled thermometer with digital display (Amarell, Kreutzwertheim, Germany). Shifts of pH due to temperature increases are within a tolerable range (from 15 to 60°C a pH shift of 0.9 was detected in the implemented TEA-HCl buffer). In order to study temperature dependent stability, the enzyme (concentration 0.5  $\text{mg mL}^{-1}$  in 200  $\mu\text{L}$  of stock solutions) was incubated in the reduction buffer [TEA-HCl (50  $\text{mmol L}^{-1}$ ) + CaCl<sub>2</sub> (0.8  $\text{mmol L}^{-1}$ ), pH 7.5] in a temperature range from 0 to 40°C (Thermomixer comfort, Eppendorf) and residual activity was followed using the reduction assay until 50% deactivation was observed at the respective temperature.

### Substrate Range and Stereoselectivity

For investigation of the substrate range the assays for reduction and oxidation were applied in the presence of 10  $\text{mmol L}^{-1}$  of each substrate, if not otherwise stated (see Tables II–IV). Stereoselectivity of alpha-hydroxy ketone biotransformations catalyzed by RADH was determined as described previously (Kulig et al., 2012).

### Determination of Kinetic Parameters

Kinetic parameters for the reduction of different aldehydes, ketones, 2-HPP, and the oxidation of alcohols were determined by initial rate activity measurements in triplicate at various substrate concentrations and fixed concentrations of NADPH (0.2  $\text{mmol L}^{-1}$ ) and NADP<sup>+</sup> (0.8  $\text{mmol L}^{-1}$ ), respectively, in the respective standard buffers for reduction or oxidation. Kinetic parameters for the cofactors were determined at fixed concentrations of benzaldehyde (15  $\text{mmol L}^{-1}$ ) and cyclohexanone (100  $\text{mmol L}^{-1}$ ) for the NADPH and for NADP<sup>+</sup> using cyclohexanol (100  $\text{mmol L}^{-1}$ ) as substrate. The  $v/[S]$ -plots are given in the Supplementary Information, Fig. S7. Experimental data were fitted to suitable kinetic models with Origin 7G and kinetic parameters ( $V_{\text{max}}$ ,  $K_M$ ,  $K_i$ ,  $n$ ) were calculated with the same program.

### Determination of Half-Lives

Half-lives in this work are defined as the time after which a residual activity of 50% was experimentally observed, independent of the kinetic of the activity decay. All deactivation curves are shown in the Supplementary Information (Figs. S1–S3 and S5–S6). Only few of them show first order inactivation kinetics.

## Results and Discussion

### Purification and Storage Stability of RADH

Purification of RADH by anion exchange chromatography and subsequent desalting yielded a purity of about 90% according to SDS-PAGE (Supplementary Information, Fig. S4A). As a matter of fact the purified enzyme is relatively unstable in buffer where the half-life is only ~6 h (Supplementary Information, Fig. S1A). Even at 8°C residual activity drops to 9% within 1 day (Supplementary Information, Fig. S1B).

For long-term storage the enzyme should be frozen in TEA-HCl buffer (10 mmol L<sup>-1</sup>, pH 7.5) at -20°C, which guarantees full stability for at least 80 days. Alternatively the enzyme may be lyophilized and stored at -20°C, where full stability was observed for 20 days. However, lyophilized enzyme required relatively long reactivation, as will be discussed in Influence of Temperature on Activity and Stability Section. Still, this method can be used as an appropriate mean to concentrate the liquid enzyme sample after chromatography. Best results were obtained by addition of 50% (v/v) glycerol to the purified enzyme in TEA-HCl buffer (10 mmol L<sup>-1</sup>, pH 7.5), which surprisingly led to an increase of initial activity during the first 4 days of storage at -20°C to 140% and after 80 days the enzyme retains still 120% of its initial activity (Supplementary Information, Fig. S1D).

### Effect of Salts

In order to identify factors, which allow a stable handling of dissolved RADH at room temperature, the influence of metal-ions on the enzyme activity was investigated. As stated in the introduction, several zinc- or magnesium-dependent ADHs are known, which rapidly lose activity in the absence of catalytically and/or structurally important metal-ions (Niefind et al., 2003). In order to detect any metal-ion dependency of RADH, first its initial rate activity was tested in the presence of different metal chlorides (Supplementary Information, Table I).

No activating metal-ion could be identified under initial rate conditions, since none of the salts increased initial rate activities compared to the control without additives. Also the addition of 1 mmol L<sup>-1</sup> EDTA had no visible effect. This could be taken as a hint that there is no weakly bound metal-ion in RADH, which is important for the enzyme activity. In contrast, some of the salts reduced the initial activity rate and thus are potential inhibitors of RADH. Among these are cobalt-, copper-, zinc-, manganese- and nickel chloride, with zinc chloride having the strongest impact (reduction to 39% of the initial rate activity). Copper- and manganese chloride reduced the initial activity rate to 75%, whereas the activity in the presence of cobalt and nickel chloride drops only moderately to 85–86%. All further tested salts did not show a significant influence of more than 8% on the initial activity rate of RADH.

Subsequently, all salts which did not impair the initial activity rate were tested with respect to potential enzyme stabilizing effects (Table I). Among these only calcium chloride showed a pronounced stabilizing effect. With 1.0 mmol L<sup>-1</sup> CaCl<sub>2</sub> the enzyme was completely stable at 0°C for 2 h and even after 3.5 h almost 90% of the initial activity was retained. Up to now only a pyrroloquinoline quinone (PQQ)-dependent methanol dehydrogenase was found requiring Ca<sup>2+</sup> ions for its activity and stability (Zhao et al., 2000). Thus, this is the first case, where Ca<sup>2+</sup>-ions were found to drastically enhance stability of an NADP(H)-dependent ADH.

In order to identify the optimal CaCl<sub>2</sub> concentration the stability of RADH was tested in the range of 0.2–1.0 mmol L<sup>-1</sup> CaCl<sub>2</sub>.

Addition of 0.8 mmol L<sup>-1</sup> Ca<sup>2+</sup>-ions during the purification procedure remained 50% of activity at 8°C after 163 h, whereas almost complete deactivation of RADH was observed without CaCl<sub>2</sub> within 24 h (Supplementary Information, Fig. S1B). However, the presence of CaCl<sub>2</sub> during the purification steps is not essential, since almost equal stabilities could be obtained upon addition of 0.2–1.0 mmol L<sup>-1</sup> CaCl<sub>2</sub> to the enzyme solution after purification. Further, the presence of 0.8 mmol L<sup>-1</sup> CaCl<sub>2</sub> during anion exchange chromatography hampered proper binding of the enzyme (data not shown). As no such problems were observed with 0.2 mmol L<sup>-1</sup> CaCl<sub>2</sub> and all purification steps were carried out at room temperature (20–25°C), this low CaCl<sub>2</sub> concentration of 0.2 mmol L<sup>-1</sup> was added to all buffers during the chromatographic process, remaining at least 50% of activity at 20°C for 100 h (Fig. 5). Further, 0.8 mmol L<sup>-1</sup> CaCl<sub>2</sub> were added to all buffers used for stability and activity studies since no significant influence of higher CaCl<sub>2</sub> concentrations (>0.8 mmol L<sup>-1</sup>) on the enzyme stability was observed.

### Determination of the Native Molecular Weight

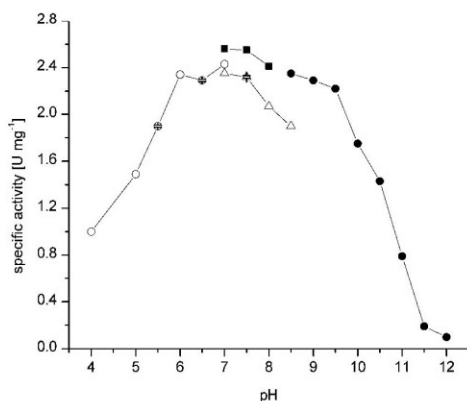
Purified RADH was subsequently used to study the native molecular weight. The calculated molecular weight based on

**Table I.** Effect of salts on the activity of RADH.

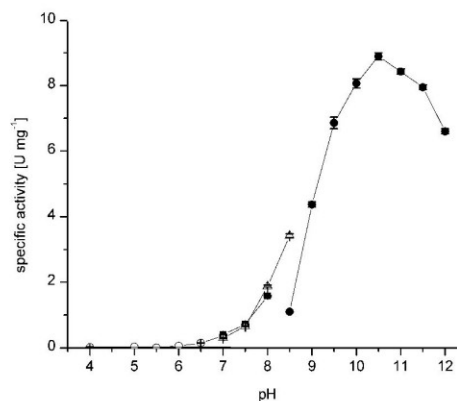
Salt	Residual activity (%)
Buffer control	100.0 ± 2.2
	79.1 ± 2.3 <sup>a</sup>
NaCl	79.6 ± 1.4 <sup>a</sup>
KCl	77.2 ± 0.8 <sup>a</sup>
MgCl <sub>2</sub>	84.0 ± 3.6 <sup>a</sup>
CaCl <sub>2</sub>	97.8 ± 1.8 <sup>b</sup>
	87.8 ± 1.6 <sup>c</sup>

The enzyme (0.2 mg mL<sup>-1</sup>) was incubated in TEA-HCl buffer (50 mmol L<sup>-1</sup>) in the presence of the respective salt (1 mmol L<sup>-1</sup>), pH 7.5 at 0°C.

The standard assay for reduction was employed. Initial rate activities were measured in triplicate following the consumption of NADPH (0.2 mmol L<sup>-1</sup>) at 340 nm at 30°C in TEA-HCl buffer (50 mmol L<sup>-1</sup>), pH 7.5. Residual activity was measured in defined time intervals: <sup>a</sup>, after 2 h; <sup>b</sup>, after 1.5 h; <sup>c</sup>, after 3.5 h.



**Figure 1.** pH-optimization of RADH for the reduction of benzaldehyde at 25°C. Initial rate activities were measured in triplicate following the consumption of NADPH ( $0.2 \text{ mmol L}^{-1}$ ) at 340 nm at 30°C in different buffer systems. Symbols: open circles: citrate-phosphate buffer ( $50 \text{ mmol L}^{-1} + \text{CaCl}_2$ ,  $0.8 \text{ mmol L}^{-1}$ , pH 4–7); filled squares: TEA-HCl buffer ( $50 \text{ mmol L}^{-1} + \text{CaCl}_2$ ,  $0.8 \text{ mmol L}^{-1}$ , pH 7–8); open triangles: TRIS-HCl ( $50 \text{ mmol L}^{-1} + \text{CaCl}_2$ ,  $0.8 \text{ mmol L}^{-1}$ , pH 7–8.5); filled circles: glycine-NaOH ( $50 \text{ mmol L}^{-1} + \text{CaCl}_2$ ,  $0.8 \text{ mmol L}^{-1}$ , pH 8.5–12).



**Figure 2.** pH-optimization of RADH for the oxidation of cyclohexanol at 25°C. Initial rate activities were measured in triplicate following the formation of NADPH ( $0.5 \text{ mmol L}^{-1}$ ) at 340 nm at 30°C in different buffer systems. Symbols: open circles: citrate-phosphate buffer ( $50 \text{ mmol L}^{-1} + \text{CaCl}_2$ ,  $0.8 \text{ mmol L}^{-1}$ , pH 4–7); filled squares: TEA-HCl buffer ( $50 \text{ mmol L}^{-1} + \text{CaCl}_2$ ,  $0.8 \text{ mmol L}^{-1}$ , pH 7–8); open triangles: TRIS-HCl ( $50 \text{ mmol L}^{-1} + \text{CaCl}_2$ ,  $0.8 \text{ mmol L}^{-1}$ , pH 7–8.5); filled circles: glycine-NaOH ( $50 \text{ mmol L}^{-1} + \text{CaCl}_2$ ,  $0.8 \text{ mmol L}^{-1}$ , pH 8.5–12).

the amino acid sequence of a single subunit is 26.7 kDa. SEC yielded a native molecular weight of 75 kDa under the tested conditions, which suggests a trimeric structure for RADH (see Supplementary Information, Fig. S5B). To the best of our knowledge this would be the first ADH with a trimeric structure in solution, although a trimeric structure was reported for some formaldehyde dehydrogenases (Eggeling and Sahm, 1985; van Ophem et al., 1992). However, as the hydrodynamic volume measured by SEC experiments is a function of the molecule form, misleading results can be expected if the three-dimensional structure is not spherically symmetrical. This will be elucidated when the crystal structure of RADH, which is currently under investigation, will be available. Further, this three-dimensional structure will be of high value to understand the stabilizing effect of calcium as described above (Effect of Salts Section).

#### Influence of pH on Activity and Stability

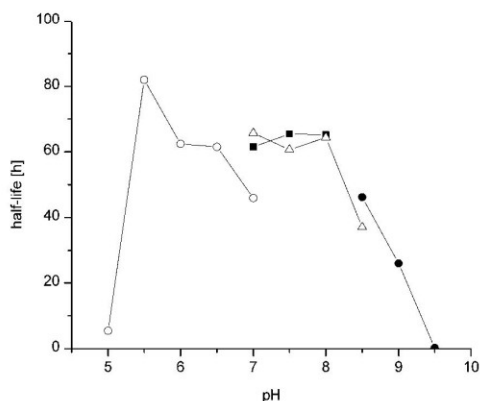
RADH exhibits two different pH-optima for the reduction and the oxidation activity (Figs. 1 and 2). The pH-optimum for the reduction activity (Fig. 1) was found in the range between pH 6 and 9.5 and is therewith significantly broader compared to the narrow pH-optimum for the oxidation between pH 10 and 11.5 (Fig. 2).

The results in Figure 1 also demonstrate that the chemical nature of the buffer influences the enzyme activity, since all activities measured in TRIS-HCl buffer were lower compared to TEA-HCl and glycine-NaOH buffer.

Besides, the reduction and oxidation negative controls containing only amine buffers (TRIS-HCl and TEA-HCl) revealed no significant activity ( $0.01 \text{ U mg}^{-1}$ ). Fortunately, TEA-HCl buffer was initially chosen for purification and storage of RADH and as buffer for the activity measurements of the reduction reaction, since amine buffers are well suited for studies with nicotinamide cofactors (Wu et al., 1986). For the oxidation reaction glycine-NaOH was implemented for initial rate activity measurements (pH 10.5), due to its broader pH-range.

The pH-dependent stability of RADH was studied in the range of pH 5–9.5 (Fig. 3) showing reasonable stability (half-lives 60–70 h) between pH 5.5 and 8 at room temperature. On the contrary, the stability drops rapidly at pH < 5.5 and pH > 8.0 (see also Supplementary Information, Fig. S5). Conclusively, the enzyme is stable at the pH-optimum for the reduction reaction, but very unstable at the pH-optimum for the oxidation reactions. Consequently, oxidation reactions (e.g. for cofactor regeneration using the substrate-coupled approach) require a careful evaluation of the optimal point of operation and should not be carried out at pH > 9.

Activity and stability detection over a broad pH range was of interest in order to elucidate its versatile applicability in multi-step reactions or for cofactor-regeneration purposes. Here reaction parameters have to be adjusted to the overall processes and not for the optimum of RADH activity alone. The broad pH-optimum for the reduction between pH 6 and 9.5 makes RADH to be a versatile catalyst for these applications.

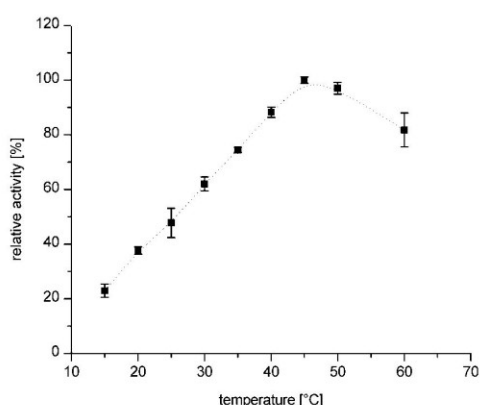


**Figure 3.** pH-dependent stability of RADH for the reduction of benzaldehyde at 25°C. Initial rate activities were measured in triplicate following the consumption of NADPH ( $0.2 \text{ mmol L}^{-1}$ ) at 340 nm at 30°C in different buffer systems. Symbols: open circles: citrate-phosphate buffer ( $50 \text{ mmol L}^{-1} + \text{CaCl}_2$ ,  $0.8 \text{ mmol L}^{-1}$ , pH 5–7); filled squares: TEA-HCl buffer ( $50 \text{ mmol L}^{-1} + \text{CaCl}_2$ ,  $0.8 \text{ mmol L}^{-1}$ , pH 7–8); open triangles: TRIS-HCl ( $50 \text{ mmol L}^{-1} + \text{CaCl}_2$ ,  $0.8 \text{ mmol L}^{-1}$ , pH 7–8.5); filled circles: glycine-NaOH ( $50 \text{ mmol L}^{-1} + \text{CaCl}_2$ ,  $0.8 \text{ mmol L}^{-1}$ , pH 8.5–9.5).

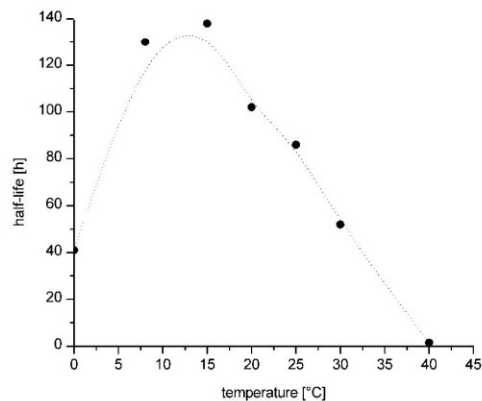
#### Influence of Temperature on Activity and Stability

The influence of temperature on the initial rate activity of RADH showed an almost linear increase of activity from 15 to 45°C by 400% (Fig. 4).

Investigation of the temperature-dependent stability revealed a stability optimum between 8 and 15°C in the presence of  $0.8 \text{ mmol L}^{-1} \text{ CaCl}_2$  (half-life: 130 h, Fig. 5).



**Figure 4.** Temperature optimum of RADH for the reduction of benzaldehyde. Initial rate activities were measured in triplicate following the consumption of NADPH ( $0.2 \text{ mmol L}^{-1}$ ) at 340 nm at 30°C in TEA-HCl buffer ( $50 \text{ mmol L}^{-1}$ ) supplemented with  $\text{CaCl}_2$  ( $0.8 \text{ mmol L}^{-1}$ , pH 7.5).



**Figure 5.** Temperature stability of RADH for the reduction of benzaldehyde. Initial rate activities were measured in triplicate in regular time intervals following the consumption of NADPH ( $0.2 \text{ mmol L}^{-1}$ ) at 340 nm at 30°C in TEA-HCl buffer ( $50 \text{ mmol L}^{-1}$ ) supplemented with  $\text{CaCl}_2$  ( $0.8 \text{ mmol L}^{-1}$ , pH 7.5).

Surprisingly, the stability at 0°C is much lower (half-life: 41 h, Fig. 5) than between 8 and 15°C and comparable to the enzyme stability at 30°C. The apparently lower stability at 0°C could be a consequence of cold inactivation. This phenomenon which has been observed with several oligomeric enzymes is assumed to be a consequence of weakened hydrophobic interactions at subunit interfaces (Almog et al., 2007; Erez et al., 2002; Ishikura et al., 2003). RADH shows highest stability at 15°C (half-life: 130 h, Fig. 5). Concerning the application of RADH for bioorganic syntheses temperatures in the range of 15–30°C should be chosen.

Almost all stability studies presented here were performed with lyophilized enzyme, which was dissolved in the respective buffer. As already mentioned above, we observed a more or less pronounced partial reactivation (up to 75%, Supplementary Information, Fig. S3F) during the first hours of incubation depending on implemented conditions (see Supplementary Information, Figs. S3 and S5). In almost all cases, where no rapid deactivation occurred, this effect could be observed (see Figure S3B, E and F; Figure 5G and H Supplementary Information). These results hint the partial reversible inactivation of RADH during lyophilization and the previous freezing step. Therefore, if lyophilized enzyme is used it should be equilibrated for some hours in buffer prior to further use, in order to ensure maximal activity and to allow quantitative measurements of, for example, maximal velocities.

#### Substrate Range

Conversion of several substrates with RADH was earlier studied using the crude cell extracts of RADH-expressing

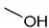
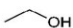

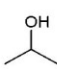
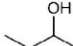



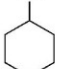
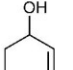
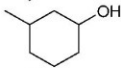
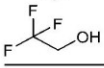


*E. coli*-cells, demonstrating a preference for sterically demanding ketones (Lavandera et al., 2008a,b). Additionally, we recently demonstrated the outstanding catalytic potential of RADH as crude cell extract and as purified enzyme for the reduction of  $\alpha$ -hydroxy ketones (Kulig et al., 2012). In order to analyze the substrate range of purified RADH in more detail, we studied its activity toward a broad range of different alcohols (Table II) and its reductase activity toward different aldehydes (Table III) and ketones (Table IV). For these studies now the calcium stabilized RADH with the optimal set of reaction parameters as described above could be implemented.

Since the kinetic parameters for the oxidation of the different alcohols are not known, the activities cannot be compared in terms of maximal velocities; they could vary significantly at different substrate concentrations due to the respective  $K_M$ -values or potential inhibition constants. As it was already demonstrated that RADH prefers sterically hindered substrates (Kulig et al., 2012; Lavandera et al., 2008a), cyclohexanol (9) was chosen as reference substrate

for the respective oxidation assay since the enzyme indicated high activity toward this alcohol. Table II shows, that RADH accepts further cyclic alcohols such as 3-methylcyclohexanol (11) and especially 2-cyclohexenol (10) very well. By contrast, small aliphatic alcohols, which could be employed, for example, for substrate-coupled cofactor regeneration, are less preferred. Only 2-butanol (5) is marginally converted ( $5.2 \text{ U mg}^{-1}$ ,  $100 \text{ mmol L}^{-1}$ ). In a previous study ethanol (2) was tested at a concentration of  $1.7 \text{ mol L}^{-1}$  [10% (v/v)] (Lavandera et al., 2008b), where 10% (v/v) of ethanol was found to be the optimal concentration for cofactor regeneration in whole cell biotransformations. Purified RADH oxidized  $1.7 \text{ mol L}^{-1}$  ethanol (2) with a specific activity of only  $0.04 \text{ U mg}^{-1}$ . At lower ethanol (2) concentrations (10 and  $100 \text{ mmol L}^{-1}$ ) no enzyme activity was detectable. This result suggests that another alcohol dehydrogenase in the previously described whole cell approach was responsible for the observed cofactor regeneration using ethanol as substrate, which became only visible by implementation of purified RADH.








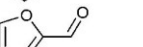

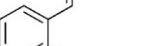
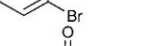
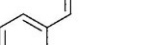


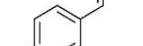
**Table II.** Investigation of the substrate range of alcohol dehydrogenase from *Ralstonia* sp. concerning the oxidation of various alcohols.

Alcohol		Concentration ( $\text{mmol L}^{-1}$ )	Specific activity ( $\text{U mg}^{-1}$ )
	1	10	n.a.
		100	n.a.
	2	10	n.a.
		100	n.a.
		1,700	$0.04 \pm 0.01$
	3	10	$0.11 \pm 0.01$
		100	$0.62 \pm 0.02$
	4	10	$0.11 \pm 0.01$
		100	$0.62 \pm 0.02$
	5	10	$1.73 \pm 0.01$
		100	$5.17 \pm 0.07$
	6	10	$0.08 \pm 0.01$
		100	$0.19 \pm 0.00$
	7	10	$0.19 \pm 0.01$
	8	10	$0.19 \pm 0.01$
	9	10	$8.36 \pm 0.31$
		100	$11.46 \pm 0.15$
	10	10	$18.83 \pm 0.22$
	11	10	$11.58 \pm 0.06$
	12	10	n.a.
		100	n.a.

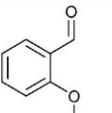
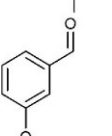
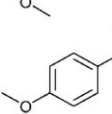
Initial rate activities were measured spectrophotometrically in triplicate in glycine-NaOH buffer ( $50 \text{ mmol L}^{-1}$ ) supplemented with  $\text{CaCl}_2$  ( $0.8 \text{ mmol L}^{-1}$ ), pH 10.5 at  $30^\circ\text{C}$  by following the increase of NADPH at 340 nm for 60 s.

Each reaction contained  $0.05 \text{ mg mL}^{-1}$  RADH and  $0.5 \text{ mmol L}^{-1}$  NADP<sup>+</sup>. n.a., activity not detectable.

**Table III.** Investigation of the substrate range of alcohol dehydrogenase from *Ralstonia* sp. concerning the reduction of various aldehydes.

Aldehyde	Concentration (mmol L <sup>-1</sup> )	Specific activity (U mg <sup>-1</sup> )
	13	10
	14	10
	15	10
	16	10
	17	10
	18	10
	19	5
	20	5
	21	Saturated
	22	5
	23	5
	24	5
	25	5
	26	5
	27	5

**Table III.** (Continued)

Aldehyde	Concentration (mmol L <sup>-1</sup> )	Specific activity (U mg <sup>-1</sup> )
	28	1-10 <sup>a</sup>
	29	1
	30	5

Initial rate activities were measured spectrophotometrically in triplicate in TEA-HCl buffer (50 mmol L<sup>-1</sup>) supplemented with CaCl<sub>2</sub> (0.8 mmol L<sup>-1</sup>), pH 7.5 at 30°C by following the decrease of NADPH (0.2 mmol L<sup>-1</sup>) at 340 nm for 60 s.

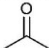
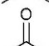


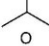
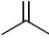





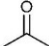
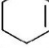

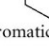
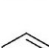
Each reaction contained 0.05 mg mL<sup>-1</sup> RADH. <sup>a</sup>, Absorption limitation occurred already at 1 mmol L<sup>-1</sup> substrate concentration; n.a., activity not detectable; n.d., not determined.

As demonstrated in Table III, RADH showed highest reductase activity towards aromatic aldehydes under the applied assay conditions. The highest initial rate activity of 23.3 U mg<sup>-1</sup> was determined for 2-bromobenzaldehyde (19), followed by 11.7 U mg<sup>-1</sup> for 3-fluorobenzaldehyde (23). The substituted aromatic aldehydes are even better converted than benzaldehyde (4.9 U mg<sup>-1</sup>) (16), while only low activity was found with small aliphatic acetaldehyde (14).

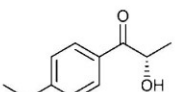
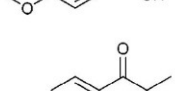
Because of the positive effect of ring-substitutions, diversely substituted benzaldehyde derivatives were compared to investigate the impact of the respective substitution (Table III, substrates 19–30). Thus, bromo-, fluoro- and methylbenzaldehyde substituted in *ortho*-, *meta*- and *para*-position were investigated as substrates. Although the specific activities measured at only one substrate concentration cannot yield valid information about the maximal velocity, they give valuable hints to substrates where a detailed investigation (e.g., at the kinetics, Steady-State Kinetics Section) is worthwhile. All substituted derivatives were converted moderately.

As demonstrated in Table IV the specific activities toward ketones resemble very much the results obtained with different aldehydes (Table III). RADH prefers cyclic and aromatic ketones such as cyclohexanone (38), acetophenone (41) and 4-phenyl-2-butanone (42), whereas aliphatic ketones such as acetone (31), or 2,5-hexandione (35) are hardly accepted by the enzyme. The highest specific activities were obtained with cyclohexanone (38) (9.8 U mg<sup>-1</sup>) and 3-methylcyclohexanone (40) (12.6 U mg<sup>-1</sup>), respectively. Furthermore, the presence of a double bond in cyclohexenone (39, 0.1 U mg<sup>-1</sup>) seems to dramatically influence the

**Table IV.** Investigation of the substrate range of alcohol dehydrogenase from *Ralstonia* sp. concerning the reduction of various ketones.

Ketone		Concentration (mmol L <sup>-1</sup> )	Specific activity (U mg <sup>-1</sup> )
Aliphatic			
	31	10	0.01 ± 0.00
	32	10	0.09 ± 0.01
	33	10	0.18 ± 0.01
	34	10	0.06 ± 0.00
	35	10	0.08 ± 0.00
	36	10	0.22 ± 0.01
	37	10	0.31 ± 0.01
	38	10	9.78 ± 0.11
	39	10	0.11 ± 0.01
	40	10	12.62 ± 0.07
Aromatic			
	41	10	4.35 ± 0.08
	42	10	0.56 ± 0.00
2-hydroxy ketones (Kulig et al., 2012)			
	43	10	362.6 ± 1.9 ( <i>R</i> )
	44	10	<i>de</i> > 99% ( <i>syn</i> ) 17.1 ± 0.3 ( <i>R</i> )
	45	10	<i>de</i> > 99% ( <i>anti</i> ) 61.9 ± 1.9 ( <i>S</i> )
	46	10	<i>de</i> > 99% ( <i>anti</i> ) 44.4 ± 0.5 ( <i>R</i> )

**Table IV.** (Continued)

Ketone	Concentration (mmol L <sup>-1</sup> )	Specific activity (U mg <sup>-1</sup> )
	47	10
		<i>ee</i> > 99% 17.4 ± 0.2 (R)
	48	10
		<i>de</i> 87% ( <i>anti</i> ) 138.7 ± 1.8 (R)
		<i>de</i> > 99% ( <i>syn</i> )

Initial rate activities were measured spectrophotometrically in triplicate in TEA-HCl buffer (50 mmol L<sup>-1</sup>) supplemented with CaCl<sub>2</sub> (0.8 mmol L<sup>-1</sup>), pH 7.5 at 30°C by following the decrease of NADPH (0.2 mmol L<sup>-1</sup>) at 340 nm for 60 s.

Each reaction contained 0.05 mg mL<sup>-1</sup> RADH. *ee*, enantiomeric excess; *de*, diastereomeric excess.

enzyme activity when compared to cyclohexanone (**38**; 9.8 U mg<sup>-1</sup>). As described earlier, alpha-hydroxy ketones such as 2-hydroxypropiophenone (2-HPP) (**43–44**) or its derivatives (**45–48**) are even better reduced by RADH with extremely high activities and high stereoselectivities (*ee* > 99%, *de* > 99%; Kulig et al., 2012).

### Steady-State Kinetics

In order to find appropriate conditions for optimal conversion with RADH in biotransformations, it is not only important to determine adequate substrate concentrations for maximal reaction velocities, but also the cofactor concentration has to be properly adjusted in order to obtain maximal performance. Furthermore kinetic investigations for four different substrates were performed. To compare kinetics of reduction and oxidation reactions, the oxidation of cyclohexanol and the reduction of cyclohexanone and benzaldehyde were exemplarily studied (Table V).

Our results in Table V demonstrate a similar range for kinetic parameters of RADH with benzaldehyde and cyclohexanone. Whereas RADH showed a difference of 50% concerning its specific activity with 10 mmol L<sup>-1</sup> of both substrates (Tables III and IV), activities differ by only ca. 30%, if the enzyme is substrate saturated (entries 6 and 7). Both *K<sub>M</sub>*-values are in the millimolar range and by a factor of 3.5–11 higher than the *K<sub>M</sub>*-value for (R)-2-HPP (entry 8). The low *K<sub>M</sub>* (1.6 mmol L<sup>-1</sup>) for (R)-2-HPP, which goes in line with an extraordinary high activity of 299.6 U mg<sup>-1</sup>, demonstrates the preference of RADH for sterically demanding compounds (e.g., alpha-hydroxy ketones; Kulig et al., 2012). Comparison of the kinetic parameters of both 2-HPP enantiomers (entries 8 and 9) demonstrates a huge difference in affinity, as can be deduced

**Table V.** Kinetic parameters of alcohol dehydrogenase from *Ralstonia* sp.

Entry	Substrate (mmol L <sup>-1</sup> )	Cofactor (mmol L <sup>-1</sup> )	V <sub>max</sub> (U mg <sup>-1</sup> )	K <sub>m</sub> (mmol L <sup>-1</sup> )	n	K <sub>i</sub> (mmol L <sup>-1</sup> )	S <sub>opt</sub> (mmol L <sup>-1</sup> )	V <sub>opt</sub> (U mg <sup>-1</sup> )	Shape of the v/[S] curve	Supplementary Figure
<b>Cofactor kinetics</b>										
1	Benzaldehyde [15] <sup>b</sup>	NADPH [0–0.2]	5.6 ± 0.1	0.005 ± 0.000	1.6 ± 0.1	—	—	—	S	S7A
2	Cyclohexanone [100] <sup>b</sup>	NADPH [0–0.2]	17.6 ± 0.10	0.008 ± 0.000	2.8 ± 0.2	—	—	—	S	S7B
3	Cyclohexanol [100] <sup>a</sup>	NADP <sup>+</sup> [0–4]	8.4 ± 0.2	0.06 ± 0.00	—	11.4	0.8	7.4	MM, I	S7C
<b>Oxidation<sup>a</sup></b>										
4	Cyclohexanol [0–200]	NADP <sup>+</sup> [0.8]	7.7 ± 0.2	5.2 ± 0.6	—	—	—	—	MM	S7D
5	Benzyl alcohol [0–150]	NADP <sup>+</sup> [0.8]	0.3 ± 0.0	12.3 ± 2.7	—	—	—	—	MM	S7E
<b>Reduction<sup>b</sup></b>										
6	Benzaldehyde [0–50]	NADPH [0.2]	12.6 ± 0.3	15.6 ± 0.9	—	—	—	—	MM	S7F
7	Cyclohexanone [0–100]	NADPH [0.2]	18.8 ± 0.6	10.8 ± 1.2	—	—	—	—	MM	S7G
8	(R)-2-HPP [0–15]	NADPH [0.2]	486.8 ± 53.2	1.6 ± 0.4	—	16.4	5.1	299.6	MM, I	S7H
9	(S)-2-HPP [0–20]	NADPH [0.2]	23.1 ± 0.4	3.6 ± 0.2	—	—	—	—	MM	S7I

Measurements were conducted spectrophotometrically in triplicates at 30 °C by following the decrease of NADPH (0.2 mmol L<sup>-1</sup>) at 340 nm for 60 s.

<sup>a</sup>, measurements were performed in TRIS–HCl buffer (50 mmol L<sup>-1</sup> + CaCl<sub>2</sub>, 0.8 mmol L<sup>-1</sup>) at pH 9.0; <sup>b</sup>, measurements were performed in TEA–HCl buffer (50 mmol L<sup>-1</sup> + CaCl<sub>2</sub>, 0.8 mmol L<sup>-1</sup>) at pH 7.5; MM, Michaelis–Menten kinetics; S, sigmoidal; I, substrate inhibition.

form the  $K_M$ -values and the maximal velocities. (S)-2-HPP (entry 9) is clearly the less preferred enantiomer showing a 2.3-fold higher  $K_M$ -value and a 13-fold lower  $V_{max}$ . However, in the concentration range tested, no substrate inhibition was observed with the (S)-enantiomer, whereas the enzyme shows a  $K_i$ -value of 16.4 mmol L<sup>-1</sup> for the (R)-enantiomer.

Measurements of the oxidation reaction were performed at pH 9.0 in TRIS–HCl buffer (50 mmol L<sup>-1</sup> with addition of CaCl<sub>2</sub>, 0.8 mmol L<sup>-1</sup>) where the enzyme showed not the highest initial rate activity for oxidation (Fig. 2) but good stability (Fig. 3). The oxidation of cyclohexanol (entry 4) and the reverse reaction, the reduction of cyclohexanone (entry 7), were compared at optimal cofactor concentrations (NADP<sup>+</sup>, 0.8 mmol L<sup>-1</sup> and NADPH, 0.2 mmol L<sup>-1</sup>). Under these conditions RADH catalyzes the reduction 2.5-fold faster than the oxidation (entries 4 and 7;  $V_{max(oxidation)} \ll V_{max(reduction)}$ ). As can be deduced from the  $K_M$ -values, the enzyme shows a twofold higher affinity for cyclohexanol (entry 4) compared to the respective ketone (entry 7) ( $K_{M(oxidation)} < K_{M(reduction)}$ ) under these conditions. A similar trend was observed for the pair benzyl alcohol and benzaldehyde (entries 5 and 6).

Kinetic investigation of the cyclohexanol oxidation (entry 4) demonstrates that the enzyme is not inhibited by high alcohol concentrations, but by high concentrations of NADP<sup>+</sup> (entry 3). The optimal concentration for the oxidized cofactor (NADP<sup>+</sup>) for biocatalytic applications was found to be 0.8 mmol L<sup>-1</sup> due to slight surplus inhibition (entry 3). By contrast, the reduced cofactor (NADPH) can be applied in lower ranges of 0.05–0.2 mmol L<sup>-1</sup> for maximal activity. For NADPH  $K_M$  values of 0.005 and 0.008 mmol L<sup>-1</sup> were determined for the reduction of benzaldehyde (entry 1) and cyclohexanone (entry 2), respectively. In both cases a slightly sigmoidal v/[S]-plot was obtained (see Supplementary Information, Fig. S7A and B), suggesting cooperative phenomena upon cofactor binding. All other v/[S]-plots followed the Michaelis–Menten equation (including substrate inhibitions for entries 3 and 8).

The presented results underline the high catalytic potential of RADH especially for the reduction of alpha-hydroxy ketones (Kulig et al., 2012). Furthermore, they demonstrate the importance of kinetic studies for efficient reaction engineering as it was demonstrated for (R)-2-HPP (entry 8) since the kinetic parameters allow an appropriate set-up of reaction parameters, for example, via a fed-batch strategy or a continuous process in order to exploit the full potential of the enzyme.

## Conclusions and Outlook

We here report a thorough characterization of the NADPH-dependent alcohol dehydrogenase from *Ralstonia* sp. Our investigation that RADH requires calcium ions for stability allowed the development of a robust purification strategy via



anion exchange chromatography and stable storage conditions as well as to identify ideal reaction conditions for biocatalytic applications. Size exclusion studies suggested a molecular weight corresponding to a trimer, which might be also the result of hydrodynamic size of the enzyme under applied experimental conditions. As enzyme crystallization is currently under investigation, this question must be left open.

The broad investigation of the substrate range for aldehydes, ketones, and alcohols complements the recently published substrate spectrum for alpha-hydroxy ketones nicely (Kulig et al., 2012), demonstrating the preference of RADH for sterically demanding compounds, which underlines the relevance of this enzyme for biotechnological applications. RADH reduces especially sterically demanding aromatic substrates much better than commonly employed ADHs from *L. brevis* and *Thermoanaerobacter* sp. (Kulig et al., 2012). Kinetic studies for selected substrates underlined these results. High affinity for alpha-hydroxy ketones such as 2-hydroxypropiophenone (2-HPP) was concomitant with a high specific activity of  $\sim 300 \text{ U mg}^{-1}$ . However, this substrate causes substrate surplus inhibition ( $K_i$   $16.4 \text{ mmol L}^{-1}$ ), which makes careful control of the reaction conditions during biotransformations necessary.

Financial support by the Marie Curie Initial Training Network in frame of project "BIOTRAINS—a European biotechnology training network for the support of chemical manufacturing", grant agreement no. 238531 is gratefully acknowledged.

## References

- Almog O, Kogan A, de Leeuw M, Gdalevsky GY, Cohen-Luria R, Parola AH. 2007. Structural insights into cold inactivation of tryptophanase and cold adaptation of subtilisin S41. *Biopolymers* 89(5):345–359.
- Bogin O, Peretz M, Burstein Y. 1997. *Thermoanaerobacter brockii* alcohol dehydrogenase: Characterization of the active site metal and its ligand amino acids. *Protein Sci* 6(2):450–458.
- Bommarius AS, Schwarm M, Stingl M, Kottenhahn K, Huthmacher K, Drauz K. 1995. Synthesis and use of enantiomerically pure tert-leucine. *Tetrahedron: Asymmetry* 6(12):2851–2888.
- Bradford MM. 1976. Rapid and sensitive method for quantitation of microgram quantities of protein utilizing principle of protein-dye binding. *Anal Biochem* 72(1–2):248–254.
- de Wildeman S, Sereinig N. 2011. Enzymatic reduction of carbonyl compounds. In: Molander GA, editor. *Stereoselective reactions of carbonyl and imino groups*. Stuttgart: Thieme p 133–208.
- Eggeling L, Sahn H. 1985. The formaldehyde dehydrogenase of *Rhodococcus erythropolis*, a trimeric enzyme requiring a cofactor and active with alcohols. *Eur J Biochem* 150(1):129–134.
- Erez T, Gdalevsky GY, Hariharan C, Pines D, Pines E, Phillips RS, Cohen-Luria R, Parola AH. 2002. Cold-induced enzyme inactivation: How does cooling lead to pyridoxal phosphate-aldimine bond cleavage in tryptophanase? *Biochim Biophys Acta* 1594:335–340.
- Faber K, Glueck SM, Seisser B, Kroutil W. 2010. Novel developments employing redox enzymes: Old enzymes in new clothes. In: Yeh W-K, Yang H-C, McCarthy JR, editors. *Enzyme technologies: Metagenomics, evolution, biocatalysis, and biosynthesis*. New Jersey: Wiley p 199–249.
- Gröger H, Hummel W, Rollmann C, Chamouveau F, Hüsken H, Werner H, Wunderlich C, Abokitse K, Drauz K, Buchholz S. 2004. Preparative asymmetric reduction of ketones in a biphasic medium with an (S)-alcohol dehydrogenase under in situ-cofactor recycling with formate dehydrogenase. *Tetrahedron* 60:633–640.
- Ishikura S, Usami N, El-Kabbani O, Hara A. 2003. Structural determinant for cold inactivation of rodent L-xylulose reductase. *Biochem Biophys Res Commun* 308:68–72.
- Katz M, Frejd T, Hahn-Hägerdal B, Growa-Graslund MF. 2003. Efficient anaerobic whole cell stereoselective bioreduction with recombinant *Saccharomyces cerevisiae*. *Biotechnol Bioeng* 84(5):573–582.
- Kulig J, Simon RC, Rose CA, Husain SM, Häckh M, Lüdeke S, Zeitler K, Kroutil W, Pohl M, Rother D. 2012. Stereoselective synthesis of bulky 1,2-diols with alcohol dehydrogenases. *Catal Sci Technol* 2(8):1580–1589.
- Laemmli UK. 1970. Cleavage of structural proteins during assembly of head of bacteriophage-T4. *Nature* 227(5259):680–685.
- Lavandera I, Kern A, Ferreira-Silva B, Glieder A, de Wildeman S, Kroutil W. 2008a. Stereoselective bioreduction of bulky-bulky ketones by a novel ADH from *Ralstonia* sp. *J Org Chem* 73(15):6003–6005.
- Lavandera I, Oberdorfer G, Gross J, de Wildeman S, Kroutil W. 2008b. Stereocomplementary asymmetric reduction of bulky-bulky ketones by biocatalytic hydrogen transfer. *Eur J Org Chem* 2008(15):2539–2543.
- Leuchs S, Greiner L. 2011. Alcohol dehydrogenase from *Lactobacillus brevis*: A versatile robust catalyst for enantioselective transformations. *Chem Biochem Eng Q* 25(2):267–281.
- Maret W, Andersson I, Dietrich H, Schneider-Bernlöhr H, Einarsson R, Zeppezauer M. 1979. Site-specific substituted cobalt(II) horse liver alcohol dehydrogenases. Preparation and characterization in solution, crystalline and immobilized state. *Eur J Biochem* 98(2):501–512.
- Niefind K, Müller J, Riebel B, Hummel W, Schomburg D. 2003. The crystal structure of R-specific alcohol dehydrogenase from *Lactobacillus brevis* suggests the structural basis of its metal dependency. *J Mol Biol* 327(2):317–328.
- Röthig TR, Kulbe KD, Bückmann F, Carrea G. 1990. Continuous coenzyme dependent stereoselective synthesis of sulcatol by alcohol dehydrogenase. *Biotechnol Lett* 12(5):353–356.
- Stillger T, Bönitz M, Filho MV, Liese A. 2002. Überwindung von thermodynamischen Limitierungen in substratgekoppelten Cofaktorregenerierungsverfahren. *Chem-Ing-Tech* 7(2):1035–1039.
- van Ophem PW, Van Beeumen J, Duine JA. 1992. NAD-linked, factor-dependent formaldehyde dehydrogenase or trimeric, zinc-containing, long-chain alcohol-dehydrogenase from *Amycolatopsis methanolica*. *Eur J Biochem* 206(2):511–518.
- Wu JT, Wu LH, Knight JA. 1986. Stability of NADPH: Effect of various factors on the kinetics of degradation. *Clin Chem* 32(2):314–319.
- Zhao Y, Wang G, Cao Z, Wang Y, Cheng H, Zhou H-M. 2000. Effects of  $\text{Ca}^{2+}$  on methanol dehydrogenase. *J Protein Chem* 19(6):469–473.

## **Biochemical characterisation of an alcohol dehydrogenase from *Ralstonia* sp.**

Justyna Kulig<sup>a</sup>, Amina Frese<sup>a</sup>, Wolfgang Kroutil<sup>b</sup>, Martina Pohl<sup>a</sup> and Dörte Rother<sup>a1</sup>

<sup>a</sup>Institute of Bio- and Geosciences, IBG-1: Biotechnology, Forschungszentrum Jülich GmbH, 52425 Jülich, Germany

<sup>b</sup>Department of Chemistry, Organic and Bioorganic Chemistry, University of Graz, Heinrichstrasse 28, 8010 Graz, Austria

### **Supporting Information**

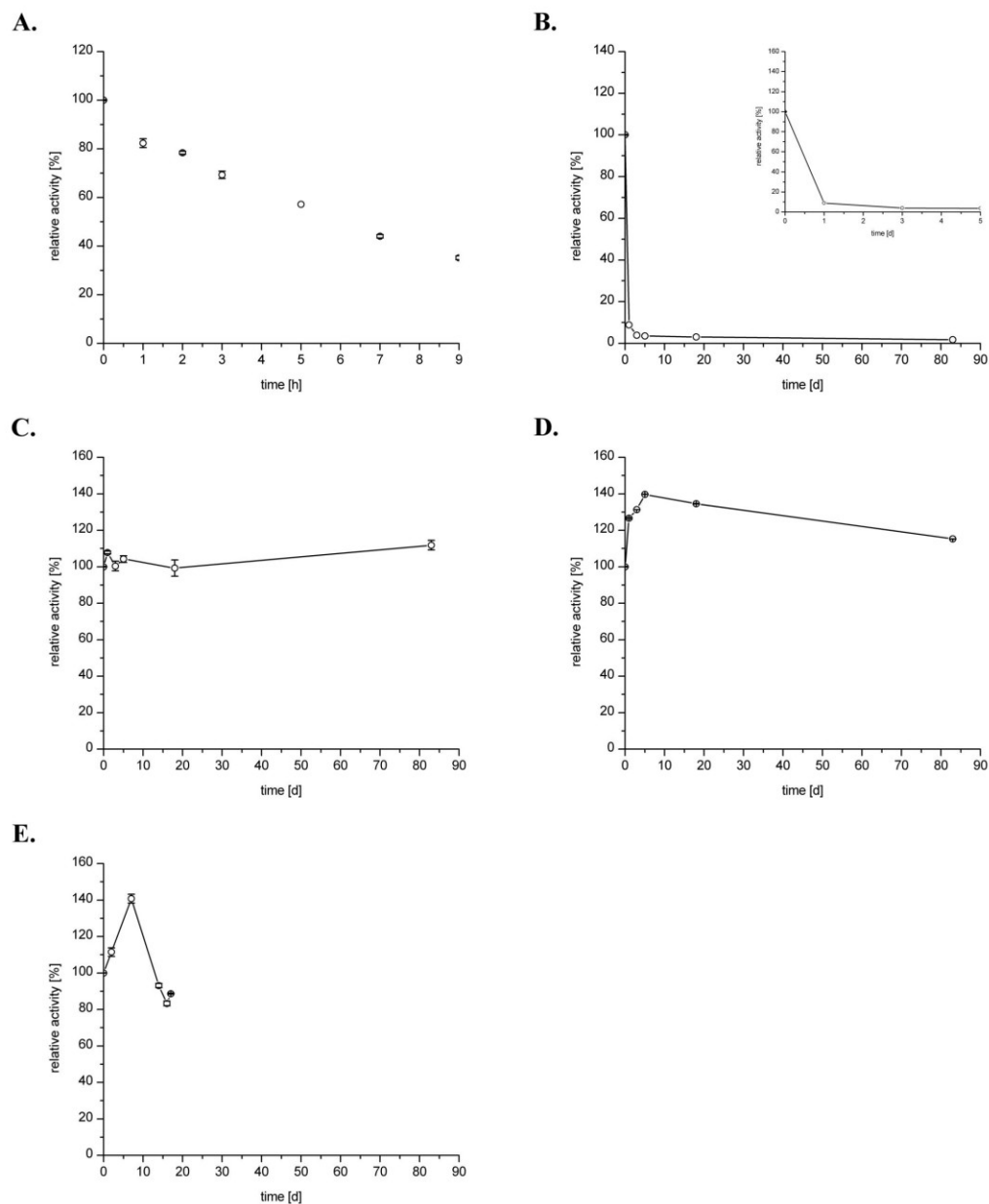
#### **Table of contents:**

1. Storage stability
2. Effect of different salts and EDTA on initial rate activity of RADH
3. Influence of Ca<sup>2+</sup> on the stability of RADH
4. Determination of the molecular weight
5. Influence of pH on RADH stability
6. Influence of temperature on RADH stability
7. Steady-state kinetic measurements

---

<sup>1</sup> Corresponding author: Fax: +49 2461-613870; Tel: +49 2461-616772; E-Mail: do.rother@fz-juelich.de

## 1. Storage stability

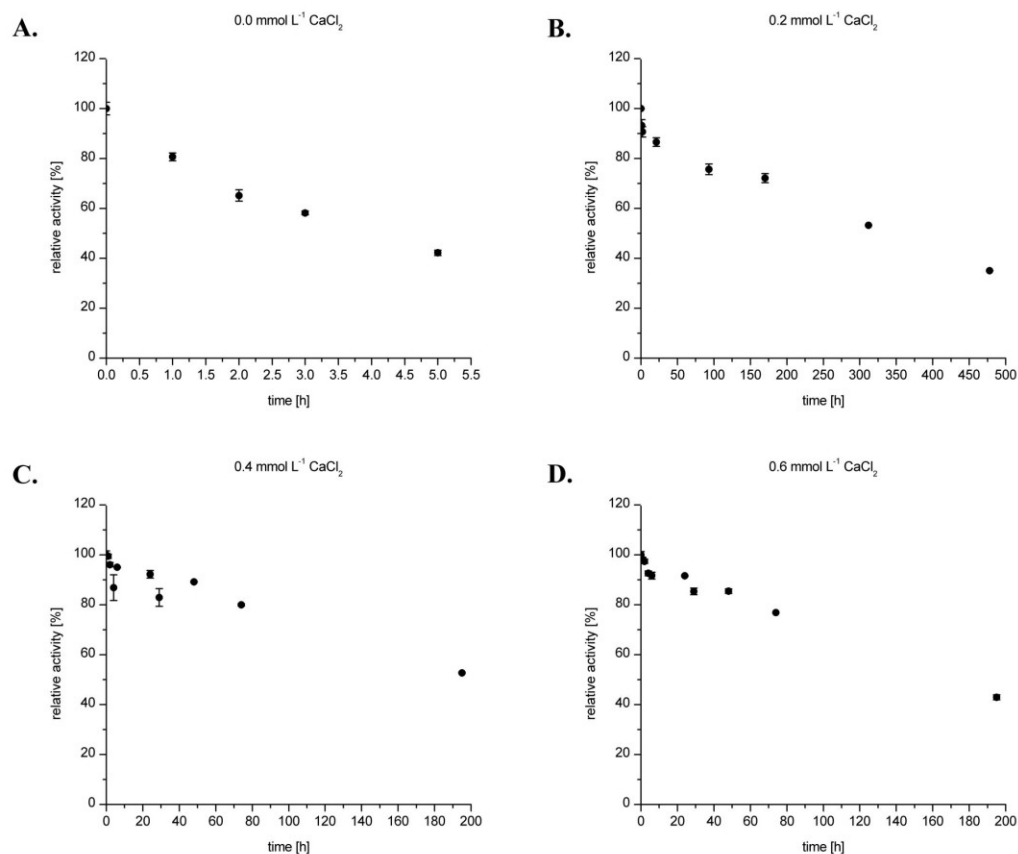


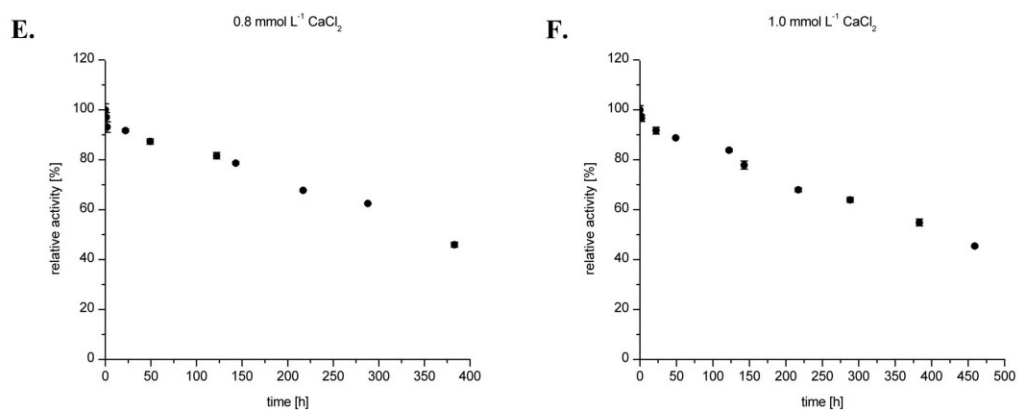
**Figure S1.** Stability study of purified RADH under different conditions. **A:** RADH (0.4 mg mL<sup>-1</sup>) in TEA-HCl buffer, 50 mmol L<sup>-1</sup>, pH 7.5 at 0 °C, **B:** RADH (0.2 mg mL<sup>-1</sup>) in TEA-HCl buffer, 10 mmol L<sup>-1</sup>, pH 7.5, T = 8 °C; **C:** RADH (0.2 mg mL<sup>-1</sup>) in TEA-HCl buffer, 10 mmol L<sup>-1</sup>, pH 7.5, T = -20 °C; **D:** RADH (0.1 mg mL<sup>-1</sup>) in 50 % glycerol (v v<sup>-1</sup>) in TEA-HCl buffer, 50 mmol L<sup>-1</sup>, pH 7.5, T = -20 °C; **E:** freeze-dried RADH (charge B) stored at T = -20 °C.

**2. Table I: Effect of different salts and EDTA on the initial rate activity of RADH.** A relative activity of 100 % corresponds to  $2.6 \text{ U mg}^{-1}$  measured in triplicate with the standard reduction activity assay following the consumption of NADPH ( $0.2 \text{ mmol L}^{-1}$ ) at 340 nm and  $30^\circ\text{C}$  in TEA-HCl buffer ( $50 \text{ mmol L}^{-1}$ ), pH 7.5. Each salt and EDTA was applied in a concentration of  $1 \text{ mmol L}^{-1}$ .

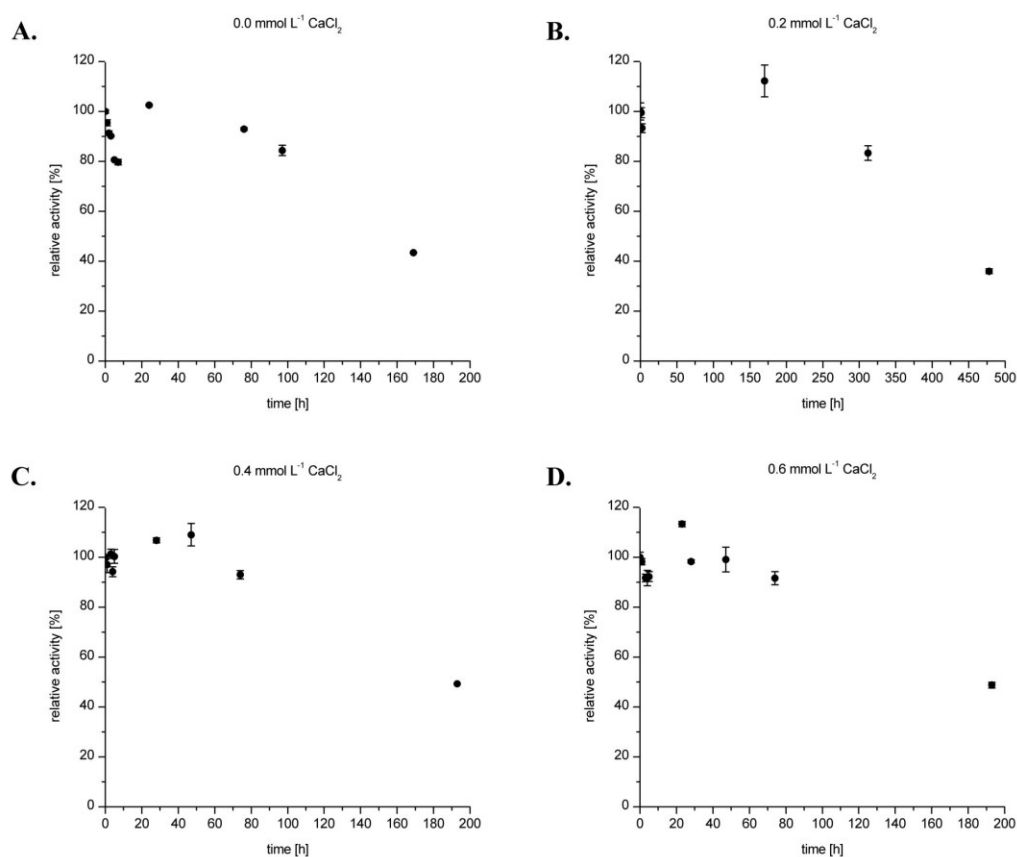
Reagent	Relative activity [%]
None	$100.0 \pm 1.7$
NaCl	$98.0 \pm 2.2$
RbCl	$97.3 \pm 3.5$
KCl	$97.1 \pm 3.1$
LiCl	$95.9 \pm 1.9$
Na-EDTA	$95.8 \pm 1.0$
$\text{CaCl}_2$	$95.3 \pm 0.8$
$\text{MgCl}_2$	$92.5 \pm 2.9$
$\text{CoCl}_2$	$86.1 \pm 4.5$
$\text{NiCl}_2$	$84.5 \pm 2.1$
$\text{CuCl}_2$	$75.5 \pm 1.1$
$\text{MnCl}_2$	$74.9 \pm 1.2$
$\text{ZnCl}_2$	$61.0 \pm 0.8$

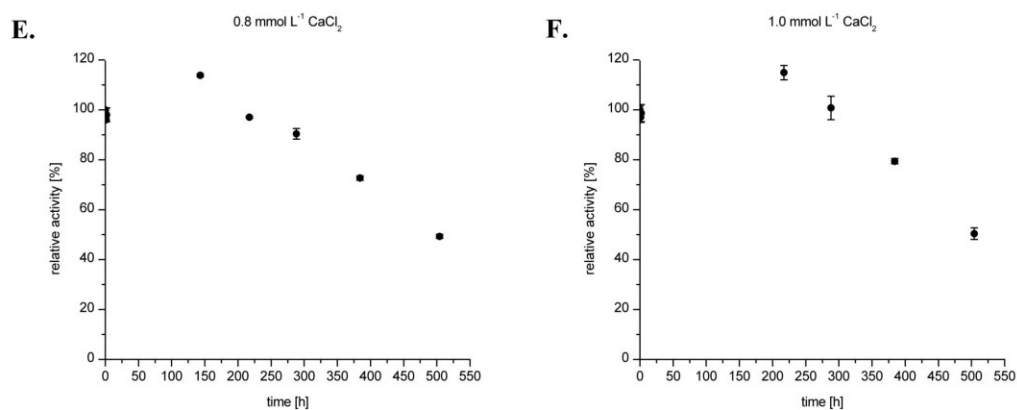
### 3. Influence of $\text{CaCl}_2$ on the stability of RADH





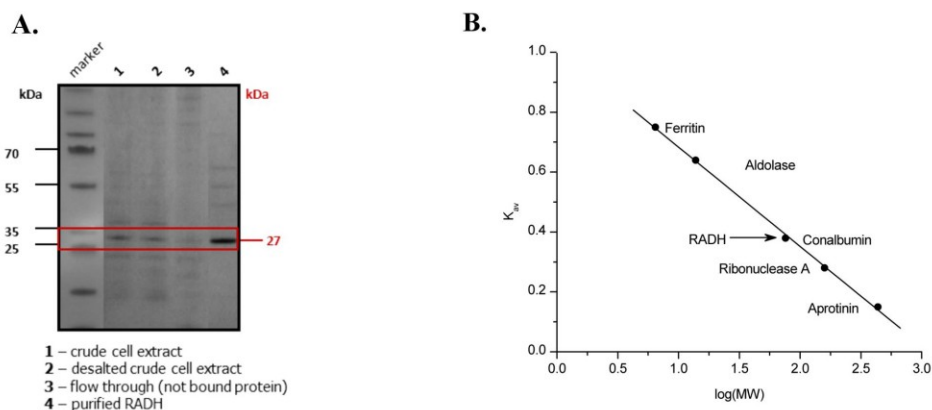
**Figure S2.** Stability studies of RADH performed with enzyme purified without  $\text{CaCl}_2$ . Lyophilized enzyme was dissolved in TEA-HCl buffer ( $50 \text{ mmol L}^{-1}$ , pH 7.5) with the given  $\text{CaCl}_2$  concentrations to a final concentration of  $0.2 \text{ mg mL}^{-1}$  and incubated at  $8^\circ\text{C}$ .





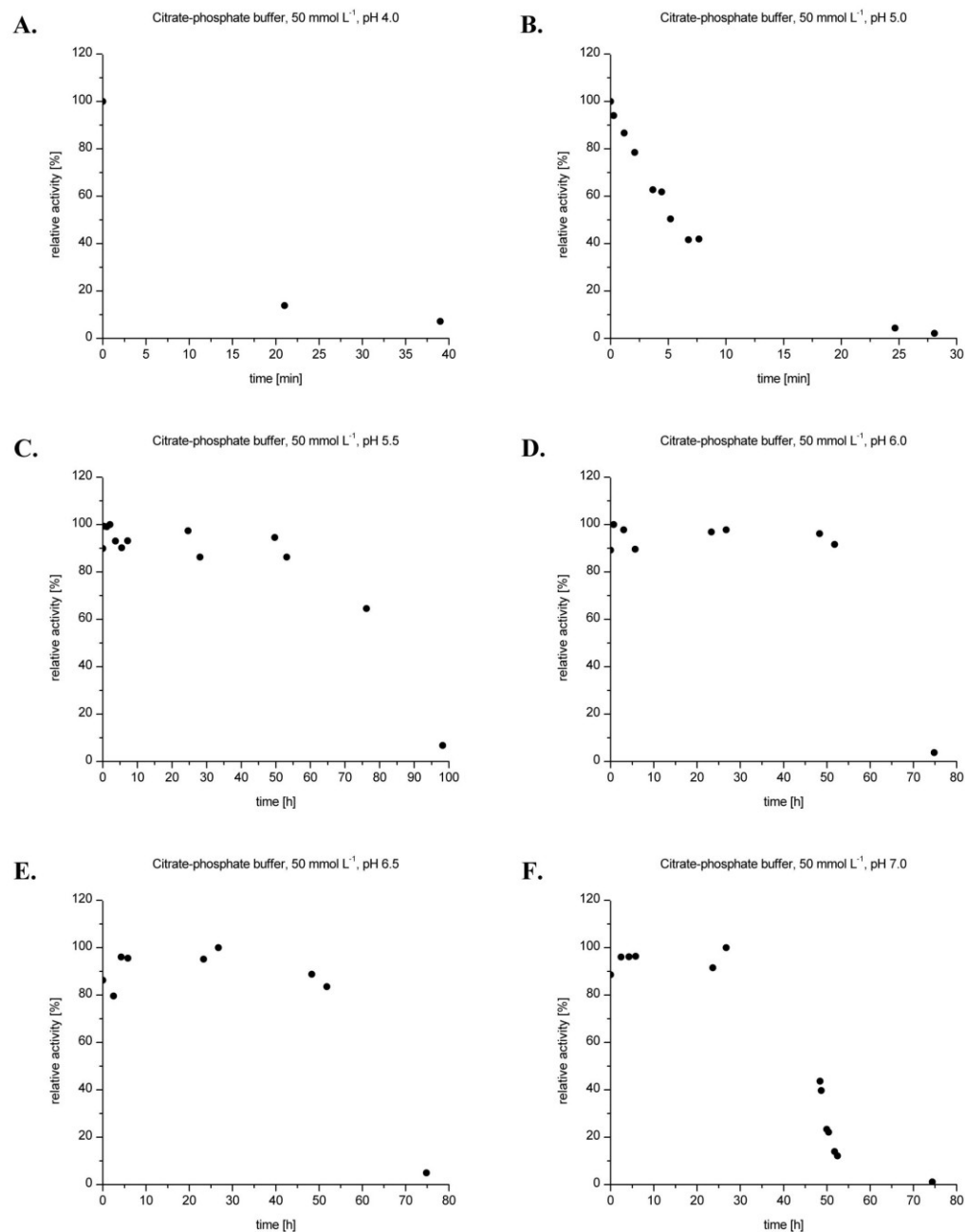
**Figure S3.** Stability studies of RADH performed with enzyme purified in the presence of 0.8 mmol L<sup>-1</sup> CaCl<sub>2</sub>. Lyophilized enzyme, stored at -20 °C, was dissolved in TEA-HCl buffer (50 mmol L<sup>-1</sup>, pH 7.5) to a final concentration of 0.2 mg mL<sup>-1</sup> with the given different CaCl<sub>2</sub> concentrations and incubated at 8 °C. Residual activity was followed using the standard assay for reduction.

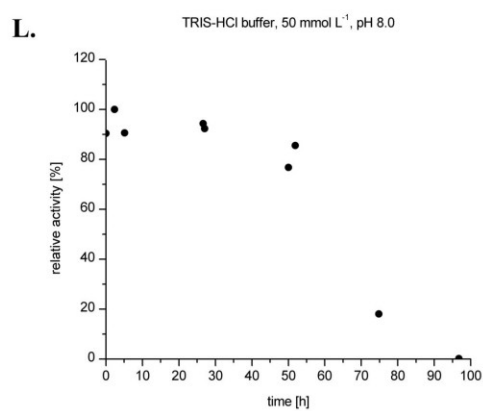
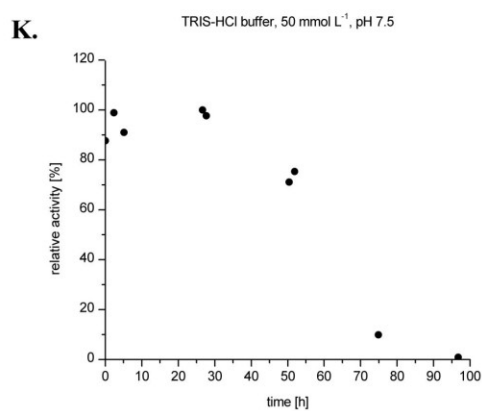
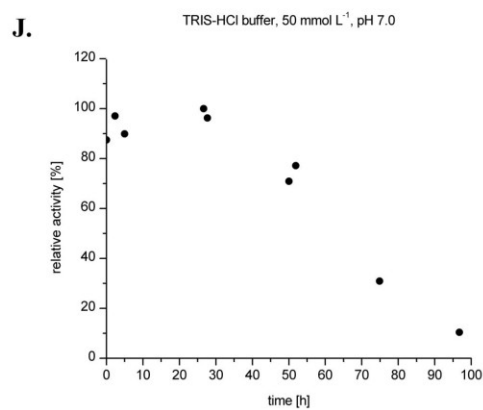
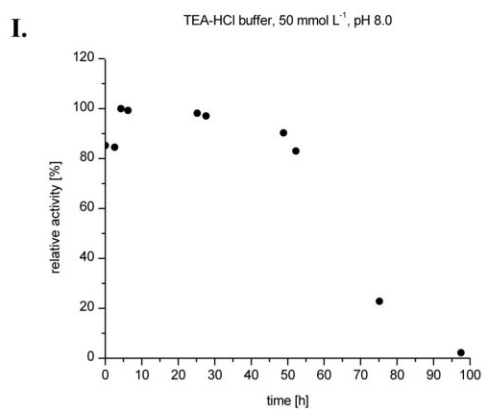
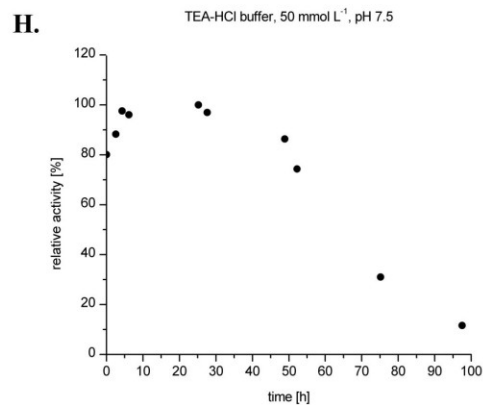
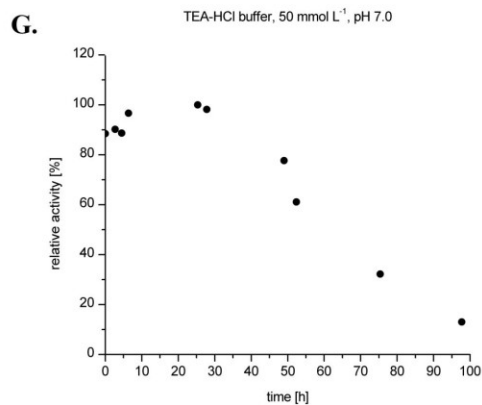
### 3. Determination of the molecular weight



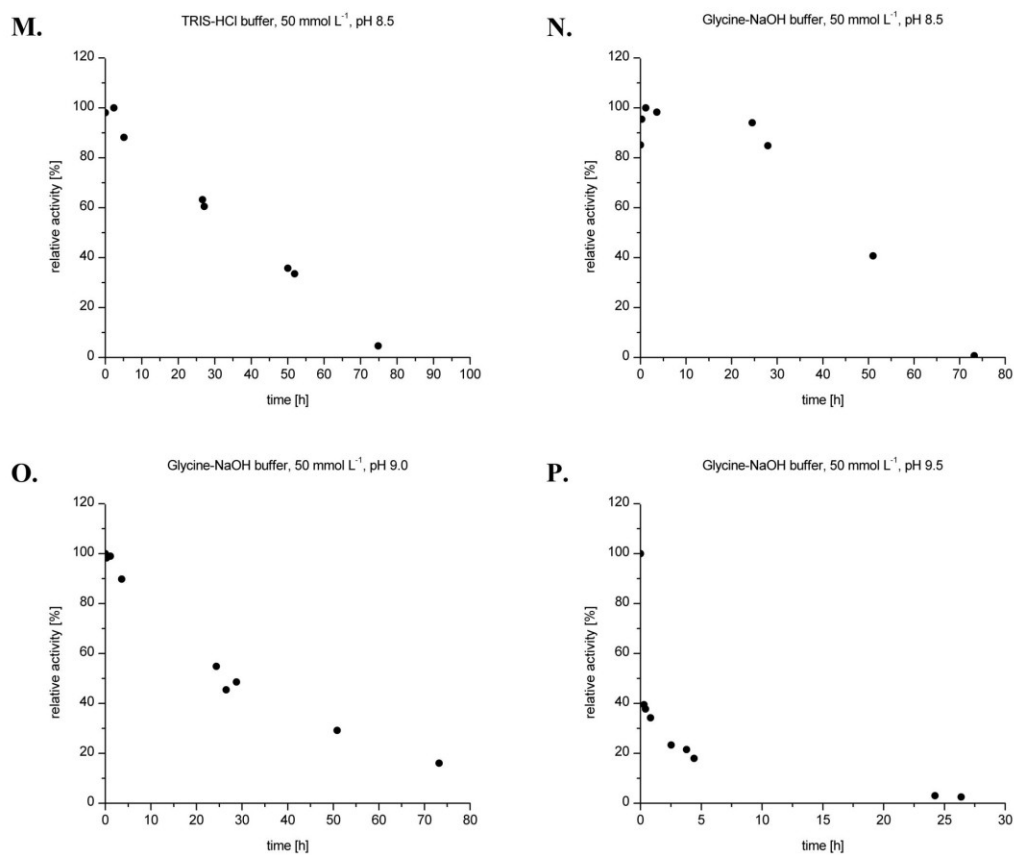
**Figure S4. A:** SDS-PAGE of a typical RADH purification **B:** The native molecular mass of RADH was determined by size exclusion chromatography using a Superdex<sup>TM</sup> 200 column (diameter: 26 mm, length: 63 cm, gel bed volume: 334 mL, RADH loaded: 1.7 mL, concentration: 3 mg mL<sup>-1</sup>). The molecular weight determination procedure was conducted in 50 mmol L<sup>-1</sup> TEA-HCl buffer, pH 7.5 containing 150 mmol L<sup>-1</sup> NaCl. According to the calibration curve  $\log(MW)$  of native RADH corresponds to 75 kDa. The results suggest a trimeric structure for the native enzyme.

#### 4. Influence of pH on the stability of RADH



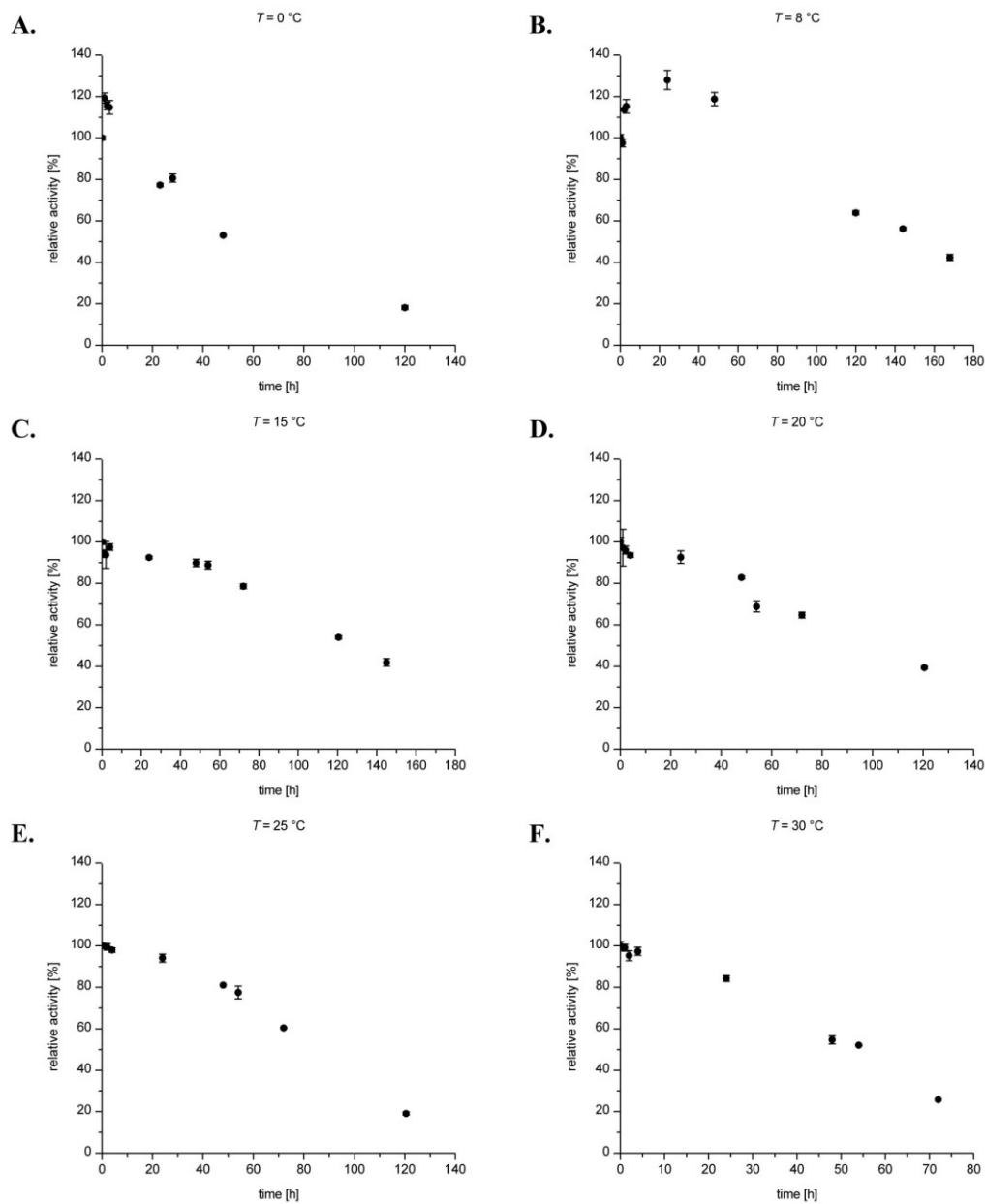


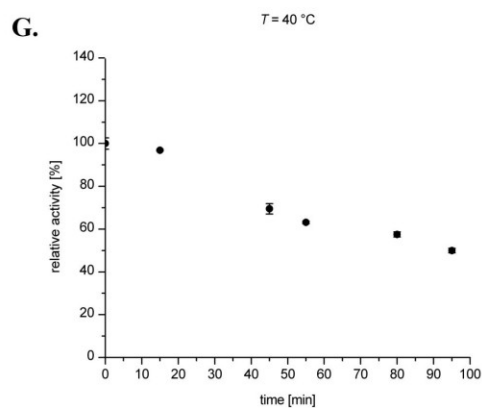




**Figure S5.** Stability studies of RADH in the presence of different buffers and pH-values. Enzyme purified with 0.2 mmol L<sup>-1</sup> CaCl<sub>2</sub> was dissolved in defined buffer supplemented with 0.8 mmol L<sup>-1</sup> of CaCl<sub>2</sub> to a final concentration of 0.8 mg mL<sup>-1</sup> and incubated under the conditions given at 25 °C.

## 5. Influence of temperature on the stability of RADH

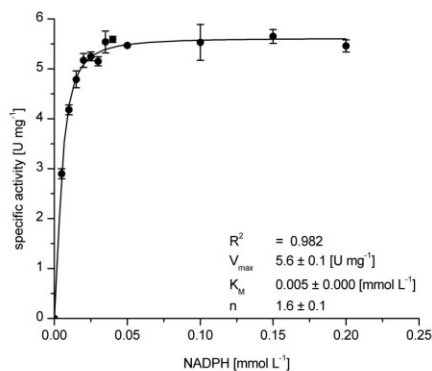




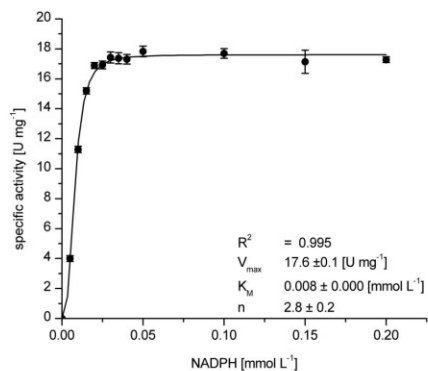
**Figure S6.** Stability investigations of RADH at different temperatures. Enzyme purified with  $0.2\text{ mmol L}^{-1}\text{ CaCl}_2$  was dissolved in TEA-HCl buffer ( $50\text{ mmol L}^{-1}\text{ TEA} + 0.8\text{ mmol L}^{-1}\text{ Ca}^{2+}$ , pH 7.5) to a final concentration of  $0.5\text{ mg mL}^{-1}$  and incubated at the given temperatures. Residual activity was determined using the standard assay (reduction of benzaldehyde).

## 6. Kinetic measurements

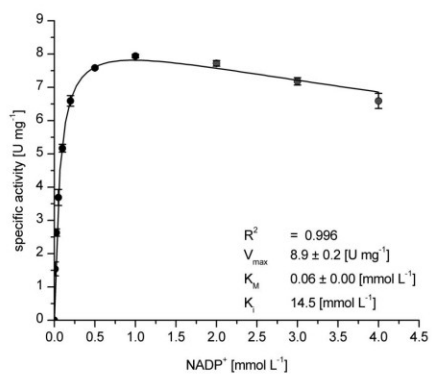
A.



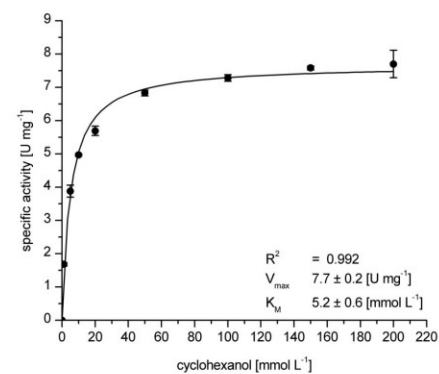
B.



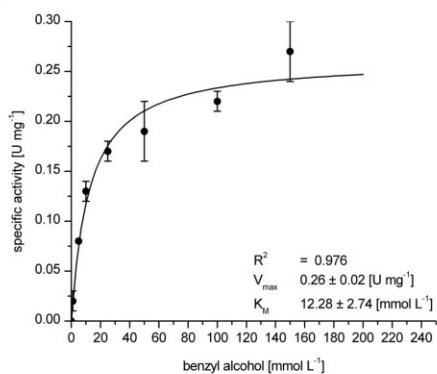
C.



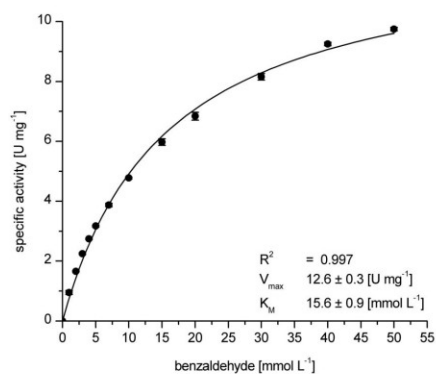
D.

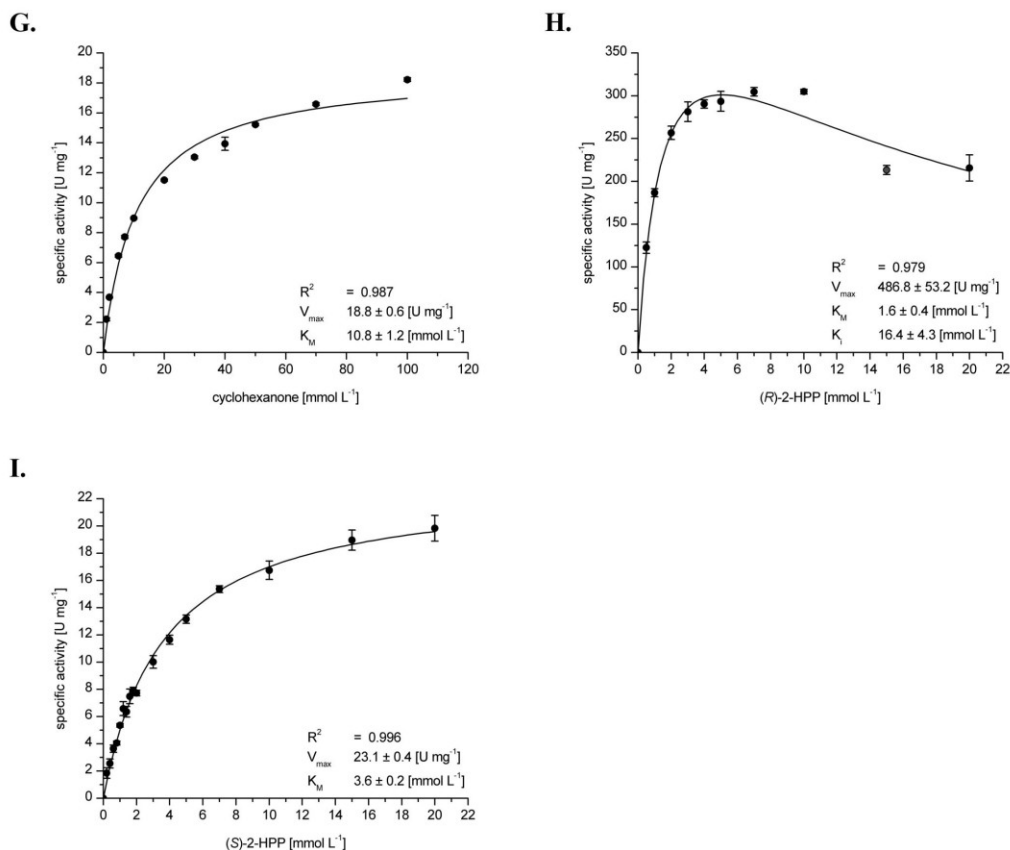


E.



F.





**Figure S7.** Kinetic measurements for oxidation and reduction. **A:** Kinetic of RADH for NADPH. Assay: TEA-HCl, 50 mmol L<sup>-1</sup> + 0.8 mmol L<sup>-1</sup> CaCl<sub>2</sub>, pH 7.5, benzaldehyde: 15 mmol L<sup>-1</sup>, NADPH: 0–0.2 mmol L<sup>-1</sup>. **B:** Kinetic of RADH for NADPH. Assay: TEA-HCl, 50 mmol L<sup>-1</sup> + 0.8 mmol L<sup>-1</sup> CaCl<sub>2</sub>, pH 7.5, cyclohexanone: 100 mmol L<sup>-1</sup>, NADPH: 0–0.2 mmol L<sup>-1</sup>. **C:** Kinetic of RADH for NADP<sup>+</sup>. Assay: TRIS-HCl, 50 mmol L<sup>-1</sup> + 0.8 mmol L<sup>-1</sup> CaCl<sub>2</sub>, pH 9.0, cyclohexanol: 100 mmol L<sup>-1</sup>, NADP<sup>+</sup>: 0–4.0 mmol L<sup>-1</sup>. **D:** Kinetic of RADH for cyclohexanol. Assay: TRIS-HCl, 50 mmol L<sup>-1</sup> + 0.8 mmol L<sup>-1</sup> CaCl<sub>2</sub>, pH 9.0, cyclohexanol: 0–200 mmol L<sup>-1</sup>, NADP<sup>+</sup>: 0.2 mmol L<sup>-1</sup>. **E:** Kinetic of RADH for benzyl alcohol. Assay: TRIS-HCl, 50 mmol L<sup>-1</sup> + 0.8 mmol L<sup>-1</sup> CaCl<sub>2</sub>, pH 9.0, benzyl alcohol: 0–150 mmol L<sup>-1</sup>, NADP<sup>+</sup>: 0.8 mmol L<sup>-1</sup>. **F:** Kinetic of RADH for benzaldehyde. Assay: TEA-HCl, 50 mmol L<sup>-1</sup> + 0.8 mmol L<sup>-1</sup> CaCl<sub>2</sub>, pH 7.5, benzaldehyde: 0–50 mmol L<sup>-1</sup>, NADPH: 0.2 mmol L<sup>-1</sup>. **G:** Kinetic of RADH for cyclohexanone. Assay: TEA-HCl, 50 mmol L<sup>-1</sup> + 0.8 mmol L<sup>-1</sup> CaCl<sub>2</sub>, pH 7.5, cyclohexanone: 0–100 mmol L<sup>-1</sup>, NADPH: 0.2 mmol L<sup>-1</sup>. **H:** Kinetic of RADH for (R)-2-HPP. Assay: TEA-HCl, 50 mmol L<sup>-1</sup> + 0.8 mmol L<sup>-1</sup> CaCl<sub>2</sub>, pH 7.5, (R)-2-HPP: 0–20 mmol L<sup>-1</sup>, NADPH: 0.2 mmol L<sup>-1</sup>. **I:** Kinetic of RADH for (S)-2-HPP. Assay: TEA-HCl, 50 mmol L<sup>-1</sup> + 0.8 mmol L<sup>-1</sup> CaCl<sub>2</sub>, pH 7.5, (S)-2-HPP: 0–20 mmol L<sup>-1</sup>, NADPH: 0.2 mmol L<sup>-1</sup>.

## Publication III

---

“Stereoselective synthesis of 1,2-diols with synthetic enzyme cascades including smart *in situ* cofactor regeneration and co-product recycling”

Justyna Kulig, Wolfgang Wiechert, Martina Pohl and Dörte Rother

Submitted to ChemCatChem, June 2013

DOI: 10.1002/cctc.200((will be filled in by the editorial staff))

# Stereoselective synthesis of 1,2-diols with synthetic enzyme cascades including in situ cofactor regeneration and co-product recycling

Justyna Kulig,<sup>[a]</sup> Wolfgang Wiechert,<sup>[a]</sup> Martina Pohl<sup>[a]</sup> and Dörte Rother<sup>\*[a]</sup>

Alcohol dehydrogenases are of high interest for stereoselective syntheses of chiral building blocks, either in single enzymatic reduction or oxidation steps or as part of enzymatic multi-step cascades. As this class of enzymes requires nicotinamide cofactors such as NAD(H) or NADP(H) in stoichiometric concentration, their application in biotechnological applications is only economically feasible with appropriate cofactor regeneration. This can be performed e.g. substrate-coupled with one enzyme catalysing the main reaction and the regeneration step or enzyme-coupled by addition of a second enzyme for the regeneration reaction. In both cases an additional co-substrate is required and oxidised to the respective co-product that accumulates in equal concentration to the desired product. In order to shift the reaction towards product formation and to avoid undesired side effects with the accumulating co-product, it is advantageous to remove the co-product during the course of the reaction. Here we report a novel highly atom efficient enzymatic cofactor regeneration system for substrate- as well as

enzyme-coupled approaches. As model reaction, two aldehydes are carbonylated by a ThDP-dependent enzyme yielding a chiral  $\alpha$ -hydroxy ketone ((*R*)-2-hydroxy-1-phenylpropan-1-one, (*R*)-2-HPP) that is subsequently reduced by an alcohol dehydrogenase to a 1,2-diol ((1*R*,2*R*)-1-phenylpropane-1,2-diol). By choice of an appropriate co-substrate for the regeneration process, the formed co-product is re-used *in situ* as substrate for the carbonylation step. This cascade design enables co-product conversions up to > 99 %, and therewith high step- and atom efficiency. Even overall conversion of the whole cascade (taking all implemented aromatic substrates and remaining co-products into account) higher than 73 % is possible. Further, enantio- as well as diastereomeric excesses up to 99 % were obtained. The example presented here for the 2-step recycling cascade can be applied for any set of enzymes, where the combination of co-substrates and co-products is possible, such that the co-products can be re-used as substrates.

## Introduction

Chiral 1,2-diols find broad application as building blocks for pharmaceuticals, agrochemicals, and chemical catalysts.<sup>[1-3]</sup> There are chemical and enzymatic methods available for the synthesis of 1,2-diols. One commonly applied chemical method for the synthesis of vicinal diols is the well-known Sharpless dihydroxylation of olefins, which requires toxic potassium osmate(VI) dihydrate ( $K_2OsO_4 \cdot 2H_2O$ ). Unfortunately, the Sharpless dihydroxylation is not suitable for the production of *anti*-1,2-diols, since the access to *Z*-olefines is limited.<sup>[4]</sup> Vicinal diols in *anti*-configuration can be produced by hydrolysis of epoxides, which requires toxic catalysts and proceeds under harsh conditions (high temperature and pressure).<sup>[5]</sup> Another synthetic strategy is a ketone reduction catalysed by hydride transfer agents, such as  $NaBH_4$  and  $LiAlH_4$ .<sup>[6-9]</sup> The main drawback of all of these reactions are low stereoselectivities. A very elegant alternative to chemical methods is an enzymatic reduction of prochiral keto function of  $\alpha$ -diketones or  $\alpha$ -hydroxy ketones using NAD(P)H-dependent alcohol dehydrogenases.<sup>[10-12]</sup> Most recently, an enzymatic reduction of diversely substituted  $\alpha$ -hydroxy ketones was conducted with high conversions and high stereoselectivities using whole cells of *Pichia glucozyma*. However, the respective enzyme(s) responsible for the catalysed reductions is/are unknown yet.<sup>[12]</sup>

A valuable alternative for the production of vicinal diols is the 2-step enzymatic synthesis. The first step is the carbonylation

of aldehydes catalysed by ThDP-dependent enzyme, whereby chiral  $\alpha$ -hydroxy ketones are formed.<sup>[13]</sup> In the second step  $\alpha$ -hydroxy ketones are reduced by isolated NAD(P)H-dependent alcohol dehydrogenases yielding vicinal 1,2-diols.<sup>[10,11]</sup>

Since nicotinamide cofactors are very expensive, prohibiting their implementation in equimolar amounts, there is a need for developing solutions of efficient cofactor regeneration systems. According to the classification of Chenault and Whitesides<sup>[14]</sup> there are five general methods exist: biological, chemical, electrochemical, photochemical and enzymatic methods. The last one is the most frequently used system<sup>[15-17]</sup> and can be further classified into substrate- and enzyme-coupled approaches. In the substrate- coupled approach only one enzyme for the main and for the regeneration reaction is implemented. There are a number of lab- and industrial-scale applications of this system using alcohol dehydrogenases from *Thermoanaerobium brockii* (TBADH)<sup>[18-20]</sup>, *Candida parapsilosis*<sup>[21,22]</sup>, horse liver<sup>[23]</sup> and *Lactobacillus brevis*.<sup>[3,24]</sup> Predominantly 2-propanol and ethanol

[a] Justyna Kulig, Prof. Dr. Wolfgang Wiechert, Prof. Dr. Martina Pohl, Dr. Dörte Rother  
Forschungszentrum Jülich GmbH  
Institute of Bio- and Geosciences 1: Biotechnology  
Wilhelm-Johnen-Strasse, 52428 Jülich (Germany)  
Fax: (+) 49 2461 61 3870  
E-mail: do.rother@fz-juelich.de

Supporting information for this article is available on the WWW under <http://dx.doi.org/10.1002/cctc.200xxxxx>. ((Please delete if not appropriate))



are oxidised in a regeneration step to acetone or acetaldehyde, respectively. Some biocatalytic processes implementing substrate-coupled cofactor regeneration systems require the removal of formed co-product, since it negatively affects the activity and stability of the enzyme<sup>[25]</sup> when present in high amounts. Furthermore, reversibility of the reaction has to be considered when a poor equilibrium constant strongly affects the yield of the reaction. Thus, high conversions can be achieved by the combination of high co-substrate concentrations and co-product removal.<sup>[21]</sup>

In enzyme-coupled approaches two different enzymes are involved in the main reaction and the cofactor regeneration step. Selected examples of effectively employed enzymes for enzyme-coupled cofactor regeneration in lab- and industrial scales are glucose dehydrogenases from *Bacillus cereus*<sup>[26,27]</sup> and *Bacillus subtilis*<sup>[27,28]</sup>, formate dehydrogenase from *Candida boidinii*<sup>[29]</sup> and *Pseudomonas* sp.<sup>[30-32]</sup> or alcohol dehydrogenases from *Thermoanaerobacter brockii*<sup>[33,34]</sup>, *Saccharomyces cerevisiae*<sup>[35,36]</sup>, and *Lactobacillus brevis*.<sup>[37-39]</sup> For latter, primary or secondary alcohols (e.g. ethanol, 2-propanol) are employed for cofactor regeneration.

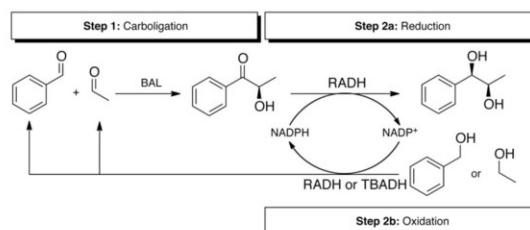
If co-product separation is not already performed during the course of the reaction, it has to be separated from the product during the final work-up. This process is very often time- and capacity-consuming and therewith a crucial cost-factor of downstream processing.<sup>[40-42]</sup> If a cascade consists of several oxidation and reduction steps, a effective approach to circumvent by-product formation is the self-sufficient cofactor regeneration by an internal recycling cascade.

For the here represented cascade this intrinsic cofactor regeneration is not possible, since only one NADPH consuming reduction step occurs. Instead, we found a novel cascade design, where the co-substrate is chosen in a way, that formed co-product can in situ be used as substrate for the first step of the main cascade reaction (see Figure 1). The here presented one-pot multi-enzymatic system combines many advantages: i) high atom economy due to in situ co-product recycling into the first step of the synthetic enzyme cascade, ii) no by-product formation (and therewith no additional purification effort) iii) high step economy and therewith high process economy (carboligation, reduction and cofactor regeneration are carried out simultaneously in one-pot; the number of required steps for product work up is significantly reduced), iv) highly stereoselective access to valuable chiral 1,2-diols from inexpensive starting materials and v) avoidance of toxic compounds.

For the model cascade reaction benzaldehyde lyase from *Pseudomonas fluorescens* Biovar I (BAL) and an alcohol dehydrogenase from *Ralstonia* sp. (RADH) were chosen. BAL is a highly active biocatalyst from our ThDP-dependent enzyme toolbox<sup>[13]</sup> for the mixed carboligation of various aldehydes, yielding  $\alpha$ -hydroxy ketones with high chemo-, regio- and enantioselectivity ( $ee > 99\%$ ).<sup>[47,48]</sup> Most recently, a successful combination of BAL with an oxidase from *Hansenula* sp. for the production of  $\alpha$ -hydroxy ketones using aliphatic alcohols for cofactor-regeneration was reported.<sup>[49]</sup> In our case we wanted to gain valuable chiral 1,2-diols from cheap aldehydes by addition of a second enzymatic step. For the further reduction of the  $\alpha$ -hydroxy ketone to the respective 1,2-diol, an alcohol dehydrogenase from *Ralstonia* sp. suited best. As we have shown previously, the alcohol dehydrogenase from *Ralstonia* sp. (RADH) is most active for bulky  $\alpha$ -hydroxy ketones (up to  $\sim 360 \text{ U mg}^{-1}$  for the (R)-2-hydroxy-1-phenylpropane-1-one) and

shows excellent high diastereoselectivity ( $de > 99\%$ ).<sup>[11]</sup> Additionally, an alcohol dehydrogenase from *Thermoanaerobacter brockii* (TBADH) was chosen for cofactor regeneration in the enzyme-coupled approach, due to its good acceptance of primary and secondary aliphatic alcohols like ethanol, 2-propanol, and 2-butanol.<sup>[50]</sup>

By a combination of the starting compounds for carboligation (acetaldehyde and benzaldehyde), co-substrates for cofactor regeneration (ethanol or benzyl alcohol), and enzymes (BAL, RADH, and TBADH), the co-products formed by cofactor regeneration (acetaldehyde or benzaldehyde) directly acts as substrate for the first step. Therefore, this work presents a new enzyme cascade mode for the highly stereoselective production of 1,2-diols from inexpensive aldehydes in an eco-efficient way including in situ co-product removal (see Figure 1).



combining a carboligation (step 1) and oxidoreduction step (step 2a) and a substrate- or enzyme-coupled approach for cofactor regeneration. Formed co-product (step 2b) is removed by its re-use in the carboligation step, the first step of the synthetic enzyme cascade. BAL = benzaldehyde lyase from *Pseudomonas fluorescens*, RADH = alcohol dehydrogenase from *Ralstonia* sp., TBADH = alcohol dehydrogenase from *Thermoanaerobacter brockii*.

## Results and Discussion

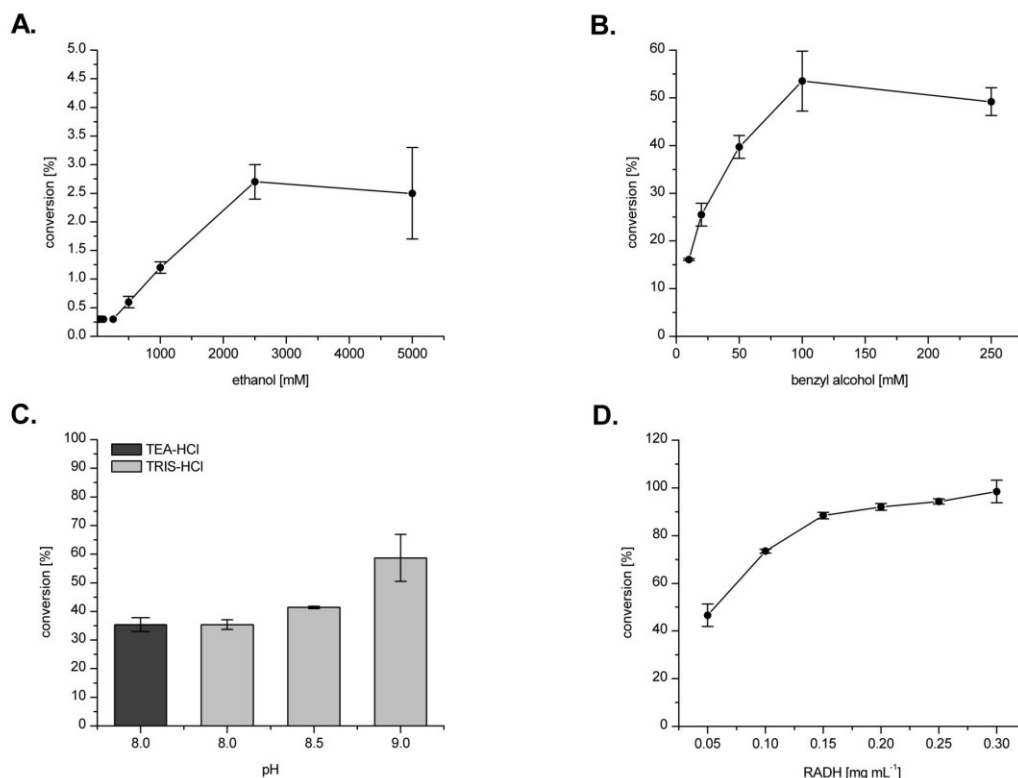
### Set-up and optimisation of cofactor regeneration

For the substrate-coupled approach the reaction of RADH with ethanol and benzyl alcohol as co-substrates were examined. For the enzyme-coupled approach oxidation of the co-substrate ethanol catalysed by TBADH was studied.

Optimisation of cofactor regeneration was performed only for the second part of the cascade using *rac*-2-HPP as substrate and varying the concentration of the co-substrates. Set-up of the synthetic cascade by applying the herein described optimal cofactor regeneration will be described afterwards,

### Substrate-coupled approach

Substrate-coupled cofactor regeneration optimisation using ethanol (20-5000 mM) as co-substrate (Figure 2A) indicated that ethanol is not well suited for this cascade reaction mode. Conversion to the respective 1-phenylpropane-1,2-diol was very low (3 %). This result is in full agreement with our previous studies, where RADH shows much higher oxidation activity towards large, cyclic and aromatic substrates compared to small aliphatic substrates.<sup>[52]</sup> For instance, the specific activity for the oxidation of ethanol (1700 mM) was determined as  $0.04 \text{ U mg}^{-1}$ . At ethanol concentrations of 10 mM and 100 mM no activity was detected at all. In contrast, cyclohexanol was oxidised with significantly higher specific activities of  $8\text{--}11.5 \text{ U mg}^{-1}$  for concentrations of 10 mM and 100 mM, respectively. Benzyl alcohol, an alternative to ethanol for substrate-coupled



**Figure 2.** Optimisation of substrate-coupled cofactor regeneration. Conversion is defined as the amount of (1*R*,2*R*)- and (1*R*,2*S*)-diol formed by reduction of *rac*-2-HPP. **A.** Optimisation of the ethanol concentration. Reaction conditions: TRIS-HCl buffer (50 mM), pH 9.0, supplemented with CaCl<sub>2</sub> (0.8 mM), *rac*-2-HPP (10 mM), ethanol (20–5000 mM), NADP<sup>+</sup> (0.2 mM), RADH (0.05 mg mL<sup>-1</sup>). **B.** Optimisation of the benzyl alcohol concentration. Reaction conditions: as in 4A, but with benzyl alcohol (10–250 mM). **C.** Identification of optimal pH for the oxidoreduction. Reaction conditions: TEA-HCl buffer (50 mM), pH 8.0 and TRIS-HCl buffer (50 mM), pH 8.0–9.0 supplemented with CaCl<sub>2</sub> (0.8 mM), *rac*-2-HPP (10 mM), benzyl alcohol (100 mM), NADP<sup>+</sup> (0.2 mM), RADH (0.05 mg mL<sup>-1</sup>). **D.** Optimisation of the enzyme concentration. Reaction conditions: as in 4A, but with RADH (0.05–0.30 mg mL<sup>-1</sup>) and benzyl alcohol (100 mM). All reactions were carried out at 20 °C for 24 h under constant shaking (500 rpm) in aliquots (1 mL each) in glass vials.

cofactor regeneration, was tested in a concentration range from 10 mM to 250 mM. Higher concentrations were not tested in order to avoid the formation of a two-phase system due to the limited solubility of benzyl alcohol in aqueous medium. As demonstrated in Figure 2B, benzyl alcohol was very well oxidised to benzaldehyde with conversions up to 53.5 % for 100 mM benzyl alcohol (0.05 mg mL<sup>-1</sup> RADH, pH 9.0).

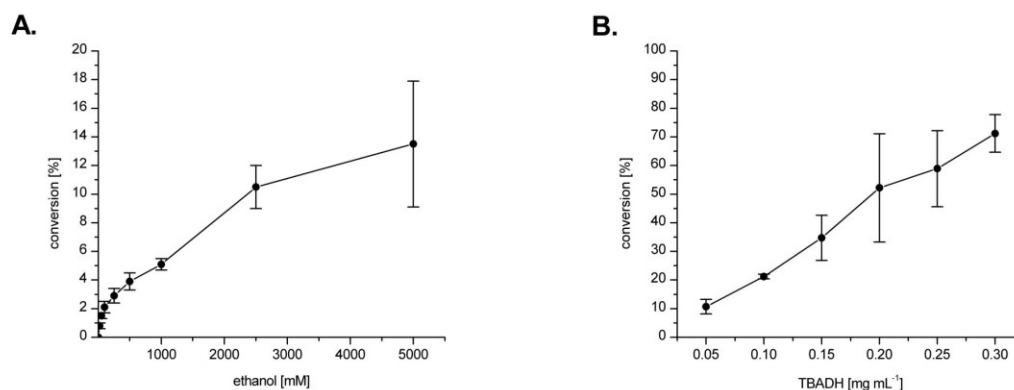
In our previous work we demonstrated that RADH exhibits different pH-optima for its reduction and oxidation activity. The pH optimum for reduction is broad (pH 6–9.5) and does not overlap with the sharp oxidation optimum of pH 10–11.5.<sup>[52]</sup> Therefore, finding suitable conditions for a simultaneous catalysis of both reactions in one-pot was a challenging task. Furthermore, stability tests indicate that RADH is rather stable at a pH range between 5.5 and 8.0 (half-life: ~60–70 h). Higher pH values (> pH 8) could promote inactivation/denaturation of the enzyme. pH 9 appeared to be a compromise for the oxidation reaction ensuring sufficient activity and stability (half-life of ~30 h). Based on these previous results, the substrate-coupled cofactor regeneration of the RADH-catalysed reduction of *rac*-2-HPP was tested between pH 8.0 to 9.0 using benzyl alcohol as a co-substrate (Figure 2C).

The pH-optimisation for the substrate-coupled approach indicated 1.7-fold higher conversions of *rac*-2-HPP to the respective 1,2-diols ((1*R*,2*R*)- and (1*R*,2*S*)-1-phenylpropane-1,2-diol) at pH 9.0 compared to pH 8.0 (35 % for pH 8 and 59 % for pH 9). The nature of the applied buffer (TEA-HCl or TRIS-HCl) had no influence at pH 8.0, resulting in 35 % conversion in both cases (Figure 2C).

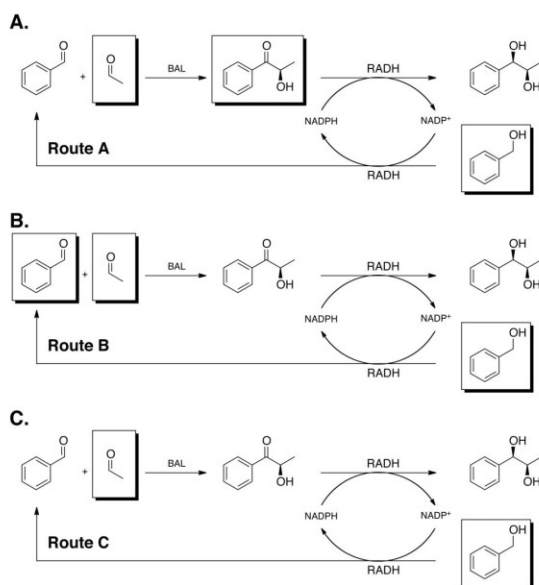
Since RADH accepts both enantiomers of *rac*-2-HPP<sup>[11,52]</sup>, and in none of these experiments conversions > 59 % of *rac*-2-HPP were observed (Figure 2A–C), the enzyme concentration was increased in order to test whether conversion could further be improved. Figure 2D demonstrates that almost full conversion (98.5 %) could be achieved with RADH concentrations > 0.15 mg mL<sup>-1</sup>, showing that previous experiments were limited by enzyme stability.

#### Enzyme-coupled approach

Ethanol is a well-accepted substrate of TBADH<sup>[50]</sup> but very poorly accepted by RADH.<sup>[52]</sup> Determination of the optimal co-substrate



**Figure 3.** Optimisation for the enzyme-coupled cofactor regeneration using TBADH for regeneration. **A.** Optimisation of the ethanol concentration. Reaction conditions: TRIS-HCl buffer (50 mM) pH 9.0 supplemented with CaCl<sub>2</sub> (0.8 mM), *rac*-2-HPP (10 mM), ethanol (20–5000 mM), NADP<sup>+</sup> (0.2 mM), RADH (0.05 mg mL<sup>-1</sup>), TBADH (0.05 mg mL<sup>-1</sup>). **B.** Optimisation of the TBADH concentration. Reaction conditions: TRIS-HCl buffer (50 mM) pH 9.0 supplemented with CaCl<sub>2</sub> (0.8 mM), *rac*-2-HPP (10 mM), ethanol (20–5000 mM), NADP<sup>+</sup> (0.2 mM), RADH (0.05 mg mL<sup>-1</sup>), TBADH (0.05–0.30 mg mL<sup>-1</sup>). All reactions were carried out at 20 °C for 24 h with constant shaking (500 rpm).



**Figure 4.** Three routes for the synthetic cascade reaction with substrate-coupled cofactor regeneration were tested (A–C). They differ in substrate supply strategy. In all cases benzyl alcohol was used as the co-substrate. The benzaldehyde formed upon oxidation with RADH is reused in the first step of the cascade. Substrates which are present in the reaction system when the reaction was started ( $t = 0$ ) are framed. BAL = benzaldehyde lyase from *Pseudomonas fluorescens*, RADH = alcohol dehydrogenase from *Ralstonia* sp.

concentration (ethanol: 20–5000 mM) gave much higher conversions of *rac*-2-HPP (~10 % conversion with 2500 mM ethanol, 0.05 mg mL<sup>-1</sup> TBADH and 0.05 mg mL<sup>-1</sup> RADH) (Figure 3A) compared to reached with the substrate-coupled approach (only 3 % conversion with 2500 mM ethanol and 0.05 mg mL<sup>-1</sup> RADH) (Figure 2A). For further investigations of all synthetic cascade modes, 2500 mM ethanol was used, which was shown to

be the optimal concentration in the presence of RADH and TBADH (Figure 2A and 3A).

For the enzyme-coupled approach pH optimisation was omitted, since pH 9.0 is suitable when RADH is implemented for the reduction step (see Figure 2C). Furthermore, TBADH shows a sharp pH optimum at pH 7.8–9.0 for oxidation.<sup>[50]</sup>

After optimisation of the enzyme concentration, conversions up to 70 % were possible with 2500 mM ethanol, when  $\geq 0.30$  mg mL<sup>-1</sup> of TBADH were used (Figure 3B).

### Synthetic enzyme cascades

#### Cascade reaction with substrate-coupled cofactor regeneration

After setting up optimal reaction conditions for substrate- and enzyme coupled cofactor regeneration, the second reduction step was combined with the first carbonylation step for the synthetic enzyme cascade.

#### Standard reaction

First conducted approaches of the cascade reactions using substrate-coupled cofactor regeneration by following routes A to C (Figure 4A–C) revealed overall conversions (for definition of overall conversion see paragraph *Experimental: Cascade with substrate-coupled cofactor regeneration*) to the (1*R*,2*R*)-diol of only 19.7 % (A), 18.6 % (B), and 11.8 % (C). Diastereoselectivities (*de*) were with values > 96 % high (Table 1, entry 8). Taking only conversions of formed co-product (conv<sub>CP</sub>) into account, measured conversions were much higher: 99.1 % (A), 99.1 % (B), and 98.6 % (C), respectively. The initial amount of the intermediate (*R*)-2-HPP (10 mM) added in route A was fully converted to the (1*R*,2*R*)-diol (24.9 mM, *de* 96 %) proving an efficiently working cofactor regeneration system. Similar high conversion with respect to co-product conversion were found (24.3 mM of (1*R*,2*R*)-diol, *de* > 99 %) when the reaction system was started with benzaldehyde (10 mM) and acetaldehyde (150 mM) for carbonylation and benzyl alcohol (120 mM) for

cofactor regeneration (Figure 4B). While route A and route B almost performed equally well, lowest conversions were obtained via route C, where only acetaldehyde and benzyl alcohol were available as starting compounds. Here only 14.9 mM (*de* > 99 %) of the (1*R*,2*R*)-diol was formed when all aromatic compounds were taken into account, which was 1.7-fold less than for routes A and B.

This standard reaction set presents the proof-of-principle of the synthetic multi-enzyme cascade in one-pot with excellent in situ co-product removal (conversion of co-product up to 99.1 %). However, overall conversion lower 20 % were unsatisfying. In order to increase the overall efficiency of the process, optimisation of reaction conditions for the cascade with substrate-coupled cofactor regeneration was done. To exploit the full potential, concentration of cofactor, enzyme, as well as pH were investigated.

#### NADP<sup>+</sup> concentration

Optimal NADP<sup>+</sup> concentration varied slightly depending on the tested route (see Table 1, entry 1–4; Supplementary Information, Figure S2.1A–C). For routes A and B (Table 1, entry 2–4; Supplementary Information, Figure S2.1A–B) NADP<sup>+</sup> concentrations > 0.2 mM have little influence on reaction velocity and overall conversion. An increase of the NADP<sup>+</sup> concentration in route A from 0.2 mM to 0.8 mM enhanced the overall conversions from 27.3 % to maximal 31.4 %. A similar trend was observed for route B (21.5 % overall conversion with 0.2 mM NADP<sup>+</sup> to 27.7 % with 0.8 mM NADP<sup>+</sup>). For route C the influence of the NADP<sup>+</sup> concentration was almost completely negligible (overall conversion only increased from 9.2 %, with 0.2 mM NADP<sup>+</sup> to 9.8 %, with 0.8 mM NADP<sup>+</sup>). For all reaction routes very good co-product conversions of 94.2 % up to > 99 % were determined (see Table 1, entry 1–4). Therefore 0.8 mM NADP<sup>+</sup> was used for further investigations.

#### pH optimisation

As mentioned above, RADH shows different pH optima for the reduction and oxidation reaction, with pH 9.0 being a compromise for RADH catalysed simultaneous oxidation and reduction reactions. The challenging task for the cascade with substrate-coupled cofactor regeneration is to find not only proper conditions for oxidation and reduction by RADH, but to further combine it with conditions that are optimal for activity and stability of the first enzyme (BAL) in the cascade.

As expected, pH optimisation revealed a pronounced influence of the pH on the overall conversion (see Table 1, entry 5–7; Figure 2.2A–C, Supplementary Information). For route A at pH 9.0, 25.1 % overall conversion and 99.2 % co-product conversion were obtained, which is higher as the results obtained at pH 8.0 (overall conversion: 19.7 %, co-product conversion: 99.1 %). A similarly high impact of the pH on the overall conversion was observed for route B (enhancement of ~ 6 % by an pH- increase from 8 to 9). In route C about 3 % increase of overall conversion was observed (pH 8.0: 11.8 %, pH 9.0: 15.3 %). Therefore pH 9.0 was applied for further investigations.

#### RADH concentration

Subsequently, the RADH concentration for effective cascade reactions with substrate-coupled cofactor regeneration was optimised. It showed a very strong influence on overall reaction conversions for all three routes (Figure 2A–C, Table 1, entry 8–

12). Using RADH concentrations up to 2.0 mg mL<sup>-1</sup>, final overall conversions up to ~ 68 % could be achieved (see Table 1, entry 12). Considering that these 68 % represent the conversion calculated for the sum of aromatic substrates added to the reaction, this conversion is very high, since the co-substrate benzyl alcohol has to be always in excess. If conversion is calculated only based on the conversion of co-product resulting only from benzyl alcohol oxidation, it reaches up to > 98 %.

It has to be mentioned that with increased concentration of the enzyme (> 0.33 mg mL<sup>-1</sup>) formation of two other stereoisomers of (1*R*,2*R*)-1-phenylpropan-1,2-diol occur. The reason of this result is discussed in the next paragraph.

#### Calculated theoretical conversions and its experimental control

The overall conversions (Table 1, entries: 1–12) obtained *via* all three routes suggested that full conversion is hampered by an unfavourable thermodynamical equilibrium. Therefore, the theoretical equilibrium constant based on obtained biochemical data was calculated (see Supplementary Information, chapter 3). According to these calculations overall conversions up to 99 % should be possible using the substrate-coupled approach with 120 mM benzyl alcohol and 150 mM acetaldehyde. (Supplementary Information, Figure S4).

Since in almost all cases route B showed best overall conversions (Table 1, entries 1–12), this route was chosen for further optimisation. Experimental data for route B showed an increased formation of the desired product with increased RADH concentrations (3.75 mg mL<sup>-1</sup>). Here, excellent co-product conversion of 97.2 % was detected (Table 1, entry 13). In total, this mode gave best results for cascades with substrate-coupled cofactor regeneration. The overall conversion biochemically detected for all implemented aromatic substrates (overall conversion) to the 1,2-diols is 73.4 % (see Table 1, entry 13; Supplementary Information, Figure S5). However, the mathematically calculated 92 % conversion (related to added benzyl alcohol and benzaldehyde as substrates) to the desired product could not completely be reached (Supplementary Information, Figure S4, Table S2). Addition of fresh enzyme to the reaction did not increase the conversion further. An explanation could be product inhibition, since the concentration of the (1*R*,2*R*)-diol reached 93 mM during the course of the reaction. However, spectrophotometric initial rate activity assays indicated that product inhibition is most likely not the reason for these limitations (data not shown). Therefore, kinetic limitations are more probable. At a certain point only a low concentration of benzyl alcohol is available, which reduces the enzyme velocity for the oxidation reaction. The *K<sub>m</sub>*-value of RADH for benzyl alcohol under the conditions applied is 12.3±2.7 mM.<sup>[52]</sup> When the apparent reaction equilibrium was reached, the measured concentration of benzyl alcohol was 13.3 mM, meaning that RADH is not operating at *V<sub>max</sub>* conditions. Most likely at high product concentration the kinetically not favoured back reaction starts, where (1*R*,2*R*)-diol is oxidised to the  $\alpha$ -hydroxy ketone. This could be proven by an elongation of time of the cascade reaction. After maximal product concentration (93 mM) was reached, the reaction was left for another 24 h with the results, that only 85.6 mM (1*R*,2*R*)-diol were left in the presence of RADH.

Thus, the assumption that the reaction was limited by the co-substrate concentration was confirmed (see Figure S6, Supplementary Information). Further, calculation of conversion is best performed based on the totally converted co-product

(benzaldehyde) that was directly applied as a substrate and produced as a co-product.

As already stated above, we observed that higher RADH concentrations negatively influence the stereoselectivity of the 1,2-diol formation. Applying an enzyme concentration of

3.75 mg mL<sup>-1</sup>, three of four possible stereoisomers of 1-phenylpropane-1,2-diol ((1*R*,2*R*) 90 %, (1*S*,2*R*) 8 %, and (1*R*,2*S*) 2 %) occur, resulting in a diastereomeric ratio (dr) of (*syn/anti*) 9:1. Formation of 8 % (1*S*,2*R*)-diol can be explained by

Table 1. Reaction engineering for cascade reactions with substrate-coupled cofactor regeneration										
Entry	Parameter	Route	conv <sub>overall</sub> <sup>[a]</sup> [%]	conv <sub>CP</sub> <sup>[b]</sup> [%]	C <sub>1,2-diol</sub> <sup>[c]</sup> [mM]	Distribution of stereoisomers of 1,2-diol [%]				de [%]
						(1 <i>R</i> ,2 <i>R</i> )	(1 <i>S</i> ,2 <i>R</i> )	(1 <i>R</i> ,2 <i>S</i> )	(1 <i>S</i> ,2 <i>S</i> )	
NADP <sup>+</sup> [mM]										
1	0.2	A	27.3±2.2	99.4±0.2	34.5	98	2	0	0	96
		B	21.5±0.2	99.1±0.1	28.6	98	2	0	0	96
		C	9.2±0.2	98.2±0.2	11.6	> 99	0	0	0	> 99
2	0.4	A	29.1±1.2	98.7±0.7	35.2	97	3	0	0	94
		B	26.8±1.6	94.2±6.7	32.4	97	3	0	0	94
		C	9.5±0.0	98.5±0.3	11.0	> 99	0	0	0	> 99
3	0.6	A	32.2±0.4	98.5±1.0	39.1	97	3	0	0	94
		B	23.4±1.0	99.0±0.0	28.5	98	2	0	0	96
		C	9.7±0.1	98.0±0.3	11.4	> 99	0	0	0	> 99
4	0.8	A	31.4±1.8	98.7±0.7	38.0	97	3	0	0	94
		B	27.7±1.8	98.4±1.0	33.8	97	3	0	0	94
		C	9.8±0.0	98.5±0.4	11.4	> 99	0	0	0	> 99
pH										
5	8.0	A	19.7±0.5	99.1±0.5	24.9	98	2	0	0	96
		B	18.6±0.9	99.1±0.4	24.3	98	2	0	0	96
		C	11.8±0.2	98.6±0.4	14.9	> 99	0	0	0	> 99
6	8.5	A	22.8±1.4	99.2±0.2	28.2	98	2	0	0	96
		B	26.5±3.5	98.8±0.0	31.8	98	2	0	0	96
		C	15.9±0.3	99.2±0.6	19.1	> 99	0	0	0	> 99
7	9.0	A	25.1±3.2	99.2±0.0	31.4	98	2	0	0	96
		B	24.3±2.9	99.1±0.1	29.7	99	1	0	0	98
		C	15.3±0.2	98.5±0.6	18.4	> 99	0	0	0	> 99
C <sub>RADH</sub> [mg mL <sup>-1</sup> ]										
8	0.10	A	19.7±0.5	99.1±0.5	24.9	98	2	0	0	96
		B	18.6±0.9	99.1±0.4	24.3	98	2	0	0	96
		C	11.8±0.2	98.6±0.4	14.9	> 99	0	0	0	> 99
9	0.24	A	27.2±1.3	99.1±0.1	34.0	99	1	0	0	98
		B	32.6±0.3	98.8±0.5	40.3	99	1	0	0	98
		C	29.5±1.3	98.5±0.6	35.0	99	1	0	0	98
10	0.33	A	42.7±3.7	98.6±0.7	53.1	98	2	0	0	96
		B	44.6±1.4	98.0±0.5	57.8	98	2	0	0	96
		C	36.1±3.6	97.9±0.1	43.3	99	1	1	0	n.a.
11	0.65	A	56.5±1.0	98.5±0.3	68.1	95	3	2	0	n.a.
		B	54.9±3.7	98.1±0.6	72.5	95	3	2	0	n.a.
		C	48.8±5.8	98.1±0.1	58.9	95	3	2	0	n.a.
12	2.00	A	68.3±3.0	98.6±0.1	82.4	97	2	1	0	n.a.
		B	67.6±4.5	98.2±0.3	88.1	96	3	1	0	n.a.
		C	68.0±2.1	98.6±0.5	78.9	96	2	2	0	n.a.
13	3.75	B	73.4	97.2	93.2	90	8	2	0	n.a.

[a] % conv<sub>overall</sub> – overall conversion is defined as the conversion of all aromatic compounds (benzyl alcohol, benzaldehyde and (*R*)-2-HPP depending on the route) at time *t* = 0 to the 1-phenylpropane-1,2-diol present; [b] % conv<sub>CP</sub> – co-product conversion is defined as the conversion of benzaldehyde formed during oxidation of benzyl alcohol; [c] C<sub>1,2-diol</sub> – concentration of (1*R*,2*R*)-1-phenylpropane-1,2-diol; de – diastereomeric excess; n.a. – not applicable since three stereoisomers of 1,2-diol are formed (see text).

non-perfect stereoselectivity of RADH. The higher the enzyme concentrations, the more prominent gets (S)-selective reduction of (R)-2-HPP. Further, formation of the (1R,2S)-diol can most likely be explained by keto-enol tautomerisation of 1,2-diol under applied conditions, during which interconversion of the vicinal diol occurs, yielding another stereoisomer. But since even with extremely high catalyst concentrations of  $3.75 \text{ mg mL}^{-1}$  only 1.8 % of this product was measured, this phenomena was too negligible to be investigated in more detail.

Besides, in all investigated routes (A–C) small amounts of benzoin (< 1 mM) were formed as a side product of the BAL-catalysed carbonylolation step.

Conclusively, taking into account that cofactor regeneration is required, with conversion of all aromatic compounds up to 73 % (route B using 10 mM benzaldehyde, 150 mM acetaldehyde and 120 mM benzyl alcohol, at pH 9 with 0.8 mM  $\text{NADP}^+$  and  $3.75 \text{ mg mL}^{-1}$  RADH) this cascade is very economically and ecologically efficient. Additionally higher final product concentration up to 93 mM 1,2-diol could be gained via route B. In the presence of only acetaldehyde and benzyl alcohol, still 78.9 mM of (1R,2R)-1-phenylpropane-1,2-diol are formed (route C), proving the effective working cofactor regeneration and the high atom-efficiency of the cascade. However, for this high conversion stereoselectivity was with 90 % good but not excellent. Therefore it was investigated, if the enzyme-coupled approach was advantageous for both, yield and selectivity.

#### Cascade reaction with enzyme-coupled cofactor regeneration

In the synthetic cascade including enzyme-coupled cofactor regeneration inexpensive ethanol was used instead of bezylalcohol. Therewith satisfying conversions from 69 % up > 95 % for all tested routes under optimised reaction conditions could be reached (see Table 2; Supplementary Information, Figure S7A–C). For route A, where initial concentrations of 10 mM (R)-2-HPP and 10 mM benzaldehyde as well as TBADH ( $0.30 \text{ mg mL}^{-1}$ ) and

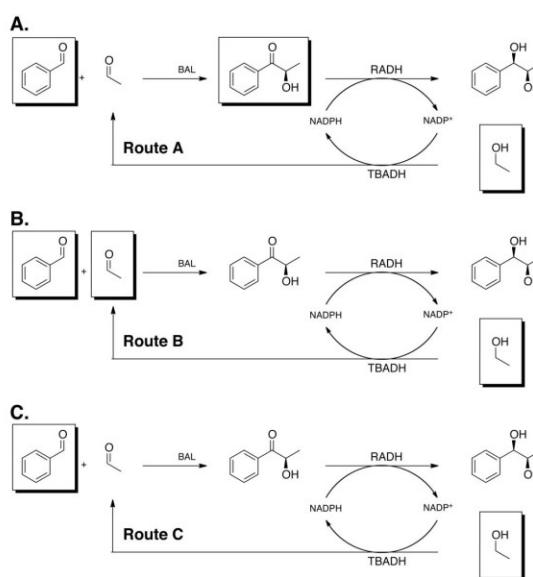
ethanol (2500 mM) were applied for enzyme-coupled cofactor regeneration, overall conversion of all aromatic compounds up to 79 % ( $de > 99\%$ ) were achieved (Supplementary Information, Figure S7A). For route B, where the reaction was started with benzaldehyde (10 mM) and acetaldehyde (100 mM) for the carbonylation step and ethanol as co-substrate for cofactor regeneration, benzaldehyde conversions of 96.1 % ( $de > 99\%$ ) were obtained (Supplementary Information, Figure S7B). Even very good benzaldehyde conversion (67.4 %,  $de > 99\%$ ) was even achieved via route C, where only ethanol and benzaldehyde were used as starting substrates for the 2-step 3-enzyme cascade reaction (Supplementary Information, Figure 7C).

Results of Route C, where no acetaldehyde was added in the beginning, show, that in situ co-product removal of built acetaldehyde is working very well. Regardless of the strategy (route A–C), recycling of the co-product (acetaldehyde) in the first carbonylation step of the synthetic enzyme cascade occurred.

Results for the different reaction modes further show that although it is advantageous for the overall conversion, if (R)-2-HPP is present in the beginning of the reaction (route A, 79 % conversion), even better conversions up to 96 % can be obtained without addition of this expensive intermediate (Table 2). Finally, the whole cascade can be performed starting from only two inexpensive substrates (ethanol and benzaldehyde). This increases step- as well as atom efficiency of the synthetic

cascade. Finally, the stereoselectivity of the cascade running with enzyme-coupled cofactor regeneration is excellent, where only one stereoisomer of 1,2-diol (here: (1R,2R)-1-phenylpropane-1,2-diol) is formed with a diastereomeric excess of > 99 %.

Besides optimal stereoselectivity of enzyme-coupled cofactor regeneration, under optimal reaction conditions the atom-economy with respect to implemented substrate and co-substrate is higher for the substrate-coupled cofactor regeneration. Also higher final product concentration up to 93 mM 1,2-diol could be reached. Before an optimal cofactor-recycling mode for a desired process can be designed, it first has to be decided, if high product yield or higher stereoselectivity is the more crucial parameter.



**Figure 5.** Three routes for the synthetic cascade reaction with enzyme-coupled cofactor regeneration were tested (A–C). They differ in substrate supply strategy. In all cases ethanol was used as the co-substrate. The acetaldehyde formed upon oxidation with TBADH is re-used in the first step of the cascade. Substrates which are present in the reaction system when the reaction was started ( $t = 0$ ) are framed. BAL = benzaldehyde lyase from *Pseudomonas fluorescens*, RADH = alcohol dehydrogenase from *Ralstonia* sp., TBADH = alcohol dehydrogenase from *Thermoanaerobium brockii*.

Entry	Route	conv <sub>overall</sub> <sup>[a]</sup> [%]	C <sub>1,2-diol</sub> <sup>[b]</sup> [mM]	de [%]
1	A	79.0±1.7	20.1	>99
2	B	96.1±1.1	9.4	>99
3	C	67.4±1.9	6.6	>99

[a] % conv<sub>overall</sub> – conversion of all aromatic compounds (benzaldehyde and (R)-2-HPP (route A)) to 1-phenylpropane-1,2-diol; [b] C<sub>1,2-diol</sub> – concentration of (1R,2R)-1-phenylpropane-1,2-diol; de – diastereomeric excess; dr – diastereomeric ratio; "n.a." – only one stereoisomer of 1,2-diol is formed and therefore dr is not given.



## Conclusion

We developed a synthetic enzyme cascade for the highly stereoselective production of (1*R*,2*R*)-1-phenylpropane-1,2-diol. Inexpensive starting materials such as benzaldehyde or acetaldehyde as substrates for the carboligation step and ethanol or benzyl alcohol as substrates for the cofactor regeneration step were employed. Atom- and step efficiency could be further increased by implementation of an enzymatic cofactor regeneration system with in situ co-product recycling. Therefore, co-substrates were chosen such that the resulting co-products are used as substrates in the carboligation step of the synthetic enzyme cascade. The reaction was successfully optimised using substrate- and enzyme-coupled cofactor regeneration, yielding high conversions.

Substrate-coupled cofactor regeneration has the big advantage that no potentially expensive third enzyme is required. With benzyl alcohol as co-substrate, overall conversions and co-product conversions (for definition see paragraph *Experimental: Cascade with substrate-coupled approach*) of up to 73.4 % and 97.2 %, respectively, were achieved under optimised conditions. 93 mM (1*R*,2*R*)-1-phenylpropane-1,2-diol were gained. Using enzyme-coupled cofactor regeneration, benzaldehyde conversions up to 96 % were reached. Here, stereoselectivity towards the (1*R*,2*R*)-diol was mostly very high with optimal results (*de* > 99 %) for all modes of enzyme-coupled cofactor regeneration.

In this work, we show that by the combination of reaction optimisation and calculation of equilibrium restrains improvement of conversions by a factor of more than four was possible. Additionally, the overall atom economy is very high since, although a cofactor recycling step is present, overall conversions (including amount of remaining co-product) > 73 % are possible.

In summary, we have developed a novel process strategy for more sustainable and eco-friendly synthetic enzyme cascades including cofactor recycling. This approach optimises the atom economy of the reaction, reduce waste production and thus increase process economy.

## Experimental Section

### Materials and Methods

#### Chemicals

All implemented chemicals were of high analytical grade. Tris-2-(hydroxyethyl)amine (TEA) was purchased from Sigma (Steinheim, Germany), 2-amino-2-hydroxymethylpropane-1,3-diol (TRIS) and calcium chloride ( $\text{CaCl}_2 \cdot 2\text{H}_2\text{O}$ ) were from Merck (Darmstadt, Germany), benzyl alcohol and benzaldehyde from Sigma-Aldrich (Steinheim, Germany), and acetaldehyde and magnesium sulfate ( $\text{MgSO}_4$ ) from Fluka (Steinheim, Germany). Cofactors: thiamine diphosphate (ThDP) and NADP<sup>+</sup> were from AppliChem (Darmstadt, Germany) and Biomol (Hamburg, Germany), respectively. Alcohol dehydrogenase from *Thermoanaerobacter brockii* (TBADH) was from Sigma (St. Louis, USA). (*R*)-2-hydroxy-1-phenylpropan-1-one ((*R*)-2-HPP)<sup>[10,47]</sup> and *rac*-2-hydroxy-1-phenylpropan-1-one (*rac*-2-HPP)<sup>[51]</sup> were synthesised as described in literature.

#### Expression and purification of the recombinant enzymes

Expression and purification of His-tagged benzaldehyde lyase from *Pseudomonas fluorescens* (BAL) employing metal chelate affinity chromatography (Ni-NTA column) was carried out as described elsewhere.<sup>[48]</sup> Alcohol dehydrogenase from *Ralstonia* sp. (RADH) was

expressed and purified by ion exchange chromatography (anion exchanger) as recently described.<sup>[11,52]</sup>

#### Determination of protein concentration

Protein concentration was determined by the Bradford method<sup>[53]</sup> using bovine serum albumin as a standard (Sigma-Aldrich, Steinheim, Germany).

#### Cofactor regeneration optimisation

Optimisation of cofactor regeneration was carried out at a 1 mL scale in screwed glass vials equipped with a Teflon-membrane in order to avoid evaporation of aldehydes. Reactions were conducted at 20 °C for 24 h with constant shaking of 500 rpm (Eppendorf thermomixer, Hamburg, Germany) and stopped by extraction with ethyl acetate (50 % v v<sup>-1</sup>). All reactions were performed in duplicate. Conversions were determined using GC-analysis based on a calibration with the formed product 1-phenylpropane-1,2-diol. For conditions of instrumental analysis and origins of reference compounds see *Experimental: Chiral analysis*.

#### Substrate-coupled approach

All reactions were conducted in TRIS-HCl buffer (50 mM) supplemented with  $\text{CaCl}_2$  (0.8 mM), pH 9.0, if not stated otherwise. For biotransformations the following standard conditions were applied (if not otherwise stated): *rac*-2-HPP (10 mM), NADP<sup>+</sup> (0.2 mM) and RADH (0.05 mg mL<sup>-1</sup>).

To determine the optimal co-substrate concentration, ethanol (20 mM to 5000 mM) and benzyl alcohol (10 mM to 250 mM) were tested under standard conditions.

To identify the optimal pH and buffer conditions, batch experiments were performed in TRIS-HCl (50 mM, pH 8.0–pH 9.0) and in TEA-HCl (50 mM, pH 8.0) buffer systems, both supplemented with  $\text{CaCl}_2$  (0.8 mM). pH studies were carried out with benzyl alcohol (100 mM) as the co-substrate.

The optimal RADH concentration was tested by varying the enzyme concentrations between 0.05–0.30 mg mL<sup>-1</sup> under standard biotransformation conditions, using benzyl alcohol (100 mM) as the co-substrate.

#### Enzyme-coupled approach

If not otherwise stated, enzyme-coupled cofactor regeneration was studied under the following standard conditions: TRIS-HCl (50 mM) supplemented with  $\text{CaCl}_2$  (0.8 mM), pH 9.0, *rac*-2-HPP (10 mM) and NADP<sup>+</sup> (0.2 mM), RADH (0.05 mg mL<sup>-1</sup>) and TBADH (0.05 mg mL<sup>-1</sup>).

In order to determine the optimal co-substrate concentration, ethanol concentrations were varied from 20 mM to 5000 mM under standard conditions.

For detection of the optimal TBADH concentration, the regenerating enzyme was tested in concentrations from 0.05 mg mL<sup>-1</sup> to 0.30 mg mL<sup>-1</sup> using ethanol (2500 mM) as a co-substrate.

#### Substrate addition strategies for synthetic enzyme cascades

Three different routes were studied differing in substrate supply strategy (Figure 4 and Figure 5). All reactions were carried out at a 1 mL scale in screwed glass vessels equipped with a Teflon membrane at 20 °C under constant shaking (500 rpm). Samples (100 µL) were taken in defined time intervals, diluted (10-times). The reaction was stopped by addition of ethyl acetate (50 % v v<sup>-1</sup>) or acetonitrile (50 % v v<sup>-1</sup>) and analysed by GC and HPLC (see



paragraph *Experimental: Chiral analysis*), respectively. All reactions were carried out in duplicate.

#### Cascade with substrate-coupled cofactor regeneration

All routes (Figure 4A–C) were conducted under the following conditions: TEA-HCl buffer (50 mM), pH 8.0, supplemented with  $\text{CaCl}_2$  (0.8 mM),  $\text{MgSO}_4$  (2.5 mM), ThDP (0.15 mM),  $\text{NADP}^+$  (0.2 mM), BAL (0.05 mg  $\text{mL}^{-1}$ ), and RADH (0.10 mg  $\text{mL}^{-1}$ ).

Depending on the mode (Figure 4), initial amounts of benzaldehyde, acetaldehyde, and (R)-2-HPP were applied: route A (Figure 4A): acetaldehyde (150 mM), (R)-2-HPP (10 mM) and benzyl alcohol (120 mM); route B (Figure 4B): acetaldehyde (150 mM), benzaldehyde (10 mM), and benzyl alcohol (120 mM); route C (Figure 4C): only acetaldehyde (150 mM) and benzyl alcohol (120 mM) were employed.

For substrate-coupled cofactor regeneration two different types of conversion are given. The co-product conversion (%  $\text{conv}_{\text{CP}}$ ) is defined as the conversion of benzaldehyde, which is only formed during oxidation of benzyl alcohol during cofactor regeneration. Initial amount of benzaldehyde (route B) for these calculations was subtracted. The overall conversion (%  $\text{conv}_{\text{overall}}$ ) is defined as the conversion of all aromatic compounds present at time  $t=0$  towards 1-phenylpropane-1,2-diol. There besides benzaldehyde (and optionally (R)-2-HPP depending on the route) also the aromats from the co-substrate (benzyl alcohol) are taken into account. This type of conversion taking remaining co-substrate into account is rarely found in biotransformations including cofactor-regeneration, since the cofactor often has to be added in excess due to equilibrium or kinetic restraints. In our special recycling cascade this overall conversion shows nicely the atom-efficiency of the whole process. Additionally, final concentration of formed 1-phenylpropane-1,2-diol is given (Table 1).

#### Cascade with enzyme-coupled cofactor regeneration

For enzyme-coupled synthetic cascade reactions three enzymes were applied: benzaldehyde lyase from *Pseudomonas fluorescens* (BAL) for the first step of carboligation to 2-hydroxypropiophenone, alcohol dehydrogenase from *Ralstonia* sp. (RADH) for the reduction of the  $\alpha$ -hydroxy ketone, and alcohol dehydrogenase from *Thermoanaerobacter brockii* (TBADH) for cofactor regeneration using ethanol as co-substrate. The resulting co-product acetaldehyde was recycled in the first carboligation step of the cascade.

Standard reaction condition for the enzyme-coupled approach: TRIS-HCl buffer (50 mM) pH 9.0 supplemented with  $\text{CaCl}_2$  (0.8 mM),  $\text{MgSO}_4$  (2.5 mM) and ThDP (0.15 mM),  $\text{NADP}^+$  (0.8 mM), BAL (0.05 mg  $\text{mL}^{-1}$ ), RADH (0.10 mg  $\text{mL}^{-1}$ ), TBADH (0.30 mg  $\text{mL}^{-1}$ ).

Here again, different substrate supply strategies were evaluated: route A (Figure 5A): (R)-2-HPP (10 mM), benzaldehyde (10 mM) and ethanol (2500 mM); route B (Figure 5B): benzaldehyde (10 mM), acetaldehyde (100 mM) and ethanol (2500 mM); route C (Figure 5C): benzaldehyde (10 mM) and ethanol (2500 mM).

Conversion of cascade reaction with enzyme-coupled approach was determined by the conversion of the aromatic starting materials (%  $\text{conv}_{\text{overall}}$ ). Additionally, concentration of formed 1-phenylpropane-1,2-diol is given (Table 2).

#### Reaction optimisation

##### Cascade with substrate-coupled cofactor regeneration

If not otherwise stated, standard reaction conditions for all three tested substrate-coupled modes for the cascade reaction (Figure 4A–

C) were: TEA-HCl buffer (50 mM), pH 8.0 supplemented with  $\text{CaCl}_2$  (0.8 mM),  $\text{MgSO}_4$  (2.5 mM), ThDP (0.15 mM) and  $\text{NADP}^+$  (0.2 mM). All biotransformations (route A–C) were carried out at 20 °C with constant shaking (500 rpm). Samples were taken in regular time intervals.

For the multi-enzymatic cascade reaction the concentration of  $\text{NADP}^+$  was varied in the range of 0.2 mM to 0.8 mM under standard conditions.

For pH optimisation TEA-HCl (pH 8.0) and TRIS-HCl buffer systems (50 mM, pH 8.0–pH 9.0) supplemented with  $\text{CaCl}_2$  (0.8 mM),  $\text{MgSO}_4$  (2.5 mM) and ThDP (0.15 mM) were tested (A–C).

To find optimal RADH concentrations, catalyst loads from 0.10 mg  $\text{mL}^{-1}$  to 2.00 mg  $\text{mL}^{-1}$  were examined.

##### Cascade reaction with enzyme-coupled cofactor regeneration

Reactions were carried out as described in paragraph above.

#### Determination of thermodynamic equilibrium for the cascade reaction with substrate-coupled cofactor regeneration

##### Carboligation reaction

The equilibrium constant ( $K_{\text{eq}}$ ) for the carboligation reaction (first step) was calculated according to Formula 1:

$$K_{\text{eq,BAL}} = \frac{[2\text{-HPP}]_{\text{eq}}}{[\text{acetaldehyde}]_{\text{eq}} \cdot [\text{benzaldehyde}]_{\text{eq}}} \quad (1)$$

##### Oxidoreduction reaction

The equilibrium constant for the oxidoreduction step was calculated according to Formula 2:

$$K_{\text{eq,RADH}_{\text{red}}} = \frac{[1,2\text{-diol}]_{\text{eq}} \cdot [\text{NADP}^+]_{\text{eq}}}{[2\text{-HPP}]_{\text{eq}} \cdot [\text{NADPH}]_{\text{eq}}} \quad (2)$$

and Formula 3:

$$K_{\text{eq,RADH}_{\text{ox}}} = \frac{[\text{benzaldehyde}]_{\text{eq}} \cdot [\text{NADPH}]_{\text{eq}}}{[\text{benzyl-alcohol}]_{\text{eq}} \cdot [\text{NADP}^+]_{\text{eq}}} \quad (3)$$

Available substrate and product concentrations are given in the Supplementary Information, Figure S2.3.

#### Calculation of the theoretical conversion from the reaction equilibrium constants

Equilibrium constants were calculated using initial and final concentrations of all available compounds in the reaction vessel measured for the respective route. The theoretical overall conversions of the whole synthetic cascade were calculated with MATLAB (The MathWorks, Germany). For details concerning calculations and scripts see Supplementary Information, paragraph 3.

### Experimental control of calculated conversions of a cascade reaction with substrate-coupled cofactor regeneration

As a proof-of-principle route B was chosen. Reactions were conducted under the following conditions: TRIS-HCl buffer system (50 mM), pH 9.0, supplemented with  $\text{CaCl}_2$  (0.8 mM),  $\text{MgSO}_4$  (2.5 mM), ThDP (0.15 mM), and  $\text{NADP}^+$  (0.8 mM). For the route B, initial concentrations of benzaldehyde (10 mM) and acetaldehyde (150 mM) were implemented. For substrate-coupled cofactor regeneration benzyl alcohol (120 mM) and initial RADH concentration of  $3.75 \text{ mg mL}^{-1}$  were applied. After 96 h additional lyophilised RADH ( $\sim 3.3 \text{ mg}$  of protein) was added to the reaction vessel. Reactions were carried out at  $20^\circ\text{C}$  with constant shaking (500 rpm). Samples were taken in defined time intervals and reaction progress was measured by GC and HPLC (see paragraph Chiral analysis).

### Chiral analysis

#### High Performance Liquid Chromatography (HPLC)

Concentrations of substrates (benzaldehyde and benzyl alcohol) and the intermediately formed (R)-2-HPP were determined by HPLC-analysis. Therefore 10  $\mu\text{L}$  sample (10-times diluted in acetonitrile with 2-methylbenzaldehyde as internal standard) was analysed by chiral HPLC using a HiBar 250-4 LiChrosphere 100 RP-8 ( $5 \mu\text{m}$ ) column (Merck KGaA, Germany; flow:  $1 \text{ mL min}^{-1}$ , temperature:  $25^\circ\text{C}$ ). As mobile phase, a gradient of 25-60 % ( $\text{v v}^{-1}$ ) acetonitrile was used, mixed with ultrapure water (0-12 min: 25 % ( $\text{v v}^{-1}$ ) acetonitrile, 12-13 min: gradient 25-60 % ( $\text{v v}^{-1}$ ) acetonitrile, 13-20 min: 60 % ( $\text{v v}^{-1}$ ) acetonitrile, 20-23 min: 60-25 % ( $\text{v v}^{-1}$ ) acetonitrile, 23-25 min: 25 % ( $\text{v v}^{-1}$ ) acetonitrile). Absorption was determined at 200 nm (benzyl alcohol) and 250 nm (2-HPP and benzaldehyde) with the following retention times:  $R_{\text{t}}(\text{benzyl alcohol}) = 7.6 \text{ min}$ ,  $R_{\text{t}}(2\text{-HPP}) = 10.5 \text{ min}$  and  $R_{\text{t}}(\text{benzaldehyde}) = 16.2 \text{ min}$ .

#### Gas Chromatography (GC)

Final concentration and diastereomeric excess (de) of the cascades product (non-derivatised stereoisomers of 1-phenyl-propane-1,2-diol) were determined via GC-analysis. Therefore samples were extracted with ethyl acetate including 1-dodecanol as internal standard. 5  $\mu\text{L}$  of the obtained organic phase were analysed by gas chromatography using a chiral CP-Chirasil-DEX CB (Varian, Germany) column ( $25 \text{ m} \times 0.25 \text{ mm} \times 0.25 \mu\text{m}$ ) with a flame ionisation detector (FID) and hydrogen as carrier gas. The following GC-program was applied:  $140^\circ\text{C}$  injection temperature, isothermic run for 30 min. Retention times of benzaldehyde and benzyl alcohol were as follows:  $R_{\text{t}}(\text{benzaldehyde}) = 3.1 \text{ min}$  and  $R_{\text{t}}(\text{benzyl alcohol}) = 4.9 \text{ min}$ , respectively. Retention times of the four stereoisomers of phenylpropan-1,2-diol:  $R_{\text{t}}(1,5,2,5) = 24.1 \text{ min}$ ,  $R_{\text{t}}(1,1,2,2) = 25.8 \text{ min}$ ,  $R_{\text{t}}(1,1,5,2) = 27.4 \text{ min}$ ,  $R_{\text{t}}(1,1,2,5) = 28.5 \text{ min}$ . Detailed chemical syntheses of reference substrates and its assignment of absolute configuration are described elsewhere.<sup>[11]</sup>

### Acknowledgements

This work was financed by the Marie Curie Initial Training Network "BIOTRAINS – a European biotechnology training network for the support of chemical manufacturing", grant agreement no. 238531. Additionally, we thank Prof. Dr. Wolfgang Kroutil (University of Graz, Graz, Austria) for provision of the radh gene.

**Keywords:** asymmetric synthesis • biocatalysis • cascade reaction • chirality • cofactor regeneration

- [1] I. Lavandera, A. Kern, B. Ferreira-Silva, A. Glieder, S. de Wildeman, W. Kroutil, *J. Org. Chem.* **2008**, *73*, 6003–6005.
- [2] R. N. Patel, *Coordin. Chem. Rev.* **2008**, *252*, 659–701.
- [3] T. Daußmann, H.-G. Hennemann, T. C. Rosen, P. Dünkermann, *Chem.-Ing.-Tech.* **2006**, *78*, 249–255.
- [4] K. B. Sharpless, W. Amberg, Y. L. Bennani, G. A. Crispino, J. Hartung, K. S. Jeong, H. L. Kwong, K. Morikawa, Z. M. Wang, D. Q. Xu, X. L. Zhang, *J. Org. Chem.* **1992**, *57*, 2768–2771.
- [5] Z. Wang, Y. T. Cui, Z. B. Xu, J. Qu, *J. Org. Chem.* **2008**, *73*, 2270–2274.
- [6] T. H. Johnson, K. C. Klein, *J. Org. Chem.* **1979**, *44*, 461–462.
- [7] R. J. McMahon, K. E. Wiegers, S. G. Smith, *J. Org. Chem.* **1981**, *46*, 99–101.
- [8] R. Noyori, I. Tomino, Y. Tanimoto, *J. Am. Chem. Soc.* **1979**, *101*, 3129–3131.
- [9] D. C. Wigfield, *Tetrahedron* **1979**, *35*, 449–462.
- [10] D. Kihumbu, T. Stillger, W. Hummel, A. Liese, *Tetrahedron: Asymmetr.* **2002**, *13*, 1069–1072.
- [11] J. Kulig, R. C. Simon, C. A. Rose, S. M. Husain, M. Häckh, S. Lüdke, K. Zeitler, W. Kroutil, M. Pohl, D. Rother, *Catal. Sci. Technol.* **2012**, *2*, 1580–1589.
- [12] S. M. Husain, T. Stillger, P. Dünkermann, M. Lödige, L. Walter, E. Breitting, M. Pohl, M. Büchner, I. Krossing, M. Müller, D. Romano, F. Molinari, *Adv. Synth. Catal.* **2012**, *353*, 2359–2362.
- [13] M. Müller, D. Gocke, M. Pohl, *FEBS J.* **2009**, *276*, 2894–2904.
- [14] H. K. Chenault, G. M. Whitesides, *Appl. Biochem. Biotech.* **1987**, *14*, 147–197.
- [15] R. Wichmann, D. Vasic-Racki, *Adv. Biochem. Engin./Biotechnol.* **2005**, *92*, 225–260.
- [16] A. Weckbecker, H. Groger, W. Hummel, *Adv. Biochem. Engin./Biotechnol.* **2010**, *120*, 195–242.
- [17] F. Hollmann, I. W. C. E. Arends, K. Bühler, *ChemCatChem* **2010**, *2*, 762–782.
- [18] F. D. Bastos, A. G. dos Santos, J. Jones, E. G. Oestreicher, G. F. Pinto, L. M. C. Paiva, *Biotechnol. Tech.* **1999**, *13*, 661–664.
- [19] F. M. Bastos, T. K. Franca, G. D. C. Machado, G. F. Pinto, E. G. Oestreicher, L. M. C. Paiva, *J. Mol. Catal. B-Enzym.* **2002**, *19*, 459–465.
- [20] T. R. Röthig, K. D. Kulbe, F. Buckmann, G. Carrea, *Biotechnol. Lett.* **1990**, *12*, 353–356.
- [21] T. Stillger, M. Bonitz, M. Villela, A. Liese, *Chem.-Ing.-Tech.* **2002**, *74*, 1035–1039.
- [22] J. Peters, T. Zelinski, T. Minuth, M. R. Kula, *Tetrahedron: Asymmetr.* **1993**, *4*, 1683–1692.
- [23] C. Virto, I. Svensson, P. Adlercreutz, B. Mattiasson, *Biotechnol. Lett.* **1995**, *17*, 877–882.
- [24] T. Daußmann, T. C. Rosen and P. Dünkermann, *Eng. Life Sci.* **2006**, *6*, 125–129.
- [25] K. Goldberg, K. Schroer, S. Lütz, A. Liese, *Appl. Microbiol. Biotechnol.* **2007**, *76*, 237–248.
- [26] C. H. Wong, D. G. Drueckhammer, *Bio/Technol.* **1985**, *3*, 649–651.
- [27] C. H. Wong, D. G. Drueckhammer, H. M. Sweers, *J. Am. Chem. Soc.* **1985**, *107*, 4028–4031.
- [28] W. Hilt, G. Pfeleiderer, P. Fortnagel, *Biochim. Biophys. Acta* **1991**, *1076*, 298–304.
- [29] T. Zelinski, A. Liese, C. Wandrey, M. R. Kula, *Tetrahedron: Asymmetr.* **1999**, *10*, 1681–1687.
- [30] V. V. Karzanov, A. Bogatsky Yu, V. I. Tishkov, A. M. Egorov, *FEMS Microbiol. Lett.* **1989**, *51*, 197–200.
- [31] U. Müller, P. Willnow, U. Ruschig, T. Hopner, *Eur. J. Biochem.* **1978**, *83*, 485–498.
- [32] V. I. Tishkov, A. G. Galkin, G. N. Marchenko, Y. D. Tsygankov, A. M. Egorov, *Biotechnol. Appl. Biochem.* **1993**, *18*, 201–207.
- [33] E. Keinan, K. K. Seth, R. Lamed, *J. Am. Chem. Soc.* **1986**, *108*, 3474–3480.
- [34] Y. Korkhin, A. J. Kalb, M. Peretz, O. Bogin, Y. Burstein, F. Frolow, *J. Mol. Biol.* **1998**, *278*, 967–981.
- [35] C. Drewke, M. Ciriacy, *Biochim. Biophys. Acta* **1988**, *950*, 54–60.
- [36] M. F. van Iersel, M. H. Eppink, W. J. van Berkel, F. M. Rombouts, T. Abee, *Appl. Environ. Microbiol.* **1997**, *63*, 4079–4082.
- [37] W. Hummel, *Adv. Biochem. Engin./Biotechnol.* **1997**, *58*, 145–184.
- [38] K. Niefind, J. Müller, B. Riebel, W. Hummel, D. Schomburg, *J. Mol. Biol.* **2003**, *327*, 317–328.

- [39] K. Niefind, B. Riebel, J. Müller, W. Hummel, D. Schomburg, *Acta Crystallogr. D* **2000**, *56*, 1696–1698.
- [40] K. Schügerl, J. Hubbuch, *Curr. Opin. Microbiol.* **2005**, *8*, 294–300.
- [41] P. Tufvesson, J. Lima-Ramos, M. Nordblad, J. M. Woodley, *Org. Process Res. Dev.* **2011**, *15*, 266–274.
- [42] J. M. Woodley, M. Bisschops, A. J. J. Straathof, M. Ottens, *J. Chem. Technol. Biot.* **2008**, *83*, 121–123.
- [43] A. W. Willetts, C. J. Knowles, M. S. Levitt, S. M. Roberts, H. Sandey, N. F. Shipston, *J. Chem. Soc. Perk. T. 1*, **1991**, *6*, 1608–1610.
- [44] C. A. Müller, B. Akkapurathu, T. Winkler, S. Staudt, W. Hummel, H. Gröger, U. Schwaneberg, *Adv. Synth. Catal.* **2013**, *355*, 1787–1798.
- [45] S. Staudt, U. T. Bornscheuer, U. Menyes, W. Hummel, H. Gröger, *Enzyme Microb. Tech.* **2013**, *53*, 288–292.
- [46] H. Mallin, H. Wulf, U. T. Bornscheuer, *Enzyme Microb. Tech.* **2013**, *53*, 283–287.
- [47] A. S. Demir, M. Pohl, E. Janzen, M. Müller, *J. Chem. Soc. Perk. T. 1*, **2001**, *7*, 633–635.
- [48] E. Janzen, M. Müller, D. Kolter-Jung, M. M. Kneen, M. J. McLeish, M. Pohl, *Bioorg. Chem.* **2006**, *34*, 345–361.
- [49] M. Perez-Sanchez, R. C. Müller, P. Dominguez de Maria, *ChemCatChem* **2013**, *5*, 2512–2516.
- [50] R. J. Lamed, J. G. Zeikus, *Biochem. J.* **1981**, *195*, 183–190.
- [51] C. Q. Chen, X. H. Feng, G. Z. Zhang, Q. Zhao, G. S. Huang, *Synthesis-Stuttgart* **2008**, *20*, 3205–3208.
- [52] J. Kulig, A. Frese, W. Kroutil, M. Pohl, D. Rother, *Biotechnol. Bioeng.* **2013**, *110*, 1838–1848.
- [53] M. M. Bradford, *Anal. Biochem.* **1976**, *72*, 248–254.

---

Received: ((will be filled in by the editorial staff))

Published online: ((will be filled in by the editorial staff))

## **Stereoselective synthesis of 1,2-diols with synthetic enzyme cascades including *in-situ* cofactor regeneration and by-product recycling**

Justyna Kulig,<sup>a</sup> Wolfgang Wiechert,<sup>a</sup> Martina Pohl,<sup>a</sup> Dörte Rother<sup>a\*</sup>

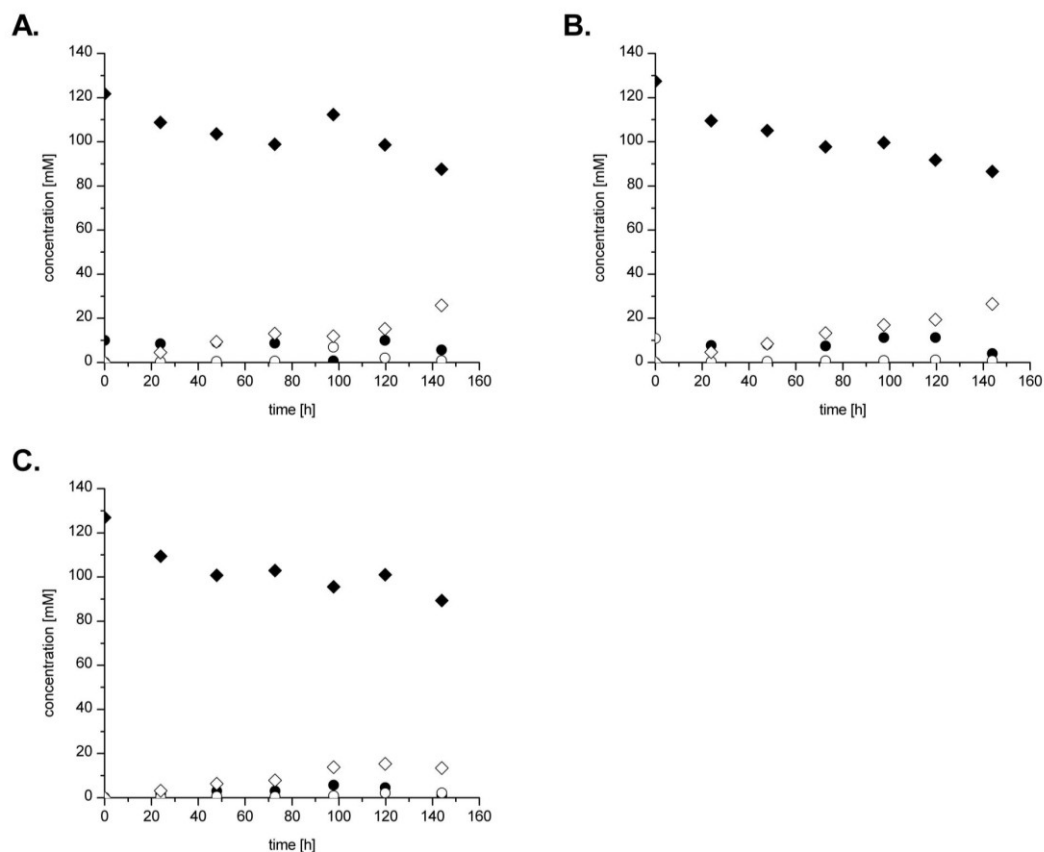
<sup>a</sup> IBG-1: Biotechnology, Forschungszentrum Jülich GmbH, 52425 Jülich, Germany

### – Supplementary Information –

Table of contents:

1. Standard synthetic cascade reaction using the substrate-coupled approach
2. Optimisation of the cascade reaction using the substrate-coupled approach  
Optimisation of:
  - a. NADP<sup>+</sup> concentration
  - b. pH
  - c. RADH concentration
3. Equilibrium computation for the cascade reaction using substrate-coupled approach
4. Experimental control of calculated theoretical conversions of the cascade reaction using the substrate-coupled approach
5. Experimental investigation of overall conversion limitations of the cascade reaction using the substrate-coupled approach
6. Cascade reaction using the enzyme-coupled approach

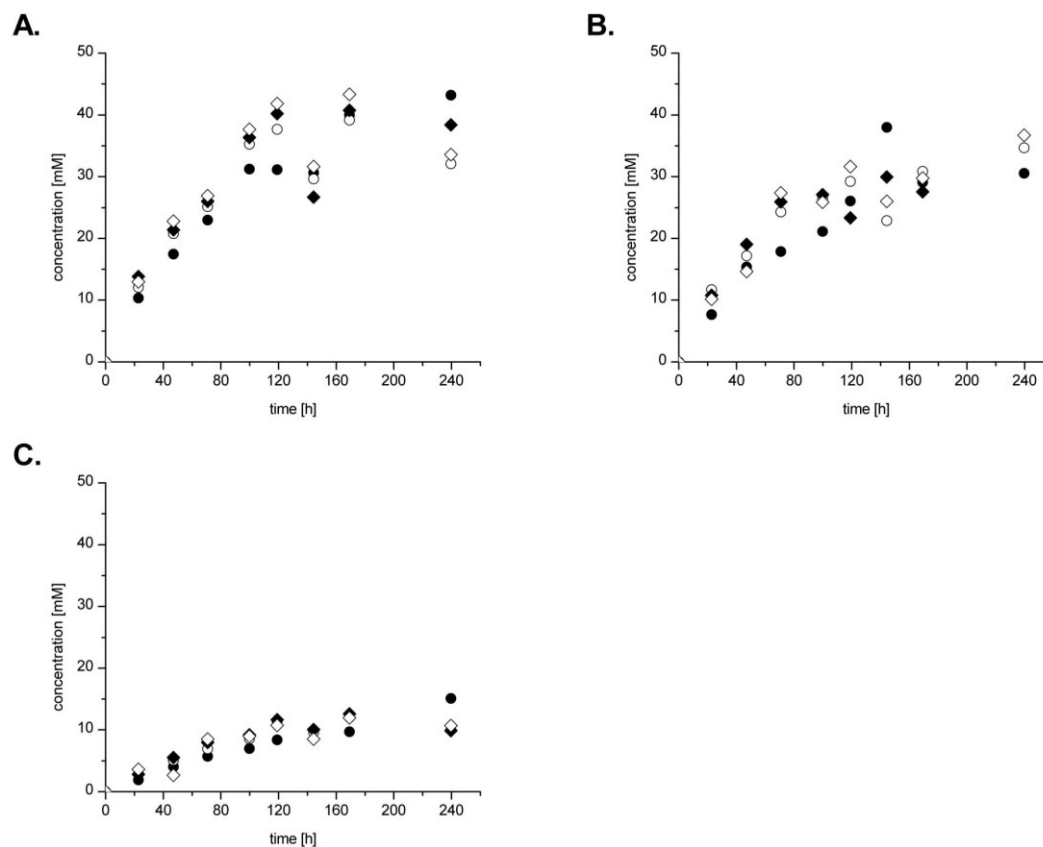
### 1. Standard synthetic cascade reaction using the substrate-coupled approach



**Figure S1.** Standard synthetic cascade reaction using the substrate-coupled approach. Reaction conditions: TEA-HCl buffer (50 mM) supplemented with  $\text{CaCl}_2$  (0.8 mM),  $\text{MgSO}_4$  (2.5 mM), ThDP (0.15 mM), pH 8.0,  $\text{NADP}^+$  (0.2 mM), BAL (0.05  $\text{mg mL}^{-1}$ ), RADH (0.05  $\text{mg mL}^{-1}$ ). **A.** Route A: (*R*)-2-HPP (10 mM), acetaldehyde (150 mM), benzyl alcohol (120 mM) **B.** Route B: benzaldehyde (10 mM), acetaldehyde (150 mM), benzyl alcohol (120 mM) **C.** Route C: acetaldehyde (150 mM), benzyl alcohol (120 mM). Reactions were carried out at 20 °C with constant shaking (150 rpm). Samples were taken in defined time intervals. Symbols:  $\blacklozenge$  – benzyl alcohol,  $\circ$  – benzaldehyde,  $\bullet$  – (*R*)-2-HPP,  $\diamond$  – 1,2-diol.

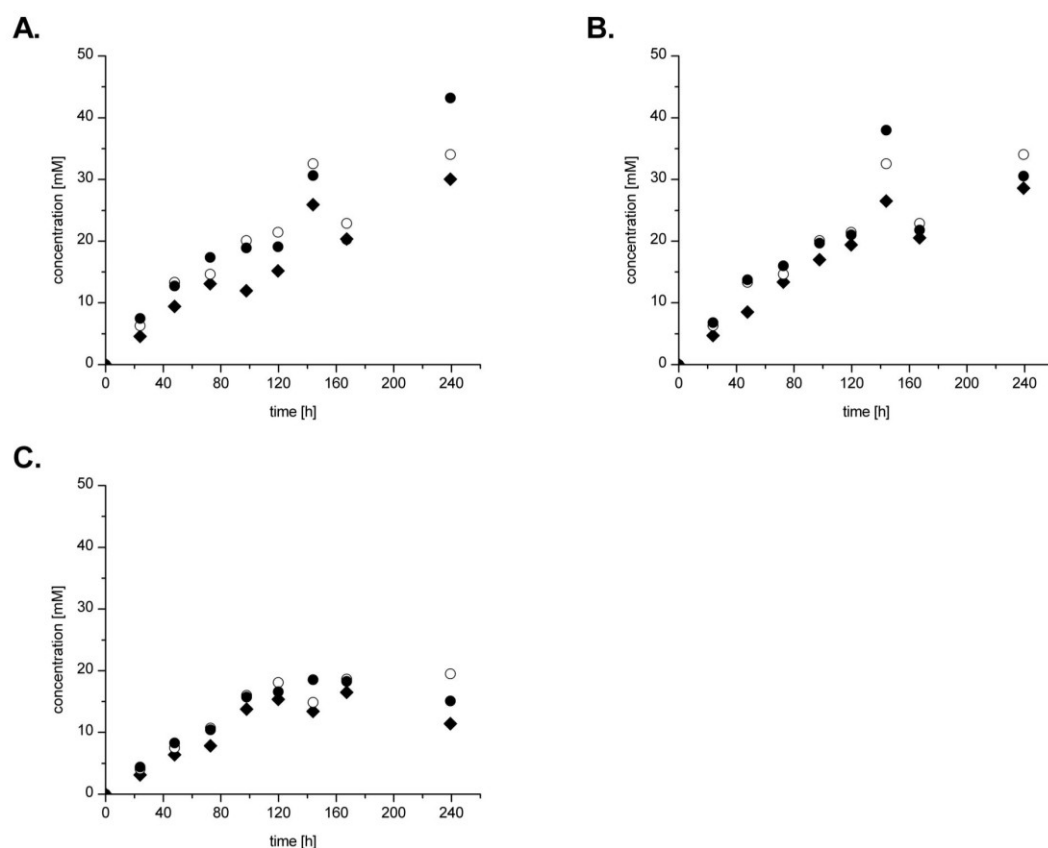
## 2. Optimisation of the cascade reaction using the substrate-coupled approach

### 2.1. $\text{NADP}^+$ concentration



**Figure S2.1.** Standard synthetic cascade reaction using the substrate-coupled approach. Reaction conditions: TEA-HCl buffer (50 mM) supplemented with  $\text{CaCl}_2$  (0.8 mM),  $\text{MgSO}_4$  (2.5 mM), ThDP (0.15 mM), pH 8.0,  $\text{NADP}^+$  (0.2–0.8 mM), BAL (0.05  $\text{mg mL}^{-1}$ ), RADH (0.10  $\text{mg mL}^{-1}$ ). **A.** Route A: (*R*)-2-HPP (10 mM), acetaldehyde (150 mM), benzyl alcohol (120 mM) **B.** Route B: benzaldehyde (10 mM), acetaldehyde (150 mM), benzyl alcohol (120 mM) **C.** Route C: acetaldehyde (150 mM), benzyl alcohol (120 mM). Reactions were carried out at 20 °C with constant shaking (150 rpm). Samples were taken in defined time intervals. Symbols: ● – 0.2 mM  $\text{NADP}^+$ , ○ – 0.4 mM  $\text{NADP}^+$ , ◆ – 0.6 mM  $\text{NADP}^+$ , ◇ – 0.8 mM  $\text{NADP}^+$ .

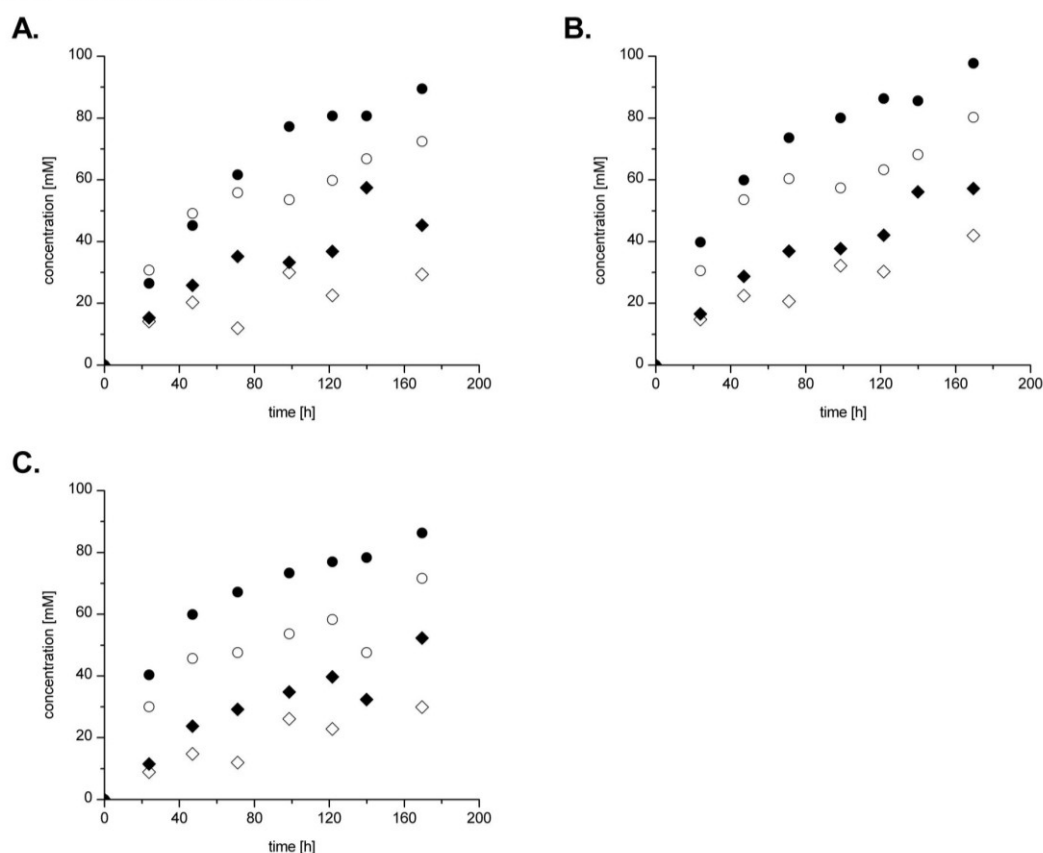
## 2.2. pH



**Figure S2.2.** Standard synthetic cascade reaction using the substrate-coupled approach. Reaction conditions: TEA-HCl buffer (50 mM) supplemented with  $\text{CaCl}_2$  (0.8 mM),  $\text{MgSO}_4$  (2.5 mM), ThDP (0.15 mM), pH 8.0-9.0,  $\text{NADP}^+$  (0.2 mM), BAL (0.05  $\text{mg mL}^{-1}$ ), RADH (0.10  $\text{mg mL}^{-1}$ ). **A.** Route A: (R)-2-HPP (10 mM), acetaldehyde (150 mM), benzyl alcohol (120 mM) **B.** Route B: benzaldehyde (10 mM), acetaldehyde (150 mM), benzyl alcohol (120 mM) **C.** Route C: acetaldehyde (150 mM), benzyl alcohol (120 mM). Reactions were carried out at 20 °C with constant shaking (150 rpm). Samples were taken in defined time intervals. Symbols:  $\blacklozenge$  – pH 8.0,  $\circ$  – pH 8.5,  $\bullet$  – pH 9.0.

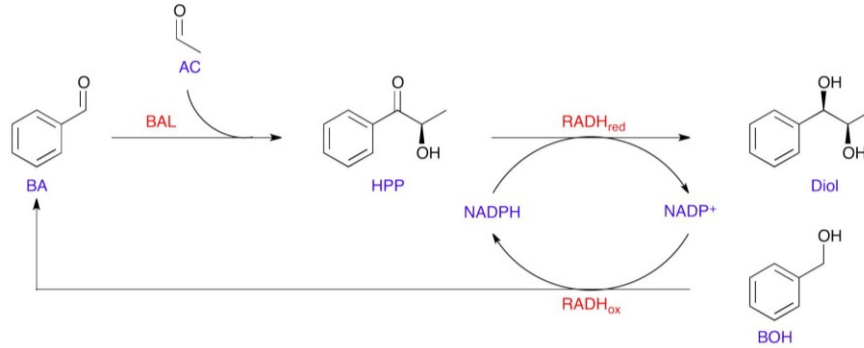


### 2.3. RADH concentration



**Figure S2.3.** Standard synthetic cascade reaction using the substrate-coupled approach. Reaction conditions: TEA-HCl buffer (50 mM) supplemented with  $\text{CaCl}_2$  (0.8 mM),  $\text{MgSO}_4$  (2.5 mM), ThDP (0.15 mM), pH 8.0,  $\text{NADP}^+$  (0.2 mM), BAL (0.05  $\text{mg mL}^{-1}$ ). **A.** Route A: (R)-2-HPP (10 mM), acetaldehyde (150 mM), benzyl alcohol (120 mM) **B.** Route B: benzaldehyde (10 mM), acetaldehyde (150 mM), benzyl alcohol (120 mM) **C.** Route C: acetaldehyde (150 mM), benzyl alcohol (120 mM). Reactions were carried out at 20 °C with constant shaking (150 rpm). Samples were taken in defined time intervals. Symbols:  $\diamond$  – RADH: 0.24  $\text{mg mL}^{-1}$ ,  $\blacklozenge$  – RADH: 0.33  $\text{mg mL}^{-1}$ ,  $\circ$  – RADH: 0.65  $\text{mg mL}^{-1}$ ,  $\bullet$  – RADH: 2.00  $\text{mg mL}^{-1}$ .

### 3. Equilibrium computation for the cascade reaction using substrate-coupled approach



**Fig. S3.** 2-step enzymatic synthesis of 1,2-diol with *in situ* co-product removal. BAL = benzaldehyde lyase from *Pseudomonas fluorescens*, RADH<sub>red</sub> = reduction catalysed by an alcohol dehydrogenase from *Ralstonia* sp., RADH<sub>ox</sub> = oxidation catalysed by an alcohol dehydrogenase from *Ralstonia* sp., BA = benzaldehyde, BOH = benzyl alcohol, AC = acetaldehyde, HPP = (R)-2-hydroxy-1-phenylpropanone.

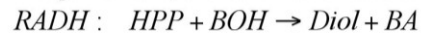
**Table S1.** Equilibrium concentration data used for the calculation of reaction equilibrium constants. RADH denotes the sum reaction of RADH<sub>red</sub> and RADH<sub>ox</sub> (see text).

	BAL	RADH
BA	0.3 mM	9.5 mM
AC	0.3 mM	·
HPP	9.7 mM	0.5 mM
Diol	·	9.5 mM
BOH	·	90.5 mM

From the data given in Table S1 the reaction equilibrium constant for the BAL reaction (Figure S3) is calculated as:

$$K_{\text{BAL}}^{\text{eq}} = \frac{[\text{HPP}]_{\text{eq}}}{[\text{AC}]_{\text{eq}} \cdot [\text{BA}]_{\text{eq}}} = 107.8 \quad (4)$$

In equilibrium, the other two reactions can be considered as one single sum reaction



because their rates must be equal and the cofactors NADPH, NADP<sup>+</sup> both behave stoichiometrically and thermodynamically neutral. The equilibrium constant of the sum reaction is (cf. Table S1):

$$K_{\text{RADH}}^{\text{eq}} = \frac{[\text{Diol}]_{\text{eq}} \cdot [\text{BA}]_{\text{eq}}}{[\text{HPP}]_{\text{eq}} \cdot [\text{BOH}]_{\text{eq}}} = 2.0 \quad (5)$$

The balance equations describing the dynamics of all substance concentrations are given by:

$$\begin{aligned}
 \dot{[BA]} &= -r_{BAL} + r_{RADH_{ox}} \\
 \dot{[AC]} &= -r_{BAL} \\
 \dot{[HPP]} &= r_{BAL} - r_{RADH_{red}} \\
 \dot{[Diol]} &= r_{RADH_{red}} \\
 \dot{[BOH]} &= -r_{RADH_{ox}} \\
 \dot{[NADPH]} &= -r_{RADH_{red}} + r_{RADH_{ox}} \\
 \dot{[NADP^+]} &= r_{RADH_{red}} - r_{RADH_{ox}}
 \end{aligned} \tag{6}$$

The reaction system equilibrium does not depend on the type of kinetics of the reaction steps. For this reason, any kinetic terms can be assumed without influencing the equilibrium. Thus, simple reversible mass action laws can be used for computing the reaction equilibrium:

$$\begin{aligned}
 r_{BAL} &= k_{BAL}^+ \cdot [BA] \cdot [AC] - k_{BAL}^- \cdot [HPP] \\
 r_{RADH_{red}} &= k_{RADH_{red}}^+ \cdot [HPP] \cdot [NADPH] - k_{RADH_{red}}^- \cdot [Diol] \cdot [NADP^+] \\
 r_{RADH_{ox}} &= k_{RADH_{ox}}^+ \cdot [BOH] \cdot [NADP^+] - k_{RADH_{ox}}^- \cdot [BA] \cdot [NADPH]
 \end{aligned} \tag{7}$$

The kinetic constants must be chosen to reproduce the equilibrium constants (notice that  $[NADPH]$ ,  $[NADP^+]$  cancel out):

$$\begin{aligned}
 \frac{k_{BAL}^+}{k_{BAL}^-} &= K_{BAL}^{eq} \\
 \frac{k_{RADH_{red}}^+}{k_{RADH_{red}}^-} \cdot \frac{k_{RADH_{ox}}^+}{k_{RADH_{ox}}^-} &= K_{RADH_{red}}^{eq} \cdot K_{RADH_{ox}}^{eq} = K_{RADH}^{eq}
 \end{aligned} \tag{8}$$

Any choice of the 6 reaction parameters

$$k_{BAL}^+, k_{BAL}^-, k_{RADH_{red}}^+, k_{RADH_{red}}^-, k_{RADH_{ox}}^+, k_{RADH_{ox}}^-$$

which is consistent with Eqs. (8) will lead to a proper reaction equilibrium. To obtain the theoretical reaction equilibrium corresponding to a specific experiment, also the initial concentrations

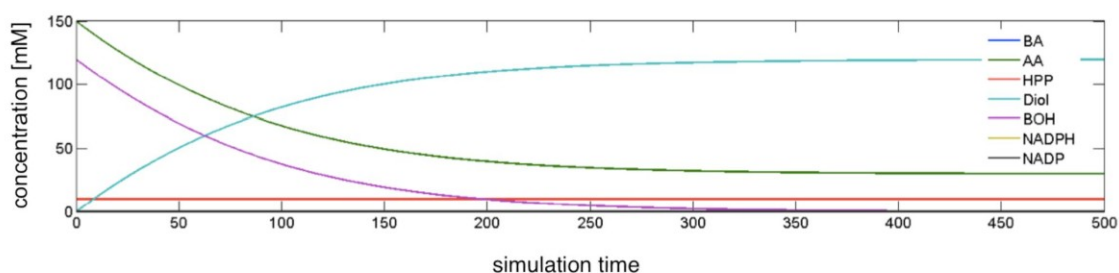
$$[BA]_0, [AC]_0, [HPP]_0, [BOH]_0, [Diol]_0, [NADPH]_0, [NADP^+]_0$$

must be supplied. Implementing equations (6), (7) in MATLAB and using the built-in numerical differential equation solver ode45 reaction equilibria can now be computed. To this end the simulation is run long enough for establishing a steady state. Figure S4 gives an example of a simulation run. Notice that the simulation is not meant as a proper model for the true process but just as a computational vehicle to compute the theoretical conversion rates. The computed rates are shown in Table S2.

As a final remark, the differential equation solver implicitly cares for the following four independent mass conservation relations which can be derived from the reaction stoichiometry:

$$\begin{aligned}
 [\text{NADPH}] + [\text{NADP}^+] &= \text{const.} \\
 [\text{BA}] + [\text{HPP}] + [\text{Diol}] + [\text{BOH}] &= \text{const.} \\
 [\text{AC}] + [\text{HPP}] + [\text{Diol}] &= \text{const.} \\
 [\text{Diol}] + [\text{BOH}] + [\text{NADPH}] &= \text{const.}
 \end{aligned} \tag{9}$$

These conservation equations can be used for plausibility checking of the computed result.



**Figure 4.** Simulation of the theoretical overall conversion for route A. Initial values implemented for the simulation:  $[\text{BA}]_0=0$ ,  $[\text{AC}]_0=150$ ,  $[\text{BAOH}]_0=120$ ,  $[\text{NADP}^+]_0=0.20$ ,  $[\text{HPP}]_0=10$ ,  $[\text{Diol}]_0=0$ ,  $K_{\text{BAL}}^{\text{eq}} = 107.8$ ,  $K_{\text{RADH}}^{\text{eq}} = 2.0$ .

**Table S2.** Theoretical overall conversions (related to benzyl alcohol (120 mM) and HPP (10 mM)) calculated for routes A, B, C (see main text)

#### Route A

	concentration [mM]						
	BA	AC	HPP	Diol	BOH	NADPH	NADP <sup>+</sup>
Initial	0.00	150.00	10.00	0.00	120.00	0.00	0.20
Equilibrium	0.00	30.15	10.17	119.68	0.15	0.17	0.03

Theoretical conversion: **92.06%**

#### Route B

	concentration [mM]						
	BA	AC	HPP	Diol	BOH	NADPH	NADP <sup>+</sup>
Initial	10.00	150.00	0.00	0.00	120.00	0.00	0.20
Equilibrium	0.00	20.16	10.17	119.67	0.16	0.17	0.03

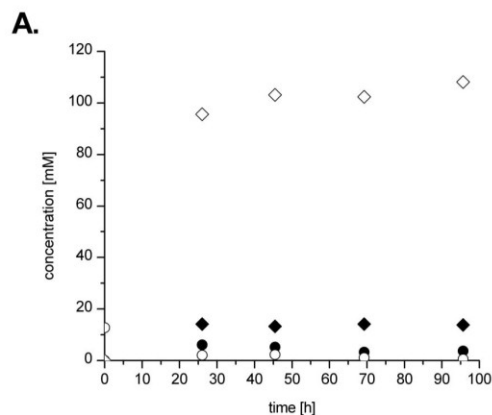
Theoretical conversion: **92.05%**

#### Route C

	concentration [mM]						
	BA	AC	HPP	Diol	BOH	NADPH	NADP <sup>+</sup>
Initial	0.00	150.00	0.00	0.00	120.00	0.00	0.20
Equilibrium	0.00	30.07	0.20	119.73	0.07	0.20	0.00

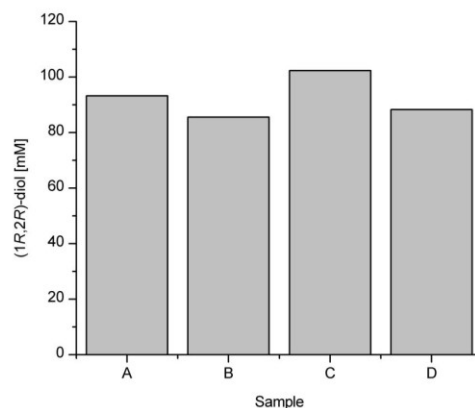
Theoretical conversion: **99.78%**

#### 4. Experimental control of calculated theoretical conversions of the cascade reaction using the substrate-coupled approach



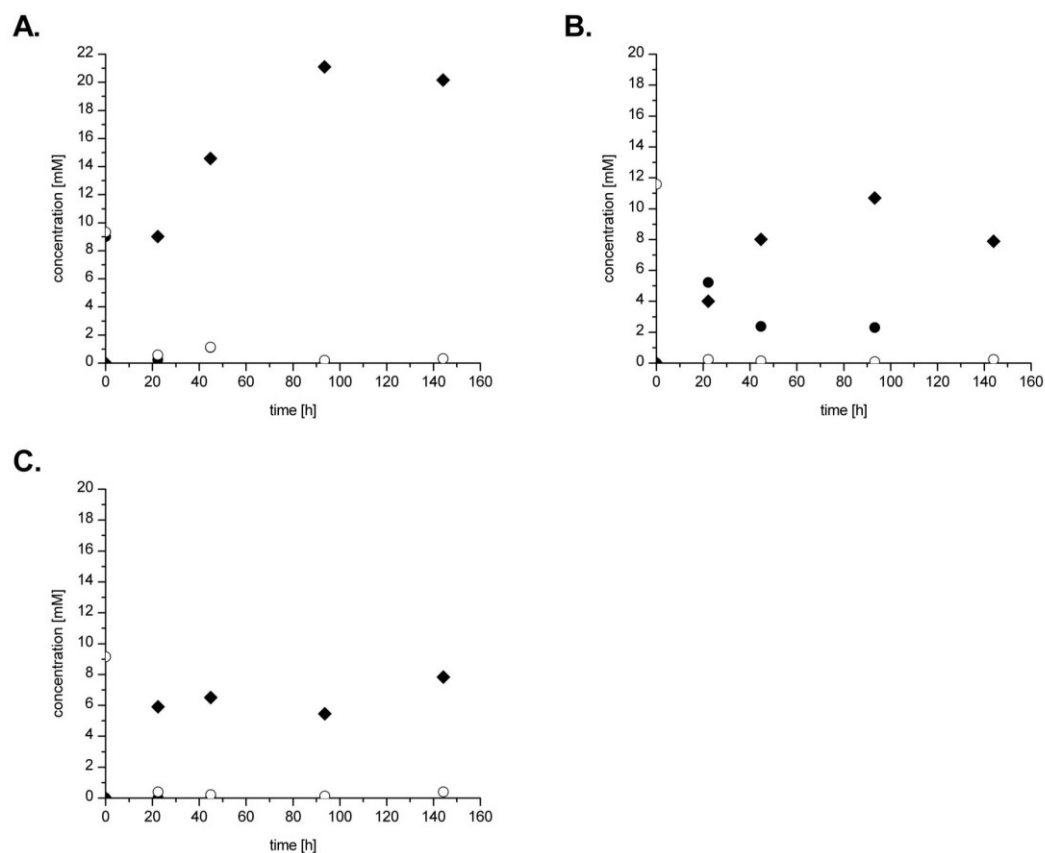
**Figure S5.** Standard synthetic cascade reaction using the substrate-coupled approach. Reaction conditions: TRIS-HCl buffer (50 mM) supplemented with  $\text{CaCl}_2$  (0.8 mM),  $\text{MgSO}_4$  (2.5 mM), ThDP (0.15 mM), pH 9.0,  $\text{NADP}^+$  (0.8 mM), benzaldehyde (10 mM), acetaldehyde (150 mM), benzyl alcohol (120 mM), BAL (0.05  $\text{mg mL}^{-1}$ ), RADH (3.75  $\text{mg mL}^{-1}$ ). Reactions were carried out at 20 °C with constant shaking (150 rpm). Samples were taken in defined time intervals. Symbols: ◆ – benzyl alcohol, ○ – benzaldehyde, ● – (R)-2-HPP, ◇ – 1,2-diol.

#### 5. Experimental investigation of overall conversion limitations of the cascade reaction using the substrate-coupled approach



**Figure S6.** Investigation of limitations of the overall conversion of the cascade reaction using the substrate-coupled approach. Reaction conditions: TRIS-HCl buffer (50 mM) supplemented with  $\text{CaCl}_2$  (0.8 mM),  $\text{MgSO}_4$  (2.5 mM), ThDP (0.15 mM), pH 9.0,  $\text{NADP}^+$  (0.8 mM), benzaldehyde (10 mM), acetaldehyde (150 mM), benzyl alcohol (120 mM), BAL (0.05  $\text{mg mL}^{-1}$ ), RADH (3.75  $\text{mg mL}^{-1}$ ). After 45 h addition of fresh, reduced cofactor (NADPH, 30 mM) and benzyl alcohol (50 mM). Samples were taken in defined time intervals: **A:** 45 h, **B:** 119 h (reference – without any addition of benzyl alcohol and NADPH), **C:** 119 h, addition of 50 mM benzyl alcohol, **D:** 119 h, addition of 30 mM NADPH.

## 6. Cascade reaction using the enzyme-coupled approach



**Figure S7.** Synthetic cascade reaction using the enzyme-coupled approach. Reaction conditions: TRIS-HCl buffer (50 mM) supplemented with  $\text{CaCl}_2$  (0.8 mM),  $\text{MgSO}_4$  (2.5 mM), ThDP (0.15 mM), pH 9.0,  $\text{NADP}^+$  (0.8 mM), BAL (0.05  $\text{mg mL}^{-1}$ ), RADH (0.10  $\text{mg mL}^{-1}$ ), TBADH (0.30  $\text{mg mL}^{-1}$ ). **A.** Route A: (R)-2-HPP (10 mM), benzaldehyde (10 mM), ethanol (2500 mM) **B.** Route B: benzaldehyde (10 mM), acetaldehyde (100 mM), ethanol (2500 mM) **C.** Route C: benzaldehyde (10 mM), ethanol (2500 mM). Reactions were carried out at 20 °C with constant shaking (150 rpm). Samples were taken in defined time intervals. Symbols:  $\circ$  – benzaldehyde,  $\bullet$  – (R)-2-HPP,  $\blacklozenge$  – 1,2-diol.

## Publication IV

---

“Structures of alcohol dehydrogenases from *Ralstonia* and *Sphingobium* spp. reveal the molecular basis for their recognition of ‘bulky-bulky’ ketones”

Henry Man, Kinga Kedziora, Justyna Kulig, Annika Frank, Ivan Lavandera-Garcia, Vincente Gotor-Fernandez, Dörte Rother, Sam Hart, Johan P. Turkenburg and Gideon Grogan

Submitted to Topics in Catalysis, *accepted*



## Abstract

Alcohol dehydrogenases (ADHs) are applied in industrial synthetic chemistry for the production of optically active secondary alcohols. However, the substrate spectrum of many ADHs is narrow, and few, for example, are suitable for the reduction of prochiral ketones in which the carbonyl group is bounded by two bulky and/or hydrophobic groups; so-called ‘bulky-bulky’ ketones. Recently two ADHs, RasADH from *Ralstonia* sp. DSM 6428, and SyADH from *Sphingobium yanoikuyae* DSM 6900, have been described, which are distinguished by their ability to accept bulky-bulky ketones as substrates. In order to examine the molecular basis of the recognition of these substrates the structures of the native and NADPH complex of RasADH, and the NADPH complex of SyADH have been determined and refined to resolutions of 1.5, 2.9 and 2.5 Å respectively. The structures reveal hydrophobic active site tunnels near the surface of the enzymes that are well-suited to the recognition of large hydrophobic substrates, as determined by modelling of the bulky-bulky substrate *n*-pentyl phenyl ketone. The structures also reveal the bases for NADPH specificity and (*S*)-stereoselectivity in each of the biocatalysts for *n*-pentyl phenyl ketone and related substrates.

## Introduction

Alcohol dehydrogenases (ADHs) have been employed for many years in both academic and industrial groups for the asymmetric reduction of prochiral carbonyl groups to optically active secondary alcohols [1,2]. The natural diversity of ADHs has ensured that enzymes encompassing a host of catalytic characteristics have been made available for applications. Hence there are ADHs that offer (*R*)-[3] or (*S*)-[4] selectivity, thermostability [5,6] and an impressive tolerance to organic solvents that allows the enzymes to be used in the presence of high substrate concentration [7] or even neat substrate itself [8]. One such niche application of ADHs is served by a subgroup of these enzymes that transforms prochiral ketones that feature large hydrophobic groups on either side of the carbonyl group; ‘bulky-bulky’ ketones.

As part of a culture collection screening programme, Kroutil and co-workers described the cloning, expression and application of an ADH from *Ralstonia* sp. DSM 6428, which was able to accept these bulky-bulky ketones as substrates [9]. The *Ralstonia* ADH (RasADH from hereon) enzyme was applied to the reduction of *n*-butyl phenyl ketone and *n*-pentyl phenyl ketone **1** with (*S*)-enantioselectivity and with e.e.s of up to >99% (**Figure 1**) [9]. The excellent enantioselectivity was also extended to bulky-small ketones such as acetophenone. RasADH has subsequently been characterised in some detail by one of our groups [10]. The enzyme was reported to be of the short chain dehydrogenase (SDR) family, with a subunit molecular weight of 26.7 kDa (249 amino acids) and it was suggested that three subunits of the enzyme associated to form a trimer in solution. RasADH exhibited a broad pH optimum for the reductive transformation of

benzaldehyde and had a half-life of 80 h at 25°C. The stability of the enzyme could be augmented by the addition of calcium ions. RasADH was subsequently also applied to the reduction of  $\alpha$ -hydroxy ketones [11] and in the dynamic kinetic resolution (DKR) of  $\alpha$ -alkyl- $\beta$ -hydroxyesters such as **3** (**Figure 1**) to give (2*S*, 3*S*)- products of type **4** [12].

Further screening of microbial culture collections for the reduction of bulky-bulky ketones revealed a strain of *Sphingobium yanoikuyae* DSM 6900 that was also able to reduce *n*-pentyl phenyl ketone **1** to the (*S*)-alcohol **2** in up to 97% e.e. [13]. This short chain dehydrogenase, named SyADH, was isolated and the relevant gene cloned and expressed, and subsequently used for the non-selective oxidation of some small prochiral alcohols [14]. Like RasADH, SyADH has also recently been employed in the DKR of  $\alpha$ -alkyl- $\beta$ -hydroxyesters such as **5** [12], in this case to give (2*R*, 3*S*)- diol products **6** with excellent d.e.s and e.e.s

RasADH and SyADH therefore present distinctly useful biocatalysts as they catalyse the transformation of sterically challenging substrates and with, in some cases, complementary stereo- and diastereo-selectivities to established ADHs. In the case of each of these enzymes, knowledge of their three-dimensional structure would not only provide information for the first time on the determinants of bulky-bulky ketone recognition in such ADHs, but also serve to inform the engineering of other ADHs for transformation of those substrates, or for the expanded substrate specificity of RasADH and SyADH themselves. In this report, we present the X-ray crystal structures of the *apo*- and NADPH-complex of RasADH at 1.5 Å and 2.9 Å resolution respectively, and also the structure of the NADPH complex of SyADH at 2.5 Å resolution. These structures reveal the hydrophobic characteristics of the active site(s) that allow accommodation of large hydrophobic substrates, and also shed light on the determinants of cofactor specificity in these ‘bulky-bulky’ ADH enzymes.

## Results and Discussion

### *Structure of RasADH*

RasADH was expressed from a strain of *E. coli* BL21 (DE3) that had been transformed with the gene encoding RasADH ligated into the pET-YSBLIC-3C vector [15]. After purification using nickel affinity and gel filtration chromatography, the pure protein was initially concentrated to 8 mg mL<sup>-1</sup> and during this process problems with precipitation were encountered, but these were successfully addressed through the inclusion of both NaCl and glycerol in the cell resuspension and protein purification buffers (see Experimental Section). Gel filtration studies on the protein derived in this way were suggestive of a tetramer of RasADH monomers in solution, rather than the trimer suggested by earlier studies [10].

Crystals of RasADH were obtained in two forms, each of which was soaked with 10 mM NADPH before testing diffraction quality. It was found that the first form diffracted to a resolution of 1.5 Å with a  $C2_1$  space group. Data collection and refinement statistics can be found in Table 1. The structure of RasADH was solved by molecular replacement using a monomer of a ‘probable dehydrogenase protein’ from *Rhizobium etli* CFN42 (55% sequence identity with RasADH; PDB code 4FGS) as a model. In the structure solution there were four monomers A-D in the asymmetric unit, which made up a tetramer (**Figure 2a**), a quaternary association common to some other short-chain ADHs such as the carbonyl reductase from *Candida parapsilosis* (PDB code 3CTM, [16]) and levodione reductase from *Corynebacterium aquaticum* (1IY8, [17]).

Each monomer of RasADH (**Figure 2b**) was made up of a classical Rossmann fold with a central  $\beta$ -sheet composed of seven  $\beta$ -strands:  $\beta 1$  (residues 8-13);  $\beta 2$  (33-37);  $\beta 3$  (54-58);  $\beta 4$  (83-87);  $\beta 5$  (131-135);  $\beta 6$  (174-180) and  $\beta 7$  (239-242). The  $\beta$ -sheet was surrounded by six alpha helices:  $\alpha 1$  (residues 17-30);  $\alpha 2$  (40-50);  $\alpha 3$  (64-77);  $\alpha 4$  (101-126);  $\alpha 5$  (148-168) and  $\alpha 7$  (217-228). A further helix, the sixth in sequence order  $\alpha 6$  (195-208, as revealed by the NADPH complex structure – *vide infra*), was largely missing from the density in the *apo* structure of RasADH. This helix was part of a sequence of residues in the region of Thr185 to Phe205 that in each subunit could not be modelled (although residues Glu200 to Lys204 were present in subunit ‘C’). A possible role for this helix is discussed below. Notwithstanding helix  $\alpha 6$ , the overall fold of the RasADH monomer (**Figure 2b**) is well-conserved amongst SDR structures; a superimposition of the ‘A’-chain of RasADH with that of a monomer of 4FGS gave an rmsd of 0.71 Å over 240 C $\alpha$  atoms. The RasADH monomer is most similar to 4FGS and a putative oxidoreductase protein from *Sinorhizobium meliloti* 1021, (PDB code 4ESO; with 41% sequence identity to RasADH), as determined by analysis using the DALI server [18], with rmsd values for the latter structure 1.4 Å. over 250 residues. In this first, higher resolution, structure of RasADH no residual density in the omit map corresponding to the NADP(H) cofactor could be observed in the putative active site of the enzyme.

A monomer of RasADH (for example, subunit ‘A’) closely associates with its neighbours ‘C’ and ‘B’, and to a lesser extent, ‘D’, to form the tetramer. Subunit ‘A’ makes a contact surface area of 1540 Å<sup>2</sup> with subunit ‘C’, as calculated using PISA [19], with interactions dominated by the reciprocal association of helices  $\alpha 7$ , including stacking interactions between Phe226 residues of each subunit, and strands  $\beta 7$ , which are largely governed by hydrophobic side-chain interactions. ‘A’ also closely interacts with subunit ‘B’, with a calculated shared interface of 1670 Å<sup>2</sup>. This pair of monomers interacts most closely through reciprocal interactions between helices  $\alpha 4$  and  $\alpha 5$ , including the indole nitrogen of Trp164 of ‘A’ with the carboxylate side chain of ‘B’ Asp148 and a salt bridge between the side-chains of ‘A’ Asp105 and ‘B’ Arg 113.

The other crystal form of RasADH diffracted more poorly, to a resolution of 2.9 Å, and in the same  $C2_1$  space group as the *apo*-enzyme. Using the monomer of the *apo*-structure as a model, the structure solution in this instance yielded six monomers in the asymmetric unit, representing one full tetramer and one half-tetramer. In this case, each monomer featured extensive density in the omit map in the active site that was representative of the cofactor NADPH at full occupancy. In addition, density for the helix  $\alpha 6$  in the region of Thr185 to Phe205 was now largely complete, and could be modelled, save for one or two residues in the region of Val191. Chain 'F' was complete, however. The loop density in the NADPH complex confirmed that the loop appears to act as lid for the active site, closing over the cofactor in the *holo*-form of the enzyme (**Figure 2b**).

### *Structure of SyADH*

SyADH was also subcloned into the pET-YSBLIC-3C vector, and was again expressed well in the soluble fraction of the BL21 (DE3) strain of *E. coli*. In this case however, gel filtration analysis suggested that SyADH was predominantly a dimer in solution. Crystallisation of SyADH followed cleavage of the hexahistidine tag as described in the Experimental Section. Crystals were of the  $P2_1$  space group. The structure was solved using the programme BALBES [20], which selected a monomer of the NADPH-dependent blue fluorescent protein from *Vibrio vulnificus* (3P19; 25% sequence identity with SyADH) as a model. The solution featured five dimer pairs in the asymmetric unit (**Figure 3a**).

The monomer of SyADH (Subunit 'A' will serve as the model for the description below), again features the characteristic Rossmann-type fold, again featuring a central  $\beta$ -sheet of seven strands:  $\beta 1$  (residues 6-11);  $\beta 2$  (31-34);  $\beta 3$  (56-58);  $\beta 4$  (82-88);  $\beta 5$  (134-138);  $\beta 6$  (177-181) and  $\beta 7$  (224-225). In SyADH, the sheet is surrounded by seven  $\alpha$ -helices:  $\alpha 1$  (residues 15-27);  $\alpha 2$  (38-52);  $\alpha 3$  (66-78);  $\alpha 4$  (102-130);  $\alpha 5$  (151-171);  $\alpha 6$  (190-194) and  $\alpha 7$  (207-220). A last helix,  $\alpha 8$ , stretching from residues 234-238, is at the C-terminus of the protein and participates in pronounced monomer-monomer ('A'/'B') interactions, helping to form the dimer (**Figure 3b**). Electron density allowed the modelling of residues Thr3 or Leu 4 through Tyr258 in all subunits, with only residue Asn199 not modeled in subunits 'I' and 'J', owing to poor electron density. The monomer of SyADH was most similar to monomers of clavulanic acid dehydrogenase from *Streptomyces clavuligerus* (PDB code 2JAH; 26% sequence identity with SyADH; rmsd 2.2 Å over 245 C $\alpha$  atoms) [21] and sepiapterin reductase from *Chlorobium tepidum* (PDB code 2BD0; 25% sequence identity with SyADH; rmsd 2.4 Å over 240 C $\alpha$  atoms) [22]. The overall structural fold of the monomer of SyADH was very similar to that of 2JAH, save for a loop region Phe218-Leu223 between  $\alpha 7$  and  $\beta 7$  in SyADH which was longer in 2JAH (Ala227 –Val236). Monomer 'A' was calculated to form an

interface of 3700 Å<sup>2</sup> with its dimer partner, subunit 'B', as calculated using PISA [19]. The dimer is stabilised by reciprocal interactions between residues in helices  $\alpha$ 8, including a salt bridge between the side-chain of residues Asp248 and Arg234 in each subunit, but also reciprocal interactions between  $\alpha$ 4 and  $\alpha$ 5, which are structurally homologous with helices  $\alpha$ 4 and  $\alpha$ 5 in RasADH, described above.

### The substrate binding sites

The active site of RasADH is a hydrophobic tunnel that is formed at the top of the central  $\beta$ -sheet of the Rossmann fold as seen in **Figure 2b** and **Figure 4**, and is partially covered by helix  $\alpha$ 6 in the NADPH-complex structure. The nicotinamide ring of NADPH sits at the base of this tunnel, lined by residues Tyr150 (the likely proton donor to a nascent alcohol in the reductive ADH-catalysed reaction [23]), Ser137, Phe205, Leu144, Leu142, Val138, Tyr150, Ile91, His147 and Gln191. The strict specificity for the phosphorylated cofactor NADPH is governed by interactions of adjacent arginine residues Arg38 and Arg39 and Asn15, with Arg38 also participating in  $\pi$ -stacking interactions with the adenine ring. The interactions with the phosphate fully explain the strict specificity of RasADH for NADPH over the non-phosphorylated cofactor NADH [10].

The active site tunnel in SyADH is situated between two loops formed by Gly195-Val204 and Phe144-Met150, the former in place of helix  $\alpha$ 6 in RasADH. The nicotinamide ring again occupies the base of the tunnel, the lining of which shares significant homology with RasADH, with probable proton donor Tyr153 (RasADH-Tyr150), Ser140 (Ser137), Met150 (His147), and Val141 (Val138), conserved in respect of steric bulk, but with three larger hydrophobic residues from RasADH replaced by alanine: Ala92 (equivalent to RasADH Ile91) and Ala145 (Leu142) and Ala194 (Gln191), suggestive, at least superficially, of a greater active site volume in SyADH overall. Additional steric bulk is provided in the active site by Trp191 (Ile188) and Phe148 (Leu144). The 2'-ribose phosphate group of NADPH is less constrained in SyADH than in RasADH; Arg36 mirrors the location and function of RasADH-Arg38, but RasADH-Arg39 is not present and is replaced by an aspartate (Asp37) that points away from the phosphate binding site. Ser13 replaces RasADH Gln15 in the other direct interaction with phosphate. The side-chain of an additional arginine, Arg40, which is not present in RasADH is close to the phosphate in SyADH, but, with both terminal N-atoms of the side chain at 3.6 Å and 3.8 Å from the phosphate oxygen, too far away to suggest a major role in phosphate binding.

The nicotinamide rings of the NADPH cofactors in each case are presented to the active site cavity. The C4 atom of the nicotinamide ring, from which hydride will be delivered to the substrate carbonyl, is in each case 4.2 Å (RasADH) or 4.3 Å (SyADH) from the

phenolic hydroxyl of the tyrosine proton donor. In SyADH, the region extending from the space between the nicotinamide C4 and the phenolic hydroxyl of Tyr153, and out into the hydrophobic cavity, contained electron density although no obvious ligands that featured in the crystallization conditions could be modelled.

### Modelling bulky-bulky ketones in the active sites

RasADH and SyADH are distinctive in their ability to reduce ketones in which the prochiral carbonyl group is bounded on either side by hydrophobic groups, such as *n*-pentyl phenyl ketone **1**, which is transformed by each enzyme into the (*S*)-alcohol with excellent enantiomeric excess. With the structures of the enzymes in hand, it was now possible to model the structure of **1** into their active sites, in the knowledge that, given the known (*S*)-stereospecificity of the enzymes with this substrate, only the *re*-face of the prochiral ketone would be presented to the C4-nicotinamide atom that delivers hydride, and also that the carbonyl group must be situated within H-bonding distance of the relevant conserved serines (Ser137 in RasADH and S140 in SyADH) and tyrosine proton donors (Tyr150 in RasADH and Tyr153 in SyADH) that are involved in catalysis [23]. **1** was modelled into the active sites of RasADH and SyADH using the programme AUTODOCK-VINA [24] using a procedure described in the Experimental Section. A comparison of these models is shown in **Figure 5**.

In the model of SyADH with substrate **1**, the hydrophobic tunnel can be described in terms of a proximal region nearer the surface of the enzyme, in which the phenyl ring is bound, and a distal region towards the enzyme interior, which binds the alkyl chain. The *re*-face of the carbonyl in **1** is positioned against the nicotinamide ring of NADPH, with the C=O oxygen at a distance of 2.5 Å and 3.4 Å from the side chains of Ser140 and the proton donor Tyr153 respectively. As a consequence, the phenyl ring is accommodated in the proximal region of the tunnel, bounded by hydrophobic residues Val141, Ala184, Leu201 and Phe148. The pendant *n*-pentyl group penetrates the distal region of the tunnel and is bounded by further hydrophobic residues Trp191, Ile190, Ala92 and Met150. In RasADH, the requisite interactions of the carbonyl group with the C4 of NADPH are still observed, but the phenyl ring of the substrate is pressed further into the active site in relation to the SyADH model complex, as a result of steric repulsion by residue Phe205, which is part of the 'lid' helix  $\alpha_6$ . In the distal region of the hydrophobic tunnel, penetration of the *n*-pentyl chain is prevented by Gln191 and is displaced into the region of the active site occupied by Ile188, which would not be permitted in SyADH because of the presence of bulky Trp191 (seen behind the substrate in **Figure 5a**). The alkyl chain now makes favourable hydrophobic interactions in this position with Phe205 and Ile188 (seen behind the substrate in **Figure 4b**). The models suggest that although each accepts **1**, SyADH is better suited to accommodate the substrate. The models are useful in revealing the hydrophobic

characteristics of the active sites that permit binding of hydrophobic substrates but also the distinctive substrate ranges of SyADH and RasADH. The model suggest that while the flexible alkyl chain of **1** can be accommodated in the distal region of hydrophobic tunnel through contortion in RasADH, less flexible substituents, such as aromatics, would not be accommodated. This is supported by substrate specificity studies [10], which show that compounds such as benzoin are poor substrates for RasADH. For SyADH, however, the larger distal portion of the hydrophobic tunnel may allow for the accommodation of such bulky groups. The large capacity of the hydrophobic tunnel of SyADH also suggests a basis for its non-selectivity towards smaller prochiral ketones such as acetophenone [14] with space available for these substrates to be accommodated in such a way that presents the *si*- or the *re*-face of the carbonyl group to the NADPH hydride at C4 of the cofactor nicotinamide ring.

## Conclusion

The structures of RasADH and SyADH have revealed the structural basis for the recognition of bulky-bulky ketones in a hydrophobic tunnel near the surface of the enzymes. The structures of enzymes with potential use in biocatalytic applications can be valuable in identifying active site determinants of substrate specificity and enantioselectivity that may inform rational engineering, or randomised mutagenesis at targeted residues, for improved or altered specificity.

## Experimental Section

### *Gene cloning, expression and protein purification*

The genes encoding RasADH and SyADH were obtained from the laboratory of Professor Wolfgang Kroutil, University of Graz, Austria. Each gene was subcloned into the pET-YSBLIC-3C vector in York. RasADH was amplified by PCR from the template plasmid using the following primers: 5'-CCAGGGACCAGCAATGTATCGTCTGCTGAATAAAACCGCAGTTATTACCG - 3' (Forward) and 5'-GAGGAGAAGGCGCGTTATTAAACCTGGGTCAGACCACCATCAACAAACAG - 3' (Reverse). SyADH was amplified using primers 5'-CCAGGGACCAGCAATGACCACCCTGCCGACCGTTCTG - 3' (Forward) and 5'-GAGGAGAAGGCGCGTTATTATTATTTTCAAACCTGCGGATGTGACCATGC - 3' (Reverse). Following agarose gel analysis of the PCR products, the relevant bands were eluted from the gels using a PCR Cleanup kit® (Qiagen). The genes were then subcloned into the pET-YSBL-LIC-3C vector using previously published techniques

[15]. The resultant plasmids were then used to transform *E. coli* XL1-Blue cells (Novagen), yielding colonies which in turn gave plasmids using standard miniprep procedures that were sequenced to confirm the identity and sequence of the genes.

The recombinant vector(s) containing the RasADH and SyADH genes were used to transform *E. coli* BL21 (DE3) cells using 30  $\mu\text{g mL}^{-1}$  kanamycin as antibiotic marker on Luria Bertani (LB) agar. Single colonies from agar plate grown overnight were used to inoculate 5 mL cultures of LB broth, which were then grown overnight at 37°C with shaking at 180 r.p.m. The starter cultures served as inocula for a 1 L cultures of LB broth in which cells were grown until the optical density ( $\text{OD}_{600}$ ) had reached a value of 0.8. Expression of either RasADH or SyADH were then induced by the addition of 1 mM isopropyl  $\beta$ -D-1-thiogalactopyranoside (IPTG). The cultures were then incubated at 18°C in an orbital shaker at 180 r.p.m. for approximately 18 h. The cells were harvested by centrifugation for 15 min at 4225 g in a Sorvall GS3 rotor in a Sorvall RC5B Plus centrifuge. At this point, considerations specific to each protein applied and purification strategies diverged.

For RasADH, cell pellets were resuspended in 20 mL of 50 mM Tris-HCl buffer pH 7.5 containing 500 mM NaCl, 20 mM imidazole, 1 mM  $\text{CaCl}_2$  and 10% glycerol (v/v) (buffer 'A') per 1 L of cell culture. The cell suspensions were then sonicated for 10 x 45s bursts at 4°C with 30 s intervals. The soluble and insoluble fractions were separated by centrifugation for 30 min at 26,892 g in a Sorvall SS34 rotor. The crude cell lysate from 1L cell culture was loaded onto a 5 mL HisTrap FF crude column (GE Healthcare), which was then washed with buffer 'A') and then the protein eluted with a linear gradient of 20-300 mM imidazole. Fractions containing RasADH were combined and concentrated using a 10 kDa cut-off Centricon® filter membrane. The concentrated RasADH was then loaded onto a pre-equilibrated S75 Superdex™ 16/60 gel filtration column, which was then eluted with 120 mL of buffer 'A' without imidazole, using a flow rate of 1 ml min<sup>-1</sup>. Fractions containing pure RasADH, as determined by SDS-PAGE analysis were combined and stored at 4°C. For SyADH, an equivalent procedure was employed using, in place of buffer 'A', a 50 mM Tris-HCl buffer containing 300 mM NaCl and 20 mM imidazole only (buffer 'B'). All subsequent procedures were equivalent to the strategy employed for RasADH, with purification performed using Ni-NTA chromatography followed by gel filtration. In the case of SyADH, prior to crystallisation, the histidine tag was cleaved using C3 protease using a procedure described previously [15].



### *Protein Crystallisation*

Crystallization conditions for both enzymes were determined using commercially available screens in the sitting-drop format in 96-well plates using 300 nL drops (150 nL protein plus 150 nL precipitant solution). Positive hits were scaled up in 24 x a mL Linbro dish using the hanging-drop method of crystallisation, with crystallisation drops containing 1  $\mu$ L of protein solution and 1  $\mu$ L of precipitant reservoir. For the apo-RasADH, the best crystals were obtained in 0.1 M Bis-tris propane pH 7.0 containing 20% (w/v) PEG 3350 and 0.02 M sodium-potassium phosphate. The protein concentration was 24 mg mL<sup>-1</sup>. For the RasADH NADPH complex, the best crystals were obtained in 0.1 M Bis-tris propane pH 8.0, containing 16% (w/v) PEG 3350, 0.2 M KSCN and 5% (w/v) ethylene glycol. The protein concentration in each case was 24 mg mL<sup>-1</sup>. In each case, the crystals were picked and transferred to a solution of the mother liquor containing 20% (v/v) ethylene glycol as cryoprotectant and 10 mM NADPH, and left for 5 min. The crystals were then flash cooled in liquid nitrogen prior to diffraction analysis.

For the SyADH-NADPH complex, the best initial crystals were obtained in conditions containing 0.1 M MES buffer pH 5.5 with 0.3 M sodium acetate and 15% (w/v) PEG 4K, with a protein concentration of 20 mg mL<sup>-1</sup>. As with RasADH, crystals were picked and transferred to a solution of the mother liquor containing 20% (v/v) ethylene glycol as cryoprotectant and 10 mM NADPH, and left for 5 min. The crystals were then flash-cooled in liquid nitrogen prior to diffraction analysis.

Crystals were tested for diffraction using a Rigaku Micromax-007HF fitted with Osmic multilayer optics and a Marresearch MAR345 imaging plate detector. Those crystals that diffracted to greater than 3 Å resolution were retained for full dataset collection at the synchrotron.

### *Data Collection, Structure Solution, Model Building and Refinement of Q1EQE0*

Complete datasets for the apo-RasADH and its NADH complex, and the SyADH complex with NADPH were collected on beamlines I04, I02 and I04 respectively, at the Diamond Light Source, Didcot, Oxfordshire, U.K. Data were processed and integrated using XDS [25] and scaled using SCALA [26] as part of the Xia2 processing system [27]. Data collection statistics are given in **Table 1**. The structure of the apo-RasADH was solved using MOLREP [28], using a monomer of structure PDB code 4FGS as a search model. The solution contained four molecules in the asymmetric unit, representing one tetramer. The structure of the RasADH NADPH complex was then solved using the monomer of the apo-RasADH. The structure of SyADH was solved using the programme BALBES [20], which selected a monomer of the PDB code structure 3P19 as a model. The solution contained five dimers in the asymmetric unit.

All structures were built and refined using iterative cycles of Coot [29] and REFMAC [30] employing local NCS restraints. For NADPH complexes of both RasADH and SyADH, the omit maps, after building and refinement of the proteins, revealed residual density at the active sites, which could in each case be successfully modelled and refined as NADPH. The final structures of *apo*-RasADH, RasADH (NADPH) and SyADH (NADPH) exhibited  $R_{\text{cryst}}$  and  $R_{\text{free}}$  values of 15.8/18.8%, 26.8/29.3% and 23.4/25.1 respectively. The structures were validated using PROCHECK [31]. Refinement statistics are presented in **Table 1**. The Ramachandran plot for *apo*-RasADH showed 97.8% of residues to be situated in the most favoured regions, 1.6% in additional allowed and 0.5% outlier residues. For the RasADH-NADPH complex, the corresponding values were 95.3%, 4.6% and 0.1% respectively. For the SyADH-NADPH complex, the corresponding values were 99.0% and 1% with no residues in outlier regions. Coordinates and structure factors for *apo*-RasADH RasADH-NADPH and SyADH-NADPH have been deposited in the Protein Data Bank with the accession codes 4bmh, 4bms and 4bmj respectively.

### Docking

Automated docking was performed using AUTODOCK VINA 1.1.2 [24]. Structures for RasADH, SyADH were prepared using AUTODOCK utility scripts. Coordinates for substrate **1** were prepared using PRODRG [32]. A monomer model was used for RasADH and a dimer model was used for SyADH with the appropriate pdbqt files prepared in AUTODOCK Tools. The active site of RasADH and SyADH was contained in a grid of 20 x 30 x 20 and 24 x 18 x 14 respectively with 0.375Å spacing, centred around the catalytic centre which was generated using AutoGrid in the AUTODOCK Tools interface. The number of runs for genetic algorithm was set to 10 and the rest of the docking parameters were set to default parameters. The dockings were performed by VINA, therefore the posed dockings were below 2Å rmsd. The results generated by VINA were visualised in AUTODOCK Tools 1.5.6 where the ligand conformations were assessed upon lowest VINA energy, but also the following criteria: The known mechanisms of short-chain ADHs [23] and experimentally-determined enantioselectivity of both RasADH and SyADH for ketone **1** dictated that only poses in which the carbonyl of **1** was observed to make appropriate interactions with the phenolic hydroxyl of the catalytic tyrosine residue (Tyr150 or Tyr153 for RasADH or SyADH respectively); the conserved active site serine, which hydrogen bonds to the substrate carbonyl [23] (Ser137 or Ser140 for RasADH or SyADH respectively) and which presented the (*re*)-face of the carbonyl to the nicotinamide ring of NADPH (resulting in the (*S*)-alcohol product), were considered.

## References

- [1] Nakamura K, Yamanaka R, Matsuda T, Harada T (2003) Recent developments in asymmetric reduction of ketones with biocatalysts. *Tetrahedron: Asymmetr* 14:2659-2681.
- [2] Goldberg K, Schroer K, Lütz S, Liese A (2007) Biocatalytic ketone reduction—a powerful tool for the production of chiral alcohols—part II: whole-cell reductions. *Appl Microbiol Biotechnol* 76:249-255.
- [3] Schlieben NH, Niefind K, Müller J, Riebel B, Hummel W, Schomburg D (2005) Atomic Resolution Structures of R-specific Alcohol Dehydrogenase from *Lactobacillus brevis* Provide the Structural Bases of its Substrate and Cosubstrate Specificity. *J Mol Biol* 349: 801-813.
- [4] Nie Y, Xu Y, Mu XQ, Wang HY, Yang M, Xiao R (2007) Purification, Characterization, Gene Cloning, and Expression of a Novel Alcohol Dehydrogenase with Anti-Prelog Stereospecificity from *Candida parapsilosis*. *Appl Environ Microbiol* 73: 3759-3764.
- [5] Höllrigl V, Hollmann F, Kleeb A, Buehler K, Schmid, A (2008) TADH, the thermostable alcohol dehydrogenase from *Thermus* sp. ATN1: a versatile new biocatalyst for organic synthesis. *Appl Microbiol Biotechnol* 81:263-273.
- [6] Machielsen R, Uria AR, Kengen SWM, van der Oost J (2006) Production and Characterization of a Thermostable Alcohol Dehydrogenase That Belongs to the Aldo-Keto Reductase Superfamily. *Appl Environ Microbiol* 72:233-238.
- [7] Karabec M, Lyskowski A, Tauber KC, Steinkellner G, Kroutil W, Grogan G, Gruber, K (2010) Structural insights into substrate specificity and solvent tolerance in alcohol dehydrogenase ADH-'A' from *Rhodococcus ruber* DSM 44541. *Chem Commun* 46:6314-6316.
- [8] Jakoblinnert A, Mladenov R, Paul A, Sibilla F, Schwaneberg U, Ansorge-Schumacher MB, de Maria PD (2011) Asymmetric reduction of ketones with recombinant *E. coli* whole cells in neat substrates. *Chem Commun* 47:12230-12232.
- [9] Lavandera I, Kern A, Ferreira-Silva B, Glieder A, de Wildeman S, Kroutil W (2008) Stereoselective Bioreduction of Bulky-Bulky Ketones by a Novel ADH from *Ralstonia* sp. *J Org Chem* 6003-6005.
- [10] Kulig J, Frese A, Kroutil W, Pohl M, Rother D (2013) Biochemical characterization of an alcohol dehydrogenase from *Ralstonia* sp. *Biotechnol Bioeng* (2013) doi: 10.1002/bit.24857.

- [11] Kulig J, Simon RC, Rose CA, Husain SM, Häckh M, Lüdeke S, Zeitler K, Kroutil W, Pohl M, Rother D (2012) Stereoselective synthesis of bulky 1,2-diols with alcohol dehydrogenases. *Catal Sci Technol* 2:1580-1589.
- [12] Cuertos, A, Rioz-Martínez A, Bisogno FR, Grischek B, Lavandera I, de Gonzalo G, Kroutil W, Gotor V (2012) Access to Enantiopure  $\alpha$ -Alkyl- $\beta$ -hydroxy Esters through Dynamic Kinetic Resolutions Employing Purified/Overexpressed Alcohol Dehydrogenases *Adv Synth Catal* 354: 1743-1749.
- [13] Lavandera I, Oberdorfer G, Gross J, de Wildeman S, Kroutil, W (2008) Stereocomplementary Asymmetric Reduction of Bulky–Bulky Ketones by Biocatalytic Hydrogen Transfer. *Eur J Org Chem* 2008: 2539-2543.
- [14] Lavandera I, Kern A, Resch V, Ferreira-Silva B, Glieder A, Fabian WMF, de Wildeman S, Kroutil W (2008) One-Way Biohydrogen Transfer for Oxidation of sec-Alcohols. *Org Lett* 10: 2155-2158.
- [15] Atkin KE, Reiss R, Turner NJ, Brzozowski AM, Grogan G (2008) Cloning, expression, purification, crystallization and preliminary X-ray diffraction analysis of variants of monoamine oxidase from *Aspergillus niger*. *Acta Crystallogr Sect F* 64: 182-185.
- [16] Zhang R, Zhu G, Zhang W, Cao S, Ou X, Li X, Bartlam M, Xu Y, Zhang XC, Rao Z (2008) Crystal structure of a carbonyl reductase from *Candida parapsilosis* with anti-Prelog stereospecificity. *Protein Sci* 17:412-1423.
- [17] Sogabe S, Yoshizumi A, Fukami TA, Shiratori Y, Shimizu S, Takagi H, Nakamori S, Wada M (2003) The Crystal Structure and Stereospecificity of Levodione Reductase from *Corynebacterium aquaticum* M-13. *J Biol Chem* 278:19387-19395.
- [18] Holm L, Sander C (1996) Mapping the Protein Universe. *Science*. 273:595-560.
- [19] Krissinel E, Henrick K (2007) Inference of macromolecular assemblies from crystalline state. *J Mol Biol* 372: 774-797.
- [20] Long F, Vagin AA, Young P, Murshudov GN (2008) BALBES: a Molecular Replacement Pipeline. *Acta Crystallogr Sect D Biol Crystallogr* 64:125-132.
- [21] MacKenzie AK, Kershaw NJ, Hernandez H, Robinson CV, Schofield CJ, Andersson I (2007) Clavulanic Acid Dehydrogenase: Structural and Biochemical Analysis of the Final Step in the Biosynthesis of the  $\beta$ -Lactamase Inhibitor Clavulanic Acid. *Biochemistry* 46:1523-1533.
- [22] Supangat S, Seo KH, Choi YK, Park YS, Son D, Han C-D, Lee KH (2006) Structure of *Chlorobium tepidum* Sepiapterin Reductase Complex Reveals the Novel

Substrate Binding Mode for Stereospecific Production of l-threo-Tetrahydrobiopterin. *J Biol Chem* 281:2249-2256.

[23] Filling C, Berndt KD, Benach J, Knapp S, Prozorovski T, Nordling E, Ladenstein R, Jörnvall H, Oppermann U (2002) Critical Residues for Structure and Catalysis in Short-chain Dehydrogenases/Reductases. *J Biol Chem* 277:25677-25684.

[24] Trott O, Olson AJ (2010) AutoDock Vina: improving the speed and accuracy of docking with a new scoring function, efficient optimization and multithreading. *J Comp Chem* 31:455-461.

[25] Kabsch W (2010) XDS. *Acta Crystallogr Sect D Biol Crystallogr* 66:125-132.

[26] Evans P (2006) Scaling and assessment of data quality. *Acta Crystallogr Sect D Biol Crystallogr* 62:72-82.

[27] Winter G (2010) *xia2*: an expert system for macromolecular crystallography data reduction. *J Appl Cryst* 3:186-190.

[28] Vagin A, Teplyakov A (1997) *MOLREP*: an Automated Program for Molecular Replacement. *Appl Crystallogr* 30:1022-1025.

[29] Emsley P, Cowtan K (2004) *Coot: model-building tools for molecular graphics*. *Acta Crystallogr Sect D Biol Crystallogr* 60:2126-2132.

[30] Murshudov GN, Vagin AA, Dodson EJ (1997) Refinement of Macromolecular Structures by the Maximum-Likelihood method. *Acta Crystallogr Sect D Biol Crystallogr* 53:240-255.

[31] Laskowski RA, Macarthur MW, Moss DS, Thornton JM (1993) PROCHECK: a program to check the stereochemical quality of protein structures. *J Appl Crystallogr* 26:283-291.

[32] Schüttelkopf AW, van Aalten DMF (2004) PRODRG - a tool for high-throughput crystallography of protein-ligand complexes. *Acta Crystallogr Sect D Biol Crystallogr* 60:1355-1363.

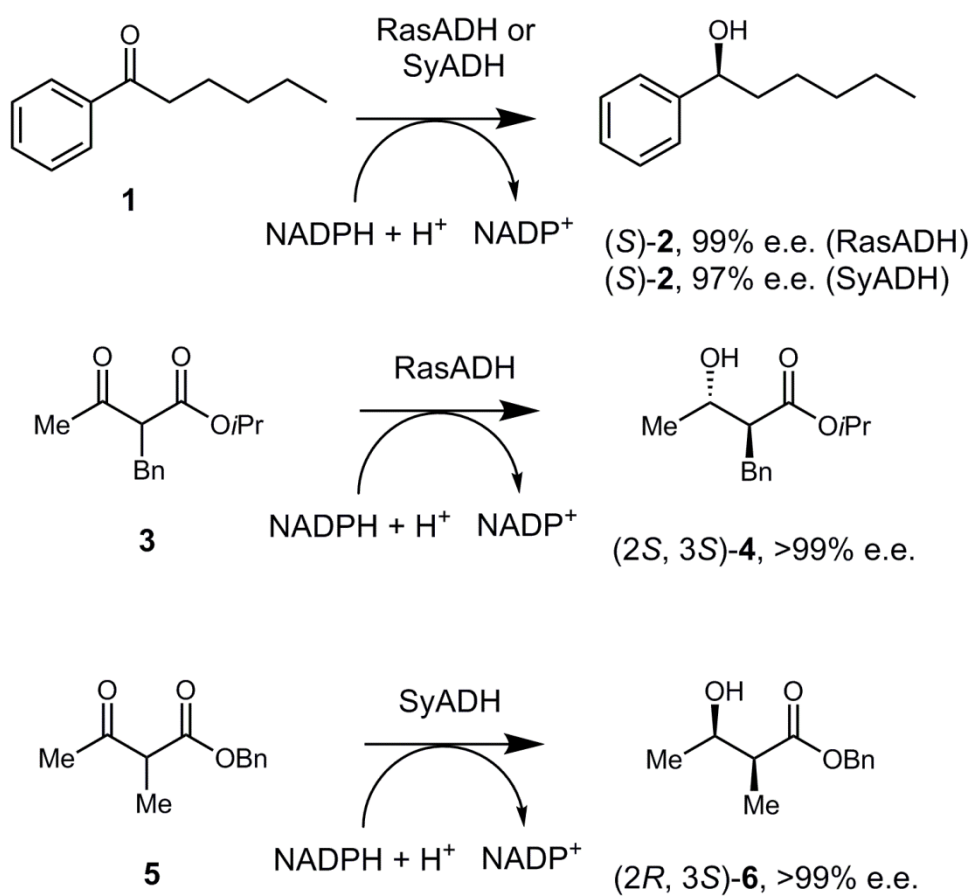
## Acknowledgements

This research was supported by a Marie Curie Network for Initial Training fellowships to K.K., J.K. and A.F. in the project BIOTRAINS (FP7-PEOPLE-ITN-2008-238531). We would also like to thank Prof. Wolfgang Kroutil of the University of Graz for genes encoding both RasADH and SyADH.

**Table 1.** Data Collection and Refinement Statistics for RasADH (*apo*- and in complex with NADPH) and SyADH in complex with NADPH. Numbers in brackets refer to data for highest resolution shells.

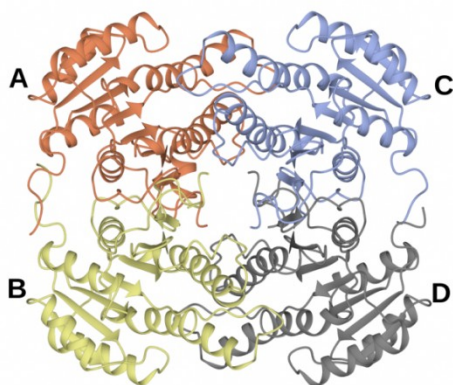
	RasADH ( <i>apo</i> )	RasADH (NADPH complex)	SyADH (NADPH complex)
Beamline	Diamond I02	Diamond I04	Diamond I02
Wavelength (Å)	0.97950	0.97950	0.97949
Resolution (Å)	60.86-1.52 (1.57-1.52)	74.54-2.89 (2.93-2.89)	139.0 - 2.5 (2.56-2.50)
Space Group	$C2_1$	$C2_1$	$P2_1$
Unit cell (Å)	a = 136.5; b = 52.5; c = 151.5; $\alpha = \gamma = 90.0$ ; $\beta = 116.6$	a = 192.3; b = 135.6; c = 93.6; $\alpha = \gamma = 90.0$ ; $\beta = 100.1$	a = 144.9; b = 86.8; c = 155.6; $\alpha = \gamma = 90.0$ ; $\beta = 106.4$
No. of molecules in the asymmetric unit	4	6	10
Unique reflections	149646 (45160)	52465 (3880)	133601 (10900)
Completeness (%)	97.7 (96.8)	99.2 (98.8)	99.7 (99.8)
$R_{\text{merge}}$ (%)	0.03 (0.25)	0.18 (0.73)	0.14 (0.54)
$R_{\text{p.i.m.}}$	0.03 (0.23)	0.16 (0.64)	0.12 (0.46)
Multiplicity	3.3 (3.5)	4.2 (4.2)	4.2 (4.3)
$\langle I/\sigma(I) \rangle$	15.6 (4.9)	7.4 (2.0)	8.2 (3.0)
CC <sub>1/2</sub>	1.00 (0.95)	0.98 (0.74)	0.99 (0.82)
Overall <i>B</i> factor from Wilson plot (Å <sup>2</sup> )	24	41	43
$R_{\text{cryst}}/R_{\text{free}}$ (%)	15.8/18.8	26.8/29.3	23.4/25.1
No. protein atoms	6942	11081	18948
No. water molecules	846	37	290
r.m.s.d 1-2 bonds (Å)	0.02	0.01	0.01
r.m.s.d 1-3 angles (°)	1.69	1.60	1.60
Avg main chain B (Å <sup>2</sup> )	20	35	35
Avg side chain B (Å <sup>2</sup> )	23	36	37
Avg water B (Å <sup>2</sup> )	33	14	20
Avg ligand B (Å <sup>2</sup> )	-	32	30

## Figures

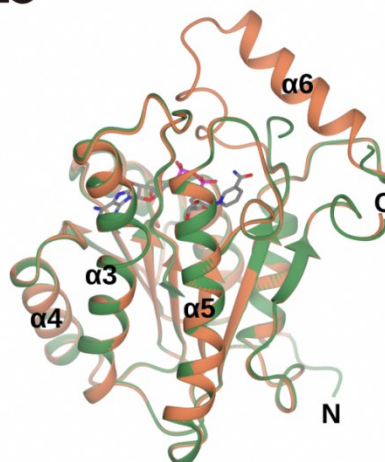


**Figure 1.** Representative asymmetric reductions of bulky-bulky ketones catalysed by alcohol dehydrogenases from *Ralstonia* sp. DSM 6428 (RasADH) and *Sphingobium yanoikuyae* DSM 6900 (SyADH).

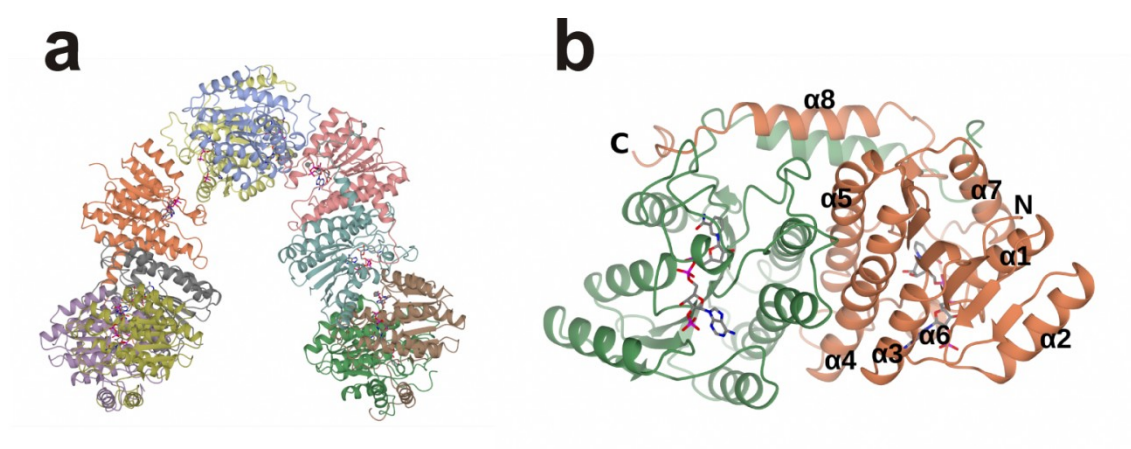
a



b

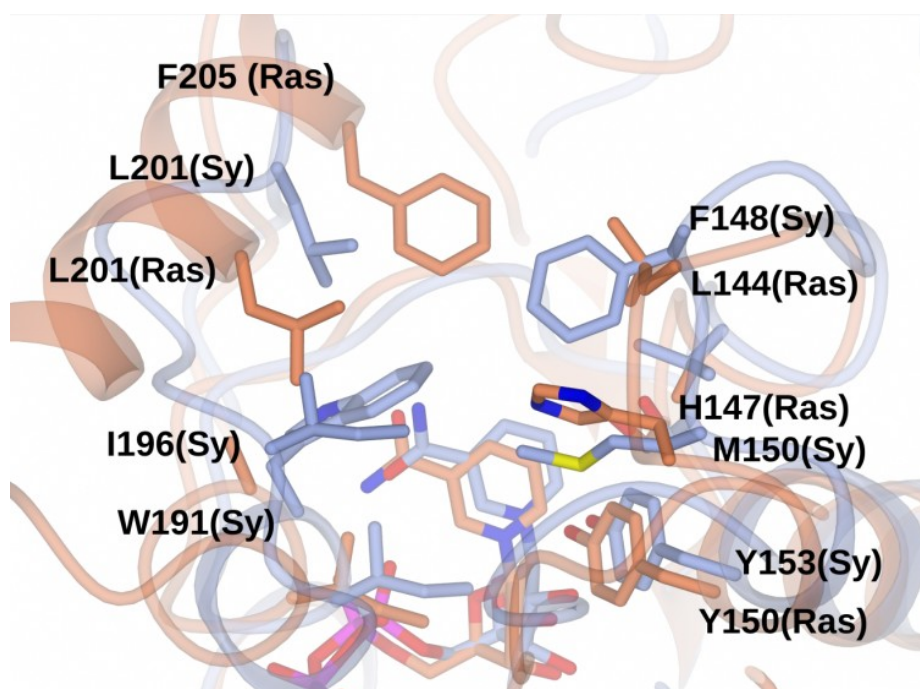


**Figure 2.** Structure of RasADH. **a:** The asymmetric unit of the *apo*-enzyme contained four monomers A-D that constituted one tetramer, which is shown in ribbon format and coloured by chain. **b:** Monomer of RasADH apoenzyme (green ribbon) superimposed with monomer of RasADH holoenzyme (coral ribbon) in complex with NADPH. The rmsd for the two structures over 201 C-alphas was 0.42 Å. The monomer(s) display the typical Rossmann fold, with a central  $\beta$ -sheet surrounded by six helices, four of which,  $\alpha 3$ ,  $\alpha 4$ ,  $\alpha 5$  and  $\alpha 6$ . Helix  $\alpha 6$ , which was absent in the apoenzyme structure, appears to act as a lid to the active site, closing over the NADPH molecule when cofactor is bound. The N and C termini of the apo enzyme monomer are also indicated. The cofactor NADPH is shown in cylinder format with carbon atoms shown in grey.

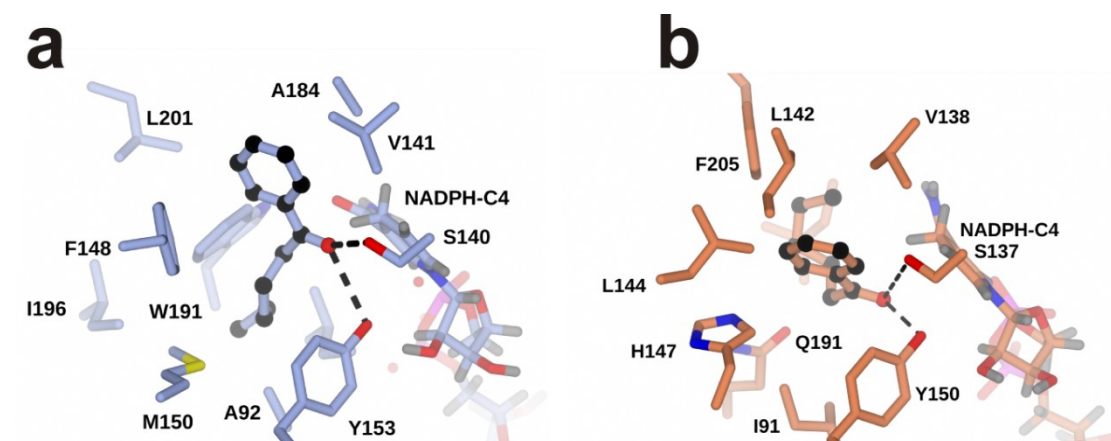


**Figure 3.** Structure of SyADH. **a:** The asymmetric unit contains ten monomers that constitute five dimers shown in ribbon format and coloured by chain. **b:** Each dimer consist of two monomers, coloured green and coral, each of which exhibits the Rossmann ( $\alpha\beta$ )<sub>8</sub> fold, with eight helices (numbered  $\alpha 1$ -4 and  $\alpha 6$ -8 for the coral monomer;  $\alpha 5$  is obscured) forming the central bundle and a ninth helix  $\alpha 9$  that associates closely with the neighbouring monomer. The N and C termini of the coral monomer are also indicated. The cofactor NADPH is shown in cylinder format with carbon atoms shown in grey.





**Figure 4.** Superimposition of active sites of RasADH and SyADH illustrating side-chain components of the hydrophobic tunnel in both active sites. RasADH is shown in ribbon format in coral with side chains projecting from the backbone and the nicotinamide ring of NADPH (centre) shown (carbon atoms in coral). SyADH is shown in light blue ribbons with NADPH and side chains (carbon atoms in light blue).



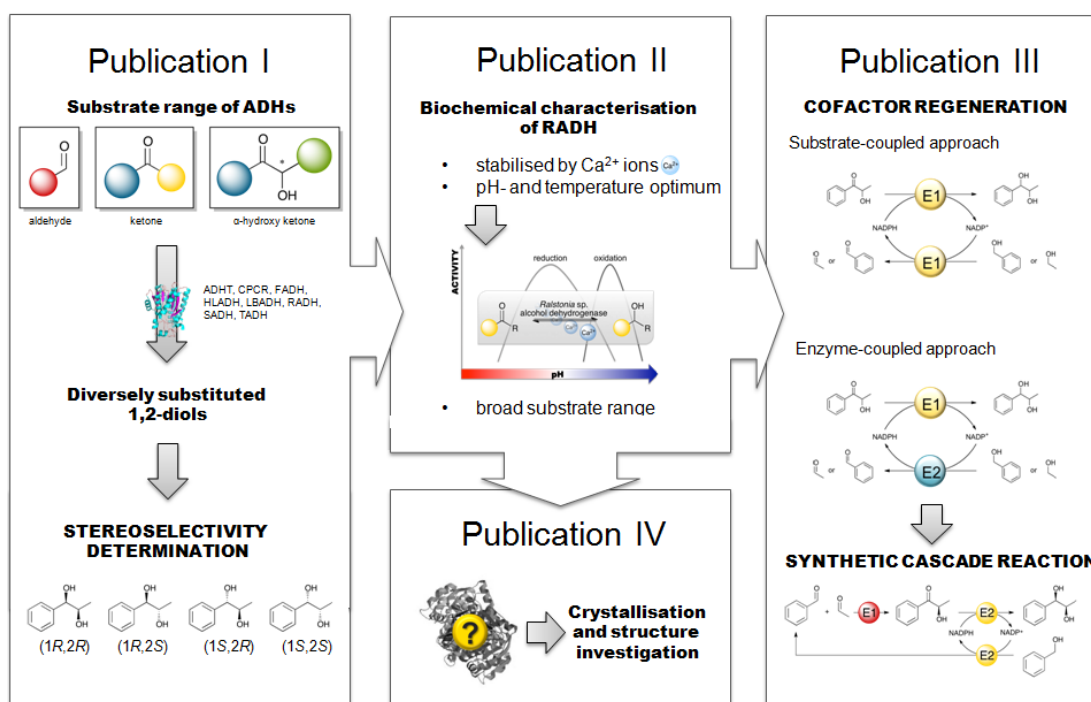
**Figure 5.** Ketone **1** modelled into the active site of a) SyADH and b) RasADH using the programme AUTODOCK VINA [24]. In a), the carbon atoms of the side chains of SyADH are shown in light blue in cylinder format; **1** is shown in ball-and-stick format with the carbon atoms in black. In b), the carbon atoms of the side chains of RasADH are shown in coral in cylinder format; **1** is again shown in ball-and-stick format with the carbon atoms in black.

## III Discussion

---

### 3.1 Overview of publications

Results obtained in this doctoral thesis were predominantly obtained at the IBG-1: Biotechnology at Forschungszentrum Jülich GmbH. Additional work packages concerning cloning, purification and crystallisation of His-tagged RADH were performed at the Department of Chemistry (York Structure Biology Laboratory), University of York, UK under supervision of Dr. Gideon Grogan. The relation of all four publications is shown in Figure 18.



**Figure 18.** Relation of publications on results obtained in this thesis.

**PUBLICATION I** describes the investigation of the substrate range of seven alcohol dehydrogenases and one carbonyl reductase towards various aldehydes, ketones and especially  $\alpha$ -hydroxy ketones. Stereoselectivities of the three most active alcohol dehydrogenases towards  $\alpha$ -hydroxy ketones was investigated in more detail. Additionally, an extended substrate range investigation of the most promising alcohol dehydrogenase, RADH from *Ralstonia* sp., is described.

**PUBLICATION II** reports the full biochemical characterisation of the alcohol dehydrogenase from *Ralstonia* sp. as the most active enzyme towards various substituted  $\alpha$ -hydroxy ketones determined so far. In this publication the effect of  $\text{Ca}^{2+}$  ions for stabilisation of RADH is discussed and the possibility of a trimeric quaternary structure is considered. Moreover, pH- and temperature dependent activities (for oxidation and reduction) and stabilities were investigated.

Subsequently, under optimal conditions the substrate range (alcohols, aldehydes and ketones) was studied. Kinetic parameters were determined for the selected substrates relevant for the 2-step enzymatic cascade reactions.

**PUBLICATION III** describes the evaluation and optimisation of suitable cofactor regeneration systems for a model cascade reaction using BAL as a ThDP-dependent lyase for the carboligation step and RADH for the oxidoreduction step. The publication is based upon the two previous publications, where substrate ranges, stereoselectivities (Publication I) and kinetic data (Publication II) were determined.

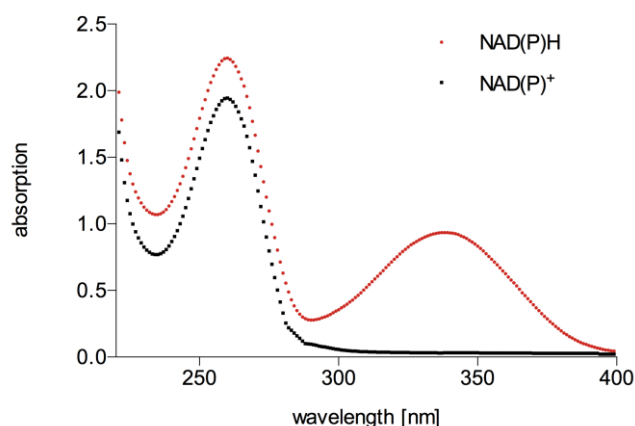
**PUBLICATION IV** reports the structure determination and refinement to resolutions of 1.5 Å and 2.9 Å, respectively, of the *apo*-enzyme and the *holo*-enzyme in complex with NADPH. In addition, the preference of RADH for bulky-bulky substrates and the specificity for NADPH could be explained.

### 3.2 Alcohol dehydrogenases as versatile catalysts

In this thesis seven alcohol dehydrogenases (ADHT, FADH, HLADH, LBADH, RADH, SADH and TADH) and the carbonyl reductase (CPCR) were investigated with respect to their substrate specificity focusing on the reduction of  $\alpha$ -hydroxy ketones. These enzymes were chosen, since it was expected from literature data that they might be able to reduce  $\alpha$ -hydroxy ketones that are significantly larger compared to small aliphatic alcohols, which are the predominant natural substrates for ADHs.

The screening was conducted employing crude cell extracts containing overexpressed enzyme. Purification at that stage was omitted, since it is a time-consuming process and not essential for a first trial. Implementation of crude cell extracts provided rapid insight into the substrate range of these all enzymes (Table 7, Publication I). For investigation of the substrate range a fast spectrophotometrical enzyme assay was applied, where the reduction or oxidation of respective substrates was monitored at 340 nm following the depletion or increase of NAD(P)H, respectively (Figure 19).

According to the obtained results three alcohol dehydrogenases were selected as most promising enzymes for the reduction of  $\alpha$ -hydroxy ketones. Among them are the recombinant alcohol dehydrogenases from *Thermoanaerobacter* sp. (ADHT), *Lactobacillus brevis* (LBADH), and *Ralstonia* sp. (RADH).

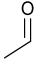
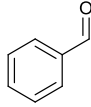
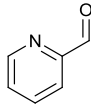
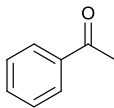
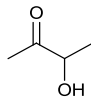
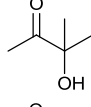
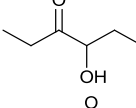
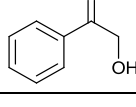


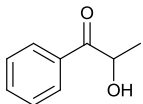
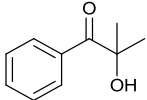
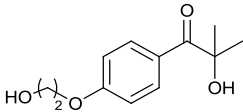
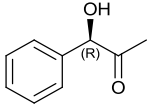
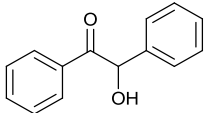
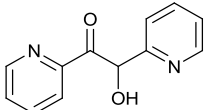
**Figure 19.** Absorption spectrum of oxidised ( $\text{NAD(P)}^+$ ) and reduced ( $\text{NAD(P)H}$ ) cofactor. Oxidised and reduced forms of the cofactor absorb ultraviolet light at about 260 nm, which is caused by the adenine moiety in the molecules. The extinction coefficient of  $\text{NAD(P)}^+$  is  $\epsilon_{260 \text{ nm}} = 16\,900 \text{ M}^{-1} \text{ cm}^{-1}$ . The reduced form of the cofactor ( $\text{NADPH}$ ) shows an additional absorption maximum at 340 nm due to the reduced nicotinamide ring ( $\epsilon_{340 \text{ nm}} = 16\,900 \text{ M}^{-1} \text{ cm}^{-1}$ ).

The investigation of substrate ranges (Table 7) demonstrated that LBADH reduces especially aliphatic  $\alpha$ -hydroxy ketones such as acetoin (**5**), its derivative (**6**), and propionin (**7**) with high specific activities. A similar tendency was found for ADHT, where as well highest activities were determined for aliphatic  $\alpha$ -hydroxy ketones (**5-7**). A different behaviour was observed for RADH, where a clear preference for the reduction of mixed araliphatic  $\alpha$ -hydroxy ketones was found. For instance,  $\alpha$ -hydroxy ketones of central interest such as 2-hydroxy-1-phenylpropan-1-one (2-HPP, **9**) and 1-hydroxy-1-phenylpropan-2-one (PAC, **12**) were reduced with extremely high initial rate activities in comparison to tested in this thesis ADHT and LBADH for the reduction of 2-HPP (**9**, see Table 7 and Publication I). A possible background reaction was excluded with an *E. coli* empty vector control.

It has to be pointed out that almost all tested  $\alpha$ -hydroxy ketones were well reduced by ADHT, LBADH, and RADH. Highest specific activities were determined with ADHT and LBADH for acetoin (**5**,  $18 \text{ U mg}^{-1}$  and  $128 \text{ U mg}^{-1}$ , respectively) and with RADH for (*R*)-2-HPP ( $240 \text{ U mg}^{-1}$ ). Low activities toward benzoin (**13**) and its derivative  $\alpha$ -pyridoin (**14**) might be caused by low solubility of these compounds in aqueous media.

**Table 7.** Substrate range of seven alcohol dehydrogenases and one carbonyl reductase towards aldehydes (1-3: 10 mM), ketones (4: 10 mM) and  $\alpha$ -hydroxy ketones (5-10 and 12: 10 mM, 11: 5 mM, 13-14: saturated). The reduction activity was measured in triplicate following the consumption of NAD(P)H (0.2 mM) at 340 nm at 30 °C (Publication I)

Substrate	No.	Specific activity [U mg <sup>-1</sup> ]							
		ADHT	CPCR	FADH	HLADH	LBADH	RADH	SADH	TADH
	1	6.0±0.3	0.3±0.0	1.4±0.0	1.0±0.0	109.8±3.1	n.a.	n.a.	0.7±0.0
	2	5.9±0.2	0.1±0.0	4.1±0.0	0.5±0.0	8.0±0.1	3.0±0.1	0.0±0.0	0.4±0.0
	3	7.7±0.2	n.a.	1.5±0.0	0.1±0.0	4.2±0.0	4.1±0.0	n.a.	0.0±0.0
	4	7.7±0.2	n.a.	n.a.	n.a.	89.6±1.0	2.4±0.0	n.a.	0.5±0.0
	5	18.1±0.1	n.a.	n.a.	n.a.	127.8±3.7	0.5±0.0	n.a.	n.a.
	6	13.3±0.3	n.a.	n.a.	n.a.	36.7±0.4	6.6±0.1	n.a.	n.a.
	7	6.4±0.3	n.a.	n.a.	n.a.	66.1±0.9	4.8±0.1	n.a.	n.a.
	8	4.2±0.1	n.a.	n.a.	n.a.	28.7±0.2	5.6±0.1	n.a.	n.a.

Substrate	No.	Specific activity [U mg <sup>-1</sup> ]							
		ADHT	CPCR	FADH	HLADH	LBADH	RADH	SADH	TADH
	<i>rac</i> - <b>9</b>	0.8±0.0	n.d.	n.d.	n.d.	3.5±0.0	112.2±7.2	n.d.	n.d.
	( <i>R</i> )- <b>9</b>	2.2±0.2	n.d.	n.d.	n.d.	3.0±0.0	239.9±7.6	n.d.	n.d.
	( <i>S</i> )- <b>9</b>	2.9±0.0	n.d.	n.d.	n.d.	3.2±0.1	10.0±0.1	n.d.	n.d.
	<b>10</b>	4.4±0.5	n.a.	n.a.	n.a.	0.3±0.0	21.5±0.4	n.a.	n.a.
	<b>11</b>	0.7±0.2	n.a.	n.a.	n.a.	0.0±0.0	4.1±0.1	n.a.	n.a.
	( <i>R</i> )- <b>12</b>	3.5±0.0	n.d.	n.d.	n.d.	20.4±0.2	36.3±1.8	n.d.	n.d.
	<b>13</b>	0.1±0.0	n.d.	n.d.	n.d.	n.d.	n.a.	n.d.	n.d.
	<b>14</b>	0.5±0.0	n.a.	n.a.	n.a.	0.1±0.0	0.6±0.0	n.a.	n.a.

ADHT = *Thermoanaerobacter* sp. alcohol dehydrogenase, CPCR = *Candida parapsilosis* carbonyl reductase, FADH = *Flavobacterium frigidimarum* alcohol dehydrogenase, HLADH = horse liver alcohol dehydrogenase, LBADH = *Lactobacillus brevis* alcohol dehydrogenase, RADH = *Ralstonia* sp. alcohol dehydrogenase, SADH = *Sphingobium yanoikuyae* alcohol dehydrogenase, TADH = *Thermus* sp. alcohol dehydrogenase, n.a. – activity not detectable, n.d. – activity not determined (for activity assay details see Publication I)

### 3.3 Stereoselectivity of ADHs

All  $\alpha$ -hydroxy ketones were reduced with high stereoselectivity. Predominantly only one stereoisomer occurred ( $de > 99\%$ ) starting from a chiral substrate ( $ee > 99\%$ ) (Table 8).

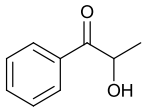
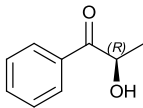
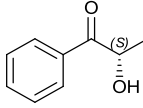
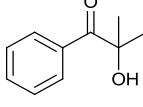
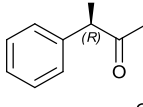
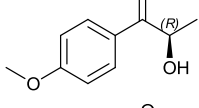
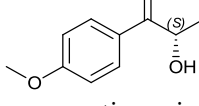
From investigations of the 2-HPP racemate the diastereomeric ratio of the resulting diastereoisomers provided information about enzyme selectivity and enzyme kinetics towards both enantiomers. For instance, reduction of *rac*-2-HPP (**9**) catalysed by ADHT showed clear preference for the reduction of (*R*)-2-HPP (dr *syn/anti* 23.6:1) under the tested conditions. A similar tendency (for the favoured reduction of (*R*)-2-HPP) was found for isolated RADH, where reduction of (*R*)-2-HPP proceeds 4-times faster (dr *syn/anti* 4:1) than the reduction of the opposite enantiomer (Table 8). This result goes in line with kinetic data, which are discussed in chapter 3.4.6. In case of LBADH the same amounts of *syn*- and *anti*-diol were formed (dr *syn/anti* 1:1) when *rac*-2-HPP was reduced. This outcome shows that LBADH shows no preference for one enantiomer of 2-HPP.

Interestingly, in all investigated cases reduction of the two isomeric compounds (*R*)-2-HPP (**9**) and (*R*)-PAC (**12**), which differ only in the position of chiral centre, resulted in inversed stereoselectivities of the product. (*R*)-PAC (**12**) was reduced by ADHT and RADH (*S*)-selectively yielding the *anti*-product, whereas reduction of (*R*)-2-HPP (**9**) proceeded (*R*)-selectively to the *syn*-product. The opposite effect was observed in case of LBADH, where reduction of (*R*)-PAC (**12**) and (*R*)-2-HPP (**9**) revealed the *syn*- and *anti*-product, respectively.

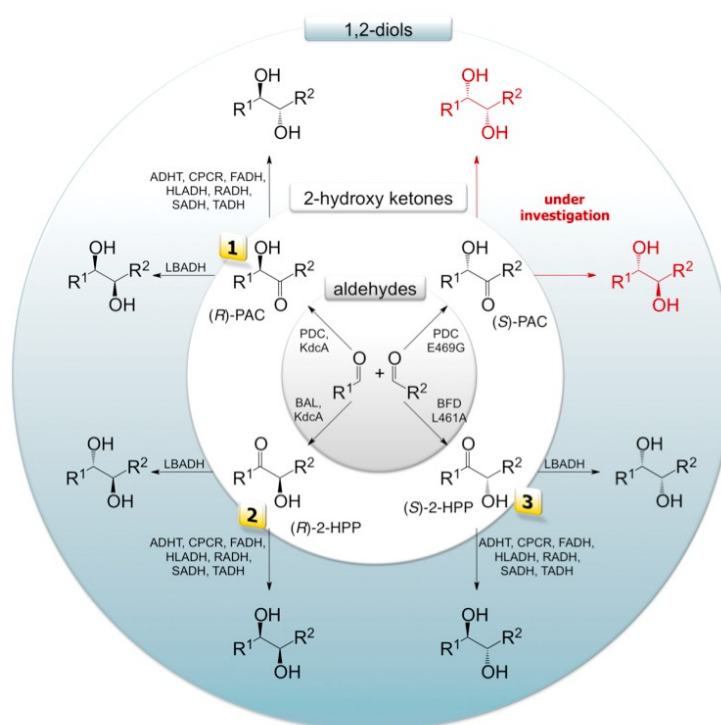
Furthermore, LBADH follows the anti-Prelog rule yielding diastereo-complementary products in comparison to products gained by catalysis with ADHT and RADH (Table 8). Therefore a broad range of highly selective products can be accessed by an appropriate combination of these biocatalysts.



**Table 8.** Stereoselectivity of tested oxidoreductases towards selected  $\alpha$ -hydroxy ketones (Publication I).

Substrate	No.	Alcohol dehydrogenase							
		ADHT	CPCR	FADH	HLADH	LBADH	RADH	SADH	TADH
	<i>rac</i> -9	<i>syn</i> -(1 <i>R</i> ,2 <i>R</i> ) and <i>anti</i> -(1 <i>R</i> ,2 <i>S</i> ) <i>dr</i> ( <i>syn/anti</i> ) 23.6:1 <sup>a</sup>	n.d.	n.d.	n.d.	<i>syn</i> -(1 <i>S</i> ,2 <i>S</i> ) and <i>anti</i> -(1 <i>S</i> ,2 <i>R</i> ) <i>dr</i> ( <i>syn/anti</i> ) 1:1 <sup>a</sup>	<i>syn</i> -(1 <i>R</i> ,2 <i>R</i> ) and <i>anti</i> -(1 <i>S</i> ,2 <i>R</i> ) <i>dr</i> ( <i>syn/anti</i> ) 2:1 <sup>a</sup> 4:1 <sup>b</sup>	n.d.	n.d.
	( <i>R</i> )-9	<i>syn</i> -(1 <i>R</i> ,2 <i>R</i> ) <i>de</i> > 99% <sup>a</sup>	n.d.	n.d.	n.d.	<i>anti</i> -(1 <i>S</i> ,2 <i>R</i> ) <i>de</i> > 99% <sup>a</sup>	<i>syn</i> -(1 <i>R</i> ,2 <i>R</i> ) <i>de</i> > 99% <sup>a,b</sup>	<i>syn</i> -(1 <i>R</i> ,2 <i>R</i> ) <i>de</i> > 99% <sup>a,b</sup>	n.d.
	( <i>S</i> )-9	<i>anti</i> -(1 <i>R</i> ,2 <i>S</i> ) <i>de</i> > 99% <sup>a</sup>	n.d.	n.d.	n.d.	<i>syn</i> -(1 <i>S</i> ,2 <i>S</i> ) <i>de</i> > 99% <sup>a</sup>	<i>anti</i> -(1 <i>R</i> ,2 <i>S</i> ) <i>de</i> > 99% <sup>a,b</sup>	n.d.	n.d.
	10	( <i>R</i> ) <i>ee</i> > 99% <sup>a</sup>	( <i>R</i> ) <i>ee</i> > 99% <sup>a</sup>	( <i>R</i> ) <i>ee</i> 81% <sup>a</sup>	( <i>R</i> ) <i>ee</i> > 15% <sup>a</sup>	( <i>S</i> ) <i>ee</i> > 99% <sup>a</sup>	( <i>R</i> ) <i>ee</i> > 99% <sup>a,b</sup>	( <i>R</i> ) <i>ee</i> > 75% <sup>a</sup>	( <i>R</i> ) <i>ee</i> > 74% <sup>a</sup>
	( <i>R</i> )-12	<i>anti</i> -(1 <i>R</i> ,2 <i>S</i> ) <i>de</i> > 99% <sup>a</sup>	<i>anti</i> -(1 <i>R</i> ,2 <i>S</i> ) <i>de</i> > 99% <sup>a</sup>	<i>anti</i> -(1 <i>R</i> ,2 <i>S</i> ) <i>de</i> > 99% <sup>a</sup>	<i>anti</i> -(1 <i>R</i> ,2 <i>S</i> ) <i>de</i> > 99% <sup>a</sup>	<i>syn</i> -(1 <i>R</i> ,2 <i>R</i> ) <i>de</i> 89% <sup>a</sup>	<i>anti</i> -(1 <i>R</i> ,2 <i>S</i> ) <i>de</i> > 99% <sup>a,b</sup>	<i>anti</i> -(1 <i>R</i> ,2 <i>S</i> ) <i>de</i> > 99% <sup>a</sup>	<i>anti</i> -(1 <i>R</i> ,2 <i>S</i> ) <i>de</i> > 99% <sup>a</sup>
	( <i>R</i> )-28	n.d.	n.d.	n.d.	n.d.	n.d.	<i>syn</i> -(1 <i>R</i> ,2 <i>R</i> ) <i>de</i> > 99% <sup>a,b,c</sup>	n.d.	n.d.
	( <i>S</i> )-28	n.d.	n.d.	n.d.	n.d.	n.d.	<i>anti</i> -(1 <i>R</i> ,2 <i>S</i> ) <i>de</i> 87% <sup>b,c</sup>	n.d.	n.d.

*ee* – enantiomeric excess, *de* – diastereomeric excess, *dr* – diastereomeric ratio, n.d. – not determined, <sup>a</sup> – employing crude cell extract with overexpressed ADH, <sup>b</sup> – employing purified RADH, <sup>c</sup> – *de* determined by <sup>1</sup>H NMR measurement, <sup>d</sup> – absolute configuration confirmed by VCD studies



**Figure 20.** Syntheses of chiral diols using enzymatic toolboxes: ThDP-dependent enzymes (centre) for carbonylation of aldehydes to  $\alpha$ -hydroxy ketones (white ring), and subsequent reduction to 1,2-diols using different oxidoreductases (blue ring).  $R^1$  = phenyl,  $R^2$  = methyl, PDC = pyruvate decarboxylase, BFD = benzoylformate decarboxylase, BAL = benzaldehyde lyase, KdcA =  $\alpha$ -keto acid decarboxylase, ADHT = *Thermoanaerobacter* sp. alcohol dehydrogenase, CPCR = *Candida parapsilosis* carbonyl reductase, FADH = *Flavobacterium frigidimaris* alcohol dehydrogenase, HLADH = horse liver alcohol dehydrogenase, LBADH = *Lactobacillus brevis* alcohol dehydrogenase, RADH = *Ralstonia* sp. alcohol dehydrogenase, SADH = *Sphingobium yanoikuyae* alcohol dehydrogenase, TADH = *Thermus* sp. ATN1 alcohol dehydrogenase.

Depending on the combination of the enzymes all four stereoisomers of 1-phenylpropane-1,2-diol could be obtained (Table 8). All of these reductions were catalysed with very high stereoselectivity ( $ee > 99\%$ ,  $de > 99\%$ ). It has to be mentioned that during reduction of the keto function, the chiral information of the hydroxy function is maintained. Therefore no loss of stereoselectivity of the educt was observed under the tested conditions.

Conclusively the 2-step enzymatic approach for the synthesis of 1,2-diols from inexpensive aldehydes is a useful and competitive method to gain highly valuable chiral precursors (see Table 8), what is not the case with chemical methods. Furthermore, it eliminates toxic catalysts, which are implemented in the chemical syntheses of these compounds (e.g.  $OsO_4$ ,  $NaBH_4$ ,  $LiAlH_4$ ) (see chapter 1.11.1). Therefore the biocatalytic synthetic cascade approach of 1,2-diols is much “greener”.

The stereoselective 2-step enzymatic synthesis allows building up a platform of diversely substituted 1,2-diols by the combination of two enzymatic toolboxes. Depending on the combination of ThDP-dependent enzyme and oxidoreductase the selective production of one stereoisomer out of a number of theoretically possible products is now achievable (Figure 20) due to the high chemo- and stereoselectivity of each enzyme.

### 3.4 Biochemical characterisation of ADH from *Ralstonia* sp.

In the group of Kroutil the alcohol dehydrogenase from *Ralstonia* sp. (RADH) was found to be an excellent catalyst for the reduction of sterically hindered compounds (e.g. ketones) (Lavandera et al. 2008a; Lavandera et al. 2008c). They investigated the great potential towards large aromatic substrates with crude cell extract from lyophilised *E. coli*-cells, but never tested activity towards  $\alpha$ -hydroxy ketones.

Initial screening of the RADHs substrate scope described in Publication I shows the high potential of alcohol dehydrogenases, especially from *Ralstonia* sp., for the reduction of the prochiral carbonyl group of  $\alpha$ -hydroxy ketones. Motivated by these results RADH was biochemically characterised in detail.

#### 3.4.1 Purification and storage stability

The *radh* gene was gratefully obtained from Prof. Dr. W. Kroutil (University of Graz, Austria) and cloned into the high copy plasmid (pET-22b). *E. coli* BL21(DE3) was transformed with this vector, cultivated and RADH was overexpressed after induction (Publication I).

*E. coli* cells containing overexpressed RADH were disrupted and purification of the enzyme was carried out in three chromatographic steps encompassing a preliminary desalting of the crude cell extract by size exclusion chromatography (SEC) (1<sup>st</sup> step), anion exchange chromatography (2<sup>nd</sup> step), and a final desalting step of the purified enzyme (3<sup>rd</sup> step) using SEC in order to remove salt from the second purification step (see Publication II). RADH was obtained with purity of about 90% according to SDS-PAGE electrophoresis.

The isolated enzyme can be stored at  $-20\text{ }^{\circ}\text{C}$  without any loss of activity over 80 days as (I) a frozen protein stock solution in desalting buffer (TEA-HCl, 10 mM, pH 7.5) or (II) a glycerine stock (50 vol%) in desalting buffer (TEA-HCl, 10 mM, pH 7.5) (Publication II). Lyophilisation of the enzyme can be also used to concentrate the liquid protein. The lyophilised protein is stable for at least 20 days

stored at  $-20\text{ }^{\circ}\text{C}$ , but requires a relatively long reactivation time after re-dissolving the lyophilised protein in buffer (Publication II).

### 3.4.2 Effect of salts

Purification of RADH gave first insights into the enzyme stability. The purified enzyme was relatively unstable at room temperature (half-life:  $\sim 6$  hours), which initiated further studies concerning essential metal-ions or other additives that might be crucial for enzyme stability.

The stability issue of ADHs is known from a number of examples, where enzyme stability and/or activity are improved in the presence of metal ions. Metal ions in the active centre of alcohol dehydrogenases may act as catalytic ions. Besides, metal ions can have a structural function, which is known for several alcohol dehydrogenases for example from horse liver (HLADH) or *Lactobacillus brevis* (LBADH). HLADH and LBADH lose their activity and stability in the absence of zinc and magnesium ions, respectively (Maret et al. 1979; Niefind et al. 2003; Niefind et al. 2000).

Examination of the influence of different metal chlorides on the activity of RADH revealed no activators under initial rate conditions. However, several metal ions displayed inhibitory effects. Among them were cobalt-, copper-, zinc-, manganese and nickel chloride with zinc chloride having the strongest impact (reduction to 39% of initial rate activity). Copper- and manganese chloride reduced the initial activity rate to 75%, whereas the activity in the presence of cobalt- and nickel chloride dropped moderately to 85-86% (Publication II).

Other tested chlorides ( $\text{CaCl}_2$ , KCl, NaCl and  $\text{MgCl}_2$ ) did not affect the enzyme activity and therefore were investigated as potential enzyme stabilisers. The time-dependent activity measurements of RADH in the presence of these salts (1 mM) resulted in the finding that the enzyme is stabilised by  $\text{Ca}^{2+}$  ions. After 2 hours RADH retained 97.8% of the initial activity in comparison to the buffer control (without any metal chlorides) where only 79.6% of initial activity was retained (Publication II). Up to now only one pyrroloquinoline quinone (PQQ)-dependent alcohol dehydrogenase was found as an enzyme, which is stabilised and activated by  $\text{Ca}^{2+}$  ions (Zhao et al. 2000).

Unfortunately,  $\text{Ca}^{2+}$  ions could not be detected in the crystal structure of RADH (Publication IV). Thus, the role of  $\text{Ca}^{2+}$  for enzyme stability remains unclear.

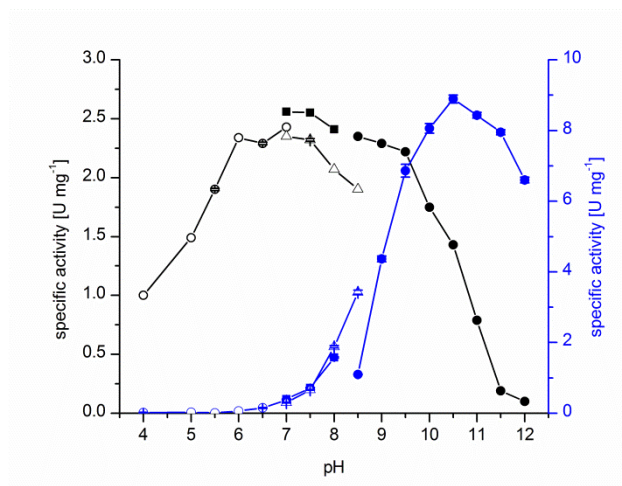
### 3.4.3 Determination of the native molecular weight of RADH

According to the calculated molecular weight of the RADH (ExPASy) based on the amino acid sequence, a single subunit of the enzyme has a molecular weight of 26.7 kDa. The estimated molecular weight of RADH by size exclusion chromatography (SEC) is 75 kDa, suggesting a trimeric structure of RADH. Trimeric enzymes are not common in nature. Up to now only several formaldehyde dehydrogenases were reported as trimeric enzymes (Eggeling and Sahm 1985; van Ophem et al. 1992). To the best of my knowledge, this would be the first trimeric NADPH-dependent alcohol dehydrogenase stabilised by  $\text{Ca}^{2+}$  ions.

Finally the crystal structure of the enzyme demonstrated a tetrameric structure of the enzyme. The structure seems to be more or less globular, so the results obtained with SEC could not be explained by structural analysis (Publication IV).

### 3.4.4 pH- and temperature optima

RADH indicates a broad pH-optimum for reduction (pH 6.0-9.5) and a sharp optimum for oxidation (pH 10.0-11.5) (Figure 21).



**Figure 21.** pH optima for the reduction of benzaldehyde (black) and the oxidation of cyclohexanone (blue), respectively. Symbols: ○ – citrate-phosphate buffer (50 mM +  $\text{CaCl}_2$ , 0.8 mM, pH 5-7), ■ – TEA-HCl buffer (50 mM +  $\text{CaCl}_2$ , 0.8 mM, pH 7-8), △ – TRIS-HCl buffer (50 mM +  $\text{CaCl}_2$ , 0.8 mM, pH 7-8.5), ● – glycine-NaOH buffer (50 mM +  $\text{CaCl}_2$ , 0.8 mM, pH 8.5-12) (Publication II).

Furthermore, pH-dependent stability investigation proved the enzyme to be stable (half-lives: 60-70 h, 25 °C) in a pH range from 5.5 to 8.0, thus including the pH range, where reduction is favoured.

According to the obtained results, application of RADH for oxidation and/or reduction requires careful selection of the pH value, under which either reduction

or oxidation, or both are catalysed simultaneously (e.g. if enzymatic cofactor regeneration is implemented, see chapter 3.6.1.1).

The temperature optimum of RADH showed highest initial rate activity at 45 °C. In contrast, highest stability was found between 8-15 °C (half-life: ~130 h).

In order to implement RADH for biocatalysis, a compromise of high enzyme activity and stability has to be found to achieve highest enzyme performance. In order to allow substrate-coupled cofactor regeneration a pH range between pH 8 and pH 9 should be chosen to gain high enzyme activity for reduction and oxidation step, and reasonable stability for the reaction time as well.

Conclusively, the pH- and temperature-dependent activity and stability profile of RADH allows the application of the enzyme under mild reaction conditions.

#### 3.4.5 Substrate range for oxidation and reduction

The extended biochemical characterisation of RADH revealed its high potential for reductions of the prochiral keto group of  $\alpha$ -hydroxy ketones (Publication I). It has to be pointed out that kinetic parameters for oxidation and reduction of the majority of investigated compounds were not determined and therefore activities cannot be compared in terms of maximal velocities. Maximal velocities can vary significantly at different substrate concentrations due to the respective  $K_M$ -values or potential substrate sur-plus inhibition.

Nevertheless, from investigation of the substrate range of RADH it became obvious that the enzyme reduces aldehydes (up to 23.3 U mg<sup>-1</sup>), ketones (up to 12.6 U mg<sup>-1</sup>) (Publication II) and especially  $\alpha$ -hydroxy ketones (up to 362 U mg<sup>-1</sup>) with high velocities (Publication I). Under these conditions (pH 7.5), oxidation is less favoured. Here maximal rates were obtained for the cyclohexanol oxidation (up to 18.8 U mg<sup>-1</sup>) (Publication II). Investigation of the substrate scope demonstrated that RADH accepts cyclic and aromatic compounds best, especially  $\alpha$ -hydroxy ketones like 2-HPP derivatives, where the pro-chiral keto group is located next to a methyl group (for details see Publication I and II).

#### 3.4.6 Steady-state kinetic parameters

In order to find optimal conditions for multi-enzymatic synthetic cascade reaction, it is not only important to determine appropriate substrate concentrations for maximal reaction velocities, but also the concentrations of cofactor have to be properly adjusted. In addition, determination of kinetic parameters allows

appropriate process design in order to avoid potential limitations by substrate, cofactor, and product inhibitions.

Since the aim of this work is a 2-step enzymatic synthesis combining a carboligation and a oxidoreduction step, all for this process relevant kinetic data are summarised in Table 9. It must be noted that kinetic studies with acetaldehyde are missing due to the impossibility to determine acetaldehyde precisely by instrumental analysis.

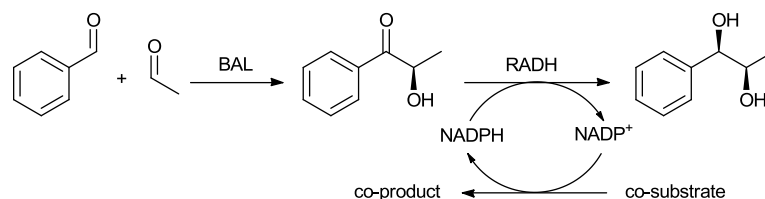
**Table 9.** Selected kinetic parameters of RADH relevant for the synthetic enzymatic 2-step cascade reaction towards 1,2-diols starting from benzaldehyde and acetaldehyde (Publication II).

Entry	Substrate [mM]	Cofactor [mM]	$V_{\max}$ [U mg <sup>-1</sup> ]	$K_M$ [mM]	$K_i$ [mM]	$S_{\text{opt}}$ [mM]	$V_{\text{opt}}$ [U mg <sup>-1</sup> ]
1	Benzyl alcohol [0–150]	NADP <sup>+</sup> [0.8]	0.3±0.0	12.3±2.7	–	–	–
2	Benzaldehyde [15]	NADPH [0–0.2]	5.6±0.1	0.005±0.000	–	–	–
3	Benzaldehyde [0–50]	NADPH [0.2]	12.6±0.3	15.6±0.9	–	–	–
4	( <i>R</i> )-2-HPP [0–15]	NADPH [0.2]	486.8±52.2	1.6±0.4	16.4	5.1	299.6±32.1
5	( <i>S</i> )-2-HPP [0–20]	NADPH [0.2]	23.1±0.4	3.6±0.2	–	–	–

Kinetic parameters determined for the reduction of (*R*)- and (*S*)-2-HPP revealed a significant difference of maximal velocities and affinities of RADH for these compounds (Publication II). Initial rate activities for the reduction of (*R*)-2-HPP (10 mM) showed extremely high activity of 362.6±1.6 U mg<sup>-1</sup>, whereas the opposite enantiomer, (*S*)-2-HPP (10 mM) was reduced 21-fold slower (17.1±0.3 U mg<sup>-1</sup>) (see Table 4, Publication I). Kinetic data go in line with previous studies of the substrate range (Table 7). However, the high calculated specific activity of 486.8±52.3 U mg<sup>-1</sup> for (*R*)-2-HPP cannot be reached because of substrate surplus inhibition, and therefore  $V_{\text{opt}}$  for the reduction was determined as 299.6±32.1 U mg<sup>-1</sup>. In contrast to (*R*)-2-HPP, the (*S*)-enantiomer did not show surplus inhibition. Further investigations showed no product inhibition (up to > 85 mM of (1*R*,2*R*)-diol) in case of (*R*)-2-HPP (data not shown). Furthermore, kinetic studies indicated differences of the enzyme affinity towards (*R*)- and (*S*)-2-HPP, where for the (*R*)-enantiomer the  $K_M$ -value is 2.2-fold lower than for the opposite enantiomer (Table 9).

Additionally, the data in Table 9 clearly demonstrate that RADH prefers (*R*)-2-HPP over benzaldehyde with respect to maximal velocity, where the velocity for benzaldehyde was found to be 23.8-fold lower compared to (*R*)-2-HPP. This goes in line with a 10-fold lower affinity for benzaldehyde compared to (*R*)-2-HPP, as can be deduced from the  $K_M$ -values. Due to these differences in kinetic parameters

RADH the enzyme can principally be applied in one pot together with substrates for the carboligation step (Figure 22).

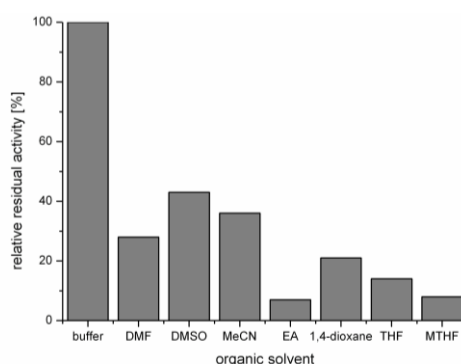


**Figure 22.** 2-Step enzymatic synthesis of chiral (1*R*,2*R*)-1-phenylpropane-1,2-diol by combining a carboligation step catalysed by the ThDP-dependent enzyme BAL and a oxidoreduction step catalysed by RADH including a cofactor regeneration system.

Determination of kinetic parameters underlines the high catalytic potential of RADH, especially for the reduction of  $\alpha$ -hydroxy ketones (Publication I and II). These studies show the high significance of efficient reaction engineering and adjustment of proper reaction parameters.

#### 3.4.7 Activity in organic solvents

One key drawback of biocatalysis for industrial applications is solubility limitation of organic substrates in aqueous media. This can be circumvented by implementation of organic solvents for enzyme-catalysed syntheses.



**Figure 23.** Influence of water-miscible organic solvents (5 vol%) on the initial rate activity of RADH. Initial rate activity was measured towards benzaldehyde (10 mM) reduction following the consumption of NADPH (0.2 mM) at 340 nm at 30 °C in TEA-HCl buffer (50 mM), pH 7.5 supplemented with 5 vol% of the respective organic solvent. DMF = dimethylformamide, DMSO = dimethyl sulfoxide, MeCN = acetonitrile, EA = ethyl acetate, THF = tetrahydrofuran, MTHF = 2-methyltetrahydrofuran. A relative activity of 100% corresponds to 3.4 U mg<sup>-1</sup> measured for the reduction of benzaldehyde under standard conditions.



But since organic solvents can influence enzyme activity negatively, the influence of various water-miscible organic solvents on the initial rate activity of RADH was studied. The results demonstrated that RADH lost activity in the presence of all tested organic solvents. Almost complete depletion of initial rate activity of RADH for the reduction of benzaldehyde is caused by ethyl acetate (7% residual activity), 2-methyltetrahydrofuran (8% residual activity), tetrahydrofuran (14% residual activity) and 1,4-dioxane (21% residual activity). DMSO, acetonitrile and DMF reduce activity also significantly, yielding residual activities of 28-43% (Figure 23).

The results indicate the limitation of water-miscible organic solvent addition in RADH catalysed syntheses in buffered systems.

### 3.5 Preparations to crystallise RADH

In order to allow crystallisation of RADH (Publication IV) the coding gene had to be cloned into a vector that allows expression of a hexahistidine-tagged enzyme for optimal purification. Further, an appropriate purification protocol had to be developed.

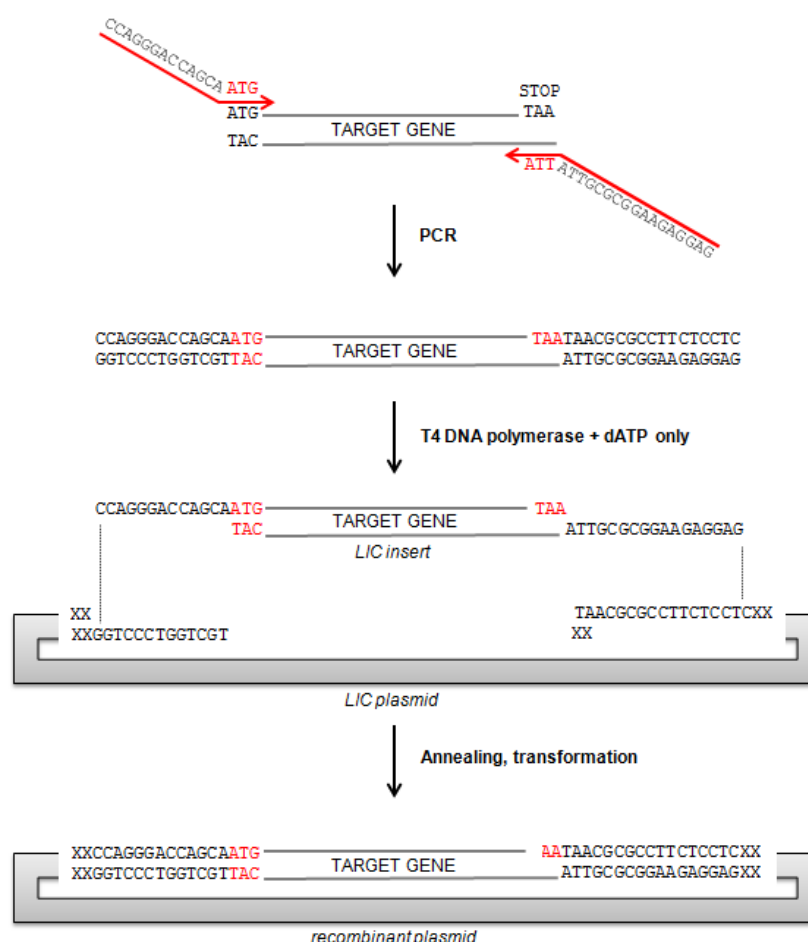
#### 3.5.1 Cloning RADH into a vector with cleavable tag

In order to gain highly pure RADH for crystallisation a cleavable His-tag was introduced into the enzyme sequence. This N-terminal His<sub>6</sub>-tag could be cleaved off by a protease (HRV 3C), if crystallisation with His-tag fails.

Cloning of the *radh* gene was conducted using a ligation independent cloning (LIC-cloning) method (Figure 24). LIC-cloning is a form of molecular cloning that is conducted without the use of restriction endonucleases or DNA ligases. This cloning strategy reduces the risk of cleavage of the insert by the restriction enzymes.

#### 3.5.2 Expression and purification of His-RADH

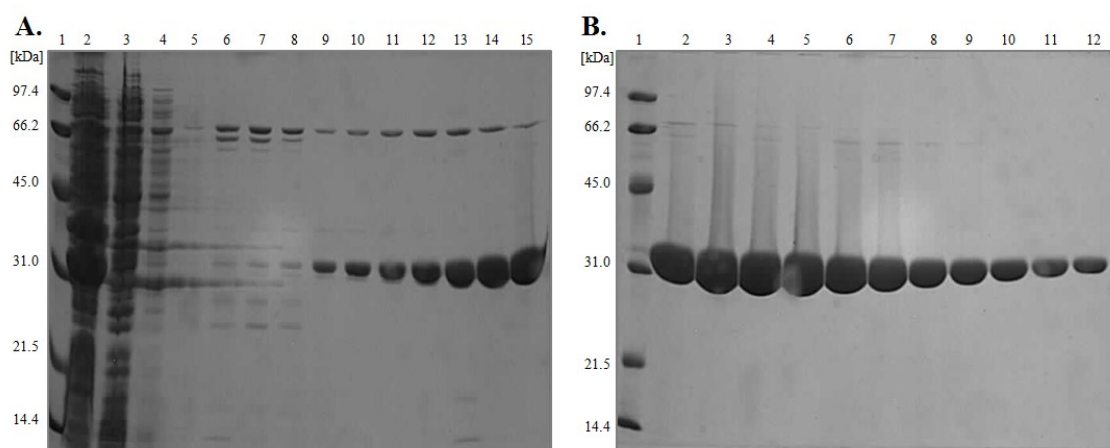
The obtained fusion protein (His-RADH) was very good expressed in the *E. coli* T7 expression system as a soluble protein (induction with 1 mM IPTG final concentration, overnight overexpression at 16 °C) (Figure 25).



**Figure 24.** Principles of ligation independent cloning (LIC-cloning) of PCR products. For cloning LIC-based primers (FOR and REV primers) are implemented, which consist of vector- and desired gene-based sequences. For this purpose vector pET-YSBLIC3C containing an N-terminal cleavable His<sub>6</sub>-tag was implemented (Fogg and Wilkinson 2008). The vector is based on pET-28a (Kan<sup>R</sup>), where the thrombin cleavage site was changed to a HRV 3C protease (3C protease human rhinovirus type 14) site. HRV 3C protease cleaves the sequence: LEVLFQ/GP. After cleavage three additional N-terminal amino acids (GPA) remain. The LIC site is introduced between the *Nco*I and *Nde*I restriction cleavage sites in the modified pET-28a vector. In the multiple cloning site all pET-28a restriction sites are intact.

His-RADH was subsequently purified in three chromatographic steps encompassing immobilised metal affinity chromatography (IMAC) and two desalting steps (for more details see Protocol, Appendix, paragraph 4.9). Set-up of the purification protocol revealed solubility limitations caused by the N-terminal His-tag. As His-RADH strongly binds to the chromatography matrix, elution required high concentrations of imidazole (up to 300 mM). For elution a flat imidazole gradient was used (50-300 mM imidazole, 20 column volumes (=100 mL), flow rate: 1 mL min<sup>-1</sup>, 100 min), since a step gradient causes rapid protein precipitation already on the Ni-NTA column. The solubility problem of the fusion protein on the Ni-NTA column was solved by several factors. Convenient purification without enzyme precipitation could finally be achieved when glycerol

(10 vol%) and NaCl (500 mM) were added to every purification step (see Appendix, paragraph 4.9). Furthermore, imidazole should not be removed by SEC after IMAC; dialysis gives much better results (see Appendix, paragraph 4.9). In order to keep the enzyme in soluble form for crystallisation trials the purified fusion protein should be stored in the following storage buffer: TRIS-HCl (50 mM) supplemented with  $\text{CaCl}_2$  (1 mM), glycerol (10 vol%) and NaCl (500 mM).



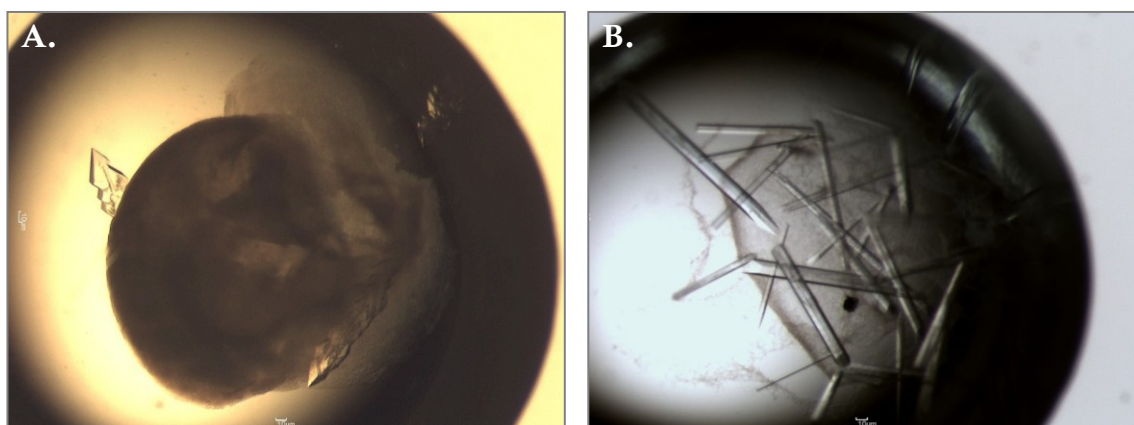
**Figure 25.** SDS-PAGE electrophoresis of His-RADH purification employing immobilised metal ion affinity chromatography (IMAC). **A:** Lane: 1 – protein ladder, low range (Bio-Rad), 2 – crude cell extract, 3 – flow through, 4 – wash 1, 5 – wash 2, 6 – fraction B10, 7 – fraction B8, 8 – fraction B6, 9 – fraction C5, 10 – fraction C7, 11 – fraction C9, 12 – fraction C11, 13 – fraction D12, 14 – fraction D10, 15 – fraction D8. **B:** Lane: 1 – protein ladder, low range (Bio-Rad), 2 – fraction D6, 3 – fraction D4, 4 – fraction D2, 5 – fraction E1, 6 – fraction E3, 7 – fraction E5, 8 – fraction E7, 9 – fraction E9, 10 – fraction E11, 11 – fraction F12, 12 – fraction F10. Collected fractions – 2 mL each.

Further investigation of solubility limitation of His-RADH showed that the enzyme starts to precipitate at concentrations  $> 5 \text{ mg mL}^{-1}$  (spectrophotometric measurement of protein concentration at 280 nm, measurement based on Eppendorf Biophotometer) in storage buffer.

Besides these solubility issues, the enzyme was obtained with very high purity ( $> 99\%$ ) according to SDS-PAGE electrophoresis (Figure 25).

### 3.5.3 Crystallisation and structure analysis of RADH

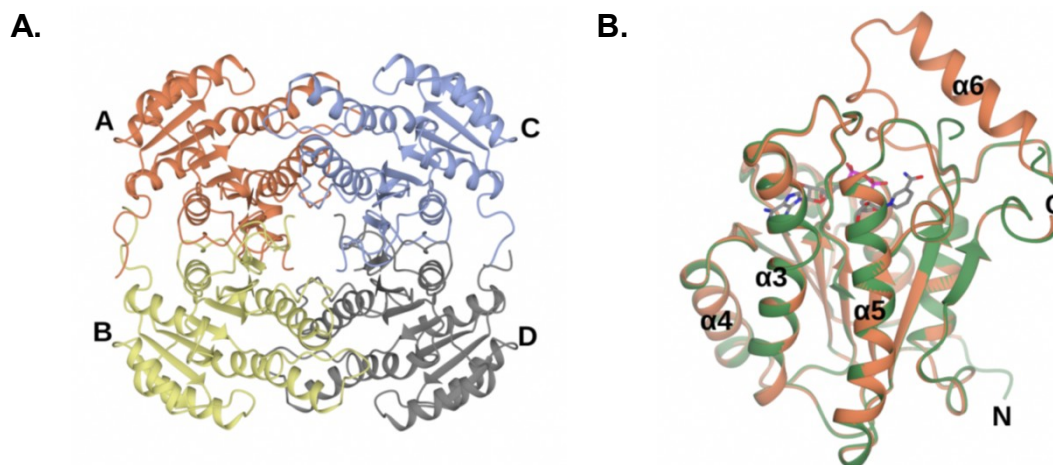
Subsequently, appropriate crystallisation conditions for His-RADH were investigated. There were a number of conditions, under which rod crystals occurred. Some examples are presented in Figure 26.



**Figure 26.** His-RADH crystals. Shown crystals were obtained under following conditions: *apo*-RADH: 0.1 M Bis-TRIS propane, pH 7.0 containing 20% (w/v) PEG 3350 and 0.02 M sodium-potassium phosphate; *holo*-RADH: 0.1 M Bis-TRIS propane, pH 8.0 containing 16% (w/v) PEG 3350, 0.2 M KSCN and 5% (w/v) ethylene glycol. For crystallisation 24 mg mL<sup>-1</sup> of purified His-RADH was used.

The crystal structure of RADH with NADPH (*holo*-RADH) and without cofactor (*apo*-RADH) was solved to a resolution of 1.5 Å and 2.9 Å, respectively.

The structure of RADH was solved by molecular replacement employing a monomer of a “probable dehydrogenase protein” from *Rhizobium etli* CFN42 (55% sequence identity with RADH; pdb code: 4FGS) as a model. Structure analysis revealed the presence of four monomers A-D (Figure 27A) in the asymmetric unit, which form a tetramer (Publication IV).



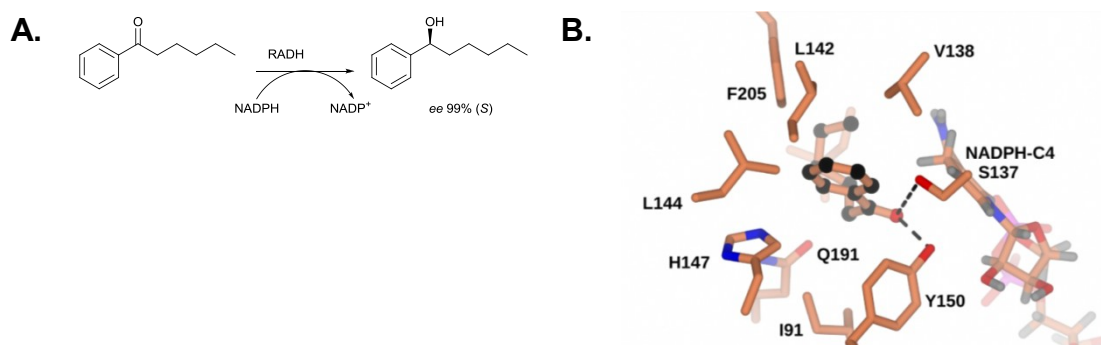
**Figure 27.** Structure of RADH. **A.** The asymmetric unit of the *apo*-enzyme contains four monomers (A-D) that constitute one tetramer. **B.** Monomer of *apo*-RADH (green ribbon) superimposed with *holo*-RADH (coral ribbon). The monomer shows the typical Rossmann fold, with a central  $\beta$ -sheet surrounded by six helices. Helix  $\alpha 6$  which was absent in the *apo*-RADH appears in *holo*-RADH and acts as a lid to the active site closing molecule over the NADPH, when cofactor is bound (Publication IV).

Comparative structural analysis of *apo*-RADH and *holo*-RADH indicated that most of the electron density of the  $\alpha 6$  helix was missing in the *apo*-RADH while the helix

was present in *holo*-RADH. This observation suggests that the helix appears upon NADPH-binding and acts as a lid for the active site, closing over the cofactor in the *holo*-form of the enzyme.

The enzyme has a large hydrophobic active site tunnel, which is formed at the top of the central  $\beta$ -sheet of the Rossmann fold and is partially covered by the  $\alpha_6$  helix in the *holo*-enzyme (Figure 27B). The Rossmann fold is a common structural motif found in proteins that bind nucleotides, e.g. cofactors. The fold consist of two repeats forming a  $\beta$ - $\alpha$ - $\beta$ - $\alpha$ - $\beta$  motif (Rossmann et al. 1974).

The strong preference of NADPH over NADH is controlled by interactions of two arginine residues (Arg38 and Arg39) and one residue of asparagine (Asn15) with the phosphate group in NADPH.



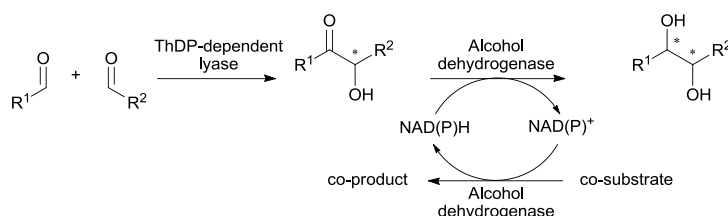
**Figure 28.** **A.** Reduction of *n*-pentyl phenyl ketone to the respective (*S*)-alcohol using RADH. **B.** *n*-Pentyl phenyl ketone modelled into the active site of RADH using the programme AUTODOCK VINA (Trott et al. 2010). Carbon atoms of RADH side chains are shown in coral; *n*-pentyl phenyl ketone is presented in ball-and-stick format with the carbon atoms in black.

The model presented in Figure 28 suggests that flexible side chain of *n*-pentyl phenyl ketone can fit in the region of hydrophobic tunnel through contortion in the enzyme. Less flexible substituents, such as aromatic rings would not be accommodated. This goes in line with substrate specificity studies, which clearly demonstrated that compounds such as benzoin or  $\alpha$ -pyridoin are poor substrates for RADH (see Table 7).

The 3D structure of RADH provides the structural explanation for the recognition of bulky-bulky ketones in a hydrophobic tunnel near the surface of the enzyme. It will further be beneficial to identify crucial amino acids in the active site for stereoselectivity and for the acceptance of sterically hindered substrates. Subsequently, rational engineering or randomised mutagenesis of target residues may improve or alter the enzyme's specificity.

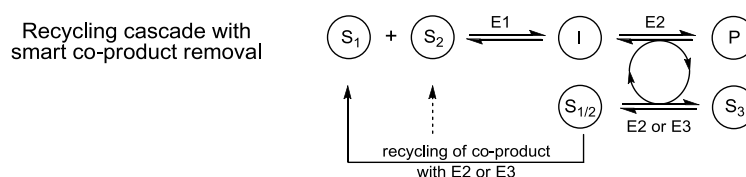
### 3.6 Reaction engineering

Since the ADHs employed in this work for the further reduction of  $\alpha$ -hydroxy ketones require NAD(P)H in stoichiometric concentration, there is a necessity to develop suitable cofactor regeneration systems (see chapter 1.7), which can be conducted either substrate-coupled (see chapter 1.7.1) or enzyme-coupled approach (see chapter 1.7.2). Both of these approaches require the application of an additionally co-substrate, which is oxidised to the co-product in stoichiometric amounts to the product of interest (Figure 29). In order to shift the potential reaction equilibrium to the desired product and to avoid unwanted side effects caused by the accumulation of the co-product, it is beneficial to remove the co-product during the course of the reaction.



**Figure 29.** 2-Step enzymatic synthesis of chiral 1,2-diols combining carbonylation and oxidoreduction with cofactor regeneration.

In frame of this work a modified approach of cofactor regeneration was developed, where by smart choice of the co-substrate for the cofactor recycling process the formed co-product is *in situ* removed by its reuse as a substrate for the carbonylation step (Figure 30).



**Figure 30.** Novel recycling cascade reaction with smart *in situ* cofactor regeneration and co-product recycling. Abbreviations: S = substrate, I = intermediate, P = product, E = enzyme (Publication III).

#### 3.6.1 Optimisation of the cofactor regeneration system

In this work the enzymatic approach of cofactor regeneration (substrate- and enzyme-coupled cofactor regeneration) was comparatively tested.

### 3.6.1.1 Substrate-coupled approach

The substrate-coupled approach of cofactor regeneration is also called “*biocatalytic hydrogen transfer*”. For later implementation in the enzyme cascade two co-substrates, ethanol and benzyl alcohol, were tested as hydrogen donors for bioreductions catalysed by RADH. The co-substrates for cofactor regeneration were chosen such that the respective co-product could subsequently be reused in the first carboligation step of the synthetic enzyme cascade. This was done to increase atom- and therewith process economy and to reduce waste production.

Lavandera *et al.* (Lavandera et al. 2008c) showed that implementation of ethanol (10 vol%) for cofactor regeneration at pH 7.5 was suitable for the reduction of cyclohexyl(phenyl)methanone. It should be noted that these authors applied lyophilised cells containing overexpressed RADH for the reduction (Lavandera et al. 2008c). In contrast own cofactor regeneration studies were performed with purified RADH.

This study revealed that ethanol (20-5000 mM) is not a good co-substrate for the reduction of *rac*-2-HPP (10 mM) using isolated RADH since conversions of only 3% could be achieved. This result suggests that one or more further alcohol dehydrogenases present in the host *Escherichia coli* were probably responsible for cofactor regeneration using lyophilised crude cell extracts for the reduction of cyclohexyl(phenyl)methanone in the work of Lavandera *et al.* (Lavandera et al. 2008c).

Better results were obtained, when benzyl alcohol was employed as a co-substrate for cofactor regeneration. Here conversions up to 59% were achieved under not optimised conditions. Further optimisation of the enzyme concentration (0.05-0.30 mg mL<sup>-1</sup>) yielded conversions up to 98.5% (Publication III).

### 3.6.1.2 Enzyme-coupled approach

For the enzyme-coupled approach TBADH from *Thermoanaerobacter brockii* was tested, since this enzyme was already successfully used in lab- and industrial-scale (Bastos et al. 1999; Bastos et al. 2002; Röthig et al. 1990).

Oxidation of ethanol catalysed by TBADH gave more promising initial conversions (up to ~10%) than first substrate-coupled trials (up to 3%, see paragraph 3.6.1.1) under not optimised conditions. Further optimisation revealed conversions of 71% with 2 500 mM ethanol (Publication III).



### 3.6.2 Synthetic cascade reaction

Synthetic cascade reactions using enzymes have many advantages such as: elimination of dangerous and toxic catalysts, atom and energy economy, elimination of unnecessary derivatisation and last but not least reduction of waste production (see paragraph 1.12, Table 6). These benefits of enzymatic cascade reactions go in line with the 12 principles of *Green Chemistry* and the *PRODUCTIVELY* concept (see paragraph 1.1).

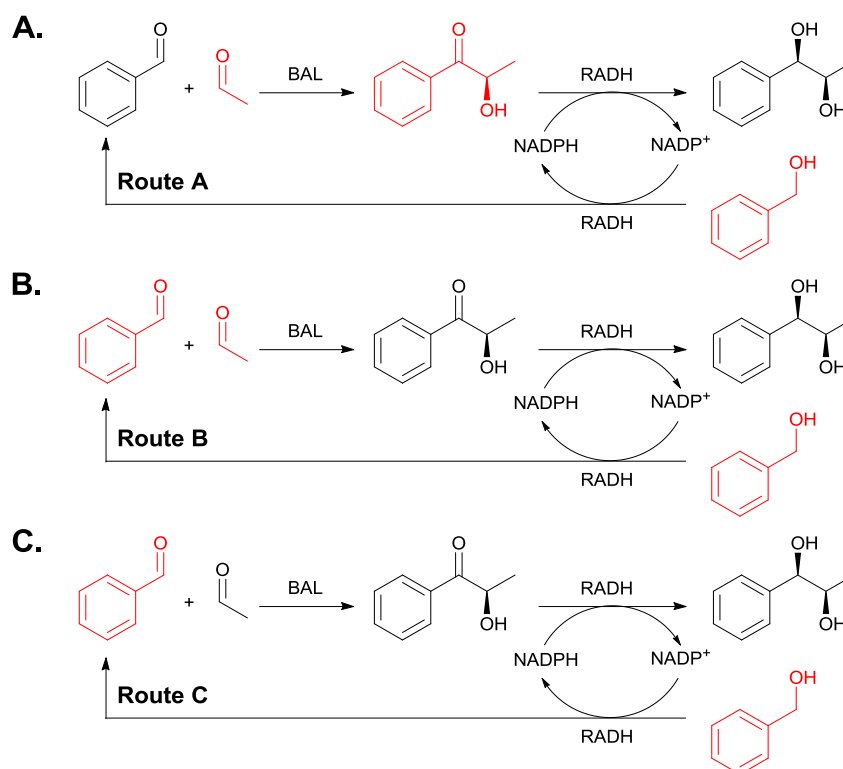
In this work a new cascade reaction was developed, encompassing carboligation and a subsequent reduction step with cofactor regeneration system in one pot (Figure 30). Furthermore, one of a key objective was the combination of cheap starting materials yielding the desired 1,2-diol with highest possible stereoselectivity and maximal conversion. Therefore, two cofactor regeneration systems (substrate- and enzyme-coupled approaches) were compared. The cascade was designed such that the by-product formed during cofactor regeneration was reused for the carboligation step. This approach ensured high atom and step economy.

#### 3.6.2.1 Cascade reaction using substrate-coupled cofactor regeneration

Three different routes for cascade reactions with substrate-coupled cofactor regeneration were investigated. They varied on the implemented starting compounds at the beginning of the cascade reaction (Figure 31):

- **ROUTE A:** where acetaldehyde (150 mM), benzyl alcohol (120 mM), and the intermediate (*R*)-2-HPP (10 mM) were applied for the production of respective 1,2-diol;
- **ROUTE B:** where benzaldehyde (10 mM), acetaldehyde (150 mM) and benzyl alcohol (120 mM) were applied;
- **ROUTE C:** where only benzyl alcohol (120 mM) and acetaldehyde (150 mM) were used to start the production of the chiral 1,2-diol. Thereby diol formation can only occur, if the cofactor regeneration system is effectively working, since benzaldehyde for carboligation has to be formed by oxidation of benzyl alcohol.





**Figure 31.** Process design for a synthetic cascade reactions using substrate-coupled cofactor regeneration. Substrates which are present in the reaction at time  $t=0$  are highlighted in red. BAL = *Pseudomonas fluorescens* benzaldehyde lyase, RADH = *Ralstonia* sp. alcohol dehydrogenase (adapted from Publication III, modified).

The first cascade reactions with substrate-coupled cofactor-regeneration under non-optimised reaction conditions (Table 10, entry 8) showed only low overall conversions of  $19.7 \pm 0.5\%$  and  $18.6 \pm 0.9\%$  for routes A and B, respectively. Thereby route A is a kind of control reaction, which gives an insight into the efficiency of the cofactor regeneration system. The overall conversion is defined as the conversion all aromatic compounds to the desired product ((1R,2R)-diol) which were applied to start the reaction. In case of route C, where only acetaldehyde and benzyl alcohol were added to start the reaction, an overall conversion of only  $11.8 \pm 0.2\%$  under not optimised conditions was achieved. However, if conversion is calculated based on the co-product  $\geq 98\%$  of the benzaldehyde produced by oxidation of benzyl alcohol was transformed into the product (Table 10, entry 5).

Optimisation of the pH-value, concentration of  $\text{NADP}^+$  and RADH increased the overall conversion up to 73% (route B, see Table 10, entry 13), when benzyl alcohol was applied for the production of benzaldehyde for the carboligation step. Here again the co-product was transformed almost completely (97.2%) into the diol (Publication III).

**Table 10.** Optimisation of the synthetic cascade reaction with the substrate-coupled approach. Depending on the mode of the cascade reaction, different initial concentrations of starting materials were applied: route A: acetaldehyde: 150 mM, (*R*)-2-HPP: 10 mM and benzyl alcohol: 120 mM; route B: acetaldehyde: 150 mM, benzaldehyde: 10 mM and benzyl alcohol: 120 mM; route C: acetaldehyde: 150 mM and benzyl alcohol: 120 mM; conv<sub>overall</sub> – overall conversion is defined as a conversion of all aromatic compounds (benzyl alcohol and benzaldehyde with (*R*)-2-HPP depending on the route) to the 1-phenylpropane-1,2-diol; conv<sub>BA</sub> – co-product conversion is defined as a conversion of benzaldehyde formed during oxidation of benzyl alcohol (Publication III).

Entry	Optimised parameter	Route	conv <sub>overall</sub> [%]	conv <sub>BA</sub> [%]	Distribution of stereoisomers [%] (1 <i>R</i> ,2 <i>R</i> ) : (1 <i>S</i> ,2 <i>R</i> ) : (1 <i>R</i> ,2 <i>S</i> ) : (1 <i>S</i> ,2 <i>S</i> )			
NADP <sup>+</sup> [mM]								
1	0.2	A	27.2±2.2	99.4±0.2	98	2	0	0
		B	21.5±0.2	99.1±0.1	98	2	0	0
		C	9.2±0.2	98.2±0.2	> 99	0	0	0
2	0.4	A	29.1±1.2	98.7±0.7	97	3	0	0
		B	26.8±1.6	94.2±6.7	97	3	0	0
		C	9.5±0.0	98.5±0.3	> 99	0	0	0
3	0.6	A	32.2±0.4	98.5±1.0	97	3	0	0
		B	23.4±1.0	99.0±0.0	98	2	0	0
		C	9.7±0.1	98.0±0.3	> 99	0	0	0
4	0.8	A	31.4±1.8	98.7±0.7	97	3	0	0
		B	27.7±1.8	98.4±1.0	97	3	0	0
		C	9.8±0.0	98.5±0.4	> 99	0	0	0
pH-value								
5	8.0	A	19.7±0.5	99.1±0.5	98	2	0	0
		B	18.6±0.9	99.1±0.4	98	2	0	0
		C	11.8±0.2	98.6±0.4	> 99	0	0	0
6	8.5	A	22.8±1.4	99.2±0.2	98	2	0	0
		B	26.5±3.5	98.8±0.0	98	2	0	0
		C	15.9±0.3	99.2±0.6	> 99	0	0	0
7	9.0	A	25.1±3.2	99.2±0.0	98	2	0	0
		B	24.3±2.9	99.1±0.1	99	1	0	0
		C	15.3±0.2	98.5±0.6	> 99	0	0	0
RADH concentration [mg mL <sup>-1</sup> ]								
8	0.10	A	19.7±0.5	99.1±0.5	98	2	0	0
		B	18.6±0.9	99.1±0.4	98	2	0	0
		C	11.8±0.2	98.6±0.4	> 99	0	0	0
9	0.24	A	27.2±1.3	99.1±0.1	99	1	0	0
		B	32.6±0.3	98.8±0.5	99	1	0	0
		C	29.5±1.3	98.5±0.6	99	1	0	0
10	0.33	A	42.7±3.7	98.6±0.7	98	2	0	0
		B	44.6±1.4	98.0±0.5	98	2	0	0
		C	36.1±3.6	97.9±0.1	99	1	1	0
11	0.65	A	56.5±1.0	98.5±0.3	95	3	2	0
		B	54.9±3.7	98.1±0.6	95	3	2	0
		C	48.8±5.8	98.1±0.1	95	3	2	0
12	2.00	A	68.3±3.0	98.6±0.1	97	2	1	0
		B	67.6±4.5	98.2±0.3	96	3	1	0
		C	68.0±2.1	98.6±0.5	96	2	2	0
13	3.75	B	73.4	97.2	90	8	2	0

Full conversion of the synthetic cascade reaction with substrate-coupled cofactor regeneration cannot be achieved, since benzyl alcohol always has to be present in a defined concentration for the oxidation reaction in order to enable cofactor regeneration. In the presence of high RADH concentrations (up to 3.75 mg mL<sup>-1</sup>) conversion of benzyl alcohol reached a maximum of 89.8% (t=0 h: c<sub>benzyl alcohol</sub>: 127 mM, t=45 h: c<sub>benzyl alcohol</sub>: 13 mM). Conversion is strongly restricted by the benzyl alcohol concentration in the batch reaction. The K<sub>M</sub>-value for the RADH-

catalysed oxidation of benzyl alcohol (at pH 9.0) was determined to be  $12.3 \pm 2.7$  mM (Publication II). When the concentration of benzyl alcohol in the reaction vessel dropped below a concentration of ca. 230 mM ( $V_{\max}$ ) the enzyme catalyses the oxidation of benzyl alcohol no longer with maximal activity. This is the reason, why the co-substrate has to be applied in excess.

This conclusively also means that the calculation of conversion to the desired 1,2-diol should be based on the amount of converted benzaldehyde (resulting from direct implementation of benzaldehyde and/or oxidation of benzyl alcohol to benzaldehyde) and not based on the sum of all aromatic substrates and products apparent in the vessel.

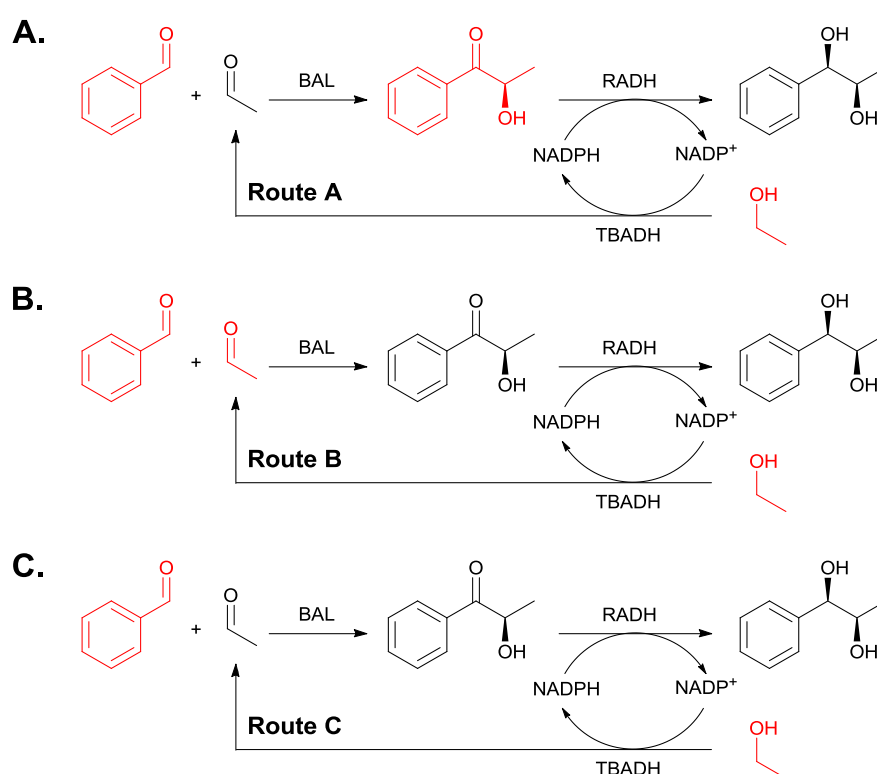
Further, the application of higher amounts of benzyl alcohol is limited by its solubility in aqueous media, which is  $\sim 47$  g L<sup>-1</sup> ( $\sim 435$  mM, at pH 9, 25 °C) (O'Neil 2006), albeit its additional organic compounds in buffer system will decrease the solubility further. It was observed that solubility problems occurred already with 250 mM benzyl alcohol, in the cascade reaction, leading in the formation of emulsions (visual observation). In the presence of very high enzyme concentrations ( $\geq 0.33$  mg mL<sup>-1</sup>), a drop of stereoselectivity of the catalysed reaction was observed. When the overall conversion of the cascade reaction was exceeding  $> 40\%$ , two another stereoisomers (1*S*,2*R*) and (1*R*,2*S*) of 1-phenylpropane-1,2-diol were formed. When 3.75 mg mL<sup>-1</sup> RADH was implemented, the following stereoisomers were detected: (1*R*,2*R*): 90.4%, (1*S*,2*R*): 7.8% and (1*R*,2*S*): 1.8%. The formation of the (1*S*,2*R*)-diol can be explained by a non-perfect stereoselectivity of RADH. Under the conditions tested the high concentration of the enzyme obviously results also in the (*S*)-selective reduction of (*R*)-2-HPP to a certain extend. The presence of the (1*R*,2*S*)-diol (1.8%) can most probably be explained by keto-enol tautomerism of the 1,2-diol at pH 9. The fourth possible stereoisomer, the (1*S*,2*S*)-diol, could not be detected in the course of the reaction.

One solution for the stereoselective production of only one stereoisomer of the 1,2-diol with substrate-coupled cofactor regeneration in the cascade reaction could be a fed-batch process, where benzyl alcohol is continuously fed enabling a constant concentration of benzyl alcohol during the reaction. Moreover, an appropriate enzyme concentration should be applied in order to produce only one stereoisomer of the desired product and to avoid the side reaction of "stereoinversion" or use of a 2-phase reaction system should be tried, since in organic solvent (methyl *tert*-butyl ether, MTBE) no formation of the other unwanted stereoisomers of the 1,2-diol were observed (discussion with Jochen Wachtmeister).

## 3.6.2.2 Cascade reaction using enzyme-coupled cofactor regeneration

As described for the substrate-coupled cofactor regenerations synthetic cascade reaction employing enzyme-coupled cofactor regeneration were conducted in three routes (Figure 32):

- **ROUTE A:** where, similarly to the cascade approach mentioned above, two substrates, benzaldehyde (10 mM) and ethanol (2500 mM), and the intermediate (*R*)-2-HPP (10 mM) were applied for the production of respective 1,2-diol;
- **ROUTE B:** where benzaldehyde (10 mM), acetaldehyde (100 mM), and ethanol (2500 mM) were applied;
- **ROUTE C:** where only two substrates, benzaldehyde (10 mM) and ethanol (2500 mM), were used for the production of chiral 1,2-diol. Thereby diol formation can only occur, if the cofactor regeneration system is working, since acetaldehyde for the carboligation step has to be formed by oxidation of ethanol.



**Figure 32.** Process strategies for a synthetic cascade reaction using enzyme-coupled cofactor regeneration. Substrates which are present in the reaction at time  $t=0$  are highlighted in red. BAL = *Pseudomonas fluorescens* benzaldehyde lyase, RADH = *Ralstonia* sp. alcohol dehydrogenase, TBADH = *Thermoanaerobacter brockii* alcohol dehydrogenase (adapted from Publication III, modified).

Synthetic cascade reactions using the enzyme-coupled approach for cofactor regeneration revealed very good overall conversions. Best overall conversions were obtained for route B, where 95% conversion was determined. Very good conversions were also obtained for route A (78%) and route C (69%). In all tested routes only the (1*R*,2*R*)-diol (Figure 20) was obtained (*de* > 99%).

### 3.6.2.3 Comparison of cascade reactions using the substrate- and enzyme coupled approach

As demonstrated above the studied synthetic cascade reactions with two types of cofactor regeneration systems showed differences in the overall conversions. Conclusively it depends very much on the set-up of the cascade, which regeneration system is to be favoured. In terms of economic efficiency, implementation of a third enzyme for the cascade should be circumvented, if possible, since enzyme costs (especially of purified enzymes) are one major cost factor of the reaction. However, if highest possible stereoselectivities are most important, the enzyme-coupled cofactor regeneration is the favoured mode for the studied reaction.

### 3.6.2.4 Further cascade reactions

Apart from the described reactions system, a synthetic enzyme cascaded using BFD from *Pseudomonas putida* in combination with the alcohol dehydrogenase from *Ralstonia* sp. (RADH) was additionally studied. In contrast to BAL, BFD catalyses the carboligation of benzaldehyde and acetaldehyde yielding (*S*)-2-HPP. Subsequent reduction by RADH should give access to the respective (1*R*,2*S*)-diol.

Preliminary results gave overall conversions of 13.5%. Nevertheless, similar initial results were obtained for the non-optimised reaction employing BAL and RADH. As was demonstrated in chapter 3.6.2.1 reaction engineering and mathematical modelling increased conversion (up to 73.4%). Therefore the BFD-RADH enzyme combination seems to be a good starting point for a future optimisation to obtain the (1*R*,2*S*)-diol.

## IV Conclusion and future perspectives

---

In this thesis the high potential of biocatalysis for the stereoselective synthesis of chiral vicinal diols was demonstrated.

Reduction of various  $\alpha$ -hydroxy ketones allowed the setup of a platform of diversely substituted and stereocomplementary vicinal diols. Investigation of the substrate scope of eight different alcohol dehydrogenases gave insight into the potential of  $\alpha$ -hydroxy ketones reduction catalysed by oxidoreductases and resulted in the investigation of one outstanding catalyst, the alcohol dehydrogenase from *Ralstonia* sp. (RADH).

Isolated for the first time and biochemically characterised, RADH confirmed its extremely high potential for bulky compounds, and its surprisingly high affinity for the reduction of  $\alpha$ -hydroxy ketones compared to aldehydes was confirmed by kinetic studies.

In collaboration with the University of York, crystallisation of RADH was performed in order to elucidate the enzyme structure and to understand its high preference for bulky substrates. The solved structure gives insight into the architecture of the enzymes active centre. It further opens the way for protein engineering in a rational manner in order to expand the substrate range of the enzyme for the reduction of e.g. benzoin-derivatives.

Moreover, synthetic enzyme cascade reactions for the stereoselective production of (1*R*,2*R*)-diols could be established, where atom- and step economy could be increased by implementation of an enzymatic cofactor regeneration system with smart *in situ* by-product recycling. Thus, by reaction engineering and modelling studies, optimised synthetic cascade reactions produced vicinal diols more sustainable than described so far. Due to the improvement, atom economy could be increased, waste production reduced and thus overall process economy increased.

The presented work was performed either by implementation of crude cell extracts containing overexpressed alcohol dehydrogenases or by the usage of purified enzyme in order to exclude potent side reactions. In order to make the process for

the production of chiral diols faster and therewith more efficient, investigation of catalyst implementation in form of whole cells are ongoing in a follow-up project. This would circumvent costs and time spending enzymes purification. Furthermore, increase of substrate load for the biotransformations by implementation of neat substrates or addition of organic co-solvents can increase space-time yields of the synthetic cascade reaction, if a system can be established, under which all enzymes are still active even under non-conventional reaction conditions.

## V Appendix

---



## 5.1. DNA sequence of RADH (without His-tag)

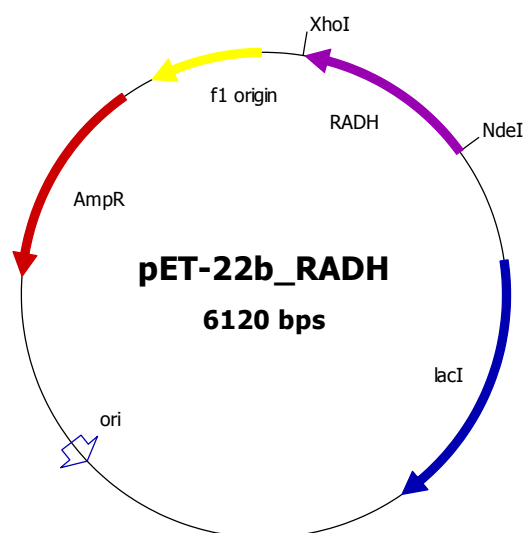
```

1  ATGTATCGTC TGCTGAATAA AACCGCAGTT ATTACCGGTG GTAATAGCGG TATTGGTCTG
61 GCAACCGCAA AACGTTTTGT TGCCGAAGGT GCCTATGTTT TTATTGTTGG TCGTCGTCGT
121 AAAGAACTGG AACAGGCAGC AGCAGAAATT GGTCTGTAATG TTACCGCAGT TAAAGCCGAT
181 GTTACCAAAC TGAAGATCTT GGATCGTCTG TATGCAATTG TTCGTGAACA GCGTGGTAGC
241 ATTGATGTTT TGTTCGAAA TAGCGGTGCC ATTGAACAGA AAACCCCTGA AGAAATTACA
301 CCGGAACATT ATGATCGCAC CTTTGATGTT AATGTGCGTG GTCTGATTTT TACCGTTCAG
361 AAAGCACTGC CGCTGCTGCG TGATGGTGGT AGCGTTATTC TGACCAGCAG CGTTGCCGGT
421 GTTCTGGGTC TGCAGGCACA TGATACCTAT AGCGCAGCAA AAGCAGCAGT TCGTAGCCTG
481 GCACGTACCT GGACCACCGA ACTGAAAGGT CGTAGCATTG GTGTTAATGC AGTTAGTCCG
541 GGTGCAATTG ATACCCCGAT TATTGAAAAT CAGGTTAGCA CCCAGGAAGA AGCAGACGAA
601 CTGCGCGCAA AATTTGCAGC AGCAACACCG CTGGGTCGTG TTGGTCGTCC GGAAGAACTG
661 GCAGCAGCCG TTCTGTTTCT GGCAAGTGAT GATAGCAGCT ATGTTGCAGG TATTGAACTG
721 TTTGTTGATG GTGGTCTGAC CCAGGTTTAA

```

ATG - start codon

TAA - stop codon



## 5.2. Protein sequence of RADH (without His-tag)

```

1  MYRLNKTAV ITGNSGIGL ATAKRFVAEG AYVFIVGRRR KELEQAAAEI GRNVTAVKAD
61 VTKLEDLDR LYAIVREQRGS IDVLFANSGA IEQKTL EEIT PEHYDR TFDV NVRGLIFTVQ
121 KALPLL RDG SVILTSSVAG VLGLQAHDTY SAAKAAVRS LARTWT TELKG RSIRVNAVSP
181 GAIDTPI ENQVSTQEEADE LRAKFAAATP LGRVGRPEEL AA AVLFLASD DSSYVAGIEL
241 FVDGGLTQV-

```

M - methionine

"-" - stop codon

### 5.3. Primers for RADH subcloning

RADH\_FOR:

**C CAG GGA CCA GCA** ATG TAT CGT CTG CTG AAT AAA ACC GCA GTT ATT ACC G

RADH\_REV:

**GA GGA GAA GGC GCG** TTA TTA AAC CTG GGT CAG ACC ACC ATC AAC AAA CAG

Bolded: standard LIC3C sequences

ATG - start codon

TAA - stop codons

not bolded: sequence of RADH

Universal LIC3C sequences for LIC-cloning:

3C FOR: CCA GGG ACC AGC A (LIC3C forward primer addition)

REV: GAG GAG AAG GCG CGT TTA (Universal reverse primer addition)

TTA – stop codon

### 5.4. DNA sequence of His-RADH

```

1 ATGGGCAGCA GCCATCATCA TCATCATCAC AGCAGCGGCC TGGAAGTTCT GTTCCAGGGA
61 CCAGCAATGT ATCGTCTGCT GAATAAAACC GCAGTTATTA CCGGTGGTAA TAGCGGTATT
121 GGTCTGGCAA CCGCAAAACG TTTTGTGGCC GAAGGTGCCT ATGTTTTTAT TGTGGTTCGT
181 CGTCGTAAAG AACTGGAACA GGCAGCAGCA GAAATTGGTC GTAATGTTAC CGCAGTTAAA
241 GCCGATGTTA CCAAACCTGA AGATCTGGAT CGTCTGTATG CAATTGTTTCG TGAACAGCGT
301 GGTAGCATTG ATGTTCTGTT TGCAAATAGC GGTGCCATTG AACAGAAAAC CCTGGAAGAA
361 ATTACACCGG AACATTATGA TCGCACCTTT GATGTTAATG TGCGTGGTCT GATTTTTTACC
421 GTTCAGAAAG CACTGCCGCT GCTGCGTGAT GGTGGTAGCG TTATTCTGAC CAGCAGCGTT
481 GCCGGTGTTT TGGGTCTGCA GGCACATGAT ACCTATAGCG CAGCAAAAGC AGCAGTTCGT
541 AGCCTGGCAC GTACCTGGAC CACCGAAGTG AAAGGTCGTA GCATTCTGTG TAATGCAGTT
601 AGTCCGGGTG CAATTGATAC CCCGATTATT GAAAATCAGG TTAGCACCCA GGAAGAAGCA
661 GACGAACTGC GCGCAAAATT TGCAGCAGCA ACACCGCTGG GTCGTGTTGG TCGTCCGGAA
721 GAACTGGCAG CAGCCGTTCT GTTTCTGGCA AGTGATGATA GCAGCTATGT TGCAGGTATT
781 GAACTGTTTG TTGATGGTGG TCTGACCCAG GTTTAA

```

### 5.5. Protein sequence of His-RADH

```

1 MGSSHHHHHH SSGLEVLFG PAM+YRLLNKT AVITGGNSGI GLATAKRFVA EGAYVFIVGR
61 RRKELEQAAA EIGRNVTA VK ADVTKLEDLD RLYAIVREQR GSIDVLFANS GAIEQKTL EE
121 ITPEHYDRTF DVNVRGLIFT VQKALPLL RD GGSVILTSSV AGVLGLQAH D TYSAAKAAVR
181 SLARTWTTEL KGRSIRVNAV SPGAIDTPII ENQVSTQEEA DELRAKFAAA TPLGRVGRPE
241 ELAAAVLFLA SDDSSYVAGI ELFVDGGLTQ V-

```

MGSSHHHHHH SSGLEVLFGQ PA  
LEVLFG/G P

- introduced additional amino acids
- sequence recognition motif for HRV 3C

protease cleavage

Underlined  
GPA

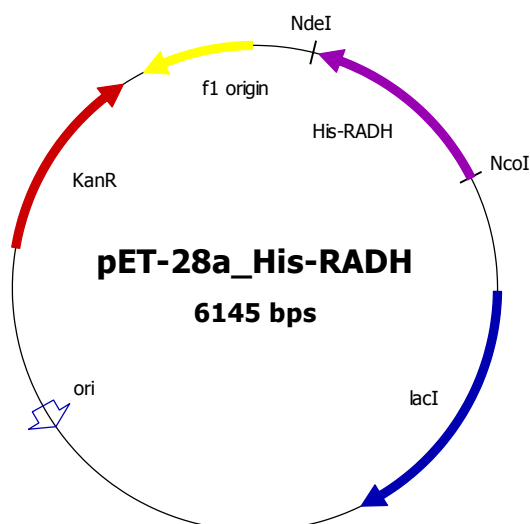
- His<sub>6</sub>-tag
- amino acids remained after HRV 3C protease cleavage

## 5.6. Protein sequence of His-RADH: after His-tag cleavage

```

1  GPA MYRLLNK TAVITGGNSG IGLATAKRFV AEGAYVFIVG RRRKELEQAA AEIGRNVTA
61 KADVTKLEDL DRLYAIVREQ RGSIDVLFAN SGAIEQKTLE EITPEHYDRT FDNVVRGLIF
121 TVQKALPLLR DGGSVILTSS VAGVLGLQAH DTYSAAKAAV RSLARTWTTE LKGRSIRVNA
181 VSPGAIDTPI IENQVSTQEE ADELRAKFAA ATPLGRVGRP EELAAAVLFL ASDSSSYVAG
241 IELFVDGGLT QV-

```



## 5.7. General procedure for subcloning

Component	Volume [μL]			
	Control	#1	#2	#3
FOR_Primer	1.0	1.0	1.0	1.0
REV_Primer	1.0	1.0	1.0	1.0
dNTP's	5.0	5.0	5.0	5.0
KOD Hot Start Polymerase	1.0	1.0	1.0	1.0
MgSO <sub>4</sub> (25 mM)	2.0	2.0	2.0	2.0
Buffer (10X)	5.0	5.0	5.0	5.0
Template DNA (50 ng μL <sup>-1</sup> )	–	0.5	0.5	0.5
DMSO	–	–	1.0	2.0
Water	35.0	34.5	33.5	32.5
Total volume [μL]	50	50	50	50

## 5.8. Thermocycler program for LIC-cloning

Step	Temperature [°C]	Time	N° cycles
Initial denature	94	2 min	1
Denature	94	30 sec	35
Anneal	50	30 sec	
Extension	72	30 sec	
Final extension	72	3 min	1
Hold	4	n	1

## 5.9. Protocol for His-RADH purification using IMAC

Purification of His-RADH proceeds in three chromatographic steps encompassing immobilised metal affinity chromatography, desalting and gel filtration.

1. STEP: Immobilised metal affinity chromatography (IMAC) using HiTrap Chelating HP column (bed volume: 5 mL, Amersham Biosciences). The fusion protein was purified as follows:
  - a. WASH I: 10 column volumes (50 mL total wash step) with buffer A, flow rate: 2 mL min<sup>-1</sup>
  - b. WASH II: 10 column volumes (50 mL total wash step) with buffer B, flow rate: 2 mL min<sup>-1</sup>
  - c. ELUTION: 20 column volumes, gradient (0-100% buffer C) (100 mL total elution step) and next ~10-20 column volumes with buffer C, flow rate: 1 mL min<sup>-1</sup>
2. STEP: Desalting using gel filtration, HiPrep 26/10 Desalting column (bed volume: 53 mL, Amersham Biosciences). To this purpose buffer D was applied. Onto column 10-15 mL of purified protein was loaded. Desalting procedure was carried out with flow rate of 5 mL min<sup>-1</sup>. Fractions containing the enzyme of interest were next concentrated using ultrafiltration membrane (VIVASPIN 20, cut-off: 30 000 Da, MWCO 30) and are a subject of the last purification step.
3. STEP: Gel filtration using Superdex HiLoad 75/16 PrepGrade (bed volume: 120 mL, Amersham Biosciences). Collected and concentrated (up to 2 mL) sample was loaded onto the column and purification proceeded under flow rate of 0.5-1.0 mL min<sup>-1</sup>. Fractions containing purified enzyme were concentrated as described above

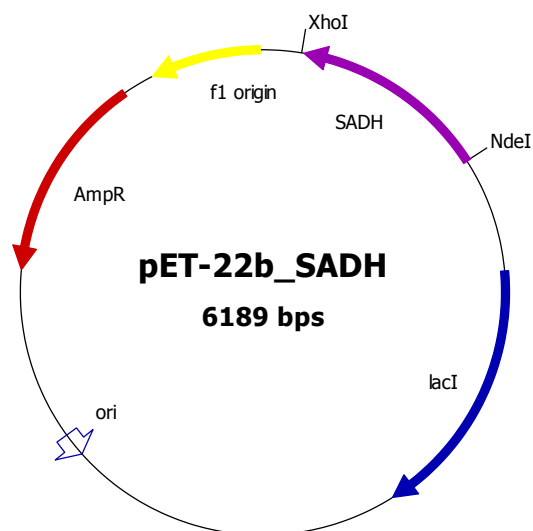
Description	Component	Concentration [mM]
<b>Buffer A</b> (resuspension and wash I)	TRIS	50
	NaCl	500
	CaCl <sub>2</sub>	1.0
	Imidazole	20
	Glycerol	10 vol%
<b>Buffer B</b> (wash II)	TRIS	50
	NaCl	500
	CaCl <sub>2</sub>	1.0
	Imidazole	50
	Glycerol	10 vol%
<b>Buffer C</b> (elution)	TRIS	50
	NaCl	500
	CaCl <sub>2</sub>	1.0
	Imidazole	300
	Glycerol	10 vol%
<b>Buffer D</b> (desalting and gel filtration)	TRIS	50
	NaCl	150
	CaCl <sub>2</sub>	1.0

### 5.10. DNA sequence of strep-SADH

```

1  ATGACCACCC  TGCCGACCGT  TCTGATTACC  GGTGCAAGCA  GCGGTATTGG  TGCAACCTAT
61  GCAGAACGTT  TTGCACGTCG  TGGTCATGAT  CTGGTTCTGG  TTGCACGTGA  TAAAGTTCGT
121  CTGGATGCAC  TGGCAGCACG  TCTGCGTGAT  GAAAGCGGTG  TTGCAGTTGA  AGCACTGCAG
181  GCAGATCTGA  CCCGTCCGGC  AGATCTGGCA  GCAGTTGAAA  TTCGTCTGCG  TGAAGATGCA
241  CGTATTGGCA  TTCTGATTAA  TAATGCAGGT  ATGGCACAGA  GCGGTGGTTT  TGTTTCAGCAG
301  ACCGCAGAAG  GTATTGAACG  TCTGATTACC  CTGAATACCA  CCGCACTGAC  CCGTCTGGCT
361  GCAGCAGTTG  CACCGCGTTT  TGTTTCAGAGC  GGCACCGGTG  CAATTGTTAA  TATTGGTAGC
421  GTTGTGGTT  TTGCACCGGA  ATTTGGTATG  AGCATTTATG  GTGCAACCAA  AGCCTTTGTT
481  CTGTTTCTGA  GCCAGGGTCT  GAATCTGGAA  CTGAGCCCGA  GCGGTATTTA  TGTTTCAGGCA
541  GTTCTGCCTG  CAGCAACCCG  TACCGAAATT  TGGGGTCGTG  CAGGTATTGA  TGTTAATACC
601  CTGCCGGAAG  TTATGGAAGT  TGATGAACTG  GTTGATGCAG  CACTGGTTGG  TTTTGATCGT
661  CGTGAACCTG  TTACCATTC  TCCGCTGCAT  GTTGCAGCAC  GTTGGGATGC  ACTGGATGGT
721  GCACGTCAGG  GTCTGATGAG  CGATATTCGT  CAGGCACAGG  CAGCAGATCG  TTATCGTCCG
781  GAAGCAAGCG  CATGGTCACA  TCCGCAGTTT  GAAAAATAA

```



### 5.11. Protein sequence of strep-SADH

```

1  MTTLP TVLIT  GASSGIGATY  AERFARRGHD  LVLVARDKVR  LDALAARLRD  ESGVAVEALQ
61  ADLTRPADLA  AVEIRLREDA  RIGILINNAG  MAQSGGFVQQ  TAEGIERLIT  LNTTALTRLA
121 AAVAPRFVQS  GTGAIVNIGS  VVGFAPEFGM  SIYGATKAFV  LFLSQGLNLE  LSPSGIYVQA
181 VLPAAATREI  WGRAGIDVNT  LPEVMEVDEL  VDAALVGFD R  RELVTIPPLH  VAARWDALDG
241 ARQGLMSDIR  QAQAADRYRP  EASAWSH PQF  EK-

```

WSHPQF EK - strep-tag sequence

## VI References

---

- Adolph HW, Maurer P, Schneiderbernlohr H, Sartorius C, Zeppezauer M. (1991).** Substrate specificity and stereoselectivity of horse liver alcohol dehydrogenase. Kinetic evaluation of binding and activation parameters controlling the catalytic cycles of unbranched, acyclic secondary alcohols and ketones as substrates of the native and active-site-specific Co(II)-substituted enzyme. *European Journal of Biochemistry* 201(3): 615-625.
- Agranat I, Caner H, Caldwell A. (2002).** Putting chirality to work: the strategy of chiral switches. *Nature Reviews Drug Discovery* 1(10): 753-768.
- Anastas PT, Warner JC. (1998).** Green chemistry: theory and practice. New York: Oxford University Press.
- Anastas PT, Williamson TC. (1996).** Green chemistry: designing chemistry for the environment. Washington, DC: American Chemical Society.
- Auld DS. (2001).** Zinc coordination sphere in biochemical zinc sites. *BioMetals* 14(3-4): 271-313.
- Bala N, Chimni SS. (2010).** Recent developments in the asymmetric hydrolytic ring opening of epoxides catalysed by microbial epoxide hydrolase. *Tetrahedron: Asymmetry* 21(24): 2879-2898.
- Bar-Ilan A, Balan V, Tittmann K, Golbik R, Vyazmensky M, Hübner G, Barak Z, Chipman DM. (2001).** Binding and activation of thiamin diphosphate in acetohydroxyacid synthase. *Biochemistry* 40(39): 11946-11954.
- Barrowman MM, Fewson CA. (1985).** Phenylglyoxylate decarboxylase and phenylpyruvate decarboxylase from *Acinetobacter calcoaceticus*. *Current Microbiology* 12(4): 235-239.
- Barrowman MM, Harnett W, Scott AJ, Fewson CA, Kusel JR. (1986).** Immunological comparison of microbial TPP-dependent nonoxidative alpha-keto acid decarboxylases. *FEMS Microbiology Letters* 34(1): 57-60.
- Bastos FD, dos Santos AG, Jones J, Oestreicher EG, Pinto GF, Paiva LMC. (1999).** Three different coupled enzymatic systems for *in situ* regeneration of NADPH. *Biotechnology Techniques* 13(10): 661-664.
- Bastos FM, Franca TK, Machado GDC, Pinto GF, Oestreicher EG, Paiva LMC. (2002).** Kinetic modelling of coupled redox enzymatic systems for *in situ* regeneration of NADPH. *Journal of Molecular Catalysis B-Enzymatic* 19-20: 459-465.
- Bellucci G, Capitani I, Chiappe C, Marioni F. (1989).** Product enantioselectivity of the microsomal and cytosolic epoxide hydrolase catalysed hydrolysis of *meso* epoxides. *Journal of the Chemical Society D – Chemical Communications* 16: 1170-1171.



- Besse P, Bolte J, Fauve A, Veschambre H. (1993).** Baker's yeast reduction of  $\alpha$ -diketones: investigation and control of the enzymatic pathway. *Bioorganic Chemistry* 21(3): 342-353.
- Blaschke G, Kraft HP, Fickentscher K, Kohler F. (1979).** Chromatographic separation of racemic Thalidomide and teratogenic activity of its enantiomers. *Arzneimittel-Forschung/Drug Research* 29-2(10): 1640-1642.
- Blée E, Schuber F. (1995).** Stereocontrolled hydrolysis of the linoleic acid monoepoxide regioisomers catalyzed by soybean epoxide hydrolase. *European Journal of Biochemistry* 230(1): 229-234.
- Bogin O, Peretz M, Burstein Y. (1997).** *Thermoanaerobacter brockii* alcohol dehydrogenase: characterization of the active site metal and its ligand amino acids. *Protein Science* 6(2): 450-458.
- Bommarius AS, Riebel BR. (2004).** Biocatalysis. Weinheim: Wiley-VCH.
- Borchert S, Burda E, Schatz J, Hummel W, Gröger H. (2012).** Combination of Suzuki cross-coupling reaction using a water-soluble palladium catalyst with an asymmetric enzymatic reduction towards a one-pot reaction in aqueous medium at room temperature. *Journal of Molecular Catalysis B-Enzymatic* 84(SI): 89-93.
- Bortolini O, Fantin G, Fogagnolo M, Giovannini PP, Guerrini A, Medici A. (1997).** An easy approach to the synthesis of optically active vic-diols: a new single-enzyme system. *Journal of Organic Chemistry* 62(6): 1854-1856.
- Boutoute P, Mousset G, Veschambre H. (1998).** Regioselective or enantioselective electrochemical and microbial reductions of 1,2-diketones. *New Journal of Chemistry* 22(3): 247-251.
- Bowen WR, Pugh SYR, Schomburgk NJD. (1986).** Inhibition of horse liver and yeast alcohol dehydrogenase by aromatic and aliphatic aldehydes. *Journal of Chemical Technology and Biotechnology* 36(4): 191-196.
- Bowlus SB, Katzenellenbogen JA. (1974).** Aluminium hydride reduction of  $\alpha$ -ketols. II. Additional evidence for conformational flexibility in the transition state. *Journal of Organic Chemistry* 39(23): 3309-3314.
- Boyce S, Tipton KF. (2005).** Enzyme classification and nomenclature. eLS. Chichester: John Wiley & Sons Ltd.
- Boyd DR, Sheldrake GN. (1998).** The dioxygenase-catalysed formation of vicinal *cis*-diols. *Natural Product Report* 15(3): 309-324.
- Bradshaw CW, Fu H, Shen GJ, Wong CH. (1992a).** A *Pseudomonas* sp. alcohol dehydrogenase with broad substrate specificity and unusual stereospecificity for organic synthesis. *Journal of Organic Chemistry* 57(5): 1526-1532.

- Bradshaw CW, Hummel W, Wong CH. (1992b).** *Lactobacillus kefir* alcohol dehydrogenase – a useful catalyst for synthesis. *Journal of Organic Chemistry* 57(5): 1532-1536.
- Bradshaw CW, Lalonde JJ, Wong CH. (1992c).** Enzymatic synthesis of (*R*)- and (*S*)-1-deuterohexanol. *Applied Biochemistry and Biotechnology* 33(1): 15-24.
- Bränden CI, Eklund H, Nordstrom B, Boiwe T, Soderlund G, Zeppezauer E. (1973).** Structure of liver alcohol dehydrogenase at 2.9 Å resolution. *Proceedings of the National Academy of Sciences of the United States of America* 70(8): 2439-2442.
- Brown DA, Khorlin AA, Lesiak K, Ren WY. (1998).** Pharmaceutical compositions and methods. WO 98/11882.
- Brown DA, Khorlin AA, Lesiak K, Ren WY. (2001).** Dermatological compositions and methods. US 6,290,937 B1.
- Brown DA, Ren WY. (2002).** Treatment of neurodegenerative diseases. WO 02/051395 A1.
- Chen M, Doherty SD, Hsu S. (2010).** Innovative uses of Thalidomide. *Dermatologic Clinics* 28(3): 577-586.
- Chen XJ, Archelas A, Furstoss R. (1993).** Microbiological transformations. 27. The first examples for preparative-scale enantioselective or diastereoselective epoxide hydrolases using microorganisms. An unequivocal access to all four bisabolol stereoisomers. *Journal of Organic Chemistry* 58(20): 5528-5532.
- Chenault HK, Whitesides GM. (1987).** Regeneration of nicotinamide cofactors for use in organic synthesis. *Applied Biochemistry and Biotechnology* 14(2): 147-197.
- Chiappe C, Leandri E, Hammock BD, Morisseau C. (2007).** Effect of ionic liquids on epoxide hydrolase-catalyzed synthesis of chiral 1,2-diols. *Green Chemistry* 9(2): 162-168.
- Chien PN, Moon JY, Chao JH, Leo SJ, Park JS, Kim DE, Park Y, Yoon MY. (2010).** Characterisation of acetohydroxyacid synthase I from *Escherichia coli* K-12 and identification of its inhibitors. *Bioscience, Biotechnology and Biochemistry* 74(11): 2281-2286.
- Chipman DM, Barak Z, Schloss JV. (1998).** Biosynthesis of 2-aceto-2-hydroxy acids: acetolactate synthases and acetohydroxyacid synthases. *Biochimica et Biophysica Acta* 1385(2): 401-419.
- Chipman DM, Duggleby RG, Tittmann K. (2005).** Mechanism of acetohydroxyacid synthase. *Current Opinion in Chemical Biology* 9(5): 475-481.
- Chir TU-Berlin. (2011).** Technische Universität Berlin. [www.chir.tu-berlin.de](http://www.chir.tu-berlin.de)

- Dalziel K, Dickinso FM. (1966).** Kinetics and mechanism of liver alcohol dehydrogenase with primary and secondary alcohols as substrates. *Biochemical Journal* 100(1): 34-46.
- Daußmann T, Hennemann HG; (2009).** Alcohol dehydrogenase for the stereoselective production of hydroxy compounds. US 2009/0162893 A1.
- Daußmann T, Hennemann HG, Rosen TC, Dünkelfmann P. (2006a).** Enzymatic technologies for the synthesis of chiral alcohol derivatives. *Chemie Ingenieur Technik* 78(3): 249-255.
- Daußmann T, Rosen TC, Dünkelfmann P. (2006b).** Oxidoreductases and hydroxynitrilase lyases: complementary enzymatic technologies for chiral alcohols. *Engineering in Life Sciences* 6(2): 125-129.
- Davies J, Jones JB. (1979).** Enzymes in organic synthesis. 16. Heterocyclic ketones as substrates of horse liver alcohol dehydrogenase. Stereospecific reductions of 2-substituted tetrahydrothiopyran-4-ones. *Journal of the American Chemical Society* 101(18): 5405-5410.
- de Torres M, Dimroth J, Arends IWCE, Keilitz J, Hollmann F. (2012).** Towards recyclable NAD(P)H regeneration catalysts. *Biomolecules* 17(8): 9835-9841.
- de Wildeman SM, Sonke T, Schoemaker HE, May O. (2007).** Biocatalytic reductions: from lab curiosity to "first choice". *Accounts of Chemical Research* 40(12): 1260-1266.
- Demir AS, Pohl M, Janzen E, Müller M. (2001).** Enantioselective synthesis of hydroxy ketones through cleavage and formation of acyloin linkage. Enzymatic kinetic resolution via C–C bond cleavage. *Journal of the Chemical Society-Perkin Transactions 1*(7): 633-635.
- Ding S, Mannhardt B, Graf P, Mayerl C, Kästner C. (2012).** Die deutsche Biotechnologie-Branche. Daten & Fakten. Berlin: www.biotechnologie.de.
- Drauz K, Waldmann H. (2002).** Enzyme catalysis in organic synthesis: a comprehensive handbook. Weinheim: Wiley-VCH.
- Drueckhammer DG, Barbas CF, Nozaki K, Wong CH, Wood CY, Ciufolini MA. (1988).** Chemoenzymic synthesis of chiral furanderivatives: useful building blocks for optically active structures. *Journal of Organic Chemistry* 53(8): 1607-1611.
- Drueckhammer DG, Sadozai SK, Wong CH, Roberts SM. (1987).** Biphasic one-pot synthesis of two useful and separable compounds using nicotinamide cofactor-requiring enzymes: syntheses of (*S*)-4-hydroxyhexanoate and its lactone. *Enzyme and Microbial Technology* 9(9): 564-570.
- Dunn MF, MacGibbon AKH, Pease K. (1986).** Zinc enzymes. Boston: Birkhauser Boston.

- Dutler H, Vanderbaan JL, Hochuli E, Kis Z, Taylor KE, Prelog V. (1977).** Dihydroxyacetone reductase from *Mucor javanicus*. 1. Isolation and properties. *European Journal of Biochemistry* 75(2): 423-432.
- Eap CB, Crettol S, Rougier JS, Schlapfer J, Grilo LS, Deglon JJ, Besson J, Croquette-Krokar M, Carrupt PA, Abriel H. (2007).** Stereoselective block of hERG channel by (S)-methadone and QT interval prolongation in CYP2B6 slow metabolizers. *Clinical Pharmacology & Therapeutics* 81(5): 719-728.
- Edegger K, Stampfer W, Seisser B, Faber K, Mayer SF, Oehrlein R, Hafner A, Kroutil W. (2006).** Regio- and stereoselective reduction of diketones and oxidation of diols by biocatalytic hydrogen transfer. *European Journal of Organic Chemistry* 2006(8): 1904-1909.
- Efstathiou E, Logothetis CJ. (2009).** Thalidomide for prostate cancer: is there progress? *Nature Reviews Urology* 6(5): 248-250.
- Eggeling L, Sahm H. (1985).** The formaldehyde dehydrogenase of *Rhodococcus erythropolis*, a trimeric enzyme requiring a cofactor and active with alcohols. *European Journal of Biochemistry* 150(1): 129-134.
- Eklund H, Bränden CI, Jörnvall H. (1976).** Structural comparison of mammalian, yeast and bacillar alcohol dehydrogenases. *Journal of Molecular Biology* 102(1): 61-73.
- Engel S, Vyazmensky M, Berkovich D, Barak Z, Chipman DM. (2004a).** Substrate range of acetohydroxyacid synthase I from *Escherichia coli* in the stereoselective synthesis of  $\alpha$ -hydroxy ketones. *Biotechnology and Bioengineering* 88(7): 825-831.
- Engel S, Vyazmensky M, Berkovich D, Barak Z, Mershuk J, Chipman DM. (2005).** Column flow reactor using acetohydroxyacid synthase I from *Escherichia coli* as catalysts in continuous synthesis of (R)-phenylacetylcarbinol. *Biotechnology and Bioengineering* 89(6): 733-740.
- Engel S, Vyazmensky M, Geresh S, Barak Z, Chipman DM. (2003).** Acetohydroxyacid synthase: a new enzyme for chiral synthesis of (R)-phenylacetylcarbinol. *Biotechnology and Bioengineering* 83(7): 833-840.
- Engel S, Vyazmensky M, Vinogradov M, Berkovich D, Bar-Ilan A, Qimron U, Rosiansky Y, Barak Z, Chipman DM. (2004b).** Role of conserved arginine in the mechanism of acetohydroxyacid synthase. *Journal of Biological Chemistry* 279(23): 24803-24812.
- Eriksson T, Bjorkman S, Hoglund P. (2001).** Clinical pharmacology of Thalidomide. *European Journal of Clinical Pharmacology* 57(5): 365-376.
- Eriksson T, Bjorkman S, Roth B, Hoglund P. (2000).** Intravenous formulations of the enantiomers of Thalidomide: pharmacokinetic and initial

- pharmacodynamic characterization in man. *Journal of Pharmacy and Pharmacology* 52(7): 807-817.
- Faber K. (2001).** Non-sequential processes for the transformation of a racemate into a single stereoisomeric product: proposal for stereochemical classification. *Chemistry – A European Journal* 7(23): 5004-5010.
- Faber K. (2011).** Biotransformations in organic chemistry. A textbook. Berlin Heidelberg: Springer-Verlag.
- Faber K, Patel R. (2000).** Chemical biotechnology. A happy marriage between chemistry and biotechnology: asymmetric synthesis *via* green chemistry. *Current Opinion in Biotechnology* 11(6): 517-519.
- Fanelli M, Sarmiento R, Gattuso D, Carillio G, Capaccetti B, Vacca A, Roccaro AM, Gasparini G. (2003).** Thalidomide: a new anticancer drug? *Expert Opinion on Investigational Drugs* 12(7): 1211-1225.
- Fang JM, Lin CH, Bradshaw CW, Wong CH. (1995).** Enzymes in organic synthesis: oxidoreductions. *Journal of the Chemical Society-Perkin Transactions* 1(8): 967-978.
- Ferreira-Silva B, Lavandera I, Kern A, Faber K, Kroutil W. (2010).** Chemo-promiscuity of alcohol dehydrogenases: reduction of phenylacetaldoxime to the alcohol. *Tetrahedron* 66(19): 3410-3414.
- Fogg MJ, Wilkinson AJ. (2008).** Higher-throughput approaches to crystallization and crystal structure determination. *Biochemical Society Transactions* 36(4): 771-775.
- Fraga D, Hinrichsen RD. (1994).** The identification of a complex family of low-molecular-weight GTP-binding protein homologues from *Paramecium tetraurelia* by PCR cloning. *Gene* 147(1): 145-148.
- Freire RS, Morais SM, Catunda-Junior FEA, Pinheiro DCSN. (2005).** Synthesis and antioxidant, anti-inflammatory and gastroprotector activities of anethole and related compounds. *Bioorganic & Medicinal Chemistry* 13(13): 4353-4358.
- Gadler P, Glueck SM, Kroutil W, Nestl BM, Larissegger-Schnell B, Ueberbacher BT, Wallner SR, Faber K. (2006).** Biocatalytic approaches for the quantitative production of single stereoisomers from racemates. *Biochemical Society Transactions* 34(Pt2): 296-300.
- Gauchot V, Kroutil W, Schmitzer AR. (2010).** Highly recyclable chemo-/biocatalyzed cascade reactions with ionic liquids: one-pot synthesis of chiral biaryl alcohols. *Chemistry – A European Journal* 16(23): 6748-6751.
- Gerhards T, Mackfeld U, Bocola M, von Lieres E, Wiechert W, Pohl M, Rother D. (2012).** Influence of organic solvents on enzymatic asymmetric carbonylations. *Advanced Synthesis & Catalysis* 354(14-15): 2805-2820.

- Giacomini D, Galletti P, Quintavalla A, Gucciardo G, Paradisi F. (2007).** Highly efficient asymmetric reduction of arylpropionic aldehydes by horse liver alcohol dehydrogenase through dynamic kinetic resolution. *Chemical Communications* (39): 4038-4040.
- Gocke D, Walter L, Gauchenova E, Kolter G, Knoll M, Berthold CL, Schneider G, Pleiss J, Müller M, Pohl M. (2008).** Rational protein design of ThDP-dependent enzymes-engineering stereoselectivity. *ChemBioChem* 9(3): 406-412.
- Goldberg K, Schroer K, Lütz S, Liese A. (2007).** Biocatalytic ketone reduction-a powerful tool for the production of chiral alcohols-part I: processes with isolated enzymes. *Applied Microbiology and Biotechnology* 76(2): 237-248.
- Guillena G, Hita MC, Nájera. (2006).** Organocatalyzed direct aldol condensation using L-proline and BINAM-prolinamides: regio- diastereo-, and enantioselective controlled synthesis of 1,2-diols. *Tetrahedron: Asymmetry* 17(7): 1027-1031.
- Hailes HC, Rother D, Müller M, Westphal R, Ward JM, Pleiss J, Pohl M. (2013).** Engineering stereoselectivity of ThDP-dependent enzymes. *FEBS Journal* – submitted.
- Hashimoto Y, Tanatani A, Nagasawa K, Miyachi H. (2004).** Thalidomide as a multitarget drug and its application as a template for drug design. *Drugs of the Future* 29(4): 383-391.
- Haslett PAJ, Klausner JD, Makonkawkeyoon S, Moreira A, Metatrati P, Boyle B, Kunachiwa W, Maneekarn N, Vongchan P, Corral LG and others. (1999).** Thalidomide stimulates T cell responses and interleukin 12 production in HIV-infected patients. *Aids Research and Human Retroviruses* 15(13): 1169-1179.
- Hegeman GD. (1970).** Benzoylformate decarboxylase (*Pseudomonas putida*). In: Herbert Tabor CWT, editor. *Methods in Enzymology*: Academic Press. 674-678.
- Heger W, Schmahl HJ, Klug S, Felies A, Nau H, Merker HJ, Neubert D. (1994).** Embryotoxic effects of Thalidomide derivatives in the nonhuman primate *Callithrix jacchus*. 4. Teratogenicity of Mu-G/Kg Doses of the Em12 enantiomers. *Teratogenesis Carcinogenesis and Mutagenesis* 14(3): 115-122.
- Hilt W, Pfeleiderer G, Fortnagel P. (1991).** Glucose dehydrogenase from *Bacillus subtilis* expressed in *Escherichia coli*. 1. Purification, characterization and comparison with glucose dehydrogenase from *Bacillus megaterium*. *Biochimica et Biophysica Acta* 1076(2): 298-304.
- Hinrichsen P, Gomez I, Vicuna R. (1994).** Cloning and sequencing of the gene encoding benzaldehyde lyase from *Pseudomonas fluorescens* biovar I. *Gene* 144(1):137-138.

- Hochuli E, Taylor KE, Dutler H. (1977).** Dihydroxyacetone reductase from *Mucor javanicus*. 2. Identification of physiological substrate and reactivity towards related compounds. *European Journal of Biochemistry* 75(2): 433-439.
- Hodgson DM, Gibbs AR, Lee GP. (1996).** Enantioselective desymmetrisation of achiral epoxides. *Tetrahedron* 52(46): 14361-14384.
- Höfer R, Clark JH, Kraus GA, Saling P, Spicher P, Schröder R, Kaltschmitt M, Dinjus E, Seyfried F, Hill K and others. (2009).** Sustainable solutions for modern economies. RSC Green chemistry, Cambridge: Royal Society of Chemistry.
- Hoglund P, Eriksson T, Bjorkman S. (1998).** A double-blind study of the sedative effects of the Thalidomide enantiomers in humans. *Journal of Pharmacokinetics and Biopharmaceutics* 26(4): 363-383.
- Hollmann F, Arends IWCE, Holtmann D. (2011).** Enzymatic reductions for the chemist. *Green Chemistry* 13(9): 2285-2314.
- Höllrigl V, Hollmann F, Kleeb AC, Buehler K, Schmid A. (2008).** TADH, the thermostable alcohol dehydrogenase from *Thermus* sp. ATN1: a versatile new biocatalyst for organic synthesis. *Applied Microbiology and Biotechnology* 81(2): 263-273.
- Horvath IT, Anastas PT. (2007).** Innovations and green chemistry. *Chemical Reviews* 107(6): 2169-2173.
- Huisman GW, Liang J, Krebber A. (2010).** Practical chiral alcohol manufacture using ketoreductases. *Current Opinion in Chemical Biology* 14(2): 122-129.
- Hult K, Berglund P. (2007).** Enzyme promiscuity: mechanism and applications. *Trends in Biotechnology* 25(5): 231-238.
- Husain SM, Stillger T, Dünkelfmann P, Lödige M, Walter L, Breitling E, Pohl M, Büchner M, Krossing I, Müller M, Romano D, Molinari F. (2011).** Stereoselective reduction of 2-hydroxy ketones towards *syn*- and *anti*-1,2-diols. *Advanced Synthesis & Catalysis* 353(13): 2359-2362.
- Ideka H, Sato E, Sugai T, Ohta H. (1996).** Yeast mediated synthesis of optically active diols with C<sub>2</sub>-symmetry and (*R*)-4-pentanolide. *Tetrahedron* 52(24): 8113-8122.
- Iding H, Dünwald T, Greiner L, Liese A, Müller M, Siegert P, Grötzinger J, Demir AS, Pohl M. (2000).** Benzoylformate decarboxylase from *Pseudomonas putida* as stable catalyst for the synthesis of chiral 2-hydroxy ketones. *Chemistry – A European Journal* 6(8): 1483-1495.
- Ikariya T, Blacker AJ. (2007).** Asymmetric transfer hydrogenation of ketones with bifunctional transition metal-based molecular catalysts. *Accounts of Chemical Research* 40(12): 1300-1308.

- Ito C, Itoigawa M, Furukawa H, Tokuda H, Okuda Y, Mukainaka T, Okuda M, Nishino H. (1999).** Anti-tumor-promoting effects of 8-substituted 7-methoxycoumarins on Epstein-Barr virus activation assay. *Cancer Letters* 138(1-2): 87-92.
- Itozawa T, Kise H. (1993).** Highly efficient coenzyme regeneration system for reduction of cyclohexanone by horse liver alcohol dehydrogenase in organic solvent. *Biotechnology Letters* 15(8): 843-846.
- Itozawa T, Kise H. (1995).** Immobilization of HLADH on polymer materials for reduction of cyclohexanone with NADH regeneration under 2-phase conditions. *Journal of Fermentation and Bioengineering* 80(1): 30-34.
- Jakoblinnert A, Bocola M, Bhattacharjee M, Steinsiek S, Bonitz-Dulat M, Schwaneberg U, Ansorge-Schumacher MB. (2012).** Who's who? Allocation of carbonyl reductase isoenzymes from *Candida parapsilosis* by combining bio- and computational chemistry. *ChemBioChem* 13(6): 803-809.
- Jakoblinnert A, Mladenov R, Paul A, Sibilla F, Schwaneberg U, Ansorge-Schumacher MB, Dominguez de Maria P. (2011).** Asymmetric reduction of ketones with recombinant *E. coli* whole cells in neat substrates. *Chemical Communications* 47(44): 12230-12232.
- Janzen E, Müller M, Kolter-Jung D, Kneen MM, McLeish MJ, Pohl M. (2006).** Characterization of benzaldehyde lyase from *Pseudomonas fluorescens*: a versatile enzyme for asymmetric C-C bond formation. *Bioorganic Chemistry* 34(6): 345-61.
- Jörnvall H. (1970).** Horse liver alcohol dehydrogenase. Primary structure of the protein chain of the ethanol active isoenzyme. *European Journal of Biochemistry* 16(1): 25-40.
- Jörnvall H, Hedlund J, Bergman T, Oppermann U, Persson B. (2010).** Superfamilies SDR and MDR: from early ancestry to present forms. Emergence of three lines, a Zn-metalloenzyme and distinct variabilities. *Biochemical and Biophysical Research Communications* 396(1): 125-130.
- Joglekar S, Levin M. (2004).** The promise of Thalidomide: evolving indications. *Drugs of Today* 40(3): 197-204.
- Johnson TH, Klein KC. (1979).** Asymmetric chemistry. Alcohol effects upon the (+)-1,2,2-trimethyl-1,3-bis(hydroxymethyl)cyclopentane-lithium aluminium hydride reduction to acetophenone. *Journal of Organic Chemistry* 44(3): 461-462.
- Jones JB. (1986).** Enzymes in organic synthesis. *Tetrahedron* 42(13): 3351-3403.
- Jones JB, Lok KP. (1979).** Enzymes in organic synthesis. 14. Stereoselective horse liver alcohol dehydrogenase catalyzed oxidations of diols containing a



- prochiral center and of related hemiacetals. *Canadian Journal of Chemistry-Revue Canadienne de Chimie* 57(9): 1025-1032.
- Jones JB, Schwartz HM. (1981).** Enzymes in organic syntheses. 19. Evaluation of the stereoselectivities of horse liver alcohol dehydrogenase; catalyzed oxidoreductions of hydroxythiolanes and ketothiolanes, thianes, and thiepanes. *Canadian Journal of Chemistry-Revue Canadienne de Chimie* 59(11): 1574-1579.
- Jones JB, Sih CJ, Perlman D. (1976).** Applications of biochemical systems in organic chemistry. New York: Wiley.
- Jones JB, Takemura T. (1982).** Enzymes in organic synthesis. 28. Reinvestigation of the horse liver alcohol dehydrogenase-catalyzed reductions of 2-alkylcyclohexanones; identification of *cis*-alkylcyclohexanols as minor products. *Canadian Journal of Chemistry-Revue Canadienne de Chimie* 60(23): 2950-2956.
- Junceda L. (2008).** Multi-step enzyme catalysis biotransformations and chemoenzymatic synthesis. Weinheim: Wiley-VCH.
- Karzanov VV, Bogatsky Yu A, Tishkov VI, Egorov AM. (1989).** Evidence for the presence of a new NAD<sup>+</sup>-dependent formate dehydrogenase in *Pseudomonas* sp. 101 cells grown on a molybdenum-containing medium. *FEMS Microbiology Letters* 51(1): 197-200.
- Katzenellenbogen JA, Bowlus SB. (1973).** Stereoselectivity in the reduction of aliphatic  $\alpha$ -ketols with aluminium hydride reagents. *Journal of Organic Chemistry* 38(4): 627-632.
- Kazuoka T, Oikawa T, Muraoka I, Kuroda S, Soda K. (2007).** A cold-active and thermostable alcohol dehydrogenase of a psychrotolerant from Antarctic seawater, *Flavobacterium frigidimaris* KUC-1. *Extremophiles* 11(2): 257-267.
- Keinan E, Hafeli EK, Seth KK, Lamed R. (1986a).** Thermostable enzymes in organic synthesis. 2. Asymmetric reduction of ketones with alcohol dehydrogenase from *Thermoanaerobium brockii*. *Journal of the American Chemical Society* 108(1): 162-169.
- Keinan E, Seth KK, Lamed R. (1986b).** Organic synthesis with Enzymes. 3. TBADH-catalyzed reduction of chloro ketones. Total synthesis of (+)-(*S,S*)-(cis-6-methyltetrahydropyran-2-yl)acetic acid: a civet constituent. *Journal of the American Chemical Society* 108(12): 3474-3480.
- Kihumbu D, Stillger T, Hummel W, Liese A. (2002).** Enzymatic synthesis of all stereoisomers of 1-phenylpropane-1,2-diol. *Tetrahedron-Asymmetry* 13(10): 1069-1072.

- Kim YH, Yoo YJ. (2009).** Regeneration of the nicotinamide cofactor using a mediator-free electrochemical method with a thin oxide electrode. *Enzyme and Microbial Technology* 44(3): 129-134.
- Kirk O, Borchert TV, Fuglsang CC. (2002).** Industrial enzyme applications. *Current Opinion in Biotechnology* 13(4): 345-351.
- Kjellin M, Johansson I. (2010).** Surfactants from renewable resources. Chichester: Wiley.
- Kleifeld O, Frenkel A, Martin JML, Sagi I. (2003a).** Active site electronic structure and dynamics during metalloenzyme catalysis. *Nature Structural Biology* 10(2): 98-103.
- Kleifeld O, Shi SP, Zarivach R, Eisenstein M, Sagi I. (2003b).** The conserved Glu-60 residue in *Thermoanaerobacter brockii* alcohol dehydrogenase is not essential for catalysis. *Protein Science* 12(3): 468-479.
- Kolb HC, van Nieuwenhze MS, Sharpless KB. (1994).** Catalytic asymmetric dihydroxylation. *Chemical Reviews* 94(8): 2483-2547.
- Korkhin Y, Kalb AJ, Peretz M, Bogin O, Burstein Y, Frolow F. (1998).** NADP-dependent bacterial alcohol dehydrogenases: crystal structure, cofactor-binding and cofactor specificity of the ADHs of *Clostridium beijerinckii* and *Thermoanaerobacter brockii*. *Journal of Molecular Biology* 278(5): 967-981.
- Krantz MJ, Martin J, Stimmel B, Haigney MCP. (2009a).** Concerns about consensus guidelines for QTc interval screening in Methadone treatment response. *Annals of Internal Medicine* 151(3): 218-219.
- Krantz MJ, Martin J, Stimmel B, Mehta D, Haigney MCP. (2009b).** QTc interval screening in Methadone treatment. *Annals of Internal Medicine* 150(6): 387-395.
- Krawczyk AR, Jones JB. (1989).** Enzymes in organic synthesis. 46. Regiospecific and stereoselective horse liver alcohol dehydrogenase-catalyzed reductions of *cis*-bicyclo[4.3.0]nonanone and *trans*-bicyclo[4.3.0]nonanone. *Journal of Organic Chemistry* 54(8): 1795-1801.
- Kropff M, Baylon HG, Hillengass J, Robak T, Hajek R, Liebisch P, Goranov S, Hulin C, Blade J, Caravita T and others. (2012).** Thalidomide versus dexamethasone for the treatment of relapsed and/or refractory multiple myeloma: results from optimum, a randomized trial. *Haematologica – The Hematology Journal* 97(5): 784-791.
- Kroutil W, Mischitz M, Faber K. (1997).** Deracemisation of ( $\pm$ )-2,3-substituted oxiranes *via* biocatalytic hydrolysis using bacterial epoxide hydrolases: kinetics of an enantioconvergent process. *Journal of the Chemical Society, Perkin Transactions 1* 24: 3629-3636.

- Kulishova L. (2010).** Analysis of factors influencing enzyme activity and stability in the solid state. PhD thesis. Düsseldorf: Heinrich-Heine Universität Düsseldorf.
- Kurina-Sanz M, Bisogno F, Lavandera I, Orden, AA, Gotor V. (2009).** Promiscuous substrate binding explains the enzymatic stereo- and regiocontrolled synthesis of enantiopure hydroxy ketones and diols. *Advanced Synthesis & Catalysis* 351(11-12): 1842-1848.
- Lam LKP, Gair IA, Jones JB. (1988).** Enzymes in organic synthesis. 41. Stereoselective horse liver alcohol dehydrogenase catalyzed reductions of heterocyclic bicyclic ketones. *Journal of Organic Chemistry* 53(8): 1611-1615.
- Lamed RJ, Zeikus JG. (1981).** Novel NADP-linked alcohol-aldehyde/ketone oxidoreductase in thermophilic ethanogenic bacteria. *Biochemical Journal* 195(1): 183-190.
- Lang H-J, Kleemann H-W, Scholz W, Albus U. (1994).** Substituierte Benzoylguanidine, Verfahren zu ihrer Herstellung, ihre Verwendung als Medikament oder Diagnostikum sowie sie enthaltendes Medikament. DE 4318658.
- Laue S, Greiner L, Wöltinger J, Liese A. (2001).** Continuous application of chemzymes in membrane reactor: asymmetric transfer hydrogenation to acetophenone. *Advanced Synthesis & Catalysis* 6(343): 711-720.
- Lavandera I, Kern A, Ferreira-Silva B, Glieder A, de Wildeman S, Kroutil W. (2008a).** Stereoselective bioreduction of bulky-bulky ketones by a novel ADH from *Ralstonia* sp. *Journal of Organic Chemistry* 73(15): 6003-6005.
- Lavandera I, Kern A, Resch V, Ferreira-Silva B, Glieder A, Fabian WMF, de Wildeman S, Kroutil W. (2008b).** One-way biohydrogen transfer for oxidation of *sec*-alcohols. *Organic Letters* 10(11): 2155-2158.
- Lavandera I, Oberdorfer G, Gross J, de Wildeman S, Kroutil W. (2008c).** Stereocomplementary asymmetric reduction of bulky-bulky ketones by biocatalytic hydrogen transfer. *European Journal of Organic Chemistry* 2008(15): 2539-2543.
- Lee SW, Li G, Lee KS, Jung JS, Xu ML, Seo CS, Chang HW, Kim SK, Song DK, Son JK. (2003).** Preventive agents against sepsis and new phenylpropanoid glucosides from the fruits of *Illicium verum*. *Planta Medica* 69(9): 861-864.
- Lemiere GL, Lepoivre JA, Alderweireldt FC. (1988).** Ring-size effects in horse liver alcohol dehydrogenase-catalyzed redox reactions. *Bioorganic Chemistry* 16(2): 165-174.
- Leuchs S, Greiner L. (2011).** Alcohol dehydrogenase from *Lactobacillus brevis*: a versatile robust catalyst for enantioselective transformations. *Chemical and Biochemical Engineering Quarterly* 25(2): 267-281.

- Liese A, Seelbach K, Wandrey C. (2006).** Industrial biotransformations. Weinheim: Wiley-VCH.
- Liese A, Zelinski T, Kula MR, Kierkels H, Karutz M, Kragl U, Wandrey C. (1998).** A novel reactor concept for the enzymatic reduction of poorly soluble ketones. *Journal of Molecular Catalysis B-Enzymatic* 4(1-2): 91-99.
- Lin G-Q, You Q-D, Cheng J-F. (2011).** Chiral drugs chemistry and biological action. Hoboken: Wiley.
- Linderman RJ, Walker EA, Haney C, Roe RM. (1995).** Determination of the regiochemistry of insect epoxide hydrolase catalyzed epoxide hydration of juvenile hormone by  $^{18}\text{O}$ -labeling studies. *Tetrahedron* 51(40): 10845-10856.
- Lingen B, Kolter-Jung D, Dünkelfmann P, Feldmann R, Grötzinger J, Pohl M, Müller M. (2003).** Alteration of the substrate specificity of benzoylformate decarboxylase from *Pseudomonas putida* by directed evolution. *ChemBioChem* 4(8): 721-726.
- Liu WF, Wang P. (2007).** Cofactor regeneration for sustainable enzymatic biosynthesis. *Biotechnology Advances* 25(4): 369-384.
- Liu X, Wang Y, Gao HY, Xu JH. (2012).** Asymmetric reduction of  $\alpha$ -hydroxy aromatic ketones to chiral aryl vicinal diols using carrot enzyme system. *Chinese Chemical Letters* 23(6): 635-638.
- Maret W, Andersson I, Dietrich H, Schneiderbernlöhr H, Einarsson R, Zeppezauer M. (1979).** Site-specific substituted cobalt(II) horse liver alcohol dehydrogenases. Preparation and characterization in solution, crystalline and immobilized state. *European Journal of Biochemistry* 98(2): 501-512.
- Margolin AL. (1993).** Enzymes in the synthesis of chiral drugs. *Enzyme and Microbial Technology* 15(4): 266-280.
- Matsuyama A, Yamamoto H, Kawada N, Kobayashi Y. (2001).** Industrial production of (*R*)-1,3-butanediol by new biocatalysts. *Journal of Molecular Catalysis B-Enzymatic* 11(4-6): 513-521.
- McCourt JA, Duggleby RG. (2005).** How an enzyme answers multiple-choice questions. *TRENDS in Biochemical Sciences* 30(5): 222-225.
- McMahon RJ, Wiegers KE, Smith SG. (1981).** Stereoselectivity of lithium aluminium hydride and lithium alkoxyaluminumhydride reductions of 3,3,5-trimethylcyclohexanone in diethyl ether. *Journal of Organic Chemistry* 46(1): 99-101.
- Menger FM. (1993).** Enzyme reactivity from an organic perspective. *Accounts of Chemical Research* 26(4): 206-212.

- Merritt AD, Tomkins GM. (1959).** Reversible oxidation of cyclic secondary alcohols by liver alcohol dehydrogenase. *Journal of Biological Chemistry* 234(10): 2778-2782.
- Meyer HP, Eichhorn E, Hanlon S, Lütz S, Schürmann M, Wohlgemuth R, Coppolecchia R. (2013).** The use of enzymes in organic synthesis and the life sciences: perspectives from the Swiss Industrial Biocatalysis Consortium (SIBC). *Catalysis Science & Technology* 3(1): 29-40.
- Mischitz M, Faber K, Willetts A. (1995a).** Isolation of a highly enantioselective epoxide hydrolase from *Rhodococcus* sp. NCIMB 11216. *Biotechnology Letters* 17(9): 893-898.
- Mischitz M, Kroutil W, Wandel U, Faber K. (1995b).** Asymmetric microbial hydrolysis of epoxides. *Tetrahedron: Asymmetry* 6(6): 1261-1272.
- Morisseau C, Nellaiah H, Archelas A, Furstoss R, Baratti JC. (1997).** Asymmetric hydrolysis of racemic *para*-nitrostyrene oxide using an epoxide hydrolase preparation from *Aspergillus niger*. *Enzyme and Microbial Technology* 20(6): 446-452.
- Mueller MJ, Samuelsson B, Haeggström JZ. (1995).** Chemical modification of leukotriene A<sub>4</sub> hydrolase. Indications for essential tyrosyl and arginyl residues at the active site. *Biochemistry* 34(11): 3536-3543.
- Müller M, Gocke D, Pohl M. (2009).** Thiamin diphosphate in biological chemistry: exploitation of diverse thiamin diphosphate-dependent enzymes for asymmetric chemoenzymatic synthesis. *FEBS Journal* 276(11): 2894-2904.
- Müller M, Sprenger GA, Pohl M. (2013).** C-C bond formation using ThDP-dependent lyases. *Current Opinion in Chemical Biology* 17(2): 261-270.
- Müller U, Willnow P, Ruschig U, Hopner T. (1978).** Formate dehydrogenase from *Pseudomonas oxalaticus*. *European Journal of Biochemistry* 83(2): 485-498.
- Murata K, Okano K, Miyagi M, Iwane H, Noyori R, Ikariya T. (1999).** A practical stereoselective of chiral hydrobenzoin via asymmetric transfer hydrogenation of benzils. *Organic Letters* 1(7): 1119-1121.
- Nakamura K, Shiraga T, Miyai T, Ohno A. (1990).** Stereochemistry of NAD(P)-coenzyme in the reaction catalyzed by glycerol dehydrogenase. *Bulletin of the Chemical Society of Japan* 63(6): 1735-1737.
- Nakamura K, Takano S, Terada K, Ohno A. (1992).** Asymmetric reduction of butyl pyruvate catalyzed by immobilized glycerol dehydrogenase in organic-aqueous biphasic media. *Chemistry Letters* 21(6): 951-954.
- Nakamura K, Yoneda T, Miyai T, Ushio K, Oka S, Ohno A. (1988).** Asymmetric reduction of ketones by glycerol dehydrogenase from *Geotricum*. *Tetrahedron Letters* 29(20): 2453-2454.

- Nakata T, Tanaka T, Oishi T. (1983).** Stereoselective reduction of  $\alpha$ -hydroxy ketones. *Tetrahedron Letters* 24(26): 2653-2656.
- Nguyen M, Tran C, Barsky S, Sun JR, McBride W, Pegram M, Pietras R, Love S, Glaspy J. (1997).** Thalidomide and chemotherapy combination: preliminary results of preclinical and clinical studies. *International Journal of Oncology* 10(5): 965-969.
- Niefind K, Müller J, Riebel B, Hummel W, Schomburg D. (2003).** The crystal structure of (*R*)-specific alcohol dehydrogenase from *Lactobacillus brevis* suggests the structural basis of its metal dependency. *Journal of Molecular Biology* 327(2): 317-328.
- Niefind K, Riebel B, Müller J, Hummel W, Schomburg D. (2000).** Crystallization and preliminary characterization of crystals of (*R*)-alcohol dehydrogenase from *Lactobacillus brevis*. *Acta Crystallographica Section D – Biological Crystallography* 56(Pt12): 1696-1698.
- Notz W, List B. (2000).** Catalytic asymmetric synthesis of *anti*-1,2-diols. *Journal of the American Chemical Society* 122(30): 7386-7387.
- Noyori R, Tomino I, Tanimoto Y. (1979).** Virtually complete enantioface differentiation in carbonyl group reduction by complex aluminium hydride reagent. *Journal of the American Chemical Society* 101(11): 3129-3131.
- Oesch F. (1972).** Mammalian epoxide hydrolases: inducible enzymes catalysing the inactivation of carcinogenic and cytotoxic metabolites derived from aromatic and olefinic compounds. *Xenobiotica* 3(5): 305-340.
- O’Neil MJ. (2006).** The Merck Index: an encyclopedia of chemicals, drugs and biologicals. New Jersey: Merck.
- Orru RVA, Archelas A, Furstoss R, Faber K. (1999).** Epoxide hydrolases and their synthetic applications. *Advances in Biochemical Engineering/ Biotechnology* 63: 145-167.
- Osprian I, Kroutil W, Mischitz M, Faber K. (1997).** Biocatalytic resolution of 2-methyl-(aryl)alkyloxiranes using novel bacterial epoxide hydrolases. *Tetrahedron: Asymmetry* 8(1): 65-71.
- Pace-Asciak CR, Lee WS. (1989).** Purification of hepoxilin epoxide hydrolase from rat liver. *Journal of Biological Chemistry* 264(16): 9310-9313.
- Palumbo A. (2010).** Is Thalidomide combination a new option for myeloma? *Nature Reviews Clinical Oncology* 7(8): 425-426.
- Patel RN. (2000).** Stereoselective biocatalysis. New York: Kluwer Academic Publishers-Plenum Publishers.

- Pedragosa-Moreau S, Archelas A, Furstoss R. (1996).** Microbial transformations. 31. Synthesis of enantiopure epoxides and vicinal diols using fungal epoxide hydrolase mediated hydrolysis. *Tetrahedron Letters* 37(19): 3319-3322.
- Peretz M, Bogin O, Tel-Or S, Cohen A, Li G, Chen JS, Burstein Y. (1997).** Molecular cloning, nucleotide sequencing, and expression of genes encoding alcohol dehydrogenases from the thermophile *Thermoanaerobacter brockii* and the mesophile *Clostridium beijerinckii*. *Anaerobe* 3(4): 259-270.
- Peretz M, Burstein Y. (1989).** Amino acid sequence of alcohol dehydrogenase from the thermophilic bacterium *Thermoanaerobium brockii*. *Biochemistry* 28(16): 6549-6555.
- Periasamy M. (1996).** Syntheses of chiral amino alcohols and diols. *Pure and Applied Chemistry* 68(3): 663-666.
- Peters J, Minuth T, Kula MR. (1993a).** A novel NADH-dependent carbonyl reductase with an extremely broad substrate range from *Candida parapsilosis*: purification and characterization. *Enzyme and Microbial Technology* 15(11): 950-958.
- Peters J, Zelinski T, Minuth T, Kula MR. (1993b).** Synthetic applications of the carbonyl reductases isolated from *Candida parapsilosis* and *Rhodococcus erythropolis*. *Tetrahedron-Asymmetry* 4(7): 1683-1692.
- Peters J, Minuth T, Kula MR. (1993c).** Kinetic and mechanistic studies of a novel carbonyl reductase isolated from *Candida parapsilosis*. *Biocatalysis and Biotransformation* 8(1): 31-46.
- Prelog V. (1964).** Specification of the stereospecificity of some oxidoreductases by diamond lattice sections. *Pure and Applied Chemistry* 9(1): 119-130.
- Putman DG, Hogenkamp DJ, Dasse OA, Whittemore ER, Jensen MS. (2007).** Enantiomerically pure (*R*)-etifoxine pharmaceutical compositions thereof and methods of their use. WO 2007/109288 A2.
- Raj KC, Ingram LO, Maupin-Furlow JA. (2001).** Pyruvate decarboxylase: a key enzyme for the oxidative metabolism of lactic acid by *Acetobacter pasteurianus*. *Archives of Microbiology* 176(6): 443-451.
- Ramaswamy S, Eklund H, Plapp BV. (1994).** Structures of horse liver alcohol dehydrogenase complexed with NAD<sup>+</sup> and substituted benzyl alcohols. *Biochemistry* 33(17): 5230-5237.
- Reck M, Gatzemeier U. (2010).** Targeted therapies Thalidomide in lung cancer therapy-what have we learned? *Nature Reviews Clinical Oncology* 7(3): 134-135.
- Reist M, Carrupt PA, Francotte E, Testa B. (1998).** Chiral inversion and hydrolysis of Thalidomide: mechanisms and catalysis by bases and serum albumin, and chiral stability of teratogenic metabolites. *Chemical Research in Toxicology* 11(12): 1521-1528.

- Ricca E, Brucher B, Schrittwieser JH. (2011).** Multi-enzymatic cascade reactions: overview and perspectives. *Advanced Synthesis & Catalysis* 353(13): 2239-2262.
- Richards A, McCague R. (1997).** The impact of chiral technology on the pharmaceutical industry. *Chemistry & Industry* 11: 422-425.
- Riebel B. (1996).** Biochemische und molekularbiologische Charakterisierung neuer NAD(P)-abhängiger Alkoholdehydrogenasen. PhD thesis. Düsseldorf: Heinrich-Heine University of Düsseldorf.
- Rossmann MG, Moras D, Olsen KW. (1974).** Chemical and biological evolution of a nucleotide-binding protein. *Nature* 250(463): 194-198.
- Rother D, Kolter G, Gerhards T, Berthold CL, Gauchenova E, Knoll M, Pleiss J, Müller M, Schneider G, Pohl M. (2011).** (*S*)-Selective mixed carboligation by structure-based design of the pyruvate decarboxylase from *Acetobacter pasteurianus*. *ChemCatChem* 3(10): 1587-1596.
- Röthig TR, Kulbe KD, Buckmann F, Carrea G. (1990).** Continuous coenzyme-dependent stereoselective synthesis of sulcatol by alcohol dehydrogenase. *Biotechnology Letters* 12(5): 353-356.
- Sabale A, Rane V. (2012).** Enzymes – for today and tomorrow. *Colourage* 59(5): 33-39.
- Schlieben NH, Niefind K, Müller J, Riebel B, Hummel W, Schomburg D. (2005).** Atomic resolution structures of (*R*)-specific alcohol dehydrogenase from *Lactobacillus brevis* provide the structural bases of its substrate and cosubstrate specificity. *Journal of Molecular Biology* 349(4): 801-813.
- Schmitz C. (2012).** Untersuchung der Stereoselectivität und des Substratspektrums von AHASI & II aus *Escherichia coli*. Bachelor thesis. Jülich: Fachhochschule Aachen.
- Schubert T, Hummel W, Kula MR, Müller M. (2001).** Enantioselective synthesis of both enantiomers of various propargylic alcohols by use of two oxidoreductases. *European Journal of Organic Chemistry* 22: 4181-4187.
- Scott AK. (1993).** Stereoisomers and drug toxicity - the value of single stereoisomer therapy. *Drug Safety* 8(2): 149-159.
- Serour E, Antranikian G. (2002).** Novel thermoactive glucoamylases from the thermoacidophilic Archaea *Thermoplasma acidophilum*, *Picrophilus torridus* and *Picrophilus oshimae*. *Antonie Van Leeuwenhoek International Journal of General and Molecular Microbiology* 81(1-4): 73-83.
- Sgalla S, Fabrizi G, Cirilli R, Macone A, Bonamore A, Boffi A, Cacchi S. (2007).** Chiral (*R*)- and (*S*)-allylic alcohols *via* a one-pot chemoenzymatic synthesis. *Tetrahedron-Asymmetry* 18(23): 2791-2796.



- Sharpless KB, Amberg W, Bennani YL, Crispino GA, Hartung J, Jeong KS, Kwong HL, Morikawa K, Wang ZM, Xu DQ and others. (1992).** The osmium-catalyzed asymmetric dihydroxylation: a new ligand class and a process improvement. *Journal of Organic Chemistry* 57(10): 2768-2771.
- Shigematsu H, Matsumoto T, Kawauchi G, Hirose Y, Naemura K. (1995).** Horse liver alcohol dehydrogenase-catalyzed enantioselective reduction of cyclic ketones: The effect of the hydrophobic side chain of the substrate on the stereoselectivity of the reaction. *Tetrahedron-Asymmetry* 6(12): 3001-3008.
- Siau WY, Zhang Y, Zhao Y. (2012).** Stereoselective synthesis of Z-alkenes. *Topics in Current Chemistry* 327: 33-58.
- Singhal S, Mehta J. (2001).** Thalidomide in cancer. Potential uses and limitations. *Biodrugs* 15(3): 163-172.
- Song DK, Son JK. (2003).** Novel therapeutical use of erythro-1(4'-methoxyphenyl)1,2-propanediol. WO 03/084522 A1.
- Sotolongo V, Johnson DV, Wahnon D, Wainer IW. (1999).** Immobilized horse liver alcohol dehydrogenase as an on-line high-performance liquid chromatographic enzyme reactor for stereoselective synthesis. *Chirality* 11(1): 39-45.
- Stillger T, Bonitz M, Villela M, Liese A. (2002).** Overcoming thermodynamic limitations in substrate-coupled cofactor regeneration processes. *Chemie Ingenieur Technik* 74(7): 1035-1039.
- Tang SLY, Smith RL, Poliakoff M. (2005).** Principles of green chemistry: PRODUCTIVELY. *Green Chemistry* 7(11): 761-762.
- Tishkov VI, Galkin AG, Marchenko GN, Tsygankov YD, Egorov AM. (1993).** Formate dehydrogenase from methylotrophic bacterium *Pseudomonas* sp. 101: gene cloning and expression in *Escherichia coli*. *Biotechnology and Applied Biochemistry* 18(2): 201-207.
- Tokunaga M, Larrow JF, Kakiuchi F, Jacobsen EN. (1997).** Asymmetric catalysis with water: efficient kinetic resolution of terminal epoxides by means of catalytic hydrolysis. *Science* 277(5328): 936-938.
- Torres CE, Negro C, Fuente E, Blanco A. (2012).** Enzymatic approaches in paper industry for pulp refining and biofilm control. *Applied Microbiology and Biotechnology* 96(2): 327-344.
- Trivedi AH, Heinemann H, Spiess AC, Daußmann T, Büchs J. (2005).** Optimisation of adsorptive immobilization of alcohol dehydrogenases. *Journal of Bioscience and Bioengineering* 99(4): 340-347.
- Trivedi AH, Spiess AC, Daußmann T, Büchs J. (2006).** Effect of additives on gas-phase catalysis with immobilised *Thermoanaerobacter* species alcohol

- dehydrogenase (ADH T). *Applied Microbiology and Biotechnology* 71(4): 407-414.
- Trost BM, Malhotra S, Koschker P, Ellerbrock P. (2012).** Development of the enantioselective addition of ethyl diazoacetate to aldehydes: asymmetric synthesis of 1,2-diols. *Journal of the American Chemical Society* 134(4): 2075-2084.
- Trott O, Olson AJ. (2010).** AutoDock Vina: improving the speed and accuracy of docking with a new scoring function, efficient optimization and multithreading. *Journal of Computational Chemistry* 31(2): 455-461.
- Tsai CS. (1982).** Multifunctionality of liver alcohol dehydrogenase: kinetic and mechanistic studies of esterase reaction. *Archives of Biochemistry and Biophysics* 213(2): 635-642.
- Turner NJ. (2010).** Deracemisation methods. *Current Opinion in Chemical Biology* 14(2): 115-121.
- van Ophem PW, Van Beeumen J, Duine JA. (1992).** NAD-linked, factor-dependent formaldehyde dehydrogenase or trimeric, zinc-containing, long-chain alcohol dehydrogenase from *Amycolatopsis methanolica*. *European Journal of Biochemistry* 206(2): 511-518.
- van den Wittenboer A, Schmidt T, Müller P, Ansorge-Schumacher MB, Greiner L. (2009).** Biphasic mini-reactor for characterisation of biocatalyst performance. *Biotechnology Journal* 4(1): 44-50.
- Vellard M. (2003).** The enzyme as drug: application of enzymes as pharmaceuticals. *Current Opinion in Biotechnology* 14(4): 444-450.
- Velonia K, Tsigos I, Bouriotis V, Smonou I. (1999).** Stereospecificity of hydrogen transfer by the NAD<sup>+</sup>-linked alcohol dehydrogenase from the Antarctic psychrophile *Moraxella* sp. TAE123. *Bioorganic & Medicinal Chemistry Letters* 9(1): 65-68.
- Vinogradov V, Vyazmensky M, Engel S, Belenky I, Kaplun A, Kryukov O, Barak Z, Chipman DM. (2006).** Acetohydroxyacid synthase isoenzyme I from *Escherichia coli* has unique catalytic and regulatory properties. *Biochimica et Biophysica Acta* 1760(3): 356-363.
- Villahermosa LG, Fajardo TT, Abalos RM, Balagon MV, Tan EV, Cellona RV, Palmer JP, Wittes J, Thomas SD, Kook KA and others. (2005).** A randomized, double-blind, double-dummy, controlled dose comparison of Thalidomide for treatment of erythema nodosum leprosum. *American Journal of Tropical Medicine and Hygiene* 72(5): 518-526.
- Virto C, Svensson I, Adlercreutz P, Mattiasson B. (1995).** Catalytic activity of noncovalent complexes of horse liver alcohol dehydrogenase, NAD<sup>+</sup> and polymers, dissolved or suspended in organic solvents. *Biotechnology Letters* 17(8): 877-882.

- Wang L, Cui J, Liu L, Sheng Z. (2012).** Postrelapse survival rate correlates with first-line treatment strategy with Thalidomide in patients with newly diagnosed multiple myeloma: a meta-analysis. *Hematological Oncology* 30(4): 163-169.
- Wang Z, Cui YT, Xu ZB, Qu J. (2008).** Hot water-promoted ring-opening of epoxides and aziridines by water and other nucleophiles. *Journal of Organic Chemistry* 73(6): 2270-2274.
- Watabe T, Kanai M, Isobe M, Ozawa N. (1981).** The hepatic microsomal biotransformation of  $\Delta^5$ -steroids to  $5\alpha,6\beta$ -glycols via  $\alpha$ - and  $\beta$ -epoxides. *Journal of Biological Chemistry* 256(5): 2900-2907.
- Wichmann R, Vasic-Racki D. (2005).** Cofactor regeneration at the lab scale. *Advances in Biochemical Engineering/Biotechnology* 92: 225-260.
- Wilcocks R, Ward OP, Collins S, Dewdney NJ, Hong Y, Prosen E. (1992).** Acyloin formation by benzoylformate decarboxylase from *Pseudomonas putida*. *Applied and Environmental Microbiology* 58(5): 1699-1704.
- Willaert JJ, Lemiere GL, Joris LA, Lepoivre JA, Alderweireldt FC. (1988).** Enzymatic *in vitro* reduction of ketones. 15. The influence of reaction conditions on the stereochemical course of HLAD-catalyzed reductions: 3-cyano-4,4-dimethylcyclohexanone as a sensitive probe. *Bioorganic Chemistry* 16(3): 223-231.
- Wolfenden R. (2011).** Benchmark reaction rates, the stability of biological molecules in water and the evolution of catalytic power in enzymes. *Annual Review of Biochemistry* 80: 645-667.
- Wolfenden R, Snider MJ. (2001).** The depth of chemical time and the power of enzymes as catalysts. *Accounts of Chemical Research* 34(12): 938-945.
- Wong CH, Drueckhammer DG. (1985).** Enzymatic synthesis of chiral hydroxy compounds using immobilized glucose dehydrogenase from *Bacillus cereus* for NAD(P)H regeneration. *Bio-Technology* 3(7): 649-651.
- Wong CH, Drueckhammer DG, Sweers HM. (1985).** Enzymatic vs fermentative synthesis - thermostable glucose dehydrogenase catalyzed regeneration of NAD(P)H for use in enzymatic synthesis. *Journal of the American Chemical Society* 107(13): 4028-4031.
- Wu S, Li A, Chin YS, Li Z. (2013).** Enantioselective hydrolysis of racemic and meso-epoxides with recombinant *Escherichia coli* expressing epoxide hydrolase from *Sphingomonas* sp. HXN-200: preparation of epoxides and vicinal diols in high *ee* and high concentrations. *ACS Catalysis* 3(4): 752-759.
- Yakoub-Agha I, Mary JY, Hulin C, Doyen C, Marit G, Benboubker L, Voillat L, Moreau P, Berthou C, Stoppa AM and others. (2012).** Low-dose vs. high-dose Thalidomide for advanced multiple myeloma: a prospective trial from

- the Intergroupe Francophone du Myelome. *European Journal of Haematology* 88(3): 249-259.
- Yamada SI, Koga K. (1970).** Asymmetric induction through hydride reductions. *Selective Organic Transformations* 1: 1-33.
- Yamamoto H, Kawada N, Matsuyama A, Kobayashi Y. (1999).** Cloning and expression in *Escherichia coli* of a gene coding for a secondary alcohol dehydrogenase from *Candida parapsilosis*. *Bioscience, Biotechnology and Biochemistry* 63(6): 1051-1055.
- Zechel DL, Withers SG. (2000).** Glycosidase mechanisms: anatomy of a finely tuned catalyst. *Accounts of Chemical Research* 33(1): 11-18.
- Zeldin DC, Wei S, Falck JR, Hammock BD, Snapper JR, Capdevila JH. (1995).** Metabolism of epoxyeicosatrienoic acids by cytosolic epoxide hydrolase: substrate structural determinants of asymmetric catalysis. *Archives of Biochemistry and Biophysics* 316(1): 443-451.
- Zeldis JB. (2005).** Methods and compositions using Thalidomide for the treatment and management of cancers and other diseases. WO 2005/046686.
- Zelinski T, Liese A, Wandrey C, Kula MR. (1999).** Asymmetric reductions in aqueous media: enzymatic synthesis in cyclodextrin containing buffers. *Tetrahedron-Asymmetry* 10(9): 1681-1687.
- Zhao YF, Wang GF, Cao ZF, Wang YS, Cheng H, Zhou HM. (2000).** Effects of  $\text{Ca}^{2+}$  on the activity and stability of methanol dehydrogenase. *Journal of Protein Chemistry* 19(6): 469-473.
- Zhou SF, Kestell P, Tingle MD, Paxton JW. (2002).** Thalidomide in cancer treatment. A potential role in the elderly? *Drugs & Aging* 19(2): 85-100.